THE APPLICATION OF THE BOUNDARY INTEGRAL EQUATION METHOD TO FOUNDATION DYNAMICS

by

FESTUS OLATUNDE DAMISAH

B.Sc., M.Sc., D.I.C.

Thesis submitted for the degree of

Doctor of Philosophy

in the Faculty of Engineering of the

University of London

Department of Mechanical Engineering,

Imperial College of Science and Technology,

London SW7 2BX, England.

May 1981

in

Sweet Memory of my Grandmother

and to my

Parents and Teachers

ABSTRACT

A new approach is developed for analysing the dynamics of a foundation on an elastic half space. It is the Boundary Integral Equation (BIE) method derived from the on-going development in the field of elastostatics. The formulation of the method is based on the fundamental singular solution of the equations of linear elastodynamics in an infinite domain subjected to a point force - the Stoke's problem - together with the dynamic counterpart of the classical reciprocal theorem of Betti-Rayleigh in elastostatics. Combining these two well-known results yields the BIE, a vector integral identity that corresponds to Somigliana's identity in elastostatics and Green's third identity in potential theory.

As its name sounds, the BIE is an integral equation that establishes a relation between the physical data at the boundary of an elastic body. The use of the method to meet the requirements of the dynamics of foundations, as well as details of its numerical implementation, is presented. The method is formulated for foundations of arbitrary shape, but results are presented for the pure modes of vibration of a rectangular infinite strip foundation, as well as the coupled modes. Results are also presented for vertical and horizontal vibrations of finite rectangular foundation. The well known problems of vertical

and torsional vibrations of a circular foundation are revisited to highlight the accuracy of the method.

To underline the versatility of the BIE method some new aspects of foundation dynamics are investigated. Results are presented for the three degrees-of-freedom (i.e., coupled vertical-horizontal-rocking) vibration of the rectangular infinite strip. The results justify the intrinsic assumption that the vertical mode is not coupled to any of the other modes, which fact is probably responsible for absence of reference to such coupling in the literature. The vertical vibration is also analysed for a rectangular foundation with length/width ratio of up to 16. As a natural follow-up, the question is investigated of the errors involved in the often used approximation whereby a "long" rectangular foundation is treated as a rectangular infinite strip in the prediction of resonance frequency.

Finally an indication is given of how the method can be more easily applied to the analysis of interaction of foundations on the elastic half space than previous methods. An outline is also given of the application to the combined problem of a flexible foundation on an elastic half space.

ACKNOWLEDGEMENTS

I am greatly indebted to my supervisor, Professor P. Grootenhuis for his invaluable guidance, advice and encouragement throughout the entire period of this research.

I am very grateful also to my supervisor's secretary, Miss A.N. Berthoud, for making her IBM golfball typewriter available together with the golfball for Scientific Symbols. Thanks to the staff at Imperial College Computer Center, especially Tony Davison, for their patience and help on the Diablo printer.

Thanks are also due to my colleagues in the Dynamics Section of this Department, especially Dare Afolabi and Jerry Antonio, for discussions, arguments and suggestions on academic matters and on the layout of this thesis.

Finally I deeply appreciate the financial support of the University of Lagos during this research.

London,

May, 1981 F.O. Damisah

CONTENTS

GENERAL NOTATION

A_1, A_2, A_3, A_4	Functions appearing in the expressions for the fundamental singular stress matrix T_{jk} (same symbols for the two- and three-dimensional cases)
a_r	Width/length ratio of a rectangular foundation.
b	A characteristic length of a foundation, e.g., radius of circular foundation or semi-length of a rectangular one.
$\underline{b}$	Body force vector in an elastic medium.
c_1	Dilatation wave speed, $\sqrt{(\lambda + 2\mu)/\rho}$.
c_2	Shear wave speed, $\sqrt{\mu/\rho}$.
e, exp	Used for base of natural logarithms.
F	Some convenient unit of force.
F_j, j=1,2,3	Excitation forces applied to a massive foundation along the coordinate axes x_1, x_2, x_3.
F_j, j=4,5,6	The form Υ_j/b of couples Υ_j applied to massive foundation about the coordinate axes x_1, x_2, x_3.
f_j, j=1,2,...,6	F_j/F.
$H_n^{(1)}$, H_n	Hankel function of the first kind of order

	n.
Im	Imaginary part of
i	$\sqrt{-1}$
$J(\xi)$, $J(\underline{\xi})$	Jacobian of transformation from coordinates ξ ($\underline{\xi}$) to x_j in two (three) dimensions.
$\bar{J}_o$	Mass moment of inertia of infinitely long rectangular strip about the rocking axis.
$\bar{J}_j$, j=1,2,3	Mass moments of inertia of foundation of finite arbitrary shape about the coordinate axes.
k_1	ω/c_1, a convenient definition. ω is frequency in radians/sec, see below.
k_2	ω/c_2, a convenient difinition. ω is frequency in radians/sec, see below.
M_j, j=1,2,3	Reaction moments of the supporting medium on the foundation.
m	The mass per unit length of an infinitely long rectangular strip. Same symbol is used for the mass of a foundation of finite arbitrary shape.
m_{jj}, j=1,2,3	= m, a convenient notation. Translational inertia properties in the directions of motion.
m_{jj}, j=4,5,6	$= \bar{J}_{j-3}/b^2$, a convenient notation. Rotational inertia properties about the

	axes of ratation.
$\bar{m}_{jj}$	$m_{jj}/\rho b^3$, mass ratio.
$\hat{n}$	Outward pointing unit normal vector at a given point on the surface of a body.
$P(\underline{y})$	A point P (in or on an elastic domain) whose Cartesian coordinates are y_1, y_2, y_3.
$Q(\underline{x})$	A point Q (on an elastic domain) whose Cartesian coordinates are x_1, x_2, x_3.
Q_j, j=1,2,3	Reaction forces of the supporting medium on a foundation in the coordinate axes.
Q_j, j=4,5,6	M_{j-3}/b, a convenient definition indicating reaction moments.
R(P,Q)	Magnitude of the position vector of Q relative to P, i.e., $\lvert\underline{x} - \underline{y}\rvert$
$\bar{R}$	R/b
Re	Real part of
S	Boundary of an elastic domain.
S_t	Portion of S on which stress values are prescribed.
S_u	Portion of S on which displacement values are prescribed.
T_{jk}	The fundamental singular stress matrix (corresponding to Stoke's problem). Same symbol used for two- and three-dimensional cases.

t	Time coordinate.
$\underline{t}$, t_k	Traction vector (components of) on a given surface.
$(t_k)_o$	Prescribed values of t_k on some portion S_t of boundary S.
U_{jk}	The fundamental singular displacement matrix, the Stoke's tensor. Same symbol used for the two- and three-dimensional cases.
$\underline{u}$, u_k	Displacement vector (components of) of points in an elastic material.
$(u_k)_o$	Prescribed values of u_k on some portion S_u of boundary S.
V_j, $j=1,2,\ldots,6$	Translations and rotations of a massless rigid body in the coordinate directions.
W_j, $j=1,2,\ldots,6$	Translations and rotations of a massive rigid body in the coordinate directions.
x_1, x_2, x_3	Cartesian coordinates
$\bar{x}_j$	x_j/b
$\underline{x}$	The point (x_1,x_2,x_3)
$\underline{y}$	The point (y_1,y_2,y_3)

GREEK SYMBOLS:

λ, μ	Lamé constants, μ is shear modulus.
ρ	Mass density.
δ_{jk}	Kroenecker delta.
σ_{jk}	The stress tensor.
γ	c_2/c_1
Φ, χ, Ψ	Functions appearing in the expressions for the fundamental singular matrices U_{jk} and T_{jk}. Same symbols for two- and three-dimensional cases.
θ_j, j=1,2,3	Rotations of a massless rigid foundation about the respective coordinate axes.
Θ_j, j=1,2,3	Rotations of a massive rigid foundation about the respective coordinate axes.
Υ_j, j=1,2,3	Excitation moments applied to massive foundation about the respective coordinate axes.
ω	Frequency of harmonic motion in radians/sec.
η_1	$b\omega/c_1$
η_2	$b\omega/c_2$, frequency factor.
∇	Del vector operator
∇^2	Laplacian operator
ξ_j, ζ_j	Local coordinates defined over a boundary element.

The usual Cartesian tensor notation is employed: repeated suffixes imply summation and partial differentiation with respect to the coordinate directions is indicated by the comma-suffix notation. Occasionally it is convenient to indicate a vector quantity by underscoring the appropriate symbol, e.g., the displacement vector $\underline{u}$.

chapter 1

INTRODUCTION

1.1 MOTIVATION FOR THE PRESENT WORK

The subject of the dynamics of a rigid body on an elastic soil has received much attention over a number of decades, and many a great researcher has contributed to the fundamental concepts. The subject is important because it is often necessary at the design stage to estimate the dynamic response of a foundation which is supported by an elastic soil. The disturbance may arise either from within the machinery to be supported on the foundation or from adjacent plant and railways, or due to an earthquake. An understanding of foundation dynamics is essential in designs supporting such delicate structures as nuclear reactors, tall buildings and dams. A worldwide interest on the dynamic behaviour of dams is manifested at such meetings as the International Commission on Large Dams (1979). A complete analysis of the response of dams should include the dynamics of the foundation, and will provide a good theoretical basis to those engaged in actual tests on existing dams, such as Severn, Jeary and Ellis (1980). In seeking to understand the dynamic behaviour of ground-borne structures, it is generally accepted as a first step to regard the foundation as a rigid body resting on the soil modelled as a homogeneous isotropic elastic half space. The dynamic response of such a foundation is then sought as a function of input frequency for a harmonic force in different directions.

Attention was first brought to this problem by the works of Lamb (1904) on the dynamics of the earth due to application of an idealised point force. The amount of work involved in this relatively straightforward problem of Lamb gave a foretaste of the tremendous mathematical difficulties that awaited any attempt on analysing the dynamic response of foundations on the earth surface. Ever since then researchers have sought various ways of solving the problem. The major contributions made so far may be grouped under four categories depending on the method of approach, namely (a) Finite Model of the Semi-Infinite Half Space, (b) Analytical Methods of Dual Integral Equations, (c) Numerical methods based on the Green Function approach, and (d) Conformal Mapping of the Half Space. Detailed discussion of these is deferred to section (1.2) below. But one important observation that can be made straightaway about all these attempts is that the motion of the foundation has been constrained within the limits that the particular method of analysis can cope with. For example, considering just the vertical vibration, we find that on the one hand users of the conventional dual integral equation approach such as Awojobi and Grootenhuis (1965) prescribe zero shear stress (i.e. frictionless contact) at the contact between the foundation and the soil in order to avoid writing a third integral equation for the unknown stress, while on the other hand the conformal mapping technique by Alabi (1979)

requires zero horizontal displacement (i.e. perfect bonding) between the foundation and the soil in order to avoid numerical transformation of the unknown displacement. Attempts such as those of Luco and Westman (1972) based on Green function (or influence function) approach made to correct some of these defects introduced some other integral equations which either present considerable difficulties from the numerical point of view, according to Luco and Westman (1972), or require considerable amount of computer time to handle, according to Wong and Luco (1975).

However, more important is the question of how much the various attempts have been able to address themselves to questions of, say, partial bonding between soil and foundations, interaction between many foundations, and above all, allowing for the elasticity of the foundation itself rather than assuming it to be a rigid body. The question of allowing for the flexibility of the foundation is particularly intriguing. The foundation has always been assumed rigid because there is no known strightforward method of analysing the elastodynamics of a finite body. The assumption of rigidity may be considered good enough for small machine foundations, but is questionable for the case of long bodies such as dams and buildings. By the way, the thought of the flexibility of foundations would be very useful to geophysicists who may be interested in the effect of topography on seismic waves - what happens to

Rayleigh surface waves upon striking a mountain? Perhaps we may ponder on the less mathematically formidable aspects of foundation dynamics for the moment. It is usual in the literature to approximate a "long" rectangular foundation as an infinite rectangular strip in order to simplify analysis, but no quantitative evidence has been supplied to determine how long the rectangle should be to justify the approximation. As far as the author is aware there is no analysis in the literature of rectangular foundations with length/width ratios going up to 10 or 16, probably because of numerical difficulties, and this is responsible for the absence of quantitative justification mentioned above. Also there has been no mention of the unconstrained motion of the rigid foundation such as the three degrees-of-freedom (coupled vertical-horizontal-rocking) vibration of the infinite rectangular strip, probably because of the analytical difficulty or because of an intuitive assertion that the vertical vibration is never coupled to either of the horizontal and rocking.

Closed-form analytical solutions of foundation dynamics are almost impossible even for simple foundation shapes as the infinite rectangular strip or circular base, with the exception of torsional vibration of circular base. Efforts are therefore concentrated on seeking numerical solutions to be made available in form of computer software. It is desirable to find a method that will impose minimum

analytical constraint on the motion of the foundation, that is cheaper and more efficient in terms of computer resources, and that promises more potentials for coping with future developments in foundation dynamics. With these requirements in mind the motivation for the present work arises from the on-going developments in the field of elastostatics. The traditional methods of solving the elastic deformation of a finite body have been the finite difference and finite element methods, see Zienkiewicz and Cheung (1967). But recently the so-called Boundary Integral Equation (BIE) method was developed. Notable pioneers in this new approach include Rizzo (1967) and Cruse (1967), (1969), (1973).

Tremendous success and advantages have been recorded with the use of this method by, among others, Rizzo (1967) in two- and three-dimensional elastostatics, Cruse and Rizzo (1968) in transient elastodynamics, Rizzo and Shippy (1968) in elastic inclusion problems, and by Tan and Fenner (1979) in crack analysis. The relative ease with which this class of elasticity problems have been successfully handled by the BIE method leads one to explore the possibility of extending the solution capabilities to steady-state elastodynamics with particular reference to the vibration of foundations, an investigation that has not yet been undertaken before now. The present work is addressed to this investigation. The integral equation is formulated

following the developments in transient elastodynamics, the parallel between the static, transient and steady-state phenomena being underlined. It is found that all the powerful advantages of the BIE method in elastostatics become available for exploitation in elastodynamics.

We begin in the next section by outlining the various important contributions to the analysis of the dynamics of foundation so far, and then, from the mere statement of the Boundary Integral Equation formulation that follows, we begin to appreciate immediately the advantages the method offers over and above any of the previous approaches, and the potentials it promises for some of the yet unattempted problems of foundation dynamics.

1.2 REVIEW OF PREVIOUS WORKS

The analysis of the dynamics of rigid foundation is basically the solution of the elastic deformation of the soil modelled as a homogeneous isotropic elastic half space. For our purpose we classify as follows the major contributions made so far on the subject in accordance with the method of approach.

(a) Finite Model of the Semi-Infinite Half Space

This approach, which involves replacing the entire half space by a finite arrangement of masses, springs and damping elements, dates back to the work of Ang and Harper (1964) on a lumped parameter model for the treatment of plane strain problems. Agabein, Parmelee and Lee (1968), and Lysmer and Kuhlemeyer (1969), among others, introduced finite boundaries into the Ang and Harper model with damping elements introduced at the boundaries to account for geometric damping. Not surprisingly they found the reliability of the model to be dependent on its size.

Many variations of this modelling exist. They include confining the computation to a restricted near-field volume of the half space, Lysmer and Wass (1972), and introduction of boundaries designed to transmit D'Alembert forces, Ang and Newmark (1971). Gupta, Permelee and Krizek (1973) used lumped parameter model to analyse coupled sliding and rocking vibration of an infinitely long rigid strip and found agreement with the analytical results of Karasudhi, Keer and Lee (1968) who only estimated the coupled motion by superposition of the pure modes. Representing the half space by a finite number of masses results in a stiff system, or the model itself may have to approach the size of the half space to obtain good results.

(b) Analytical Method of Dual Integral Equations

This method is based on Fourier transformation of the equations of elastodynamics. After taking the inverse transform the resulting pair of integral equations become formidable to solve. The first approach was the search for an expression for the contact stress distribution to insert under the integrals. Reissner (1936), and later Miller and Pursey (1954) considered uniform pressure distribution under a rigid plate in vertical translation. Quinlan (1953) tried uniform, parabolic and an approximate rigid-base pressure distribution. Arnold, Bycroft and Warburton (1955) presented four modes of response of rigid circular plate based on assumption of contact pressure distribution proportional to the static case. Their results agree fairly well with their test values. These results were extended by Richardson, Webster and Warburton (1971) to the determination of the response on the surface of the half space at distances away from a single mass, and then by some averaging technique over this surface response, Warburton, Richardson and Webster (1971) proceeded to predict the response of a nearby second mass. The first attempt to solve the problem free of any pre-assumption of stress distribution was made by Awojobi and Grootenhuis (1965) using some iterative procedure, and obtained results which agreed better with the experimental results of Arnold, Bycroft and Warburton (1955). Awojobi (1971) proceeded to give approximate results for

high frequencies for some pure modes of circular plate and a long rectangular body.

It is observed that this dual integral equation approach presents considerable mathematical difficulty, except in simple cases like torsional vibration of rigid circular plate Reissner and Sagoci (1944), Sagoci (1944), Awojobi and Grootenhuis (1965), Thomas (1968), and the pure modes of long rectangular bodies, Awojobi (1966), Karasudhi, Keer and Lee (1968). We quote for our reference the pair of integral equations that has to be solved for, say, the vertical translation of infinitely long rigid rectangular body, see Awojobi and Grootenhuis (1965) for details.

$$\int_0^\infty \frac{\alpha_1}{\phi(\eta)} F(\eta)\, J_{-\frac{1}{2}}(\eta\bar{x})\, d\eta = C_b/\sqrt{\bar{x}}\ , \qquad 0 < \bar{x} < 1$$

$$\int_0^\infty F(\eta)\, J_{-\frac{1}{2}}(\eta\bar{x})\, d\eta = 0, \qquad \bar{x} > 1 \tag{1.2.1}$$

$$C_b = \left(- \frac{\mu V_o}{\sqrt{b}} \sqrt{2\pi} \right) / \eta_2^2$$

Integration is with respect to the dimensionless form η, of the Fourier transform parameter, $\phi(\eta)$ is the usual Rayleigh function, $F(\eta)$ the desired normal stress distribution function, α_1 a function of η, and V_o the harmonic vertical displacement of the body.

This approach has limited use, if any, in the analysis of foundations of arbitrary shape whose area of contact with the half space cannot be described by any simple algebraic expression. Also coupled pairs of integral equations would be required for solving coupled modes of vibration. Moreover given the approach, it would be necessary, as observed in previous section, to assume frictionless contact in order to avoid writing another set of equations for the unknown shear stresses.

(c) Green Function Approach

This consists of summing up the influence at a point of all the other points on the contact area between the body and the half space. Basically the influence function is sought from the solution to the problem of Lamb (1904) - the dynamic response of the half space to concentrated point force. The contact area is divided into a number of rectangular sub-regions, figs.(1.1) below.

Two approaches may be distinguished. Elorduy, Nieto and Szekely (1967) obtained their influence function by applying Duhamel's integral to the transient response of the half space to vertical loading obtained by Pekeris (1955). For the vertical vibration they applied an unknown vertical force at the centre of an element Q, fig.(1.1a), and considered its influence at the left corner of every element P (including Q itself).

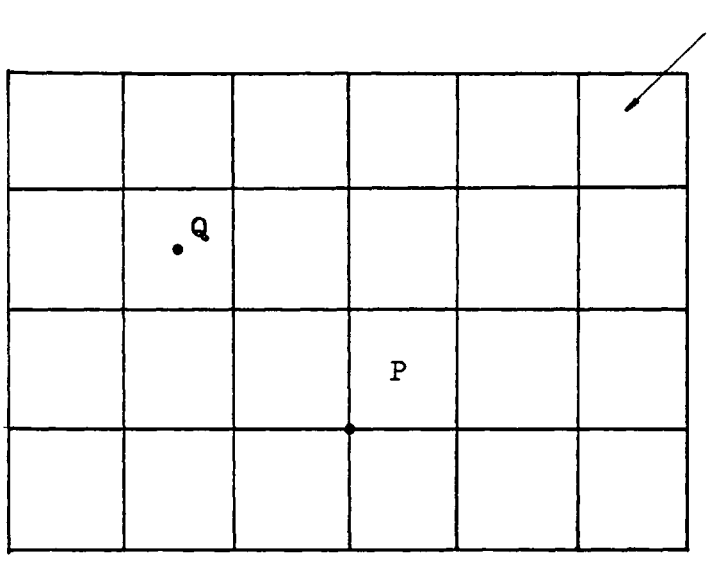

(a) Rectangular Contact Area

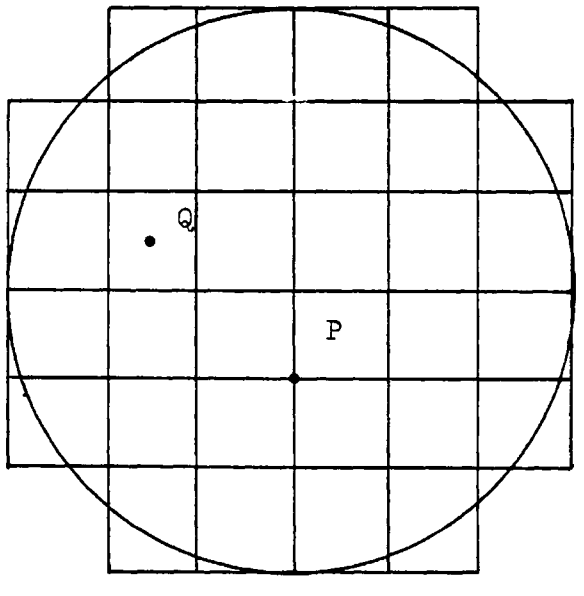

(b) Circular Contact Area

Fig 1.1 Model of Contact Area

Hamidzadeh (1978) obtained his influence function by a numerical attempt directly on Lamb's problem, and then followed Elorduy's approach with many more points on element P - all the four corners of the element - and obtained different results. To follow the approaches of the two works mentioned above for coupled modes of vibrations would require writing numerous pieces of equations before forming the overall system of algebraic equations since forces and/or couples applied in various directions are considered separately.

It is obvious that all the reactions of the supporting medium to any motion of the foundation come from the three components of traction at the contact surface. Therefore the approach of Wong and Luco (1976) looks tidier. They used boundary mesh as in fig.(1.1) above but expressed the displacement at a given point P as a sum of contributions from all the stress components σ_{k3} at point Q in the integral form

$$u_j(P) = \int_S G_{jk}(P,Q)\ \sigma_{k3}(Q)ds(Q) \qquad (1.2.2)$$

so that coupled modes can be easily handled by prescribing on the left side of the equation the displacements imparted on the half space by the chosen mode of vibration. The difficulty with the Wong and Luco's equation above lies in

the influence function G_{jk}, which is the (j)th displacement component at P generated by a unit load acting at point Q in the negative direction of the (k)th axis - which takes us back to the unsolved problem of Lamb. Wong and Luco however used functions from the works of Thomson and Kobori (1963) based on constant stress distribution. These complicated functions for G_{jk} involve infinite integrals of oscillatory functions which they found expensive to compute numerically or otherwise. We point out for our reference that the integrations involved in G_{jk} are with respect to Fourier transform parameter.

However, given this approach a better modelling of the contact area than those in fig.(1.1) can be achieved by following the boundary element modelling process commonly used in the application of Boundary Integral Equation to problems of elastostatics, see for example Lachat (1975), and the modelling used in the present study in chapter 3. The edge singularities of the contact stress distribution could then be clearly shown, see results of this study in chapter 5, and shapes like circles, fig(1.1b), or arbitrary shapes could be more adequately represented.

(d) Conformal Mapping of the Half Space

In analysing the vertical motion of a rigid infinite strip foundation, fig.(1.2a) below, Alabi (1979) transformed the Cartesian set of coordinates x_j/b to an orthogonal

curvilinear set X_j so that the half space is effectively mapped into the rectangular region of fig.(1.2b) with X_1 varying from zero to one and X_2 from zero to π. An array of mesh nodes was superposed on the rectangle over which the elastodynamic equations were integrated by finite difference method. A large system of equations resulted. It is a conceivable idea to map the whole volume of the half space in the three dimensional problem of a foundation of arbitrary shape. The resulting mapped region would be a parallelopiped and the three dimensional array of nodes required over this volume would result into an awefully massive set of equations to solve. It is observed that a lot of computing efforts are spent in this approach in calculating unwanted quantities in the interior of the half space. Excellent results have been obtained however by use of this method to static and transient problems involving the half space in plane strain, Berger and Alabi (1978).

We proceed in the next section to briefly examine the salient points of the Boundary Integral Equation method proposed in this study.

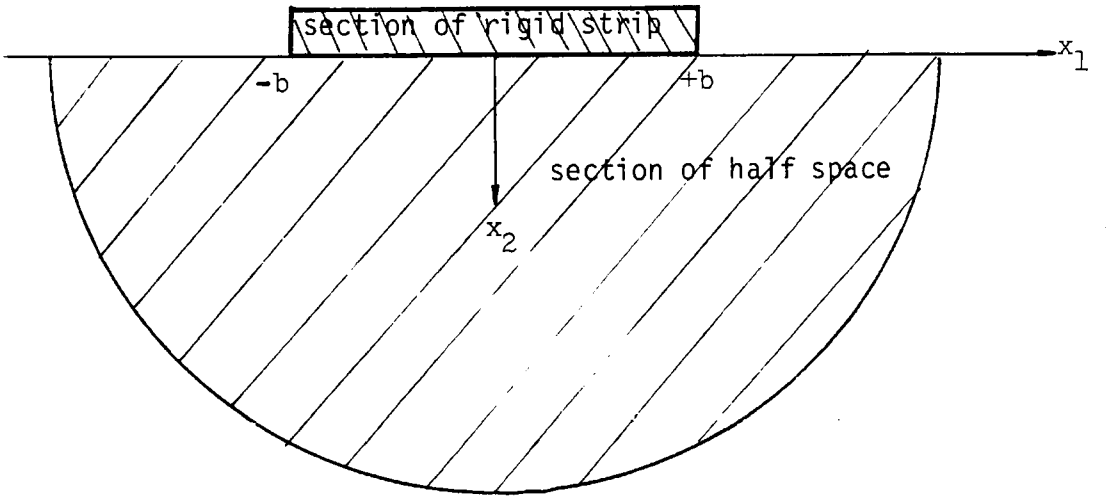

(a) Cross-section of Half Space

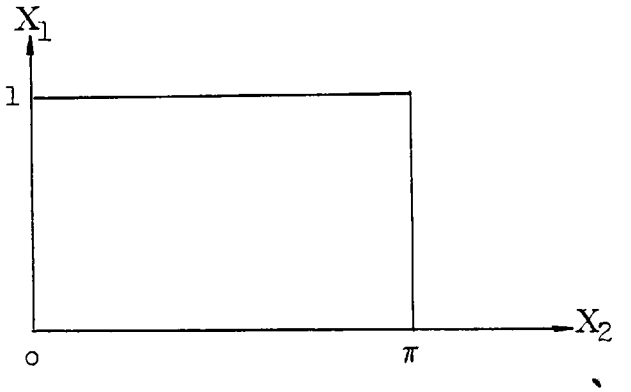

(b) Mapped Space

Fig 1.2 Mapping of the Half Space

1.3 A STATEMENT OF THE BOUNDARY INTEGRAL EQUATION METHOD

The Boundary Integral Equation method utilises the numerical solution of integral equations analogous to Green's boundary formula in Potential Theory, Symm (1963), Kellogg (1953). We give here with only brief details a statement of the BIE formulation. Simply put, the displacement vector u_j at a given point P anywhere in or on an elastic body is related to only the boundary values of the displacement vector u_k and stress vector t_k by the integral equation

$$c_{jk}u_k(P) + \int_S T_{jk}(P,Q)u_k(Q)\, ds(Q)$$

$$= \int_S U_{jk}(P,Q)t_k(Q)\, ds(Q) \qquad (1.3.1)$$

which is derivable from the equations of linear (or non-linear) elasticity. In this equation Q is the dummy integration point over the boundary of the elastic medium, $T_{jk}(P,Q)$ and $U_{jk}(P,Q)$ are second order tensors of position Q relative to P which have different expressions for elastostatics, transient elastodynamics and steady-state elastodynamics. They are functions of Poisson ratio, frequency and the space coordinates (the details start in chapter 2). S denotes the boundary of the medium. Advantageous use is made of the equation by specifying P to be on the boundary also so that attention is paid only to the boundary. c_{jk} is a tensor that depends only on the

geometry surrounding the point P. We then seek a numerical solution of this vector integral equation for displacements and/or stresses subject to given boundary conditions.

Let us examine the advantages that are immediately apparent of this equation over the categories of previous efforts listed above.

(a) The Physics of the Problem is Directly Addressed:-

One of the most important advantages of the BIE equation is that all the quantities involved are physical - displacements, stresses and space coordinates. In particular the variable of integration is the element of area of the boundary of the elastic body. Thus the physics of the problem is directly addressed. This is unlike the dual integral equation approach or Wong and Luco's Green functions in which integration is over all values of the mathematical concept of Fourier transform parameter from zero to infinity. The advantage of using only physical quantities is that if any mathematical difficulty should arise one can resort to the physics of the problem to make shrewd approximations. For example one might be tempted to argue that the BIE requires integration over the infinite area of the half space. But it can be seen firstly that the integral involving stress is only restricted to the loaded region, the stress-free surface contributing nothing to it. Secondly it can be judged physically that the displacement on the surface of the half space becomes vanishingly small

as one moves farther away from the loaded region. Hence the contribution of distant points to the displacement integral becomes insignificant. Moreover, as will be seen later, chapter 2, the tensor T_{jk} multiplying the displacement under the integral sign diminishes as the inverse of the distance from the point P under consideration. Thus the integral is actually a sort of summation technique significantly involving only the displacements in the near field. This point is examined in details in chapter 3. This cannot be said of dual integral equation (1.2.1) in which nothing is known before hand about the behavour of the integral with respect to the Fourier transform parameter. So if any analytical efforts are to be spent, it would probably pay better to focus attention on the BIE than on the dual integral equations.

(b) <u>One Step Closer to Accuracy:-</u>

The boundary integral equation is an exact statement of the problem. Thus we have moved with exact accuracy from the interior of the elastic body to its boundary. Any approximation to the equation occurs only on the boundary. This is a step closer to exactness than the lumped parameter modelling and the conformal mapping methods where approximation starts right from the interior of the medium. This question of accuracy is particularly important in steady-state wave propagation because of the discretisation error common to all numerical analysis, namely, representing

a medium which naturally has an infinite number of degrees-of-freedom with one with a finite number results in a stiffer system. This is the most serious defects of the finite modelling methods.

(c) Reduced Problem Size:-

The BIE method reduces the dimensionality of the problem by one. The two-dimensional problem of the rigid infinite strip foundation is reduced to numerical integration over the straight line that now forms the boundary of the half space in plane strain. The three- dimensional problem of foundations of arbitrary shape reduces to integration over the two-dimensional plane boundary of the half space. This reduced problem size results in much smaller set of equations to solve after discretising the integral equation. This contrasts sharply with the conformal mapping technique which requires large system of equations.

(d) Better Use of Computing Resources:-

Much of the computing resources expended in the finite modelling methods in discretising the entire half space are used in computing unwanted results - the displacements and stresses in the interior of the half space. The foundation problem is concerned only with boundary values, and these are what the BIE formulation involves. After the boundary values are computed the interior values, if and when required, are computed by direct quadrature over the boundary by placing the point P as desired.

The advantages of the BIE over other methods in elastostatics of finite bodies (particularly the benefit of reduced problem size) may be carried over to the steady-state analysis of finite bodies. Thus talking of allowing for the flexibility of foundations, the computing effort in time and storage requirements spent on calculating the interior values of the half space or in computing the Green's functions of Wong and Luco may be spent in solving for the flexibility of the non-rigid foundation over its boundary by the same BIE equation. This is discussed in chapter 6.

The Boundary Integral Equation is formulated in chapter 2. In this study the equation is being applied to the half space as an elastic body loaded at the contact area with the foundation. The question of how much the distant points contribute to the integral occurring in the BIE is examined in chapter 3 by exploiting the radiation conditions of elastodynamics established by Doyle (1965). Chapter 4 is devoted to the analysis of the pure and coupled modes of vibration of a rigid infinite rectangular strip, and chapter 5 to foundations of arbitrary shape. The flexibility and ease of the BIE method permits us to analyse the three degrees-of-freedom vibration of a rigid infinite rectangular strip also in chapter 4 in order to check whether or not the vertical mode is coupled to the horizontal and/or

rocking. Also in chapter 5 we are able to compute the resonance frequencies of rectangular foundations of length/width ratio up to 16, so that some quantitative examination is given to the question of approximating long rectangular foundation as infinite rectangular strip.

In chapter 6 an indication is given on the potentials of the BIE method as a tool for solving the general elastodynamic problem and for dealing with some of the yet unsolved problems of foundation dynamics. There the details are given of the formulation of the combined problem of elastic foundation on an elastic half space, and also of a more complete formulation than is usually given in the literature of the problem of interaction of rigid foundations on an elastic half space.

chapter 2

FORMULATION OF THE BOUNDARY INTEGRAL EQUATION

2.1 HISTORICAL BACKGROUND

The solutions of the general linear elasticity problems do admit a variety of integral representations. Here we shall be concerned with the representation employing the influence function technique based on the reciprocal work theorem of Betti (1872). The first usage of influence functions (or singular solutions) was in the field of elastostatics in the last quarter of the 19th century, employing as the singular solutions the particular solutions of the field equations for a concentrated load in an infinite elastic space attributed to Lord Kelvin (1848). These first efforts were by, among others, Betti (1872-73), Cerutti (1879), Somigliana (1892), Tedone (1879), and Fredholm (1905). Actual solutions were difficult to achieve then because of absence of fast computing aid. The advent of fast modern digital computers revived interest in this approach, and the first numerical treatment was formulated by Jaswon (1963) and Symm (1963) in the potential theory. Then Rizzo (1967) presented numerical solutions of the Boundary Integral Equation (BIE, as it is now commonly called) for plane boundary value problems in elastostatics. The method has since developed so tremendously it now handles with relative ease the problems of three dimensional elastostatics, Cruse (1969,1972,1973), and elastic fracture mechanics, Tan and Fenner (1979). A good survey can be found in the paper by Tan and Fenner (1978) of the use of the BIE method to many other applications including rock mechanics and elastoplastic analysis.

The BIE development has not progressed as rapidly in the field of transient elastodynamics. The general problem has been attempted by Doyle (1966) who used the singular solution for the Laplace-transformed field equations to obtain representations for the

displacement vector, dilatation and rotation vector. However he did not attack the general boundary value problem in terms of boundary data and did not attempt a solution and inversion to complete the problem. The treatment by Nowacki (1964) requires finding a Green's function before attempting the Laplace inversion. Numerical results have been presented by Cruse (1967), and Cruse and Rizzo (1968) I, II, for the two dimensional problem of the elastic half-space under transient load.

The boundary integral representation has also found tremendous application in problems of steady acoustic waves in which the Green's boundary formula in the theory of potentials is used to solve the governing Helmholtz equation, see Banaugh (1963), Chertock (1964) and Meyer, Bell, Zinn and Stallybrass (1978).

It is in the field of steady-state elastodynamics that the application of the BIE has been least developed. The problem of diffraction of steady elastic waves by an inclusion in an infinite elastic medium has been considered by, among others, Banaugh and Goldsmith (1963), Sharma (1967) and Shaw (1968). Their treatment was via the Lame's displacement potentials which satisfy Helmholtz equations and which, therefore, can be treated by Green's formula. Using again Lame's potentials, Banaugh (1964) formulated integral representaions for displacements for the general boundary value problems of elastodynamics. This type of formulation in terms of displacement potentials involve a lot of algebra, and Banaugh ended up with eight simultaneous integral equations to solve. This situation normally arises with displacement potentials because the Green's boundary formula requires the values of the potentials as well as their normal derivatives at the boundary. Papadopoulis (1963) used the same

approach to the problem of point source in a semi-infinite medium.

A formulation of the BIE in steady-state elastodynamics directly in terms of physical quantities of displacements and stresses may be found in the text by Eringen (1975) and also in Kupradze (1963). Applying an extension of Fredholm theory to the BIE, Kupradze formulated a number of problems ranging from linear homogeneous isotropic elastostatics to the vibrations of piecewise homogeneous bodies. He did not take advantage of the use of boundary data directly involved in the integral equation and was therefore forced to look for surface potentials to obtain solutions. His method may thus be termed an indirect approach. A direct approach (to use the terminology in elastostatics) shall be followed in this study in the sense that the BIE shall be treated directly in terms of the physical quantities it embodies - stresses, displacement and space coordinates.

The formulation of the boundary integral equation in elastodynamics is possible due to the existence of fundamental singular solution of the equations of elastodynamics in an infinite region subjected to a concentrated body force acting at a point. This is the Stoke's (1849) problem. These fundamental solutions, the well-known Stoke's tensor, in conjunction with Betti's reciprocal theorem yields a vector identity which corresponds to Somigliana's identity in elastostatics and Green's third identity in potential theory.

2.2 FIELD EQUATIONS

Let D denote a regular region described in a two- or three-dimensional Euclidean space, and S tne boundary of the region, which may be finite

or infinite. The boundary S is a plane curve if D is two-dimensional and a surface if D is three-dimensional. Associated with each differential surface element is an outward pointing unit normal vector $\hat{n}$.

The celebrated Navier's equations of motion of an isotropic homogeneous elastic body, represented by region D, are, in vector notation,

$$(c_1^2 - c_2^2)\,\nabla\nabla\cdot\underline{u} + c_2^2\,\nabla^2\underline{u} = \frac{\partial^2\underline{u}}{\partial t^2} \tag{2.2.1}$$

In the case of time-harmonic motion this equation reduces to, omitting the time harmonic factor $e^{i\omega t}$,

$$(c_1^2 - c_2^2)\,\nabla\nabla\cdot\underline{u} + c_2^2\,\nabla^2\underline{u} + \omega^2\underline{u} = 0 \tag{2.2.2}$$

If the special differential operator ∇^* is introduced as

$$\nabla^* \equiv (c_1^2 - c_2^2)\,\nabla\nabla\cdot + c_2^2\,\nabla^2 \tag{2.2.3}$$

the equation of motion takes the form

$$(\nabla^* + \omega^2)\underline{u} = 0 \tag{2.2.4}$$

The constitutive equation for the linear, isotropic and homogeneous solid relates the stress tensor σ_{jk} to the displacement gradients by Hooke's law

$$\sigma_{ks} = \lambda\delta_{ks}u_{r,r} + (u_{k,s} + u_{s,k})\,\mu \tag{2.2.5}$$

Corresponding to the displacement field $\underline{u}$ the traction vector $\underline{t}$ on a differential element of surface with unit normal $\hat{n}$ is

$$\underline{t} = 2\mu \frac{\partial \underline{u}}{\partial n} + \lambda n(\text{div}.\underline{u}) + \mu(n \times \text{curl}.\underline{u}) \qquad (2.2.6)$$

or in indicial notation

$$t_k = \sigma_{ks} n_s$$

$$t_k = \lambda u_{r,r} n_k + \mu(u_{k,s} + u_{s,k}) n_s \qquad (2.2.7)$$

The stresses and displacements are assumed to satisfy certain boundary conditions

$$t_k = \sigma_{ks} n_s = (t_k)_0 \quad \text{on} \quad S_t \qquad (2.2.8)$$

$$u_k = (u_k)_0 \quad \text{on} \quad S_u \qquad (2.2.9)$$

2.3 THE DYNAMIC BETTI-RAYLEIGH RECIPROCAL THEOREM

We refer back to the equation of steady state motion (2.2.4), namely

$$(\nabla^* + \omega^2)\underline{u} = 0 \qquad (2.3.1)$$

The corresponding equation in elastostatics is

$$\nabla^* \underline{u} = 0 \qquad (2.3.2)$$

and in transient motion

$$(\nabla^* - \alpha^2)\underline{u} = 0 \qquad (2.3.3)$$

where α is the Laplace transform parameter. For details of this see

Cruse (1967). Eqs.(2.3.1) and (2.3.2) are of similar form to the Helmholtz and Laplace equations, respectively, frequently encountered in the harmonic potential theory as

$$(\nabla^2 + k^2)\,\phi = 0 \tag{2.3.1a}$$

$$\nabla^2 \phi = 0 \tag{2.3.2a}$$

where k is a constant and ϕ an unknown variable, see for example Morse and Feshback (1953), Baker and Copson (1950). Indeed in the special case of $\lambda = -1$, $\mu = 1$ the operator ∇^* defined in eq.(2.2.3) reduces to the Laplace operator ∇^2 and equation pairs (2.3.1), (2.3.2) and (2.3.1a), (2.3.2a) become identical. The operator ∇^* plays in the theory of elasticity a similar role as the Laplace operator ∇^2 plays in the theory of harmonic potentials.

Fundamental to the formulation of the boundary integral equation is the dynamic extension of the classical reciprocal theorem of Betti-Rayleigh in elastostatics. The dynamic Betti-Rayleigh reciprocal theorem between a pair of elastodynamic states has been established and proved by Eringen and Suhubi (1975), and Kupradze (1963). Let $\underline{v}^{(1)}$ be a displacement vector field in an elastic domain. The corresponding traction vector $\underline{t}^{(1)}$ on a surface element with normal $\hat{n}$ can be found from eq.(2.2.6). These may be regarded as vector quantities in an elastodynamic state (1).† Another pair of vectors $\underline{v}^{(2)}$ and $\underline{t}^{(2)}$ may be chosen belonging to state (2). In domain D whose boundary is S, Betti's third identity is, Kupradze (1963),

---

† *The concept of "Elastodynamic State" is expounded in Appendix A.*

$$\rho \int_D \left(\underline{v}^{(1)} \cdot \nabla^* \underline{v}^{(2)} - \underline{v}^{(2)} \cdot \nabla^* \underline{v}^{(1)} \right) dD$$

$$= \int_S \left(\underline{v}^{(1)} \cdot \underline{t}^{(2)} - \underline{v}^{(2)} \cdot \underline{t}^{(1)} \right) dS \qquad (2.3.4)$$

where vector dot products is indicated. All the vectors involved are required to be regular in D and on S.

In above equation one of the elastodynamic states is usually taken to correspond to the fundamental singular solutions of the elasticity equations in an infinite region due to a concentrated body force acting at a point $P(\underline{y})$ in a fixed direction, but with harmonic time-variation for steady-state problems. These fundamental solutions, the Stoke's tensor, are discussed next.

2.4 FUNDAMENTAL SINGULAR SOLUTION OF ELASTODYNAMICS

This is the well known solution of the problem of Stoke (1849) of an infinite elastic region subjected to a unit concentrated body force acting at a point $P(\underline{y})$ in a fixed direction $\hat{\underline{e}}$, but with some (harmonic) time-variation. A detailed review of this problem is found in Eringen (1975), page 390 for time-harmonic as well as arbitrary time-varing force.

The displacement component in the j-direction at point $Q(\underline{x})$, due to a

unit concentrated force acting at the point P($\underline{y}$) in the k-direction is denoted by the Stoke's tensor $U_{jk}(P,Q)$ which is a function of the positions P and Q. In the three-dimensional infinite domain U_{jk} is given by, see Eringen (1975), page 435,

$$U_{jk}(P,Q) = \frac{1}{4\pi\rho}\left\{\frac{1}{c_2^2}\frac{e^{ik_2R}}{R}\delta_{jk} + \frac{1}{\omega^2}\frac{\partial^2}{\partial x_j \partial x_k}\left(\frac{e^{ik_1R}}{R} - \frac{e^{ik_2R}}{R}\right)\right\} \qquad (2.4.1)$$

$$j,k = 1,2,3$$

where $R = R(P,Q) = |\,\underline{x} - \underline{y}\,|$ is the distance between P and Q. The expression for U_{jk} shows that it is a symmetric tensor. It is regular everywhere in the infinite domain except at the point P($\underline{y}$) of application of the load. The traction vector for the concentrated load may be obtained by performing the differentiations indicated in eq.(2.2.7) on the row vectors of U_{jk}. If all the j rows are thus operated on the result is a matrix $T_{jk}(P,Q)$ obtainable from the differentiation

$$T_{jk} = \lambda U_{jr,r} n_k + \mu(U_{jk,s} + U_{js,k})n_s \qquad (2.4.2)$$

The matrix T_{jk} gives, on a surface element at Q($\underline{x}$) with unit normal $\hat{n}$, the traction component in the k-direction due to a unit concentrated force at the point P($\underline{y}$) in the j-direction in an infinite domain. It is also regular everywhere except point P($\underline{y}$) but it is not symmetric.

One may consider an infinite elastic domain in which the field quantities and body force vectors depend only on two independent space coordinates x_j, j=1,2, and not on the third coordinate x_3. This becomes a two-dimensional problem and the concentrated body force must

be thought of as being uniformly distributed along the line perpendicular to the infinite x_3-plane, say the plane $x_3 = 0$. We then have the two dimensional form of the Stoke's tensor, which we may represent by the same symbol U_{jk}, given by

$$U_{jk}(P,Q) = \frac{i}{4P}\left\{ \frac{1}{c_2^2} H_o^{(1)}\{k_2 R\}\delta_{jk} + \frac{1}{\omega^2}\frac{\partial^2}{\partial x_j \partial x_k}\left(H_o^{(1)}\{k_2 R\} - H_o^{(1)}\{k_1 R\}\right)\right\}$$

$$j,k = 1,2 \qquad (2.4.3)$$

where we now have

$$R(P,Q) = | \underline{x} - \underline{y} | = (x_\tau - y_\tau)(x_\tau - y_\tau)$$

$H_o^{(1)}$ is the Hankel's function of the first kind of order zero. This tensor too is symmetric. The traction vector corresponding to this two-dimensional case may be computed by eq.(2.4.2) above to obtain a corresponding matrix which we may also denote by T_{jk}. It will be convenient to adopt the following notation. With the concentrated force applied in the j-direction the resulting displacement and traction vectors, namely the j-rows of U_{jk} and T_{jk} are $(u_j)_k$ and $(t_j)_k$ respectively. It may be verified that the displacement vector $(u_j)_k$, for all j's satisfies the equation of motion (2.3.1), see Kupradze (1963).

For computational purposes the expressions for U_{jk} and T_{jk} shall be expanded. The differentiations† are carried out for U_{jk} as indicated in eqs.(2.4.1) and (2.4.3). The respective results are then substituted into eq.(2.4.2) for T_{jk}.

In two dimensions

---

† *Some algebraic details are given in Appendix B.*

$$U_{jk}(P,Q) = \frac{i}{4\mu}\left(\Psi\,\delta_{jk} + \chi\, R_{,j}R_{,k}\right) \tag{2.4.4}$$

$$T_{jk}(P,Q) = \frac{i}{4}\left(A_1 \frac{\partial R}{\partial n}\,\delta_{jk} + A_2 \frac{\partial R}{\partial n}\, R_{,j}R_{,k} + A_3\, R_{,k}n_j + A_4\, R_{,j}n_k\right) \tag{2.4.5}$$

where

$$\frac{\partial R}{\partial n} = \frac{\partial R}{\partial x_s}\, n_s \,, \quad \text{sum on } s,$$

is derivative of R along normal $\hat{n}$,

$$\Psi = H_o(k_2R) - \frac{1}{k_2R}\left(\gamma H_1(k_1R) - H_1(k_2R)\right)$$

$$\chi = \gamma^2 H_2(k_1R) - H_2(k_2R)$$

$$A_1 = -k_2H_2(k_2R) + \frac{2\chi}{R}$$

$$A_2 = 2\left(\gamma^2 k_1H_3(k_1R) - k_2H_3(k_2R)\right)$$

$$A_3 = A_1$$

$$A_4 = -(1 - 2\gamma^2)\,k_1H_1(k_1R) - \frac{2\chi}{R}$$

$$\gamma = c_2/c_1$$

R = magnitude of vector from point $P(\underline{y})$ to point $Q(\underline{x})$

$$= \left((x_1 - y_1)^2 + (x_2 - y_2)^2\right)^{1/2}$$

H_n = Hankel function of first kind of order n.

In three dimensions

$$U_{jk}(P,Q) = \frac{1}{4\pi\mu}\,\frac{1}{R}\left(\Psi\,\delta_{jk} + (3\Phi + \chi)\,R_{,j}R_{,k}\right) \tag{2.4.6}$$

$$T_{jk}(P,Q) = \frac{1}{4\pi}\,\frac{1}{R^2}\left(A_1\,\frac{\partial R}{\partial n}\,\delta_{jk} + A_2\,\frac{\partial R}{\partial n}\,R_{,j}R_{,k}\right.$$

$$\left. + A_3\,R_{,k}n_j + A_4\,R_{,j}n_k\right) \tag{2.4.7}$$

where

$$\Phi = \frac{1}{k_2^2R^2}\left(e^{ik_2R} - e^{ik_1R}\right) + \frac{i}{k_2R}\left(e^{ik_2R} - e^{ik_1R}\right)$$

$$\chi = e^{ik_2R} - \Phi$$

$$\Psi = \gamma^2\,e^{ik_1R} - \Phi$$

$$A_1 = (ik_2R - 1)\, e^{ik_2R} + 6\Phi + 2X$$

$$A_2 = 2ik_2R \left(\gamma^2 e^{ik_1R} - e^{ik_2R} \right) + 30\Phi + 12X$$

$$A_3 = A_1$$

$$A_4 = (1 - 2\gamma^2)(ik_1R - 1)\, e^{ik_1R} + 6\Phi + 2X$$

$$R = \left((x_1 - y_1)^2 + (x_2 - y_2)^2 + (x_3 - y_3)^2 \right)^{1/2}$$

2.5 THE FORMULATION OF THE INTEGRAL EQUATIONS

Returning to Betti's third identity eq.(2.3.4) we let the elastodynamic state (1) correspond to the solution for the concentrated force in the infinite space, namely displacement and traction vectors $(u_j)_k$ and $(t_j)_k$ for force in the j-direction. State (2) is taken to correspond to the set of displacements and stresses u_k, t_k which are regular in D and on S, containing the load point $P(\underline{y})$, and which consists of the unknown in the problem to be solved.

But now the vectors (in state (1)) are no longer regular everywhere in D. So to make the Betti's identity valid we enclose the singularity point P($\underline{y}$) by a small region D' of radius ε and surface S', apply the identity to the regular portion D-D', fig.2.1, and then take the limits of the integrals as the region D' is allowed to shrink towards P.

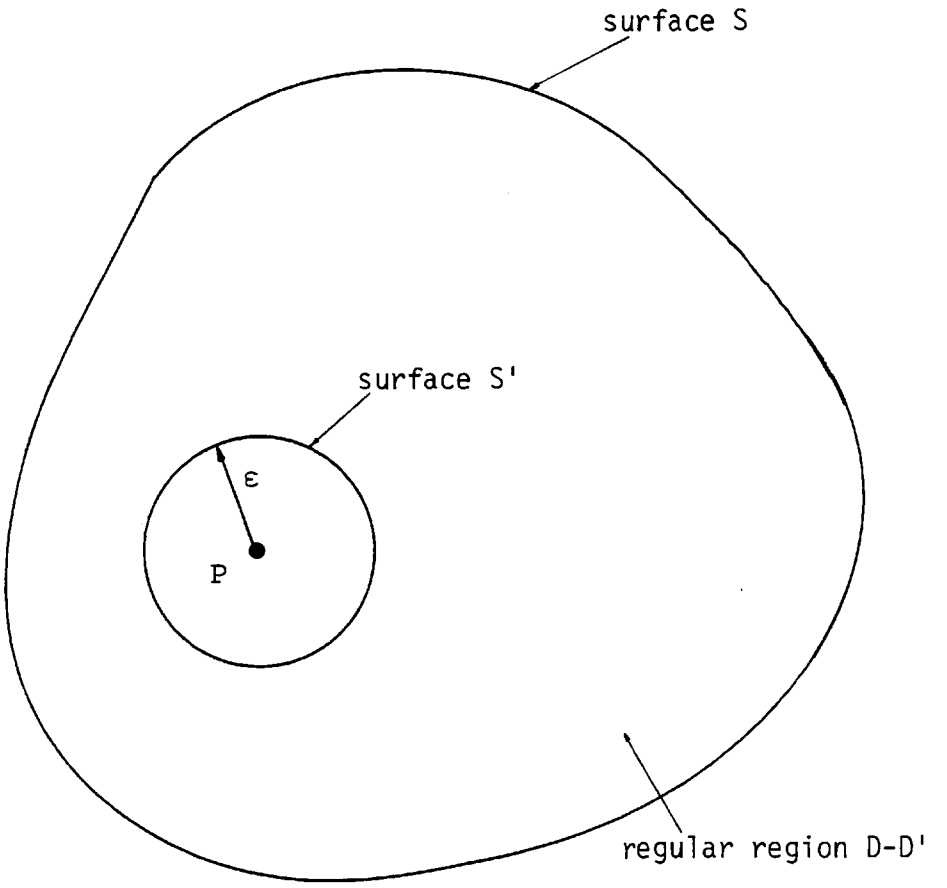

Fig 2.1 Regular Region D-D' For Application of Betti's Equation

Then Betti's equation becomes

$$\rho \int_{D-D'} \left((u_j)_k \cdot \nabla^* u_k \quad - \quad u_k \cdot \nabla^* (u_j)_k \right) \, dD \tag{2.5.1}$$

$$= \int_{S+S'} \left((u_j)_k \cdot t_k \quad - \quad u_k \cdot (t_j)_k \right) \, dS$$

If body force vector b_k is to be considered in the present problem, namely state (2), then u_k is taken to satisfy the equation of motion with the body force $\underline{b}$ introduced, ie

$$\nabla^* u_k = -\frac{1}{\rho} b_k - \omega^2 u_k$$

However in the region D-D' where body force is absent for the concentrated load problem, state (1), $(u_j)_k$ satisfies the homogeneous eq.(2.3.1), ie

$$\nabla^* (u_j)_k = -\omega^2 (u_j)_k$$

Using the last two equations above, eq.(2.5.1) reduces to

$$\int_{D-D'} (u_j)_k b_k \, dD = \int_{S+S'} \left(u_k (t_j)_k - (u_j)_k t_k \right) \, dS \tag{2.5.2}$$

Considering the set of fundamental singular solutions corresponding to the concentrated load applied in all j-directions we replace $(u_j)_k$ by U_{jk} and $(t_j)_k$ by T_{jk} in eq.(2.5.2)

$$\int_{D-D'} U_{jk} b_k \, dD = \int_{S+S'} (T_{jk} u_k - U_{jk} t_k) \, dS \tag{2.5.3}$$

If the body force b_k is ignored in the problem we have

$$\int_{S+S'} \left(T_{jk}(P,Q)u_k(Q) - U_{jk}(P,Q)t_k(Q) \right) dS(Q) = 0 \qquad (2.5.4)$$

This form of the dynamic Betti's theorem is the basis for the formulation of boundary integral equation in elasticity. The integral is taken round the boundary S+S' which encloses the domain D-D'. The integration point Q is, of course, a boundary point, and $u_k(Q)$ and $t_k(Q)$ are boundary values of the displacement and stress vectors respectively. Unit normal $\hat{n}$ points outwards at Q.

To allow the domain of exclusion D' to shrink towards point P we take the limit of the integrals as $\varepsilon \to 0$. The equation is first written in the form to separate the integrals over S and S'

$$\int_S \left(T_{jk}u_k - U_{jk}t_k \right) dS + \lim_{\varepsilon \to o} \int_{S'} \left(T_{jk}u_k - U_{jk}t_k \right) dS = 0 \qquad (2.5.5)$$

The integral over S' is in turn written in two parts

$$\lim_{\varepsilon \to o} \int_{S'} \left(T_{jk}u_k - U_{jk}t_k \right) dS = I_1 - I_2$$

where

$$I_1 = \lim_{\varepsilon \to o} \int_{S'} T_{jk} u_k \, dS$$

$$I_2 = \lim_{\varepsilon \to o} \int_{S'} U_{jk} t_k \, dS$$

The integral I_1 may be written

$$I_1 = \lim_{\varepsilon \to o} \int_{S'} T_{jk} \Big(u_k(Q) - u_k(P) \Big) \, dS(Q)$$

$$+ \lim_{\varepsilon \to o} u_k(P) \int_{S'} T_{jk} \, dS(Q) \qquad (2.5.6)$$

Since u_k is a regular vector, $u_k(P)$ tends to $u_{k(Q)}$ as the boundary S' shrinks towards P. So the first integral on the right hand side of eq.(2.5.6) vanishes and we have

$$I_1 = \lim_{\varepsilon \to o} u_k(P) \int_{S'} T_{jk}(P,Q) \, dS(Q) \qquad (2.5.7)$$

Since vector t_k is also regular throughout region D, similar reasoning may be applied to the I_2 integral to show that

$$I_2 = \lim_{\varepsilon \to o} t_k(P) \int_{S'} U_{jk}(P,Q) \, dS(Q) \qquad (2.5.8)$$

These limit integrals I_1 and I_2 are evaluated next after appropriate expressions for U_{jk} and T_{jk} are inserted.

The Boundary Integral Equation in Two Dimensions

It has been noted in the previous section that the two-dimensional Stoke's tensor U_{jk} corresponds to application of a concentrated load considered uniformly distributed along the line perpendicular to the x_3-plane. The loaded point $P(\underline{y})$ on the x_1-x_2 plane is thus the intersection of the line with the plane. The domain D is two-dimensional and boundary S a plane curve. The region D' enclosing $P(\underline{y})$ in fig.2.1 is a cylinder of radius ε with axis parallel to x_3-axis.

The expressions for U_{jk} and T_{jk} are given by eqs.(2.4.4), (2.4.5). To evaluate the limit integrals I_1 and I_2 in eqs.(2.5.7) and (2.5.8) it is necessary to determine the expressions for U_{jk} and T_{jk} on the circle S', fig.2.2

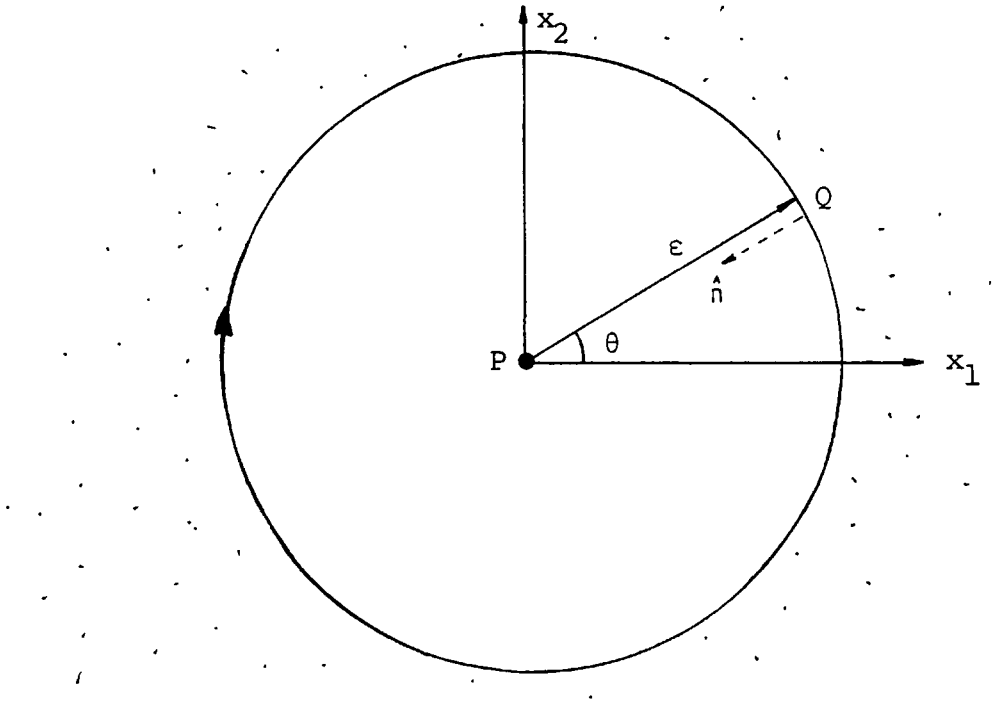

Fig 2.2 The Circle S'

On S' the following are true

$$R = \varepsilon$$

$$dS = -\varepsilon\, d\theta\,, \qquad dn = -dR$$

$$\frac{\partial R}{\partial x_1} = \cos\theta\,, \qquad \frac{\partial R}{\partial x_2} = \sin\theta$$

$$n_1 = -\cos\theta\,, \qquad n_2 = -\sin\theta$$

We take the limits, as ε tends to zero, of the following functions which have been defined for eqs.(2.4.4), (2.4.5)

$$\psi \longrightarrow \frac{2i}{\pi} \ln(k_2\varepsilon)$$

$$\chi \longrightarrow 0$$

$$A_1 \longrightarrow \frac{2i}{\pi\varepsilon}$$

$$A_2 \longrightarrow 0$$

$$A_3 \longrightarrow \frac{2i}{\pi\varepsilon}$$

$$A_4 \longrightarrow (1 - 2\gamma^2)\ \frac{2i}{\pi\varepsilon}$$

Thus on circle S', U_{jk} and T_{jk} assume the expressions

$$U_{jk} = \frac{i}{4\mu}\ \frac{2i}{\pi}\ \ln(k_2\varepsilon)$$

$$T_{jk} = \frac{i}{4}\left\{-\frac{2i}{\pi\varepsilon}\left(\delta_{jk} + \cos\theta\,\sin\theta + (1 - 2\gamma^2)\cos\theta\,\sin\theta\right)\right\}$$

The integrals I_1 and I_2 simplify to

$$I_1 = \delta_{jk}\, u_k(P) \,, \quad I_2 = 0 \tag{2.5.9}$$

It is possible, instead of locating the load point $P(\underline{y})$ inside the domain D, to place it at a point on boundary S, distinct from Q, where the boundary is "smooth", i.e. where the boundary has a continuously turning tangent. In this case the enclosing curve S' is a semi-circle in the limit, fig.2.3, giving the final results of $\frac{1}{2}\, u_k(P)\, \delta_{jk}$ and zero respectively for I_1 and I_2

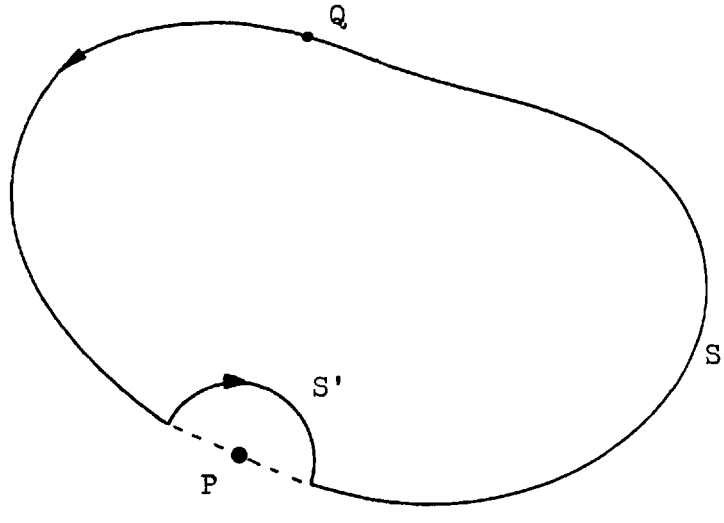

Fig 2.3 P on Boundary S

Putting the results for I_1 and I_2 back into eq.(2.5.5) we have the integral equation

$$c_{jk}u_k(P) + \int_S T_{jk}(P,Q)u_k(Q)\, ds(Q)$$

$$= \int_S U_{jk}(P,Q)t_k(Q)\, ds(Q) \qquad (2.5.10)$$

where

$c_{jk} = \delta_{jk}$ for P inside region D,

$c_{jk} = \frac{1}{2}\delta_{jk}$ for P on smooth boundary S

At a point on S where the boundary is not smooth the value of c_{jk} must be adjusted. Explicit evaluation of this value is not usually necessary as it can be obtained using the concept of rigid body motion of D as explained by Brebbia (1978) for elastostatics problems.

As R tends to zero the tensors U_{jk} and T_{jk} have singularities of orders ln(R) and 1/R respectively. Thus as the integration point Q approaches the load point P along the boundary S the first integral in eq.(2.5.10) has meaning only in the sense of Cauchy Principal Value, see Mikhlin (1957).

The Boundary Integral Equation in Three-dimensions

The region D' enclosing the point P($\underline{y}$) in fig.2.1 is a sphere of radius ε and surface S'. To evaluate the limit integrals I_1, I_2 in eqs.(2.5.7) and (2.5.8), it is necessary to determine the expressions for U_{jk} and T_{jk} on the sphere S', see fig.2.4 in which a spherical system of coordinates is indicated.

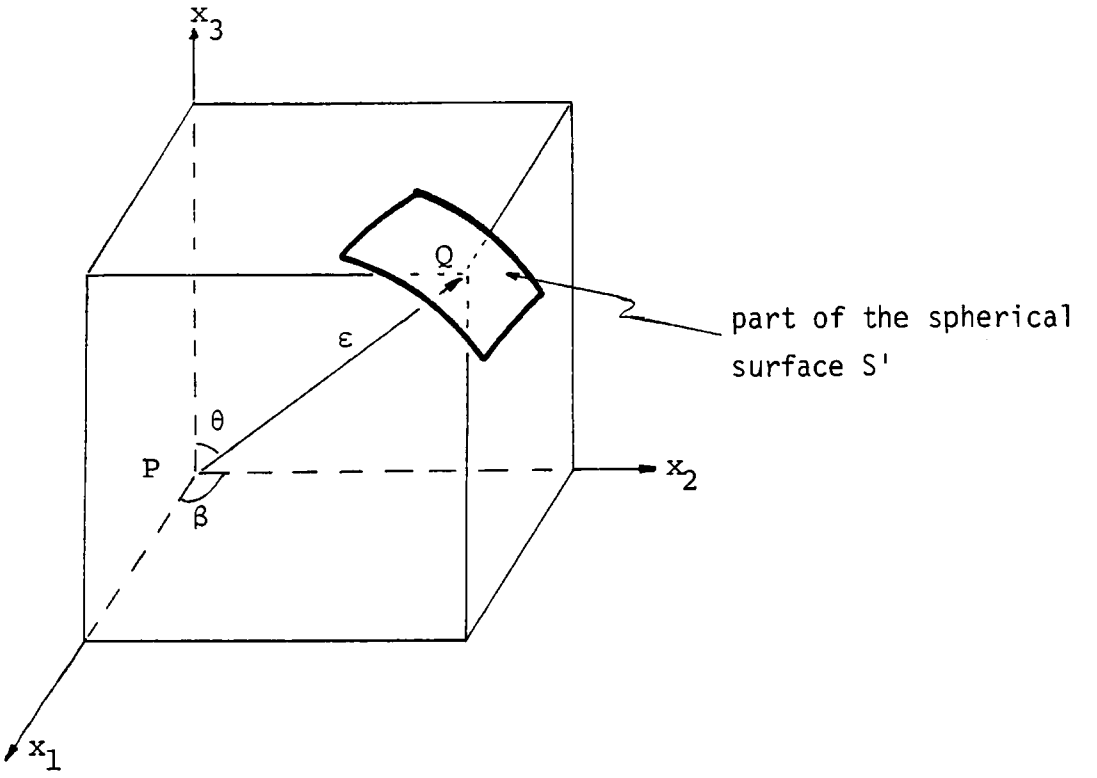

Fig 2.4 Spherical Surface S'

The following are true on S'

$$R = \varepsilon , \qquad dS = \varepsilon^2 \sin\theta \, d\theta d\beta$$

$$dn = - dR , \qquad n_1 = - \sin\theta \cos\beta$$

$$n_2 = - \sin\theta \sin\beta , \qquad n_3 = - \cos\theta$$

$$\frac{\partial R}{\partial x_1} = \frac{\varepsilon \sin\theta \cos\beta}{\varepsilon} \quad , \quad \frac{\partial R}{\partial x_2} = \frac{\varepsilon \sin\theta \sin\beta}{\varepsilon}$$

$$\frac{\partial R}{\partial x_3} = \frac{\varepsilon \cos\beta}{\varepsilon}$$

The limits of the following functions, which have been defined for eqs.(2.4.6) and (2.4.7), are taken as $\varepsilon = R$ tends to zero

$$\Phi \longrightarrow 1 - \gamma^2$$

$$\Psi \longrightarrow \gamma^2$$

$$\chi \longrightarrow \gamma^2 - 1$$

$$A_1 \longrightarrow 3 - 4\gamma^2$$

$$A_2 \longrightarrow 18(\gamma^2 - 1)$$

$$A_3 \longrightarrow A_1$$

$$A_4 \longrightarrow 3 - 2\gamma^2$$

Thus on sphere S', U_{jk} and T_{jk} assume the expressions

$$U_{jk} = \frac{1}{4\pi\mu} \frac{1}{\varepsilon}\left(\gamma^2\delta_{jk} + 2(1 - \gamma^2) f_{jk}(\theta,\beta)\right) \qquad (2.5.11)$$

$$T_{jk} = \frac{1}{4\pi}\frac{1}{\varepsilon^2}\left((4\gamma^2 - 3)\delta_{jk} + 12(1-\gamma^2)g_{jk}(\theta,\beta)\right) \qquad (2.5.12)$$

where $f_{jk}(\theta,\beta)$ and $g_{jk}(\theta,\beta)$ are 3x3 matrices whose elements are functions of θ and β only

$$f_{jk} = \begin{bmatrix} \sin^2\theta\cos^2\beta & \frac{1}{2}\sin^2\theta\sin 2\beta & \frac{1}{2}\sin 2\theta\cos\beta \\ \frac{1}{2}\sin^2\theta\sin 2\beta & \sin^2\theta\sin^2\beta & \frac{1}{2}\sin 2\theta\sin\beta \\ \frac{1}{2}\sin 2\theta\cos\beta & \frac{1}{2}\sin 2\theta\sin\beta & \cos^2\theta \end{bmatrix}$$

$$g_{jk} = f_{jk}$$

The integrals I_1 and I_2 are now

$$I_1 = \lim_{\varepsilon \to o} u_k(P)\int_o^{2\pi}\int_o^{\pi} T_{jk}(P,Q)\,\varepsilon^2\sin\theta\; d\theta d\beta$$

$$I_2 = \lim_{\varepsilon \to o} t_k(P)\int_o^{2\pi}\int_o^{\pi} U_{jk}(P,Q)\,\varepsilon^2\sin\theta\; d\theta d\beta$$

Substituting for $U_{jk}(P,Q)$ from eq.(2.5.11) it is easy to show that

$$I_2 = 0$$

Substituting for $T_{jk}(P,Q)$ from eq.(2.5.12) into the I_1 integral above, we perform the integration with respect to β first and then with respect to θ to obtain the final result

$$I_1 = \delta_{jk}u_k(P)$$

If P was at a smooth part of the boundary S distinct from Q, surface S' would be a hemisphere and the value of the integral would be

$$I_1 = \frac{1}{2}\delta_{jk}u_k(P)$$

Putting these results back into eq.(2.5.5) we find

$$c_{jk}u_k(P) + \int_S T_{jk}(P,Q)u_k(Q)\, ds(Q)$$

$$= \int_S U_{jk}(P,Q)t_k(Q)\, ds(Q) \qquad (2.5.13)$$

where

$c_{jk} = \delta_{jk}$ for P inside region D

$c_{jk} = \frac{1}{2}\delta_{jk}$ for P on smooth boundary S

For non-smooth boundary point the value of c_{jk} must be modified. As seen from eqs.(2.5.11) and (2.5.12) the singularities of U_{jk} and T_{jk}, as R tends to zero, are of order 1/R and $1/R^2$ respectively. As the integration point Q approaches P the Cauchy Principal Value of the first integral in eq.(2.5.13) is taken.

Eq.(2.5.13) is similar in form to the boundary integral equation obtained for the two-dimensional problems, see eq.(2.5.10). In fact it has the same form as those for transient motion, Cruse (1967), and elastostatics, Rizzo (1967), for both two- and three-dimensional cases. Thus it may be regarded as the governing boundary integral equation for all elasticity problems. It is the dynamic equivalence of Somigliana's identity in elastostatics.

chapter 3

APPLICATION OF THE B.I.E. TO A SEMI-INFINITE DOMAIN

3.1 ON THE APPROPRIATENESS OF THE BIE TO INFINITE/SEMI-INFINITE DOMAINS

In the formulation of the boundary integral equation for the elastic domain D in chapter 2, the domain was always considered as finite. When a boundary value problem of mathematical physics refers to a region containing a point at infinity (such as the elastic half space we shall deal with in this study), it is necessary to consider the behaviour at infinity carefully, i.e., to consider the asymptotic behaviour of the solution as a function of the spatial coordinates. There is usually no indication of this behaviour from the pure mathematical formulation of the problem, and it must be determined from indirect reasoning in agreement with physical conditions of the problem. The most important of these considerations is that the behaviour at infinity should ensure a unique solution. But it is clear that the conditions which guarantee uniqueness are, in general, by no means uniquely determined, and the problem consists in choosing these conditions in the most useful way and, especially, in such a manner that solutions with assigned character at infinity exist. Green's formulae and similar other formulae in the theory of elasticity, in particular Betti's formula, serve as a means to make this choice. The choice of the asymptotic character of the solution of boundary value problems for the Helmholtz (wave) equation

$$(\nabla^2 + k^2)\underline{u} = 0 \qquad (3.1.1)$$

which is based on the application of Green's formulae, was first derived by Sommerfeld, and has been known as the Sommerfeld radiation conditions in the theory of waves. They stipulate that the vector $\underline{u}$ assume the following asymptotic relation as the distance r from the point of observation becomes very large

$$\lim_{r \to \infty} r\left(\frac{\partial \underline{u}}{\partial r} + i k \underline{u} \right) = 0$$

$$\lim_{r \to \infty} \left(\underline{u} \right) = 0 \qquad (3.1.2)$$

For convenient reference the boundary integral equation is reproduced here.

$$c_{jk} u_k(P) + \int_S T_{jk}(P,Q) u_k(Q) \; ds(Q)$$

$$= \int_S U_{jk}(P,Q) t_k(Q) \; ds(Q) \qquad (3.1.3)$$

Applying this to the half space requires integration over the boundary S of the domain, fig.3.1, which is either a semi-circle of infinite radius or a hemisphere of infinite radius according as the problem is two- or three-dimensional.

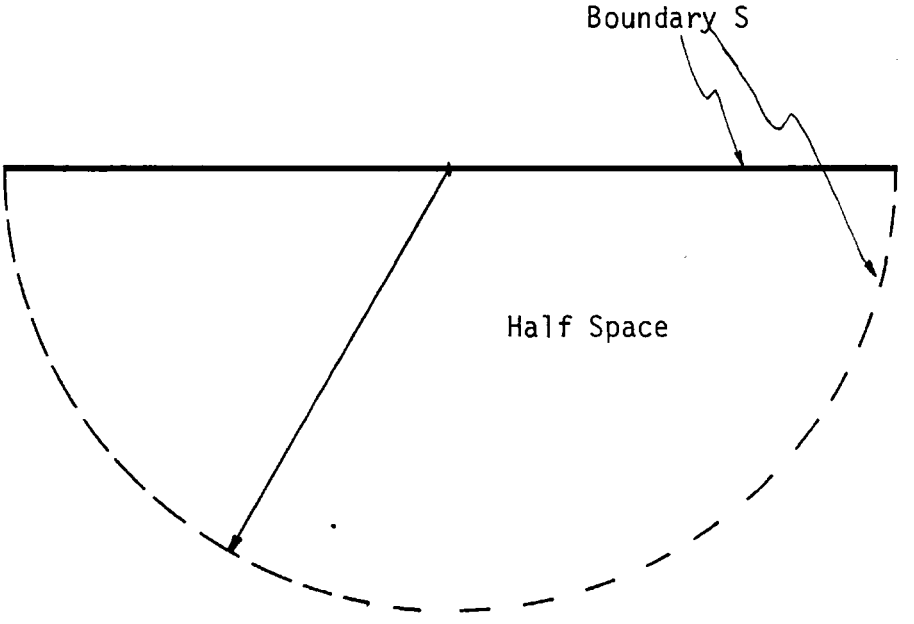

Fig 3.1 The Half Space Boundary

One way to deduce the asymptotic behaviour of vectors u_k and t_k is immediately obvious from the integral equation. We shall require that the integration over the infinitely distant parts of the boundary be zero for any chosen accessible point of observation located on the plane portion of the boundary. In particular if Σ_r is the infinitely distant portion of a sphere (or hemisphere) centered at the point of observation, we require the following integral to be zero

$$\lim_{R\to\infty} \int_{\Sigma_r} R^2 \left(T_{jk}(P,Q)u_k(Q) - U_{jk}(P,Q)t_k(Q) \right) d\Omega = 0 \qquad (3.1.4)$$

where $d\Omega$ is the solid angle at the observation point that subtends the surface element of Σ_r, and R is the distance between the element and the observation point P. From this requirement we arrive at the following so-called radiation conditions of elastodynamics, see Doyle (1965), Eringen (1975), Kupradze (1963)

$$\begin{aligned} \lim_{R\to\infty} R\{ \underline{t}^{(p)} - i\rho\omega c_1 \underline{u}^{(p)} \} &= 0 \\ \lim_{R\to\infty} R\{ \underline{t}^{(s)} - i\rho\omega c_2 \underline{u}^{(s)} \} &= 0 \end{aligned} \qquad (3.1.5)$$

in which superscripts (p) and (s) refer respectively to the irrotational and equivoluminal components of the vectors.

It is interesting to observe that the requirement (3.1.4) and its consequencies (3.1.5) are not new. Indeed Eringen (1975) and Kupradze (1963) have shown, by decomposing the displacement vector $\underline{u}$ into its irrotational part $\underline{u}^{(p)}$ and equivoluminal part $\underline{u}^{(s)}$, that these requirements result directly from the Sommerfeld radiation conditions (3.1.2) of ordinary wave equations. This link between the wave theory and elastodynamic equations is not surprising since we have observed in section 2.3, chapter 2, that the special

elastodynamic operator ∇^* defined in eq.(2.2.3) plays in the theory of elasticity a similar role as the Laplace operator ∇^2 plays in the theory of harmonic potentials.

Having chosen an asymptotic character of the solution based on indications resulting from the boundary integral formula, it is necessary to be sure that such a solution actually exists and that it is unique. The uniqueness of solutions based on these radiation conditions has been proved by Kupradze (1963) and Doyle (1965), and Doyle showed that these conditions do admit to a physical interpretation - they rule out the possibility of energy sources being located at infinity.

3.2 ADAPTATION OF THE BIE TO FOUNDATION DYNAMICS

It is now established that the integration of the BIE is restricted to the plane boundary of the half space, the contribution from the infinitely distant part of the boundary being zero. But the plane boundary itself is of infinite extent, and numerical solution of the integral equation over an infinite domain is impossible. To solve the problem we exploit the radiation conditions discussed in the previous section in the form of eq.(3.1.4).

This equation indicates that points distant from a given observation point P contribute the less to the integrals in the BIE formulation the more distant they are from P. The

formal implementation of the BIE scheme is indicated in fig.3.2 below. The shaded area in the figure is that portion of the surface of the half space on which some stress distribution is applied. O is the origin of coordinates, and P a chosen observation point. C is a circle of some radius R_c centered at O and completely enclosing the stressed region. The BIE eq.(3.1.3) gives the displacement at P in terms of integrals of displacements and stresses (multiplied by the kernel functions T_{jk} and U_{jk} respectively) taken over the entire surface. Q is the integration point and ds(Q) the element of area at Q. Now since the contribution from Q to the integrals (i.e., to the value of displacement at P) becomes less the more distant it is from the loaded area, one may wish to know the value of radius R_c of circle C beyond which one can begin to ignore contributions to the integrals, as well as the errors involved in such truncation.

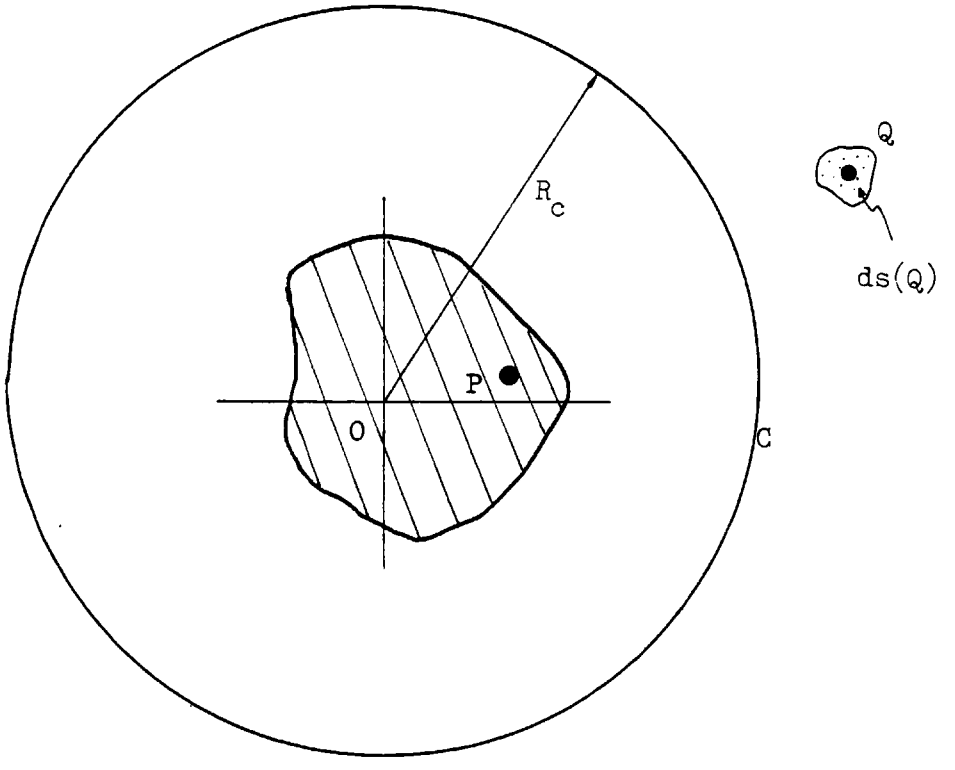

Fig 3.2 Implementation of the BIE Formulation

It is observed that the integral involving stress t_k is naturally restricted to the loaded region since it is zero on the stress-free surface. Thus the truncation applies only to the integral involving displacement, namely,

$$I_u = \int T_{jk}(P,Q)u_k(Q)\, ds(Q) \qquad (3.2.1)$$

As a rough indication of the errors involved in the truncation we compare the contribution to the integral of a portion of the surface of area Λ near P and of another portion having equal area far from P. We use the inequality

$$I_u \leq \int_\Lambda |T_{jk}| . |u_k| . |ds|$$

and note that at distances from P greater than unity the dominant part of $|T_{jk}|$ is proportional to 1/R. Also the displacement $|u_k|$ decreases with distance away from P, as may be concluded from the works of Lamb (1904). If $I_u^{(1)}$ is the value of the integral near P and $I_u^{(2)}$ the value far from P, a rough estimate of the error may be indicated by the ratio, ignoring the variation of $|u_k|$,

$$I_u^{(2)} / I_u^{(1)} \simeq (1/R_2)/(1/R_1) = R_1/R_2$$

This ratio merely compares the contribution of the area Λ to the displacement at P for near and distant positions of Λ. This error analysis, even though very approximate, does point to the fact that if a second foundation was placed near the one at the shaded area of fig.3.2, the interaction

would be greater when the bodies are closer together than when they are farther apart. Warburton, Richardson and Webster (1971) found that the disturbance of the second (circular) foundation caused by the first increased by from 50 to 100 per cent as the bodies were brought closer together from a distance apart of 30 cylinder radii to 10.

The foregoing is true for the two-dimensional problem as it is for the three-dimensional, the only alterations required being formal mathematical adjustments. In that case the region of integration is simply the solid straight line portion of the semi-circle shown in fig.3.1 (strictly speaking the region of integration is a rectangular infinite strip of unit width into the paper). The circle C of fig.3.2 to which we have truncated our integration will in this case be a straight line of length R_c on both sides of the origin.

It is expected that accuracy will improve with increasing values of R_c. By solving the given foundation problem for various values of R_c, one can observe when results have converged to a suitable accuracy compared to published works.

3.3 GENERAL APPROACH TO THE NUMERICAL SOLUTION OF THE BIE

After establishing the governing boundary integral equation, eq.(2.5.10) or (2.5.13), for steady state elastodynamics the numerical solution may now follow very much the same approach as for elastostatics, see Brebbia (1978), Latchat and Watson

(1975). In this section we outline the general numerical method of solution of the boundary integral equation for two- and three-dimensional problems. The solutions to problems described in the next chapters are based on the descriptions in this section.

Typically solutions are required for the displacements or stresses at points on the surface S of an elastic body D, given the stresses or displacements at portions of the boundary. The boundary integral equation(3.1.3) reduces to an algebraic system of equations by discretising the boundary data. In this way the boundary is assumed to be divided into finite elements. If there are L such elements then the discretised form of the integral equation is

$$c_{jk}u_k(P) + \sum_{\ell=1}^{L} \int_{S_\ell} T_{jk}(P,Q)u_k(Q)\ ds(Q)$$

$$= \sum_{\ell=1}^{L} \int_{S_\ell} U_{jk}(P,Q)t_k(Q)\ ds(Q) \qquad (3.3.1)$$

The integral sign with subscript S_ℓ indicates integration over a given element ℓ. The numerical implementation is characterised principally by the manner in which the boundary S is represented, and by what assumptions are made about the variation of displacements $u_k(Q)$ and stresses $t_k(Q)$ over each element.

Two-Dimensional Problems:-

The boundary in this case is a plane curve and the L elements are line segments. On the line element we introduce local coordinate ξ which varies from -1 to +1 over the element, fig.3.3.

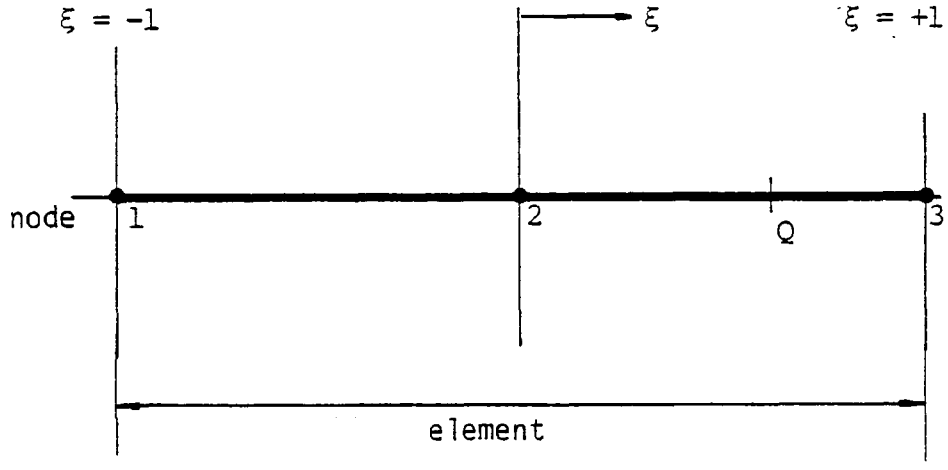

Fig 3.3 Boundary Element For Two-Dimensional Problem

The variation of u_k and t_k over the element is selected in some suitable way. We use quadratic variation in this study, i.e., the values of $u_k(Q)$, and $t_k(Q)$ at some point Q on the element are interpolated from the values at the element nodes (three nodes for quadratic variation) as

$$u_k\{Q(\xi)\} = \sum_{n=1}^{3} M_n(\xi)(u_k)_n \qquad (3.3.2)$$

$$t_k\{Q(\xi)\} = \sum_{n=1}^{3} M_n(\xi)(t_k)_n$$

where $(u_k)_n$, and $(t_k)_n$, n=1,2,3 are the values of u_k and t_k at the three nodes of the element, and $M_n(\xi)$, n=1,2,3 are the quadratic shape functions given by

$$M_1(\xi) = \tfrac{1}{2}(\xi - 1)\xi$$

$$M_2(\xi) = 1 - \xi^2 \qquad (3.3.3)$$

$$M_3(\xi) = \tfrac{1}{2}(\xi + 1)\xi$$

The element of area ds(Q) is also expressed in terms of ξ through the Jacobian of transformation from ξ to x_1

$$ds(Q) = J(\xi)d\xi$$

$$J(\xi) = \left|\frac{dx_1}{d\xi}\right| \qquad (3.3.4)$$

Let the L elements of the boundary have a total of N nodes. For ease of computer coding a global numbering scheme for the nodes is constructed whereby the number of the (c)th node of element ℓ is denoted by $d(\ell,c)$. Introducing the

functional variations (3.3.2) into the discretised equation (3.3.1) we have the following algebraic equation for the (a)th node at which point P is located

$$\frac{1}{2}\, u_j(P^a) + \sum_{\ell=1}^{L} \sum_{c=1}^{3} u_k\{d(\ell,c)\} \cdot \int_{S_\ell} T_{jk}\left(P^a, Q(\xi)\right) M_c(\xi) J(\xi)\, d\xi$$

$$= \sum_{\ell=1}^{L} \sum_{c=1}^{3} t_k\{d(\ell,c)\} \cdot \int_{S_\ell} U_{jk}\left(P^a, Q(\xi)\right) M_c(\xi) J(\xi)\, d\xi$$

$$j,k = 1,2 \qquad (3.3.5)$$

where we have made use of the fact that on the smooth boundary involved in our problem $c_{jk} = \frac{1}{2}\delta_{jk}$. If the equation is written for every position of point P along the boundary nodes, the resulting system of equations may be written in the form

$$\left[A_1\right]\left\{u\right\} = \left[A_2\right]\left\{t\right\} \qquad (3.3.6)$$

in which the unknowns are the nodal values of u_k and t_k. There are 2N equations for the 4N nodal point values of displacements and tractions, half of which are known in a well posed problem.

Since R(P,Q) is measured from P, when P coincides with one of the nodes of the integration element ℓ the integrals become singular at P. The appropriate steps taken to treat the singularities (similar to those in elastostatics problems)

are discussed in the chapters (4 and 5) where the foundation problems are analysed.

Three-dimensional Problems:-

The boundary is a surface and the L elements are area elements. We shall use quadrilateral elements which we may allow to have curved boundaries. On each element we introduce local coordinates ξ_1, and ξ_2, each varying from -1 to +1, fig.3.4

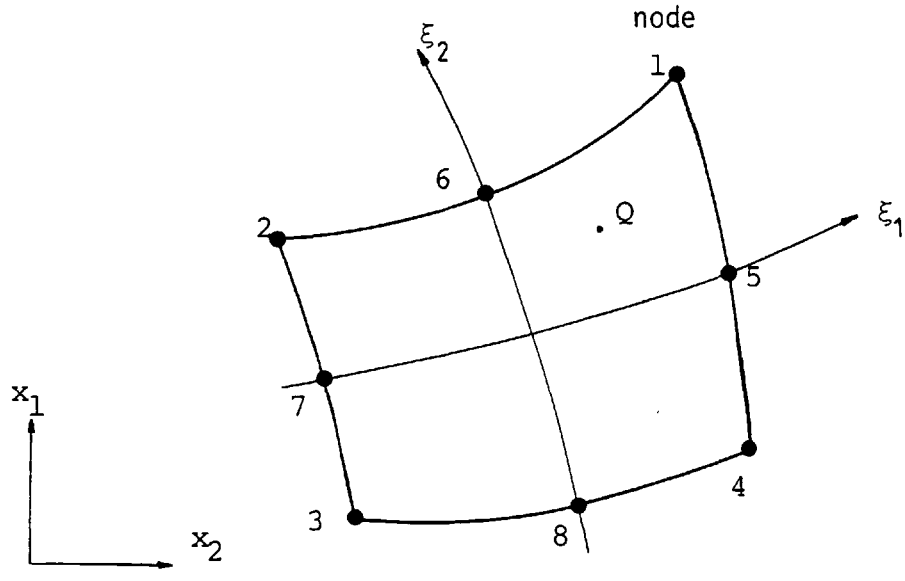

Fig 3.4 Boundary Element For Three-Dimensional Problem

Quadratic shape functions shall be used here also to interpolate variables at any given point Q on the element. In this two-dimensional element, eight nodes are required. Thus the coordinates x_j of point Q are determined in terms of the local coordinates ξ_1, ξ_2 by

$$x_j\{Q(\xi_1,\xi_2)\} = \sum_{n=1}^{8} M_n(\xi_1,\xi_2)(x_j)_n \qquad (3.3.7)$$

where $(x_j)_n$, n=1,2,...,8, are the coordinates of the eight nodes of the elements, $M_n(\xi)$, n=1,2,...,8 are the shape functions given below. By experience from the elastostatics problems, Lachat (1975), these interpolation scheme adequately models the curved boundaries of the element. The displacements and stresses are similarly interpolated

$$u_k\{Q(\xi_1,\xi_2)\} = \sum_{n=1}^{8} M_n(\xi_1,\xi_2)(u_k)_n \qquad (3.3.8)$$

$$t_k\{Q(\xi_1,\xi_2)\} = \sum_{n=1}^{8} M_n(\xi_1,\xi_2)(t_k)_n$$

The shape functions are

$$M_1(\xi_1,\xi_2) = \tfrac{1}{4}(\xi_1 + 1)(\xi_2 + 1)(\xi_1 + \xi_2 - 1)$$

$$M_2(\xi_1,\xi_2) = \tfrac{1}{4}(1 - \xi_1)(\xi_2 + 1)(\xi_2 - \xi_1 - 1)$$

$$M_3(\xi_1,\xi_2) = \tfrac{1}{4}(1 - \xi_1)(1 - \xi_2)(-\xi_1 - \xi_2 - 1)$$

$$M_4(\xi_1,\xi_2) = \tfrac{1}{4}(1 + \xi_1)(1 - \xi_2)(\xi_1 - \xi_2 - 1)$$

$$M_5(\xi_1,\xi_2) = \tfrac{1}{2}(1 + \xi_1)(1 - \xi_2^2) \qquad (3.3.9)$$

$$M_6(\xi_1,\xi_2) = \tfrac{1}{2}(\xi_2 + 1)(1 - \xi_1^2)$$

$$M_7(\xi_1,\xi_2) = \tfrac{1}{2}(1 - \xi_1)(1 - \xi_2^2)$$

$$M_8(\xi_1,\xi_2) = \tfrac{1}{2}(1 - \xi_2)(1 - \xi_1^2)$$

The element of area ds(Q) is expressed in terms of ξ_1, ξ_2 through the Jacobian of transformation from $\underline{\xi}$ to $\underline{x}$

$$ds(Q) = J(\xi_1,\xi_2)\, d\xi_1 d\xi_2$$

where $J(\underline{\xi})$ is the Jacobian given by the modulus of the vector product

$$S_{jk} = \frac{\partial x_j}{\partial \xi_k} = \frac{\partial M_n}{\partial \xi_k}(x_j)_n, \quad \text{sum on } n$$

$$\{j \in (1,2,3)\},\ k \in (1,2)$$

Introducing the functional variation (3.3.8) into the discretised boundary integral equation (3,3,1) gives the result

$$\tfrac{1}{2} u_j(P^a) + \sum_{\ell=1}^{L}\sum_{c=1}^{8} u_k\{d(\ell,c)\} \cdot \int_{S_\ell} T_{jk}\left(P^a, Q(\xi_1,\xi_2)\right) M_c(\xi_1,\xi_2) J(\xi_1,\xi_2) d\xi_1 d\xi_2$$

$$= \sum_{\ell=1}^{L}\sum_{c=1}^{8} t_k\{d(\ell,c)\} \cdot \int_{S_\ell} U_{jk}\left(P^a, Q(\xi_1,\xi_2)\right) M_c(\xi_1,\xi_2) J(\xi_1,\xi_2) d\xi_1 d\xi_2 \qquad (3.3.10)$$

Writing the equation for every position of the point P along the boundary nodes gives the algebraic system of equations

$$\left[B_1\right]\{u\} = \left[B_2\right]\{t\} \qquad (3.3.11)$$

in which the unknowns are the nodal values of u_k and t_k. There are 3N equations for the 6N nodal point values of displacements and tractions, half of which are known for a well posed problem.

Once the system of equations (3.3.6) or (3.3.11) is set up the boundary conditions of the problem are applied by rearranging the elements of the two matrices in order to have the unknowns on the left and the known on the right hand side. In the next chapter the vibrations of a rigid infinite strip is analysed. The following chapter is devoted to the vibration of foundations of finite arbitrary shape.

chapter 4

VIBRATION OF A RIGID INFINITELY LONG RECTANGULAR FOUNDATION ON AN ELASTIC HALF SPACE

4.1 INTRODUCTION

In this chapter we apply the two-dimensional form of the boundary integral equation (2.5.10) to analyse the vibration of a rigid rectangular strip of infinite length on the elastic half space. Some of the already known results are reproduced but the emphasis is on the flexibility and convenience of the method in handling different types of boundary conditions - frictionless and welded contact - as well as coupled modes of vibration. Of particular interest is the solution for the unrestricted (three degrees-of-freedom) motion of the infinite strip, namely coupled vertical, horizontal and rocking vibration, which has not been mentioned in the literature before now.

4.2 PROBLEM DEFINITION

Fig.4.1 below depicts the coordinate system x_1, x_2, x_3, and significant dimensions. The infinite length of the body runs along the x_3-axis, and the isotropic elastic half space occupies the region $x_2 \geq 0$. Since the strip is assumed rigid the displacements are assumed not to vary along the x_3-axis, so we have plane strain elasticity problem. It is therefore sufficient to consider a unit length of the body along the x_3-axis. The height is taken infinitesimally small.

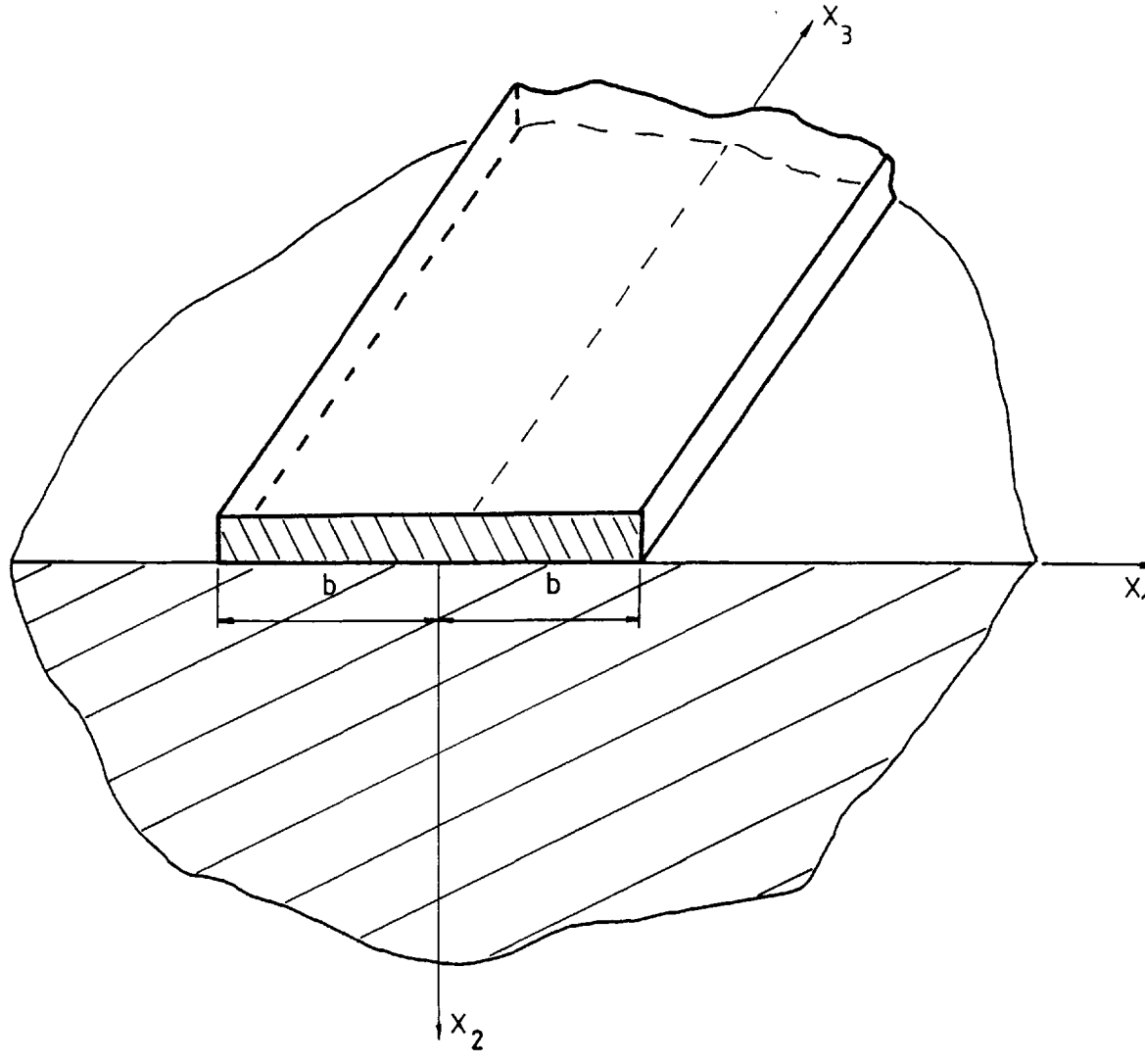

Fig.4.1 The Coordinate Axes

For the contact between the rigid body and the half space, we define two sets of conditions

Relaxed Contact Conditions:-

In the literature the following conditions are at times prescribed at the contact surface in order to relax the completely mixed boundary-value problem for convenience, as

observed in section 1.1, chapter 1. These conditions effectively decouple the modes of vibration.

(i) Vertical Vibration:- Zero shear stress t_1

(11) Horizontal Vibration:- Zero normal stress t_2

(iii) Rocking Vibration:- Zero shear stress t_1

Welded Contact Conditions:-

By this we mean the attachment in which there is complete continuity between the displacements and stresses of the footing and underlying half space in the area of contact. These conditions ensure no slip between the foundation and the half space and leave the modes coupled.

In practice it is reasonable to expect the actual conditions to be somewhere between these two extremes. However for the coupled modes of vibration the welded contact conditions prevail.

In order to apply the boundary integral method to solve this problem it will be necessary to first identify all the displacements and stresses (as knowns or as unknowns) induced on the surface of the half space by the various modes of vibration of the rigid body. For each mode the effective dynamic stiffness of the supporting medium is computed as for a massless foundation, from which the response of a foundation of a given mass is obtained.

First the following notation shall be adopted.

For a Massless Body,

the motion:-

V_1 is translation in x_1-direction

V_2, translation in x_2-direction

Θ_3, rocking about x_3-axis

$V_3 \equiv b\Theta_3$, our definition,

The applied forces per unit length of body:-

Q_1 is force applied in x_1-direction

Q_2, force applied in x_2-direction

M_3, couple applied about x_3-axis

$Q_3 \equiv M_3/b$, our definition.

It is noted that since above definitions are for a massless body, the forces Q_j, $j=1,2,3$, may be taken to correspond to the reactions of the supporting medium on the body.

Now For a Massive Body,

the motions and applied forces are modified by the inertia properties of the body.

The motion:-

W_1 is translation in x_1 - direction

W_2, translation in x_2-direction,

Θ_3, rocking about x_3-axis,

$W_3 \equiv b\Theta_3$, our difinition.

The exciting forces per unit length of body:-

F_1 is force applied in x_1-direction,

F_2, force applied in x_2-direction,

Υ_3, couple applied about the x_3-axis,

$F_3 \equiv \Upsilon_3/b$, our difinition.

These quantities are generally complex. Where the modulus is implied it will be convenient to use the same symbols. With these difinitions we have, for example, the equation of vertical motion of a body of mass m_{22} per unit length supported on the half space is, see fig.4.1a below

$$-\omega^2 m_{22} W_2 + Q_2 = F_2$$

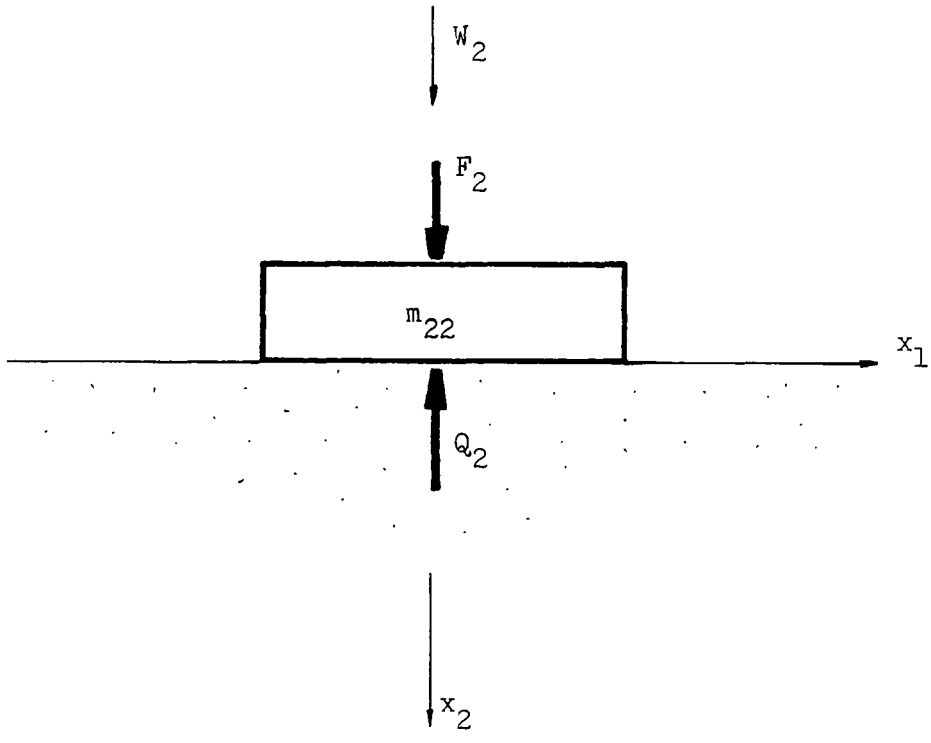

Fig 4.1a Forces on Massive Foundation

To determine, say, the vertical stiffness of the supporting medium, it is sufficient to consider a massless body, give it a known displacement V_2, compute the force (stress integral) Q_2, fig.4.1b below, and find tne ratio K_2 of Q_2 to V_2. The "compliance" is defined as the inverse of the stiffness.

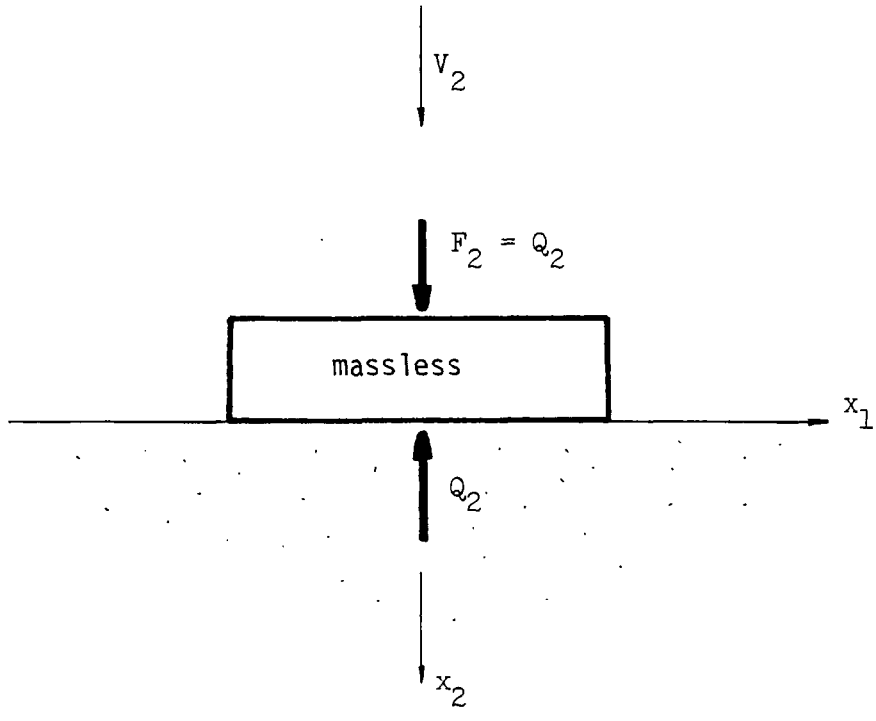

Fig 4.1b Forces on Massless Foundation

Once K_2 is determined the equation of motion of the massive body in fig.4.1a becomes

$$- \omega^2 m_{22} W_2 + K_2 W_2 = F_2$$

This is actually the so-called "impedance matching" technique.

4.3 BOUNDARY CONDITIONS IMPOSED BY THE MODES OF VIBRATION.

(i) The General Three Degrees-Of-Freedom

V_1, V_2 represent the translation of the massless rigid body in the x_1, x_2 directions while θ_3 represent the rotation (in radian measure) about x_3-axis. $V_3 = b\theta_3$. Thus the three degrees-of-freedom are described by V_1, V_2, and V_3. Considering that the body remains rigid during motion, the displacements induced on the contact area are, assuming small quantities,

$$u_1 = V_1$$

$$u_2 = V_2 + x_1\theta_3 \qquad (4.3.1)$$

The stresses on the other hand are unknown

$$t_1 = \text{unknown}, \quad |x_1| \leq b$$

$$t_2 = \text{unknown}, \quad |x_1| \leq b \qquad (4.3.1b)$$

The stresses and displacements are taken positive in the positive directions of the respective axes. The following stress integrals are defined

$$Q_1 = \int_{-b}^{+b} t_1 \, ds$$

$$Q_2 = \int_{-b}^{+b} t_2 \, ds \qquad (4.3.2)$$

$$Q_3 = \int_{-b}^{+b} (x_1 \, t_2/b) \, ds$$

$M_3 = bQ_3$ is actually a couple about x_3-axis due to the stress distribution t_2 in the contact surface. Since a unit length of body is being considered,

$$ds = dx_1$$

The harmonic time factor $e^{i\omega t}$ is being omitted in the foregoing development.

Let F be some reference force in units of force/length, m the mass per unit length of the rigid body, and $\bar{J}_o$ the mass polar inertia per unit length about the axis of rocking. These inertia properties of the body in the directions of motion will be denoted by m_{jj} where

$$m_{jj} = m, \quad j=1,2$$

$$m_{33} = \bar{J}_o/b^2$$

It is convenient to introduce the following dimensionless forms

$$\bar{u}_k = \pi\mu u_k/F$$

$$\bar{t}_k = \pi b t_k/F$$

$$\bar{V}_k = \pi\mu V_k/F$$

$$\bar{Q}_k = Q_k/F$$

$$\bar{x}_k = x_k/b$$

$$\bar{s} = s/b$$

$$\bar{m}_{jj} = m_{jj}/\rho b^2, \quad j = 1,2,3$$

$$\bar{w}_k = \pi\mu w_k/F \qquad (4.3.3)$$

$$\eta_1 = b\omega/c_1$$

$$\eta_2 = b\omega/c_2$$

The stress integrals in eqs.(4.3.2) become

$$\bar{Q}_1 = \frac{1}{\pi}\int_{-1}^{+1} \bar{t}_1 \, d\bar{s}$$

$$\bar{Q}_2 = \frac{1}{\pi}\int_{-1}^{+1} \bar{t}_2 \, d\bar{s} \qquad (4.3.4)$$

$$\bar{Q}_3 = \frac{1}{\pi}\int_{-1}^{+1} \bar{x}_1 \, \bar{t}_2 \, d\bar{s}$$

The equivalent dynamic stiffness (direct and coupled) of the supporting elastic half space are defined by

$$K_{jk} = \frac{Q_j}{\pi\mu V_k} = \frac{\bar{Q}_j}{\bar{V}_k} \tag{4.3.5}$$

K_{jk} is the force in j-direction per unit displacement in k-direction. We have the force-displacement relation

$$\begin{bmatrix} K_{11} & K_{12} & K_{13} \\ K_{21} & K_{22} & K_{23} \\ K_{31} & K_{32} & K_{33} \end{bmatrix} \begin{Bmatrix} \bar{V}_1 \\ \bar{V}_2 \\ \bar{V}_3 \end{Bmatrix} = \begin{Bmatrix} \bar{Q}_1 \\ \bar{Q}_2 \\ \bar{Q}_3 \end{Bmatrix} \tag{4.3.6}$$

To analyse the vibration problem it is necessary to first solve for the dynamic stiffnesses K_{jk}. It is observed that K_{jk} is a property of the supporting elastic medium and a function only of frequency and geometry of the loaded surface. Therefore to compute K_{jk} it is sufficient to prescribe any convenient values for motions $\bar{V}_n$ (n=1,2,3) of the body, compute the stress integral, and solve eq.(4.3.6) above for K_{jk}. However, having done this, we end up with three equations for the six unknown values K_{jk}. Therefore it is necessary to take three different sets of values for $\bar{V}_n$, namely $\bar{V}_n^{(m)}$ (m,n=1,2,3), compute the stress integrals $\bar{Q}_n^{(m)}$ in each case and then solve the following system of equations

$$\begin{bmatrix} \bar{V}_1^1 & \bar{V}_2^1 & \bar{V}_3^1 \\ \bar{V}_1^2 & \bar{V}_2^2 & \bar{V}_3^2 \\ \bar{V}_1^3 & \bar{V}_2^3 & \bar{V}_3^3 \end{bmatrix} \begin{Bmatrix} K_{j1} \\ K_{j2} \\ K_{j3} \end{Bmatrix} = \begin{Bmatrix} Q_j^1 \\ Q_j^2 \\ Q_j^3 \end{Bmatrix} \qquad (4.3.7)$$

$$j = 1,2,3$$

It is wise to select $\bar{V}_n^{(m)}$ such that the left matrix is not singular. Given an infinite strip with inertia properties m_{jj} (see eqs.(4.3.3)) the three degrees-of-freedom vibration of the body defined by $\bar{W}_1$, $\bar{W}_2$, and $\bar{W}_3$ are obtained by the usual matrix method of analysis

$$\left(-\frac{1}{\pi}\eta_2^2 \begin{bmatrix} \bar{m}_{11} & 0 & 0 \\ 0 & \bar{m}_{22} & 0 \\ 0 & 0 & \bar{m}_{33} \end{bmatrix} + \begin{bmatrix} K_{11} & K_{12} & K_{13} \\ K_{21} & K_{22} & K_{23} \\ K_{31} & K_{32} & K_{33} \end{bmatrix} \right) \begin{Bmatrix} \bar{W}_1 \\ \bar{W}_2 \\ \bar{W}_3 \end{Bmatrix} = \begin{Bmatrix} f_1 \\ f_2 \\ f_3 \end{Bmatrix} \qquad (4.3.8)$$

where F_j is the force (or moment) applied in the j-direction of motion. In indicial notation

$$\left\{ -\frac{1}{\pi}\eta_2^2 \bar{m}_{jk} + K_{jk} \right\} \bar{W}_k = f_j \qquad (4.3.9)$$

where $f_j = F_j/F$

(ii) Coupled Horizontal and Rocking Modes

The motion of the body is described by $\bar{V}_1$ and $\bar{V}_3$. The rigidness of the body requires that

$$\bar{u}_1 = \bar{V}_1, \quad |\bar{x}_1| \leq 1$$
$$\bar{u}_2 = \bar{x}_1 \bar{V}_3, \quad |\bar{x}_1| \leq 1 \qquad (4.3.10b)$$

$$\bar{t}_1 = \text{unknown}, \quad |\bar{x}_1| \leq 1$$
$$\bar{t}_2 = \text{unknown}, \quad |\bar{x}_1| \leq 1 \qquad (4.3.10b)$$

The force-displacement relations are

$$\begin{bmatrix} K_{11} & K_{13} \\ K_{31} & K_{33} \end{bmatrix} \begin{Bmatrix} \bar{V}_1 \\ \bar{V}_3 \end{Bmatrix} = \begin{Bmatrix} \bar{Q}_1 \\ \bar{Q}_3 \end{Bmatrix} \qquad (4.3.11)$$

Using two sets of displacements $\bar{V}_n^{(m)}$ we solve the following system for K_{jk}

$$\begin{bmatrix} \bar{V}_1^1 & \bar{V}_3^1 \\ \bar{V}_1^2 & \bar{V}_3^2 \end{bmatrix} \begin{Bmatrix} K_{j1} \\ K_{j3} \end{Bmatrix} = \begin{Bmatrix} \bar{Q}_j^1 \\ \bar{Q}_j^2 \end{Bmatrix} \qquad (4.3.12)$$

$$j = 1,3 \qquad (4.3.12)$$

The motions $\bar{W}_1$ and $\bar{W}_3$ of a body with inertia properties $\bar{m}_{11}$, $\bar{m}_{33}$ are determined by

$$\left(-\frac{1}{\pi} \eta_2^2 \begin{bmatrix} \bar{m}_{11} & 0 \\ 0 & \bar{m}_{33} \end{bmatrix} + \begin{bmatrix} K_{11} & K_{13} \\ K_{31} & K_{33} \end{bmatrix} \right) \begin{Bmatrix} \bar{W}_1 \\ \bar{W}_3 \end{Bmatrix} = \begin{Bmatrix} f_1 \\ f_3 \end{Bmatrix} \qquad (4.3.13)$$

(iii) Uncoupled Horizontal Vibration

The only motion of the body is $\bar{V}_1$

Relaxed Contact Conditions:-

At the contact area $|\bar{x}_1| \leq 1$

$$\begin{aligned} \bar{u}_1 &= \bar{V}_1 \\ \bar{u}_2 &= \text{unknown} \end{aligned} \tag{4.3.14}$$

$$\begin{aligned} \bar{t}_1 &= \text{unknown} \\ \bar{t}_2 &= 0 \end{aligned}$$

$\bar{V}_1 = 1$ is prescribed, and the dynamic stiffness is simply $K_{11} = \bar{Q}_1$, see eq.(3.3.4). The response $\bar{W}_1$ of a body of given mass ratio $\bar{m}_{11}$ is obtained from

$$(-\tfrac{1}{\pi}\eta_2^2\ \bar{m}_{11} + K_{11}) = f_1 \tag{4.3.16}$$

and $\bar{W}_1$ may be plotted against frequency factor η_2 for excitation $f_1 = 1$ and various mass ratios $\bar{m}_{11}$

(iv) Uncoupled Vertical Vibration:-

$\bar{V}_2$ is the only motion of the body and the contact conditions are

Relaxed Contact Conditions:-

For $|\bar{x}_1| \leq 1$

$$\begin{aligned} \bar{u}_1 &= \text{unknown} \\ \bar{u}_2 &= \bar{V}_2 \end{aligned} \tag{4.3.17}$$

$$\bar{t}_1 = 0$$

$$\bar{t}_2 = \text{unknown}$$

Welded Contact Conditions:-

$$\bar{u}_1 = 0$$

$$\bar{u}_2 = \bar{V}_2$$

(4.3.18)

$$\bar{t}_1 = \text{unknown}$$

$$\bar{t}_2 = \text{unknown}$$

$\bar{V}_2 = 1$ is prescribed, and the dynamic stiffness is $K_{22} = \bar{Q}_2$. The response $\bar{W}_2$ of a given body of mass ratio $\bar{m}_{22}$ is obtained from

$$(-\tfrac{1}{\pi}\eta_2^2\,\bar{m}_{22} + K_{22})\,\bar{W}_2 = f_2 \qquad (4.3.19)$$

for any desired excitation f_2

(v) Uncoupled Rocking Vibration

$\bar{V}_3$ is the only motion of the body

Relaxed Contact Conditions:-

For $|\bar{x}_1| \leq 1$

$$\bar{u}_1 = \text{unknown}$$

$$\bar{u}_2 = \bar{x}_1\bar{V}_3$$

(4.3.20)

$$\bar{t}_1 = 0$$

$$\bar{t}_2 = \text{unknown}$$

$\bar{V}_3 = 1$ is prescribed, and the dynamic stiffness is $K_{33} = \bar{Q}_3$. The (rocking) response $\bar{W}_3$ of a given body of inertia ratio $\bar{m}_{33}$ is obtained from

$$(-\tfrac{1}{\pi}\eta_2^2\,\bar{m}_{33} + K_{33})\bar{W}_3 = f \qquad (4.3.22)$$

In addition to the displacements and stresses mentioned above we note that on the free surface of the half space

$$\bar{u}_j = \text{unknown}, \qquad \bar{t}_j = 0, \qquad j=1,2 \qquad (4.3.23)$$

4.4 APPLYING THE BOUNDARY INTEGRAL EQUATION

In the previous section the displacements and stresses have been identified, either as knowns or as unknowns, at various points on the boundary of the elastic half space for the various modes of vibration of the rigid body. Now we recall the boundary integral equation (2.5.10) which establishes the constraint relation between these variables. The boundary S of the half space in this two-dimensional problem is the straight line

$$\bar{x}_2 = 0, \qquad -\infty < \bar{x}_1 < \infty$$

in the dimensionless coordinate system $\bar{x}_k$. The integral equation is written in the dimensionless form

$$c_{jk}\bar{u}_k(P) + \int_{\bar{S}} \bar{T}_{jk}(P,Q)\bar{u}_k(Q)\, d\bar{s}(Q)$$

$$= \int_{\bar{S}} \bar{U}_{jk}(P,Q)\bar{t}_k(Q)\, d\bar{s}(Q) \qquad (4.4.1)$$

in which we have introduced

$$\bar{T}_{jk} = bT_{jk}, \quad \bar{U}_{jk} = U_{jk} \tag{4.4.2}$$

Expressions for U_{jk} and T_{jk} on the Half Space Boundary

On the boundary of the half space, fig.(4.2), the expressions for the fundamental tensors U_{jk} and T_{jk}, eqs.(2.4.4) and (2.4.5) take simpler forms.

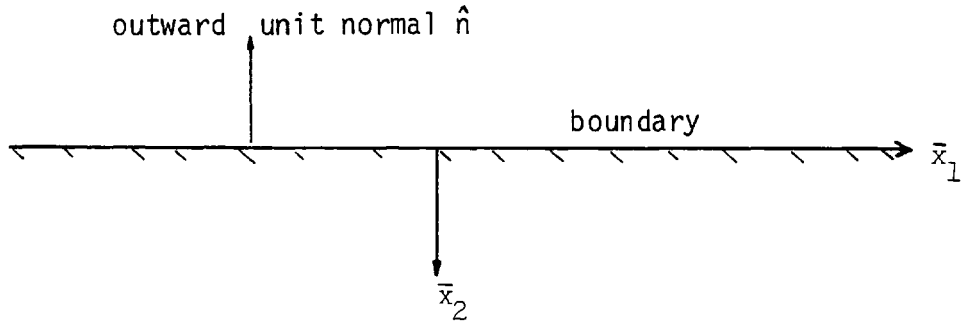

Fig.4.2 Half Space Boundary

The outward unit normal $\hat{n}$ has, at any point on the boundary, the components

$$n_1 = 0 \quad n_2 = -1$$

The distance $\bar{R}(P,Q)$ between two points $P(\bar{y}_1,\bar{y}_2)$ and $Q(\bar{x}_1,\bar{x}_2)$ on the boundary is

$$\bar{R} = \left((\bar{x}_1 - \bar{y}_1)^2 + (\bar{x}_2 - \bar{y}_2)^2 \right)^{1/2}$$

Since $\bar{x}_2 = 0$ on the boundary we have

$$\frac{\partial \bar{R}}{\partial \bar{x}_2} = 0$$

$$\frac{\partial \bar{R}}{\partial \bar{x}_1} = \frac{\bar{x}_1 - \bar{y}_1}{\left| \bar{x}_1 - \bar{y}_1 \right|} \equiv \text{(sign)}$$

Also $\frac{\partial \bar{R}}{\partial n} = 0$

We substitute these results into expressions for U_{jk} and T_{jk}, eqs.(2.4.4) and (2.4.5) and introduce the barred forms of U_{jk} and T_{jk} given by eqs.(4.4.2). Writing out the elements constituting the two tensors we obtain

$$\bar{U}_{jk} = \begin{bmatrix} \bar{U}_{11} & 0 \\ 0 & \bar{U}_{22} \end{bmatrix}$$

$$\bar{T}_{jk} = \begin{bmatrix} 0 & \bar{T}_{12} \\ \bar{T}_{21} & 0 \end{bmatrix} \qquad (4.4.3)$$

where

$$\bar{U}_{11} = \frac{i}{4} (\Psi + \chi)$$

$$\bar{U}_{22} = \frac{i}{4} \Psi$$

$$\bar{T}_{12} = -\frac{i}{4} \text{(sign)} \bar{A}_4 \qquad (4.4.4)$$

$$\bar{T}_{21} = -\frac{i}{4}\,(\text{sign})\,\bar{A}_3$$

The functions Ψ, χ, A_3 and A_4 have been defined for eqs.(2.4. 4) and (2.4. 5).

$$\Psi = H_o(\eta_2\bar{R}) + \frac{1}{\eta_2\bar{R}}\left\{\frac{c_2}{c_1}H_1(\eta_1\bar{R}) - H_1(\eta_2\bar{R})\right\}$$

$$\chi = \frac{c_2^2}{c_1^2}H_2(\eta_1\bar{R}) - H_2(\eta_2\bar{R})$$

$$\bar{A}_3 = -\eta_2 H_1(\eta_2\bar{R}) + 2\frac{\chi}{\bar{R}} \qquad (4.4.5)$$

$$\bar{A}_4 = -(1 - 2\frac{c_2^2}{c_1^2})\,\eta_1 H_1(\eta_1\bar{R}) - 2\frac{\chi}{\bar{R}}$$

The following notations have been introduced in the above equations

$$\bar{A}_j = bA_j$$

$$\bar{R} = R/b$$

$$\eta_1 = bk_1 = b\omega/c_1$$

$$\eta_2 = bk_2 = b\omega/c_2, \quad \text{frequency factor}$$

$$k_j R = bk_j R/b = \eta_j \bar{R}$$

The Boundary Elements

The half space boundary is represented by a finite number of straight line elements to cover the region to which the BIE integrals have been truncated, fig.(4.3)

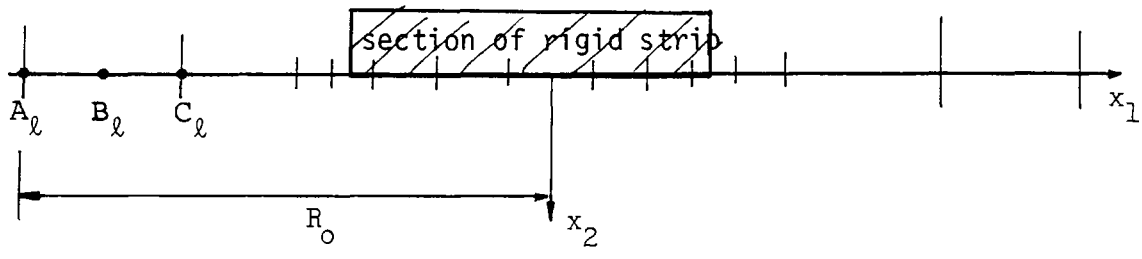

Fig.4.3 The Boundary Elements

Small elements are concentrated in and near the loaded region where functions are expected to vary more rapidly. Still smaller elements are located near the ends of the loaded region where variation is most rapid.

Quadratic variation of $\bar{u}_k$ and $\bar{t}_k$ is assumed over a given element ℓ, as discussed in chapter 3. The three nodes of the element are labelled A_ℓ, B_ℓ and C_ℓ, see fig.(4.3). The discretised boundary equation (3.3.5) may be written in the expanded form, employing the dimensionless quantities of eq.(4.4.2)

$$\frac{1}{2}\,\bar{u}_j(P^a) + \sum_{\ell=1}^{L}\left(\bar{u}_k(A_\ell)\int_{\bar{S}_\ell}\bar{T}_{jk}\left\{P^a,Q(\xi)\right\}\,M_A\,(\xi)J(\xi)\quad d\xi\right.$$

$$+\quad \bar{u}_k(B_\ell)\int_{\bar{S}_\ell}\bar{T}_{jk}\left\{P^a,Q(\xi)\right\}\,M_B(\xi)J(\xi)\quad d\xi$$

$$\left.+\quad \bar{u}_k(C_\ell)\int_{\bar{S}_\ell}\bar{T}_{jk}\left\{P^a,Q(\xi)\right\}\,M_C(\xi)J(\xi)\quad d\xi\right)$$

$$=\quad \sum_{\ell=1}^{L}\left(\bar{t}_k(A_\ell)\int_{\bar{S}_\ell}\bar{U}_{jk}\left\{P^a,Q(\xi)\right\}\,M_A(\xi)J(\xi)\quad d\xi\right.$$

$$+\quad \bar{t}_k(B_\ell)\int_{\bar{S}_\ell}\bar{U}_{jk}\left\{P^a,Q(\xi)\right\}\,M_B(\xi)J(\xi)\quad d\xi$$

$$\left.+\quad \bar{t}_k(C_\ell)\int_{\bar{S}_\ell}\bar{U}_{jk}\left\{P^a,Q(\xi)\right\}\,M_C(\xi)J(\xi)\quad d\xi\right)$$

$$j,k = 1,2 \qquad (4.4.6)$$

In this case $J(\xi) = h_\ell$ where h_ℓ is half the length of

element ℓ . Writing this equation for every nodal position of P gives the system of algebraic equations mentioned in eq.(3.3.6). We observe that the coefficients of the nodal values of $\bar{u}_k$ and $\bar{t}_k$ are integrals of the kernel-shape functions over the element ℓ . We now give details of the integration scheme with attention to the singularity at P when it occurs in the element.

4.5 NUMERICAL INTEGRATION SCHEME

The numerical integration scheme employed is the Gauss-Legendre n-point quadrature whereby the integral of a function $f(\xi)$ is approximated by

$$\int_{-1}^{+1} f(\xi)d\xi \simeq \sum_{j=1}^{n} f(\xi_j)w_j \qquad (4.5.1)$$

where w_j are the weights and ξ_j the abscissae for the n-point formula. The following cases which may arise during integration over a chosen element ℓ are considered one by one

(i) Point P Not in Element

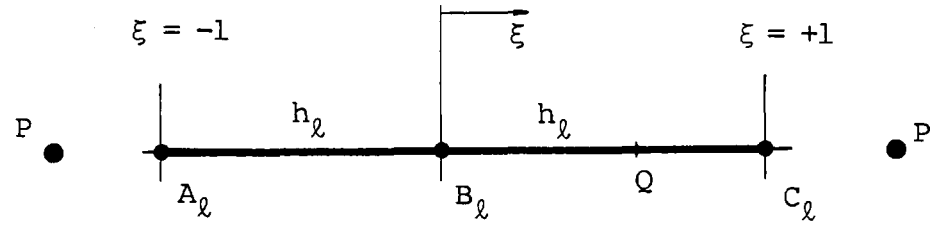

Fig 4.4 Point P Outside Integration Element ℓ

The coordinate at a point Q is

$$\bar{x}_{1Q} = \bar{x}_1(B_\ell) + \xi_Q h_\ell \qquad (4.5.2)$$

and $\bar{R}(P,Q) = |\bar{x}_{1Q} - \bar{x}_{1P}|$

There is no singularity of the integrands on the element. So all the integrands appearing in eq.(4.4.6) are evaluated easily, thus allowing the integration to proceed smoothly using the Gauss-Legendre scheme (4.5.1) above.

(ii) Point P at Node A

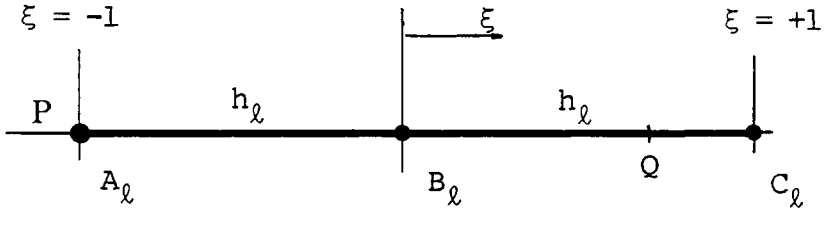

Fig 4.5 Point P at Node A

$\bar{x}_{1Q}$ and $\bar{R}(P,Q)$ are evaluated as in eqs.(4.5.2). As the integration point Q ranges over the element from A_ℓ to C_ℓ it coincides with P at A_ℓ, where $\bar{R}(P,Q) = 0$ and the kernel tensors $\bar{T}_{jk}(P,Q)$ and $\bar{U}_{jk}(P,Q)$ become singular. As observed in section 2.5 chapter 2, the singularities of $\bar{T}_{jk}$ and $\bar{U}_{jk}$ are of order O(1/R) and O(lnR) respectively. But from the shape functions $M_r(\xi)$ in eq.(3.3.3) we observe that $M_B(\xi)$ and $M_C(\xi)$ behave as O(R) as node A_ℓ is approached. Hence the products to be integrated for nodes B and C, namely $\bar{T}_{jk}M_r(\xi)J(\xi)$ and $\bar{U}_{jk}M_r(\xi)J(\xi)$, r=B,C, tend to a finite limit at A_ℓ, and so may reasonably be approximated by a polynomial over the element. The quadrature scheme eq.(4.5.1) thus applies for the coefficients at nodes B_ℓ and C_ℓ.

As for node A_ℓ the shape function $M_A(\xi)$ tends to unity at P and the integrands $\bar{T}_{jk}M_A(\xi)J(\xi)$, and $\bar{U}_{jk}M_A(\xi)J(\xi)$ remain singular. Since the singularity of $\bar{U}_{jk}$ is only logarithmic, its integral exists and can be evaluated with a quadrature scheme with logarithmic weight function. On a closer observation of the functions that make up $\bar{U}_{jk}$, see eqs.(4.4.4) and (4.4.5), the only quantity that gives rise to the logarithmic singularity is the Bessel function of the second kind $Y_o(\eta_2 R)$. So in our numerical scheme we treat all the other functions by the Gauss-Legendre scheme described above and use the following scheme

$$\int_0^1 f(\xi)\ln(\xi)\,d\xi = \sum_{j=1}^{n} f(\xi_j)b_j \qquad (4.5.2)$$

for the function $Y_o(\eta_2\bar{R})$ in the form

$$\int_o^1 \left(\left\{ Y_o\{\eta_2\bar{R}(\zeta)\}\ M_A\{\xi(\zeta)\}\ J\{\xi(\zeta)\}\ H(\zeta)\ \ln(\zeta) \right\} / \ln(\zeta) \right) d\zeta$$

$$\simeq \sum_{j=1}^{n} \left\{ \bullet \right\}_{\zeta_j} . b_j \qquad (4.5.3)$$

To this end we introduce another set of coordinates ζ as in following sketch

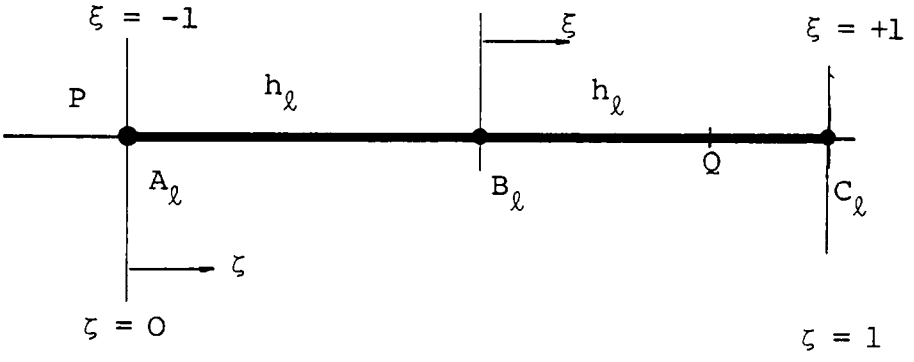

Fig 4.6 New Coordinates ζ

in which

$$\xi = -1 + 2\zeta$$

In the scheme (4.5.3) $H(\zeta)$ is the Jacobian of transformation from ξ to ζ

$$H(\zeta) = \left| \frac{\partial \xi}{\partial \zeta} \right|$$

and the special weights b_j may be obtained from Abramowitz

and Stegun (1972).

The integral containing $\bar{T}_{jk}M_A(\xi)J(\xi)$ over element ℓ alone does not exist but its principal value over the two elements on the two sides of node A exists. Since $\bar{T}_{jk}$ is anti-symmetric with respect to node A and the shape functions at A (namely M_A for element ℓ and M_C for previous element ℓ-1) are symmetric with respect to node A, the principal value is zero if the elements on both sides of A are of equal length. We shall generally ignore this value in our scheme since adjacent elements are nearly of equal length.

(iii) Point P at node C

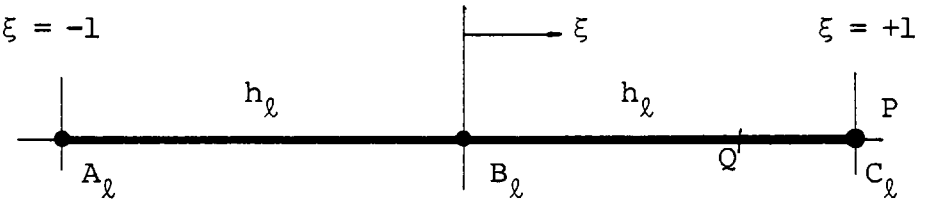

Fig 4.7 Point P at Node C

The integration is very similar to that described in above paragraph. In this case, however, the singularities are at node C. The integral coefficients for nodes A and B are evaluated ordinarily using the Gauss-Legendre scheme. The Bessel function $Y_o(\eta_2\bar{R})$ is evaluated using the scheme (4.5.3)

for node C, with the adjustment that the ζ-coordinate is defined thus

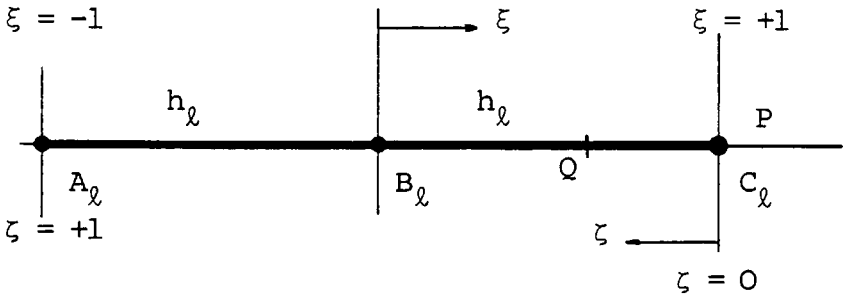

$$\xi = 1 - 2\zeta$$

Fig 4.8 New Coordinates ζ

(iv) Point P at Middle Node B

In this case it will be useful to subdivide the element into two subelements.

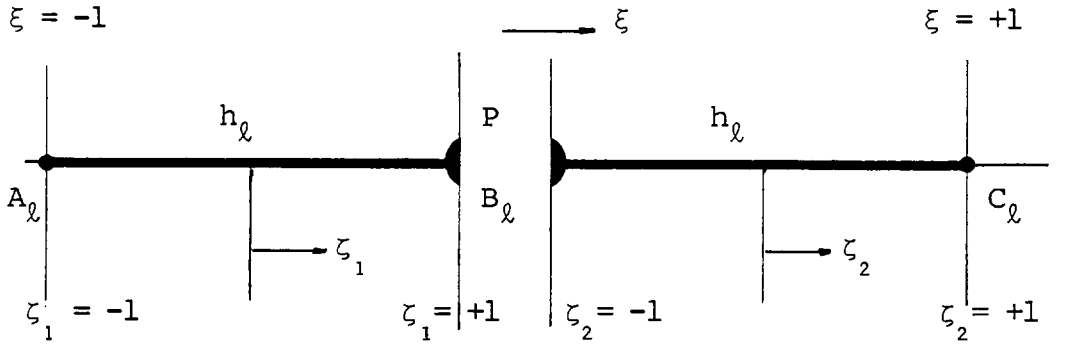

$$\xi = -\frac{1}{2} + \frac{1}{2}\zeta_1 \qquad \xi = \frac{1}{2} + \frac{1}{2}\zeta_2$$

subelement (1) subelement (2)

Fig 4.9 Element Subdivision

Over the jth subelement local coordinates ζ_j are introduced. The relationship between ζ_j and ξ are shown in the diagram and the Jacobian of transformation from ξ to ζ_j is introduced into the integrals. Thus, for example, over the first subelement,

$$\int_{-1}^{0} f(\xi)d\xi = \int_{-1}^{+1} f\{\xi(\zeta_1)\}\left|\frac{\partial \xi}{\partial \zeta_1}\right| d\zeta_1 \qquad (4.5.4)$$

The integration over each subelement becomes similar to the cases of P coinciding with an end node, paragraphs (ii) and (iii) above.

It is useful to observe that since the integrands are oscillatory, more particularly at higher frequencies, greater number of integration points (n) will be required over an element than is commonly used in elastostatics where the integrands vary less rapidly. However this does not constitute any setback here because variation over small elements can be adequately handled with few integration points for the range of interest of the frequency factor η_2 - up to 4. n=4 is found to be good for small elements and n=8,12 for the larger ones.

4.6 APPLYING THE BOUNDARY CONDITIONS TO THE ALGEBRAIC EQUATIONS

After the integration described in the previous section the resulting 2N algebraic equations are of the form

$$[A_1]\{u\} = [A_2]\{t\} \tag{4.6.1}$$

The matrices written in expanded form are

$$\begin{bmatrix} \begin{bmatrix} a^{(1)}_{11} \end{bmatrix} & \begin{bmatrix} a^{(1)}_{12} \end{bmatrix} & \begin{bmatrix} a^{(1)}_{13} \end{bmatrix} & \cdots & \begin{bmatrix} a^{(1)}_{1N} \end{bmatrix} \\ \cdots & \cdots & \cdots & \cdots & \cdots \\ \cdots & \cdots & \begin{bmatrix} a^{(1)}_{mn} \end{bmatrix} & \cdots & \cdots \\ \cdots & \cdots & \cdots & \cdots & \cdots \\ \begin{bmatrix} a^{(1)}_{N1} \end{bmatrix} & \begin{bmatrix} a^{(1)}_{N2} \end{bmatrix} & \begin{bmatrix} a^{(1)}_{N3} \end{bmatrix} & \cdots & \begin{bmatrix} a^{(1)}_{NN} \end{bmatrix} \end{bmatrix} \begin{Bmatrix} \begin{bmatrix} \bar{u}_1 \\ \bar{u}_2 \end{bmatrix}_1 \\ \cdots \\ \begin{bmatrix} \bar{u}_1 \\ \bar{u}_2 \end{bmatrix}_m \\ \cdots \\ \begin{bmatrix} \bar{u}_1 \\ \bar{u}_2 \end{bmatrix}_N \end{Bmatrix}$$

$$= \begin{bmatrix} \begin{bmatrix} a^{(2)}_{11} \end{bmatrix} & \begin{bmatrix} a^{(2)}_{12} \end{bmatrix} & \begin{bmatrix} a^{(2)}_{13} \end{bmatrix} & \cdots & \begin{bmatrix} a^{(2)}_{1N} \end{bmatrix} \\ \cdots & \cdots & \cdots & \cdots & \cdots \\ \cdots & \cdots & \begin{bmatrix} a^{(2)}_{mn} \end{bmatrix} & \cdots & \cdots \\ \cdots & \cdots & \cdots & \cdots & \cdots \\ \begin{bmatrix} a^{(2)}_{N1} \end{bmatrix} & \begin{bmatrix} a^{(2)}_{N2} \end{bmatrix} & \begin{bmatrix} a^{(2)}_{N3} \end{bmatrix} & \cdots & \begin{bmatrix} a^{(2)}_{NN} \end{bmatrix} \end{bmatrix} \begin{Bmatrix} \begin{bmatrix} \bar{t}_1 \\ \bar{t}_2 \end{bmatrix}_1 \\ \cdots \\ \begin{bmatrix} \bar{t}_1 \\ \bar{t}_2 \end{bmatrix}_m \\ \cdots \\ \begin{bmatrix} \bar{t}_1 \\ \bar{t}_2 \end{bmatrix}_N \end{Bmatrix} \tag{4.6.2}$$

The coefficient matrices A_1 and A_2 have been partitioned into 2x2 submatrices $a^{(1)}_{mn}$ and $a^{(2)}_{mn}$ respectively. $a^{(1)}_{mn}$ result from positioning P at node number m and calculating the integrals of the products of $\bar{T}_{jk}$ and the shape functions appropriate to node number n. $a^{(2)}_{mn}$ is a similar submatrix involving $\bar{U}_{jk}$ and nodes m and n. Once the system of equations (4.6.2) is set up it can be used to solve many steady state dynamic problems involving the half space in plane strain. As outlined in chapter 3, it is only necessary, after setting up the system of equations for a suitably designed boundary mesh, to shuffle or swap the elements of matrices A_1 and A_2 in order to have all known terms on the right and the unknowns on the left hand side of the system. The final system, now of the form

$$\left[A\right]\left\{z\right\} = \left\{B\right\} \tag{4.6.3}$$

is then solved by routine methods for the set of unknowns $\{z\}$, which may consist entirely of displacements, or stresses or of both, according to boundary data available.

The system of equations (4.6.2) is applicable to all modes of vibration by simply applying the boundary conditions appropriate to the mode detailed in section 4.3. To follow the procedure we let S_1 denote the loaded region of the half space boundary, and S_o the stress-free region. The algebraic equations (4.6.2) are rewritten to indicate the elements of the matrices A_1 and A_2 which pertain to

nodes in the various regions, as follows

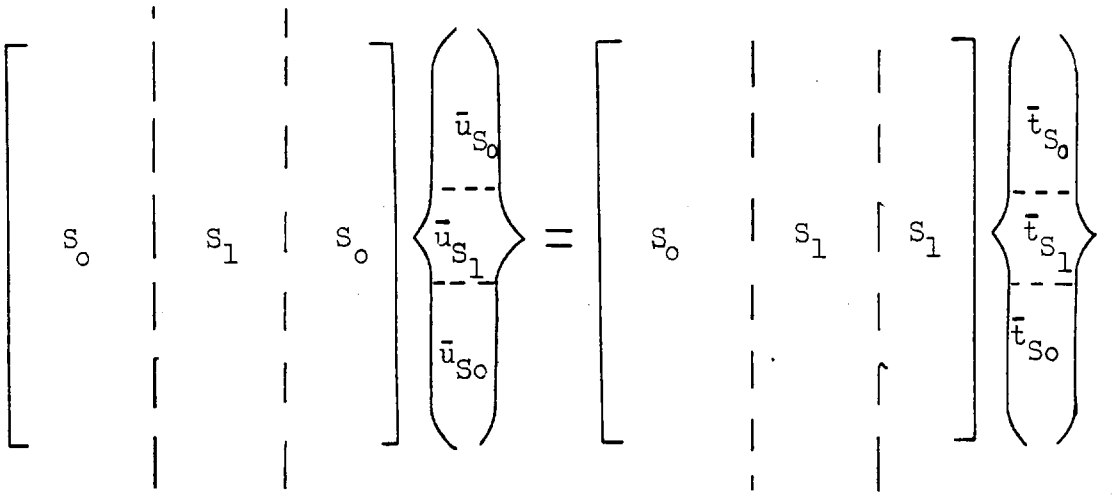

$$\left[A_1\right]\{u\} = \left[A_2\right]\{t\} \qquad (4.6.4)$$

u_{So} denotes displacements at nodes in the stress-free region S_o, etc. The odd-numbered columns of matrix A_1 are coefficients of the nodal displacement component $\bar{u}_1$ while the even-numbered columns are those of $\bar{u}_2$. The columns of A_2 refer similarly to the coefficients of nodal stresses $\bar{t}_1$ and $\bar{t}_2$. First it is noted that stresses $\bar{t}_{So} = 0$ are already known while displacements $\bar{u}_{So}$ are unknown on the stress-free region S_o. Therefore the sorting concerns only the S_1-columns of matrices A_1 and A_2. We use the cases of vertical and the three degrees-of-freedom vibration to illustrate the procedure. The other modes are similarly treated. It is observed that when a coefficient is taken across the equality sign, its sign changes, of course.

(i) Vertical Vibration:-

Refer to eqs.(4.3.17) and (4.3.18)

$\bar{V}_2$ is unity. so the even-numbered columns (S_1-columns) of

matrix A_1, are summed up and transferred to the right to the known column vector B. The even-numbered columns of matrix A_2 (coefficients of vertical stress $\bar{t}_2$) are transferred to the left to replace the even-numbered columns of A_1.

Relaxed Contact Conditions - eq.(4.3.17)

No further shuffling as the coefficients of unknown $\bar{u}_1$ are already on the left.

Welded Contact Conditions - eqs.(4.3.18)

The odd-numbered columns of A_2 (coefficients of unknown $\bar{t}_1$) are transferred to replace the odd-numbered columns of A_1.

Three Degrees-of-freedom:-

Refer to eqs.(4.3.1)a,b

The three sets of trial values $\bar{V}_n^{(m)}$ used are, see eq.(4.3.7) and subsequent discussion,

$$\begin{bmatrix} \bar{V}_1^1 & \bar{V}_2^1 & \bar{V}_3^1 \\ \bar{V}_1^2 & \bar{V}_2^2 & \bar{V}_3^2 \\ \bar{V}_1^3 & \bar{V}_2^3 & \bar{V}_3^3 \end{bmatrix} = \begin{bmatrix} 3 & 2 & 1 \\ 2 & 3 & 1 \\ 1 & 1 & 3 \end{bmatrix}$$

The values of the elements were found not to matter, as expected, as long as the array is not singular.

To effect eqs.(4.3.1a), multiply the odd-numbered columns of A_1 by $\bar{V}_n^{(m)}$, the even-numbered columns by $\bar{V}_n^{(m)} + \bar{x}_1\bar{V}_n^{(m)}$ where $\bar{x}_1$ is the $\bar{x}_1$-coordinate of the appropriate node, sum up the

result and transfer to the mth column of B (the right hand side array B of the final assembly is now required to have three columns). The operation can be represented by

$$B_{j,m} = -A_{j,2n-1}\bar{V}_1^{(m)} - A_{j,2n}\left\{\bar{V}_2^{(m)} + \bar{x}_{1n}\bar{V}_3^{(m)}\right\}$$

where n is the appropriate node number in the loaded region S_1.

To effect eqs.(4.3.1b) all the S_1-columns of A_1 are transferred to replace the similar columns of A_2 as the coefficients of the unknown $\bar{t}_1$, $\bar{t}_2$.

Some Programming Hints.

These operations can be very neatly coded into a computer subprogram. It is wasteful to bother to compute the S_o-columns of matrix A_2 as they are never used - the S_o surface has zero stresses. So only the S_1-columns need be computed for A_2, i.e., integration of the functions involving $\bar{U}_{jk}$ is done only for elements in the loaded region. Also it is not necessary to have all the rows of S_1-columns of A_2 in storage simultaneously. Space for only two rows need be allocated. For a nodal position of the point P, eq.(4.4.6) only two equations for j=1,2 are computed simultaneously. The boundary conditions may be applied immediately so that the space allocated for the two rows of array A_2 is released for computation of the next pair of equations. Of course, allocation has to be made for the entire matrices A_1 and B simultaneously unless disc-based method of solution is employed

for the equations. The problem size is small enough to need only in-core handling of the matrices. After solving the final assembly (4.6.3) one has to remember which elements of the solution vector represents stress or displacement according to the sorting done for the various modes. We have not bothered yet to consider symmetry of the problem (if any) because it will be informative to let the solutions verify this. After that one may then use symmetry to further reduce the problem size. The values of the computed nodal variables for the three degree-of-freedom vibration showed no symmetry, however.

Having solved the final assembled equations and computed the stiffnesses as outlined in section 4.3 for the various modes of vibration, the results are presented next.

4.7 RESULTS AND DISCUSSIONS

(a) Effects of Truncating the Integrals in the BIE Equation

In section 3.2 of chapter 3 it is indicated that the integrals in the BIE equation are truncated to within some region a distance of R_o from the loaded area, see fig.4.10 below

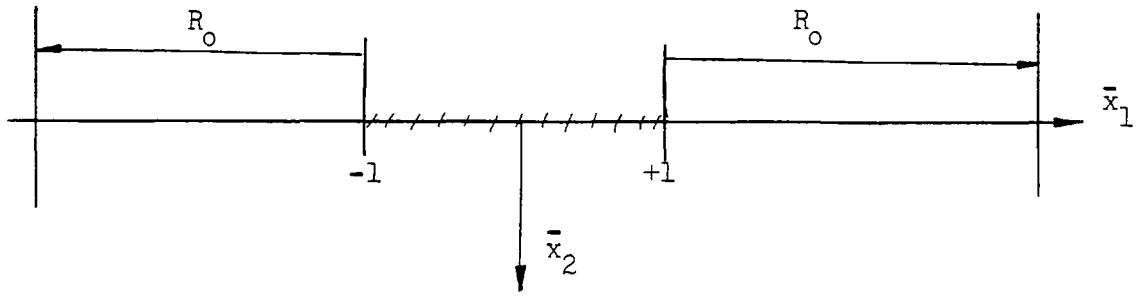

Fig 4.10 Limits of Integration

We now investigate the effect of various values of R_o on the results of the analysis of the foundation vibration. Vertical vibration is used, with Poisson ratio 1/4.

The real and imaginary parts of the dynamic stiffness for vertical vibration are plotted in fig.4.13 for values of R_o=0,3,7. A value of R_o indicates the width of the stress-free surface that is assumed to have contributed significantly to the integration, the width being measured as a number of half-widths of the rigid strip. The convergence of the dynamic stiffness to a definite limit may be observed in fig.4.13 as R_o increases. The convergence is rather more rapid that predicted by the approximate error analysis in section 3.2.

The results for R_o=3 and R_o=7 are almost identical. It is sufficient to use the smaller value R_o=3 which gives smaller area to integrate on and therefore less expensive numerical integration. The rest of the results in this chapter are based on the integration over the region indicated by R_o=3.

(b) Vertical Vibration

The equivalent dynamic stiffness is compared with the analytical results of Karasudhi, Keer and Lee (1968) in fig.4.14 where excellent agreement is observed. This is for the relaxed contact conditions. For the welded contact conditions, we compute the dynamic compliance (inverse of stiffness) in order to be able to compare directly with the works of Luco and Westman (1972) where such results are

available. This comparison is shown in fig.4.15 to be excellent.

The difference between the relaxed and welded contact conditions are also shown in the figure, and it is observed to be small. In plain words, the figure indicates that when the rigid infinite strip is considered to be executing pure vertical vibration, it makes little difference whether we assume zero shear stress between the strip and the supporting medium (relaxed contact conditions) or perfect no-slip bonding between them (welded contact conditions).

The results presented in fig.4.15 are for Poisson ratio 1/4. Luco and Westman (1972) observed that the difference between the two types of contact conditions is smaller at higher Poisson ratio but slightly larger at lower Poisson ratio.

The normal stress distribution under the rigid foundation is plotted in fig.4.16 for some values of the frequency factor η_2. The stress is symmetrical about the longitudinal axis of the body and increases with . The usual edge singularity can be observed. The shear stress was found to be anti-symmetric and to change sign very rapidly under the rigid body.

In fig.4.17 is shown the nondimensional response $\bar{W}_2 = \pi \mu W_2/F$ computed from eq.(4.3.19) and plotted against frequency factor η_2 for some values of mass ratio.

(c) Horizontal Vibration

The horizontal compliance is plotted in fig.4.18 for the relaxed problem. Agreement with Luco and Westman is again excellent. It is remembered that relaxed condition here indicates the prescription of zero normal stress at the contact between the foundation and the earth in order to preclude coupling with rocking or vertical vibration. The welded contact condition is discussed in paragraph (e) below under coupled mation.

(d) Rocking Vibration

The compliance for the relaxed condition (zero shear stress) is plotted in fig.4.19 and compared with Luco and Westmann's results. The latter results show over-estimation probably due to mathematical difficulties which forced the authors to use only the "dominant parts" of the integrals they encountered to evaluate stress distribution. The welded contact condition is discussed below under coupled horizontal-rocking vibration.

(e) Coupled Horizontal-Rocking Vibration

In this mode four compliances are involved, and are obtained from the inverse of the stiffness matrix in eq.(4.3.5). We have

C_{11} - direct horizontal-horizontal compliance

C_{13} - coupling horizontal-rocking compliance

C_{31} - coupling rocking-horizontal compliance

C_{33} - direct rocking-rocking compliance

C_{11} is plotted in fig.4.18 and is found to coincide exactly

with the compliance resulting from pure horizontal mode. C_{33} is plotted in fig.4.20 which again shows the results of Luco and Westmann to be overestimates. In fig.4.21 the direct rocking compliance C_{33} is compared with the rocking compliance resulting from pure rocking mode. Appreciable difference exists, unlike the horizontal compliance in fig.4.18. The coupling compliance is shown in fig.4.22. Theoretically the coupling compliances C_{13} and C_{31} should be equal by law of reciprocity. But due to numerical inaccuracies, differences did exist between the computed values. What is shown in fig.4.22 are the averages of the real and imaginary parts of C_{13} and C_{31} compared with similar averages taken from Luco and Westmann.

(f) The Three Degrees-of-Freedom Vibration

There are nine components of compliance involved, namely C_{jk}, $j,k=1,2,3$ obtained from the inverse of the stiffness matrix in eq.(4.3.6).

The Direct Compliances C_{jj}, $j=1,2,3$:-

The direct vertical compliance C_{22} coincides exactly with the vertical compliance resulting from pure vertical mode with welded contact conditions. This is indicated in fig.4.15. The direct horizontal compliance C_{11} coincides exactly with the horizontal compliance resulting from the pure horizontal mode as well as the coupled horizontal-rocking modes. This is indicated in fig.4.18. The direct rocking compliance C_{33} coincides exactly with the rocking compliance resulting from the coupled horizontal-rocking modes, as indicated fig.4.20 but

different from the results of the pure rocking mode in fig.4.19.

The Coupling Compliances C_{jk}, $j \neq k$:-

The horizontal-rocking, rocking-horizontal compliances are exactly the same as those for the coupled horizontal-rocking motion, and are indicated in fig.4.22. The vertical-horizontal coupling compliance and the vertical-rocking coupling compliance are found to be negligible, their maximum values being less than 2 per cent of the peaks of the horizontal-rocking compliances shown fig.4.22. Allowing for numerical inaccuracies, it may be concluded that there is no coupling between the vertical and horizontal modes, and the vertical and rocking modes.

The question of no coupling between the vertical and any other mode may be examined from the physical situation as follows. When the foundation is undergoing vertical motion, see fig.4.11 below, the normal stress is symmetric about the centre line of the rigid strip and so no rocking is induced.

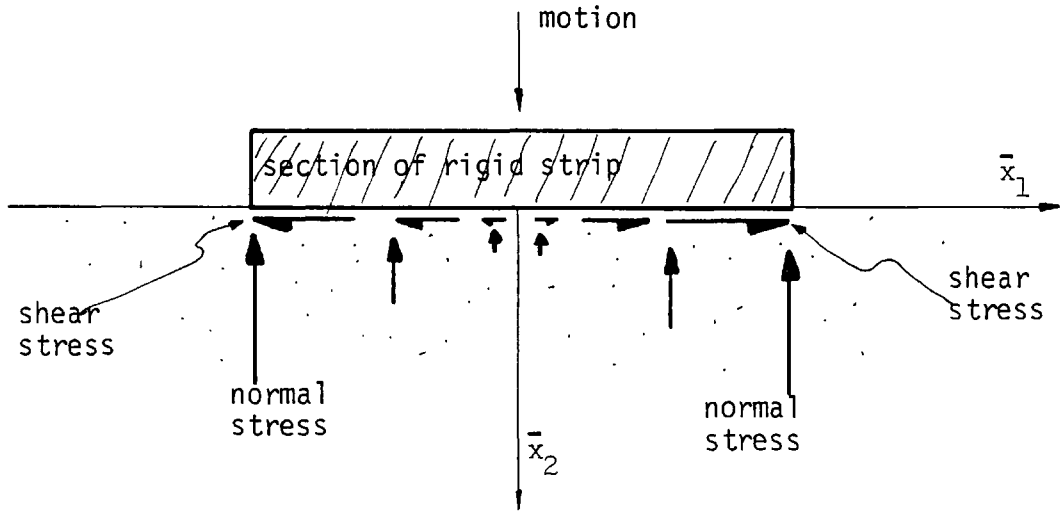

Fig 4.11 Vertical Vibration

Also the shear stress is an odd function of x_1. The resultant horizontal force on the foundation is zero and so no horizontal pull is experienced.

In the real situation it is intuitively clear that the horizontal excitation of a foundation results in rocking vibration as well. This is because the center of mass of the foundation is at a finite height above the soil surface and the horizontal reaction force of the soil which acts at the base of the foundation results in a rocking couple about a horizontal line through the center of mass.

(g) Concluding Remarks

A lot of results have been computed in this chapter. This is possible because they all result from one equation, the boundary integral equation. This is a demonstration of the power of the BIE method as well as its versatility. We did not have to formulate or write a different equation for a different mode of vibration or contact condition. Yet we have very simply reproduced most of the previously known results which were computed from series of formidable integrals. Above all a numerical verification has been presented for the results of the three degrees-of-freedom vibration which have always been assumed but not computed.

It will be relevant to mention here the cost of these computations. A hint was given in section 4.6 on the computer programming for this problem. The main body of the program is the setting up of the system of equations (4.6.2)

which then becomes applicable to any mode of vibration and contact conditions. The coding for all the modes and contact conditions is included in one program. Because of the small region of integration involved only a small system of thirty-one equations in complex variables had to be solved. As a result the program requires only 21,500 words of computer memory in the CDC Cyber 174 machine at Imperial College, and takes only 8 seconds to compute the dynamic stiffness at a particular frequency.

More demonstrations of the powers of the BIE are shown in the next chapter where the three-dimensional version is employed.

FIG.4.13 EFFECT OF TRUNCATION OF THE BIE INTEGRALS ON THE DYNAMIC STIFFNESS FOR RIGID INFINITE STRIP IN VERTICAL VIBRATION. POISSON RATIO 1/4

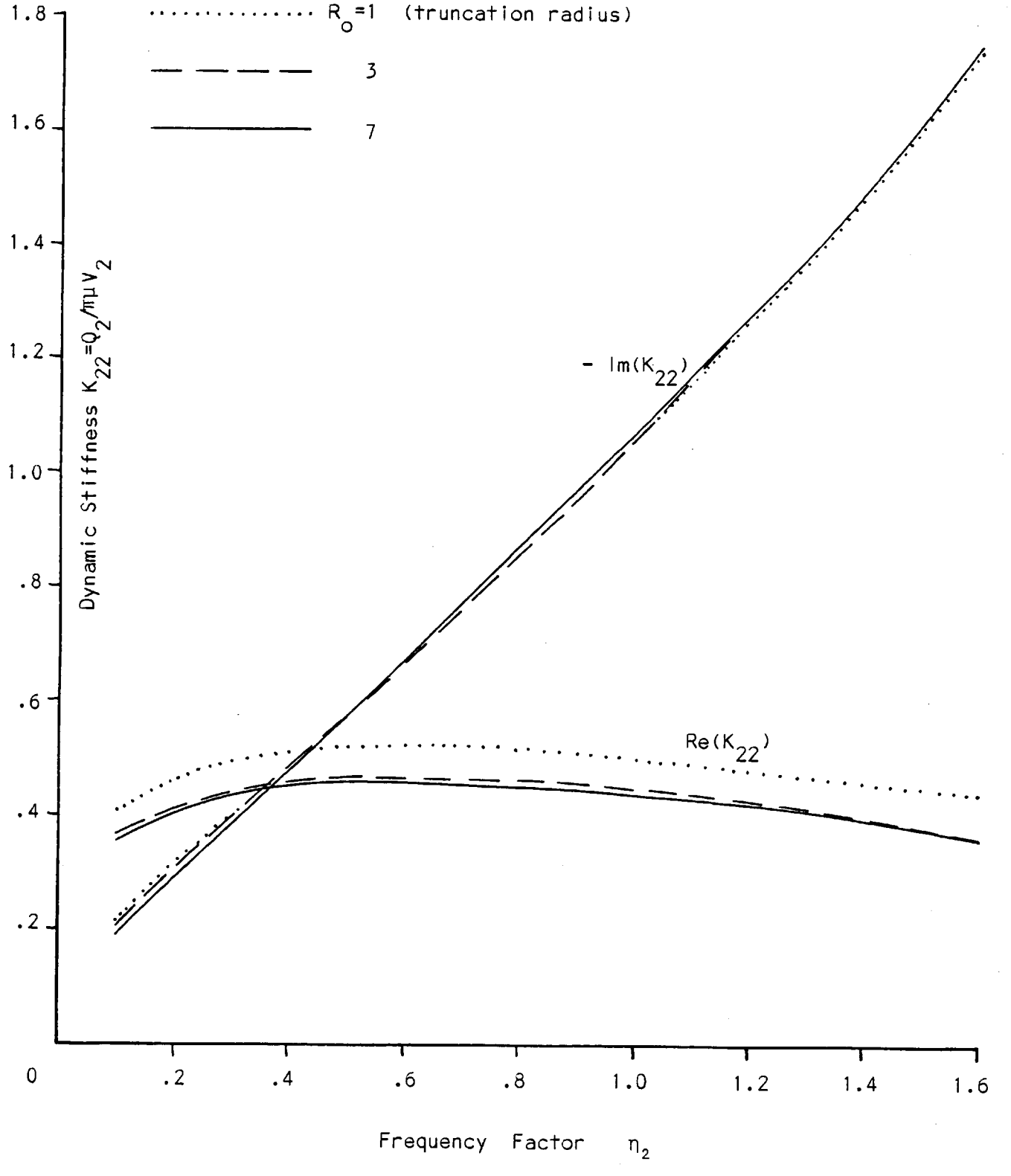

FIG.4.14 DYNAMIC STIFFNESS FOR RIGID INFINITE STRIP IN VERTICAL VIBRATION. POISSON RATIO 1/4

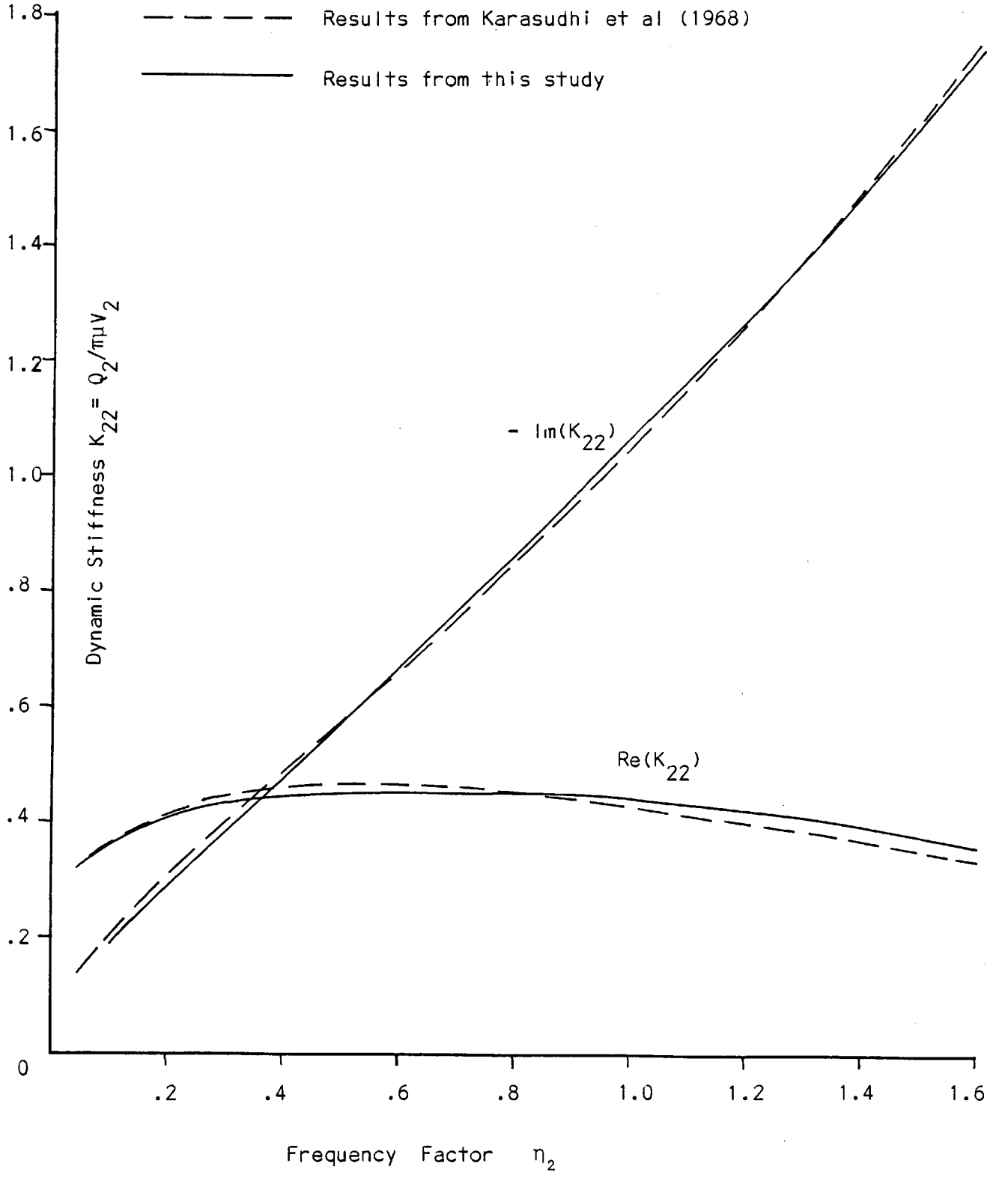

FIG. 4.15 VERTICAL COMPLIANCE FOR RIGID INFINITE STRIP RESULTING FROM:-

——— (a) pure vertical mode welded contact, (b) the three degrees-of-freedom mode

. . . . . equivalent results from Luco and Westmann (1972)

– – – – – – – pure vertical mode relaxed contact.

———···———

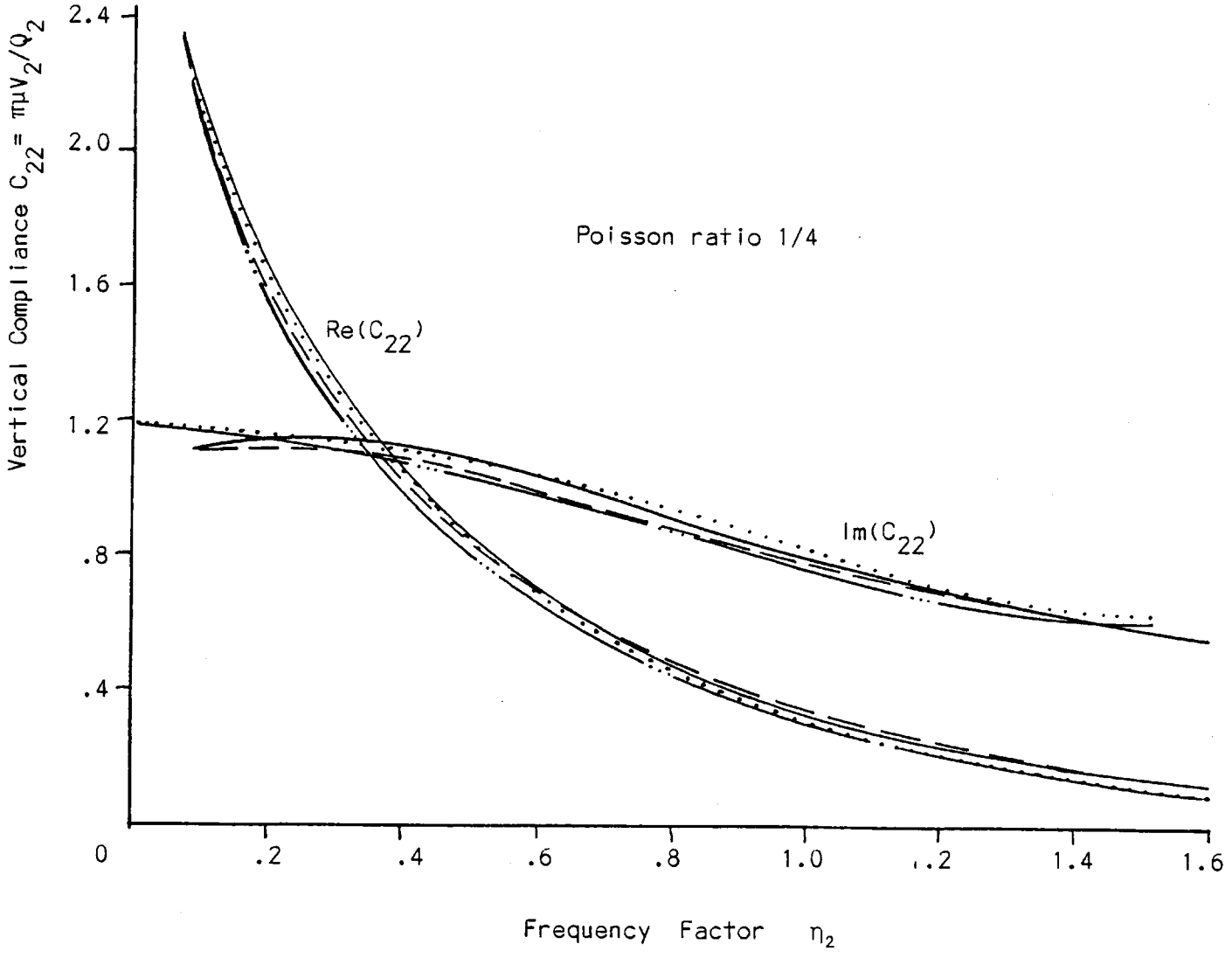

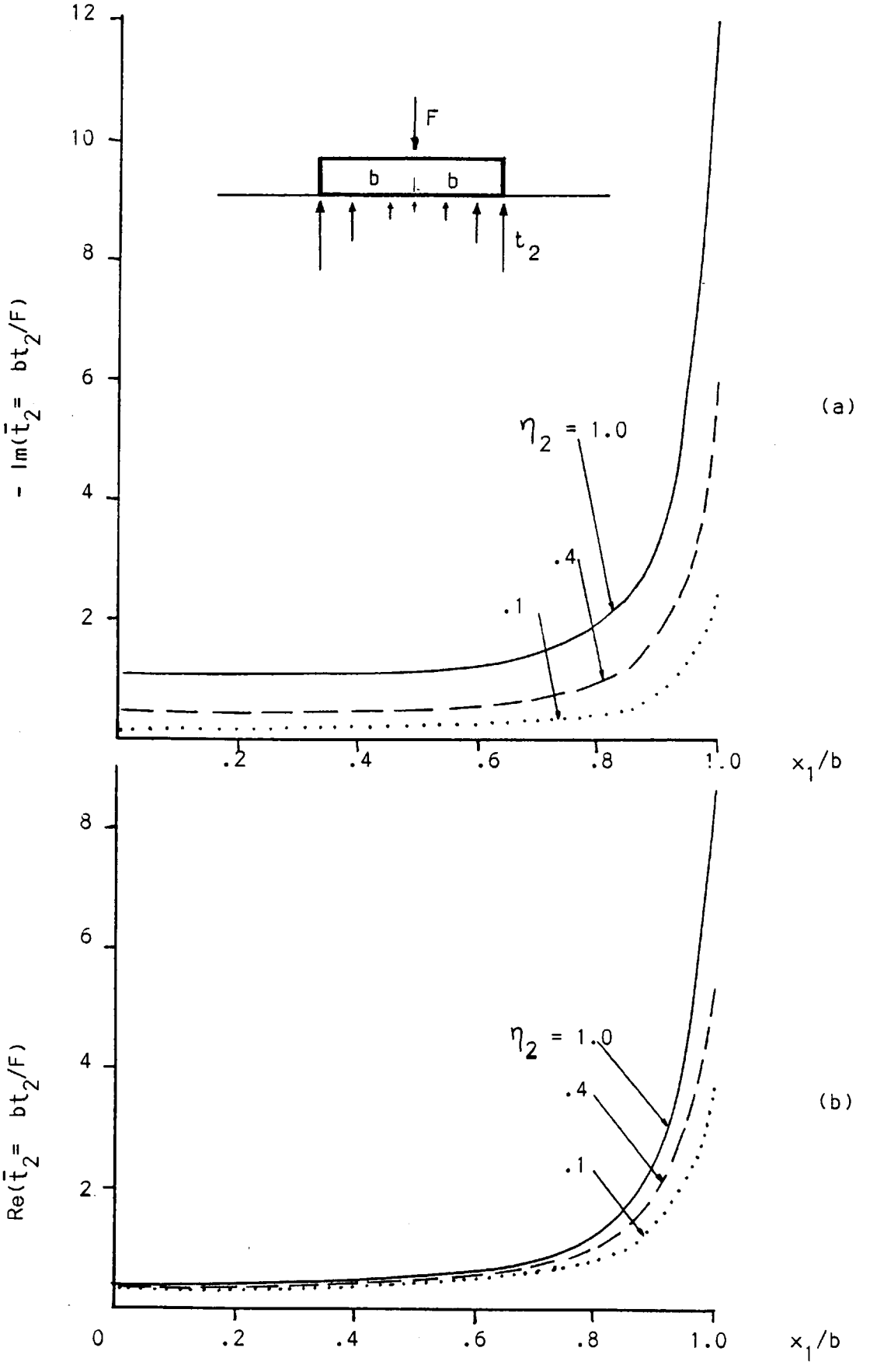

FIG.4.16 NORMAL STRESS DISTRIBUTION UNDER RIGID INFINITE STRIP IN VERTICAL VIBRATION, (a) IN QUADRATURE WITH DISPLACEMENT (b) IN PHASE WITH DISPLACEMENT

POISSON RATIO 1/4

FIG. 4.17 NON-DIMENSIONAL AMPLITUDE OF RIGID INFINITE STRIP IN VERTICAL VIBRATION. POISSON RATIO 1/4

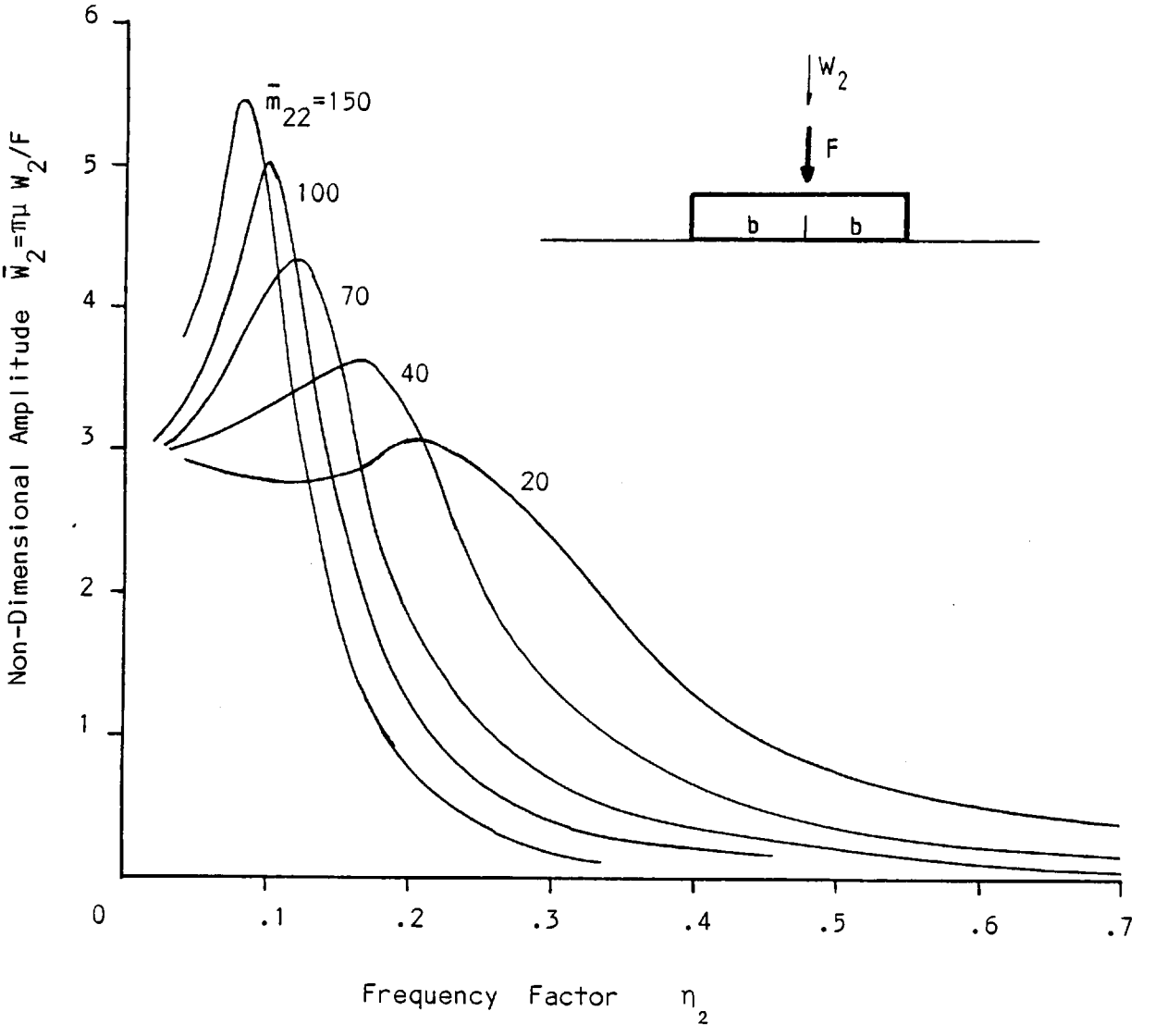

FIG.4.18 RIGID INFINITE STRIP:-
DIRECT HORIZONTAL COMPLIANCE C_{11} RESULTING FROM

——— (a) pure horizontal mode (relaxed conditions)
(b) coupled horizontal-rocking mode
(c) coupled vertical-horizontal-rocking

····· coupled horizontal-rocking from Luco and Westmann (1972)

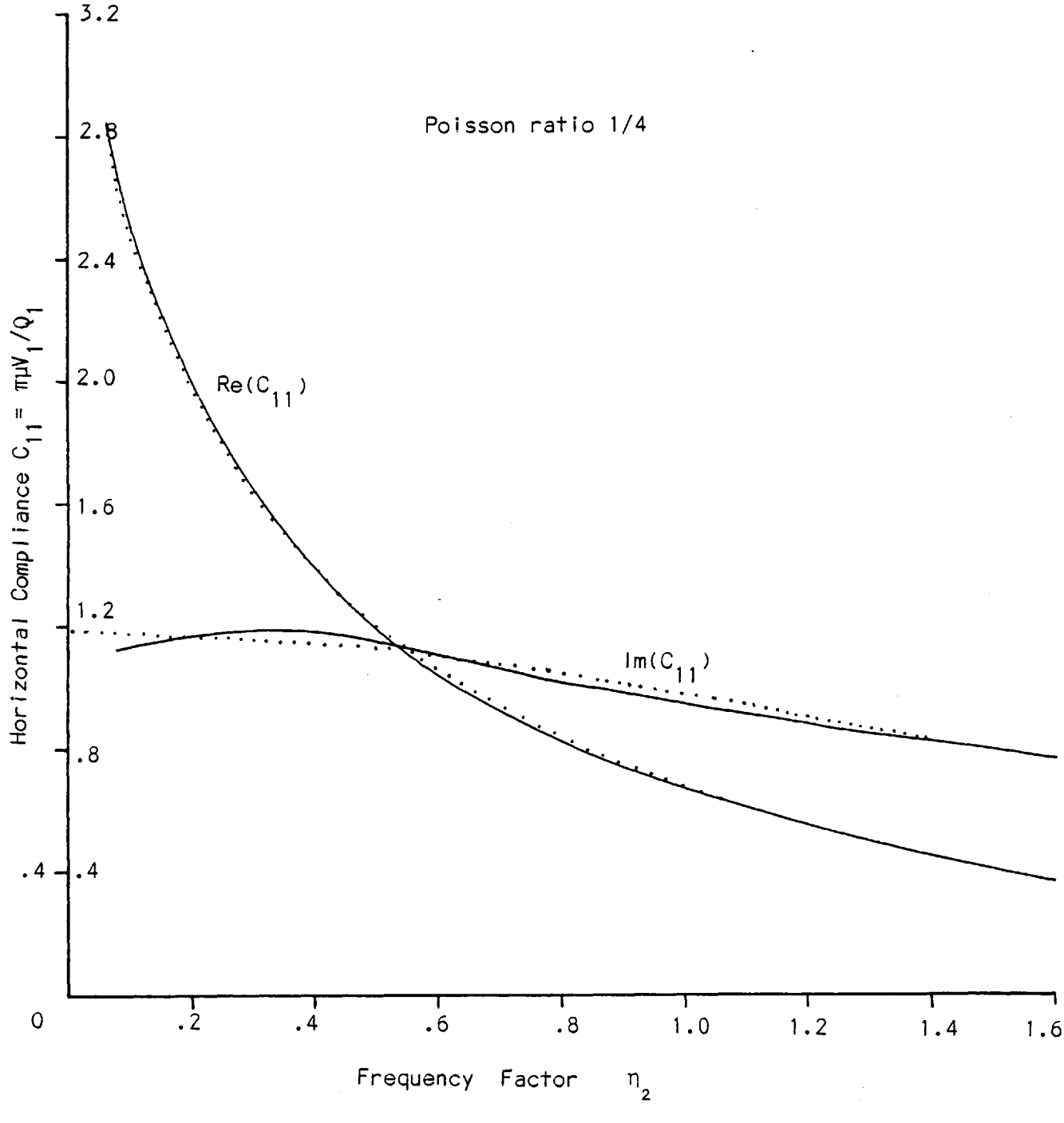

FIG.4.19 RIGID INFINITE STRIP:-
ROCKING COMPLIANCE RESULTING FROM PURE ROCKING MODE
POISSON RATIO 1/4

..... Results from Luco and Westmann (1972)

——— Present Study

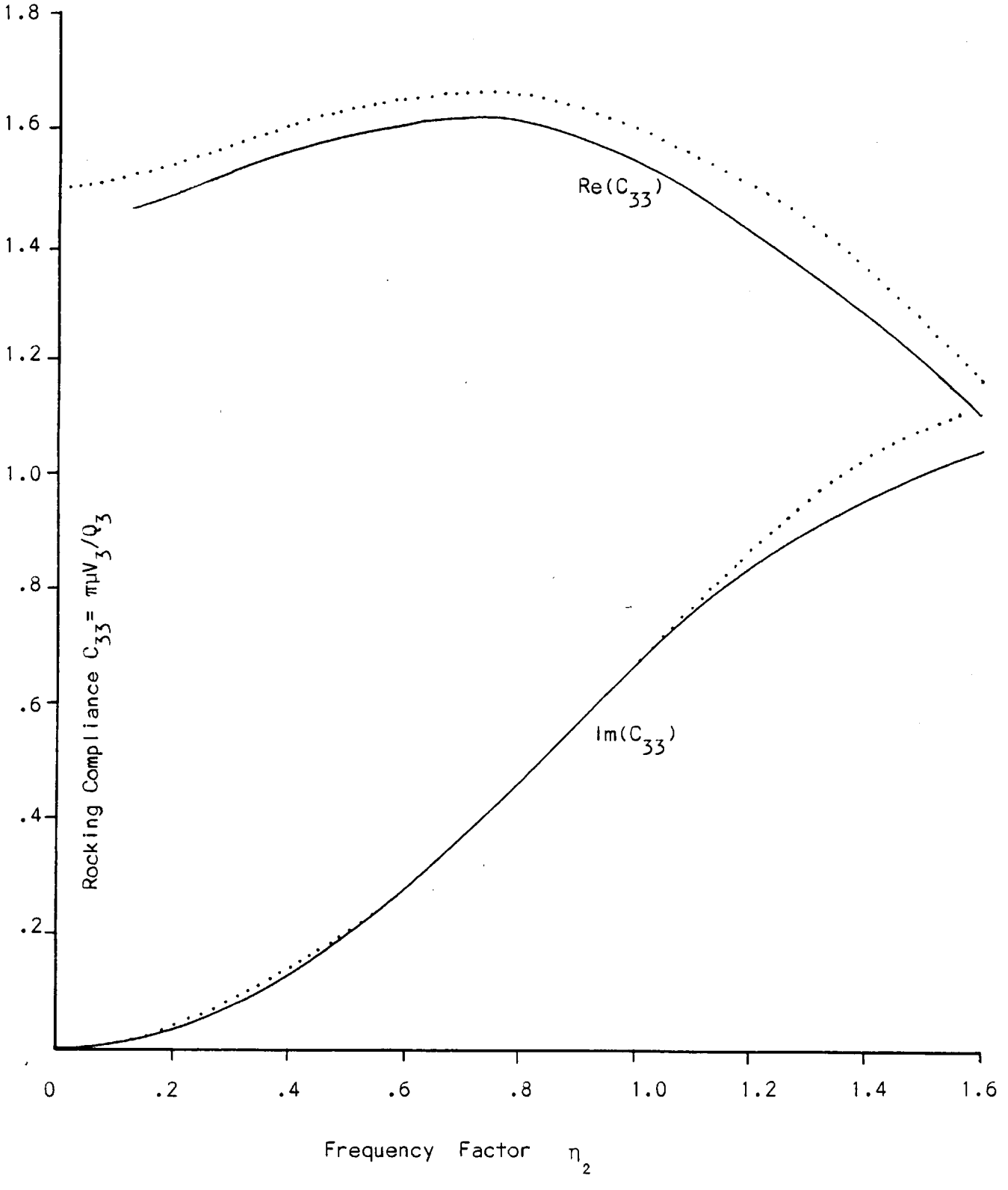

FIG.4.20 RIGID INFINITE STRIP:-
DIRECT ROCKING COMPLIANCE C_{33} RESULTING FROM

——————— (a) coupled horizontal-rocking modes
(b) coupled vertical-norizontal-rocking

. . . . . coupled horizontal-rocking from Luco and Westmann (1972)

Poisson ratio 1/4

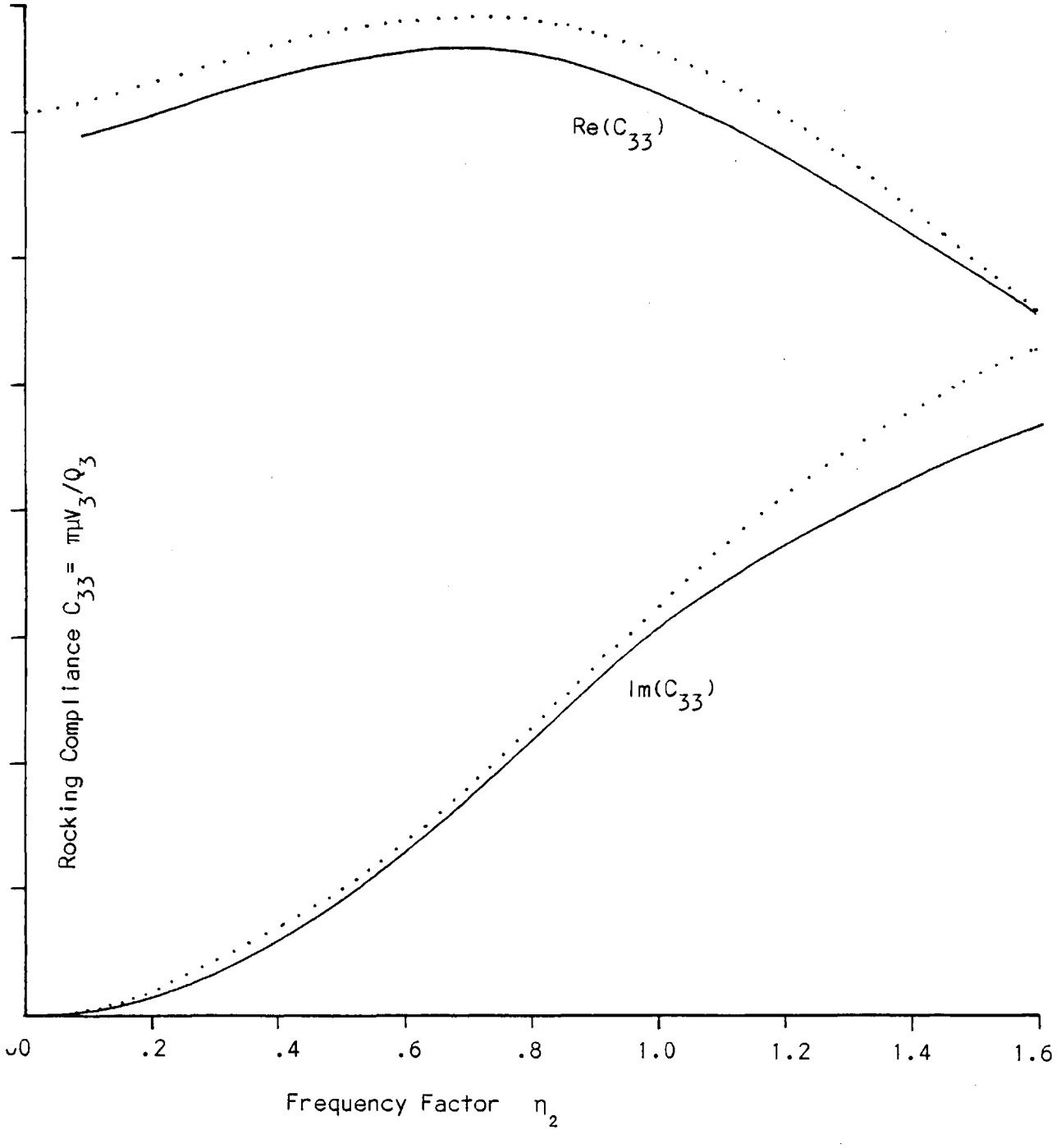

FIG.4.21 RIGID INFINITE STRIP:-
DIRECT ROCKING COMPLIANCE C_{33} RESULTING FROM

— — — — — — pure rocking mode

——···——···— coupled horizontal-rocking modes

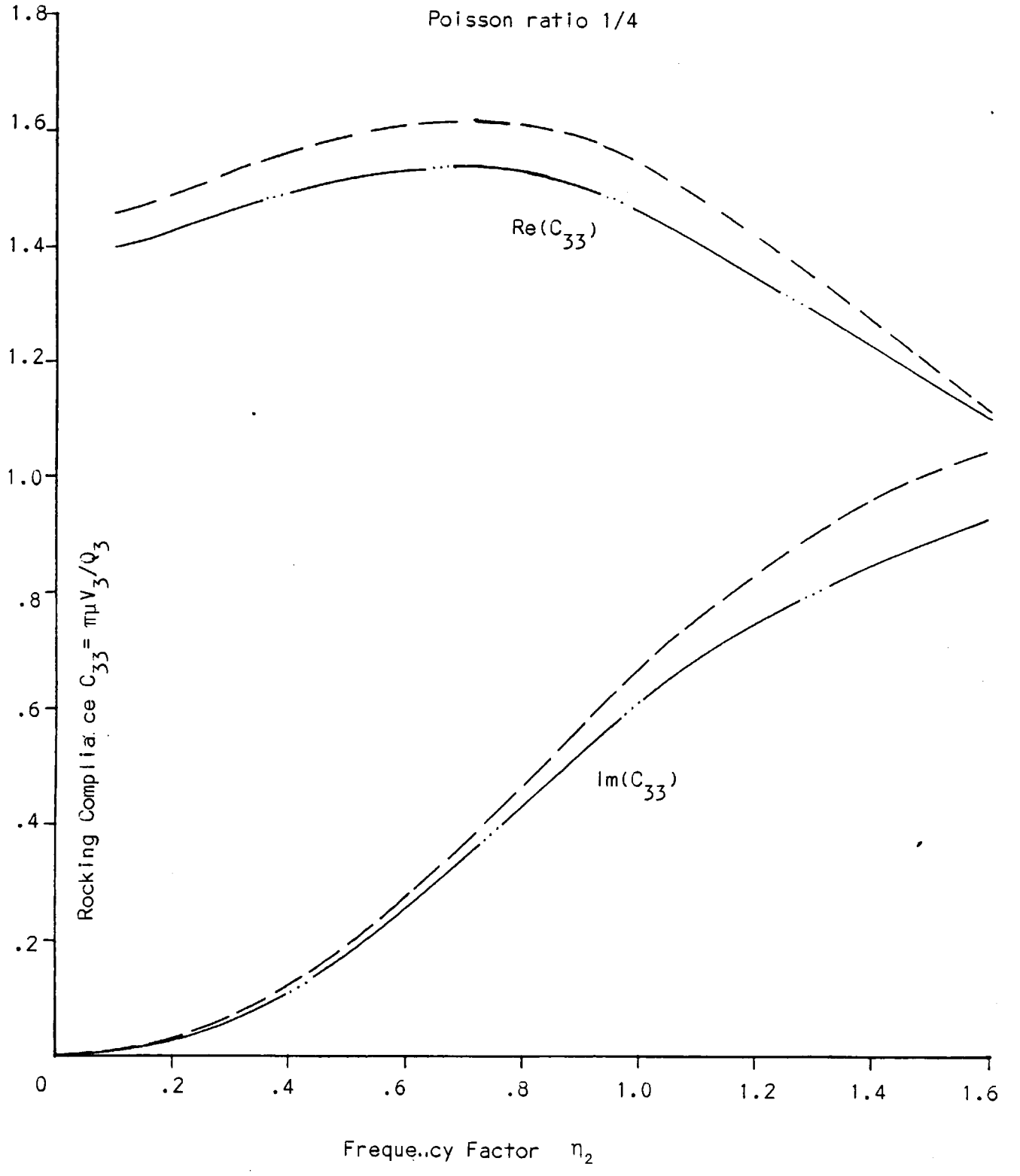

FIG.4.22 RIGID INFINITE STRIP:-
COUPLING HORIZONTAL-ROCKING COMPLIANCE RESULTING FROM

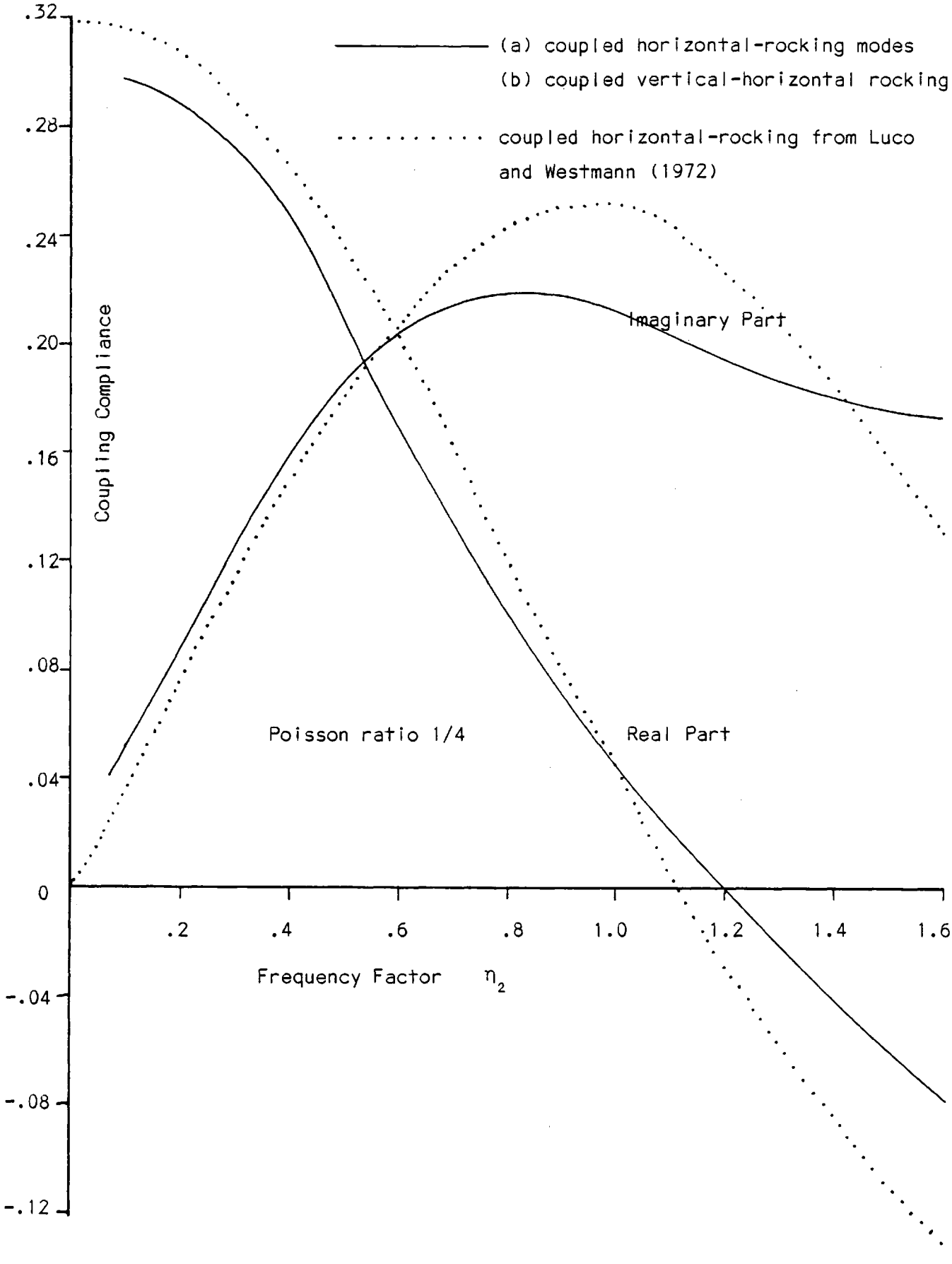

chapter 5

VIBRATION OF A RIGID FOUNDATION OF ARBITRARY SHAPE ON AN ELASTIC HALF SPACE

5.1 INTRODUCTION

The analysis of vibration of rigid foundation of arbitrary shape on the elastic half space is presented using the boundary integral equation (2.5.13). The good performance of the BIE method for the two-dimensional case in the previous chapter provides sufficient stimulus for one to proceed to this three-dimensional case. The formulation is presented for a foundation of arbitrary shape, but in order to be able to compare results with those from existing works, numerical results are presented for circular and rectangular foundations. More detailed attention is focused on rectangular foundations. The well-known circular case is mentioned in passing only to demonstrate the accuracy of the BIE formulation. Results are presented for the vertical and horizontal vibrations of rectangular foundation, and the vertical and torsional vibrations of circular foundation. Results are also presented for the vertical mode of rectangular foundations with length/width ratios of up to 16, and then compared with results obtained by idealising such "long" rectangles as infinite rectangular strip. We pay attention again to the ease of applying boundary conditions and of coping with various modes of vibration.

The development here is very much similar to that in the previous chapter, so that in this chapter we shall be able to omit much of the explanations of the steps without losing meaning.

5.2 PROBLEM DEFINITION

In fig.(5.1) is shown the contact region between the foundation and the half space, as well as the coordinate axes. b is a characteristic length of the loaded area. For example b is identified with the radius of a circular foundation or half the length of a rectangular foundation. We define the two sets of contact conditions:

Relaxed Contact Conditions:-

These decouple the motion into pure modes of vibration.

(i) Vertical Vibration - Zero shear stresses t_1, t_2

(ii) Horizontal Vibration in x_2-direction, say -
Zero shear stress t_1 and normal stress t_3

(iii) Rocking about x_1-axis - zero shear stresses t_1, t_2

(iv) Torsion Vibration - zero normal stress t_3

Welded Contact Conditions:-

The foundation is perfectly bonded to the half space. There is no interfacial slip, and the modes of vibration remain coupled. All components of contact stress are unspecified.

We now identify the boundary conditions imposed on the surface by the various modes of vibration.

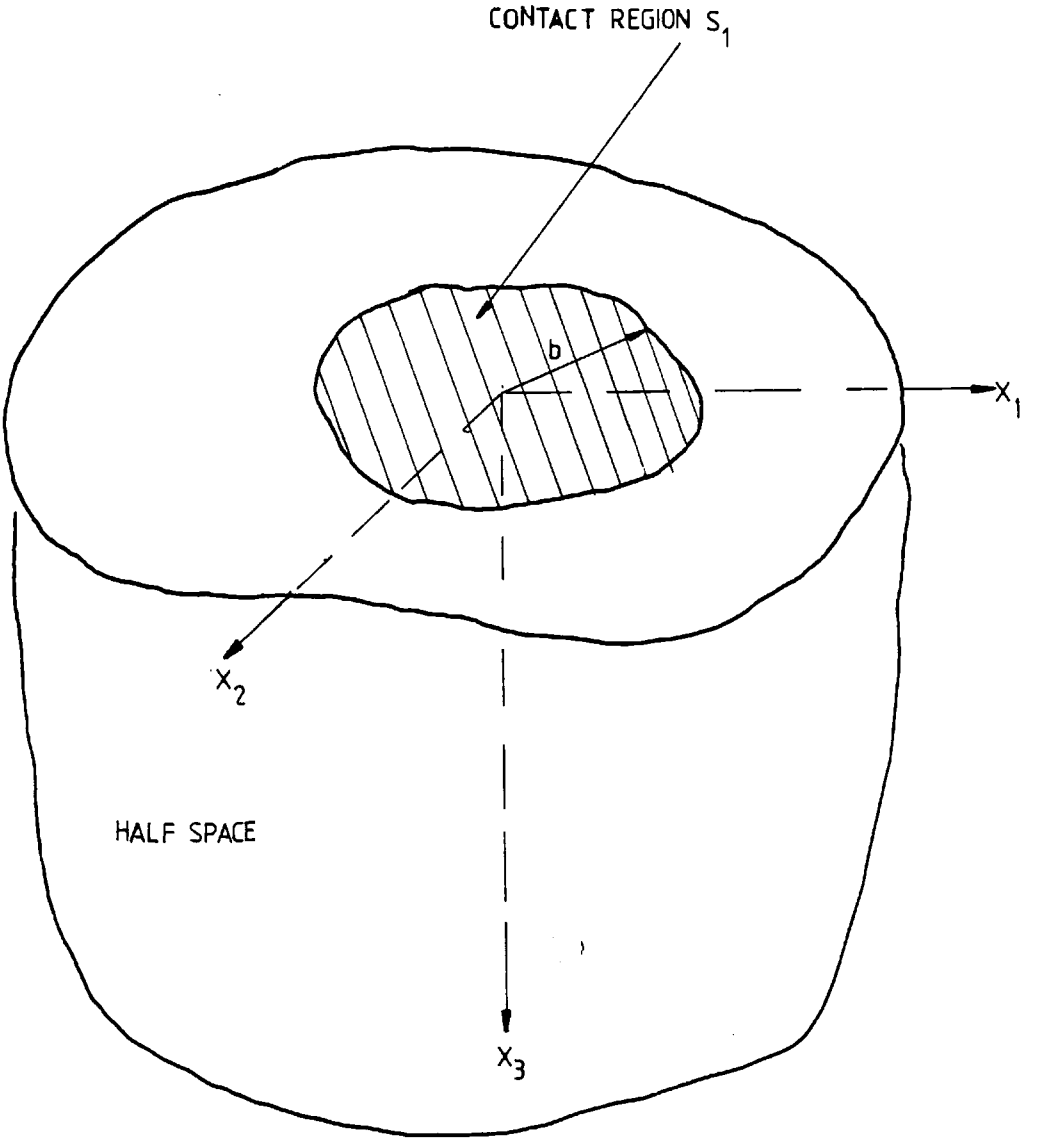

Fig 5.1 The Coordinate Axes

5.3 BOUNDARY CONDITIONS IMPOSED BY THE MODES OF VIBRATIONS

(i) The General Six Degrees-of-freedom.

Notations similar to those in chapter 4 are adopted for the general motion of and the forces on the massless rigid body. V_1, V_2, V_3 represent the translation of the body in the coordinate directions x_1, x_2, and x_3 respectively. θ_1, θ_2, and θ_3 represent the rotations in the respective coordinate axes. The motions of and the forces on a massive body are similarly defined as in chapter 4, using same symbols.

$$V_4 = b\theta_1, \quad V_5 = b\theta_2, \quad V_6 = b\theta_3$$

The displacement components induced on the contact area are

$$\begin{aligned} u_1 &= V_1 - x_2\theta_3 = V_1 - x_2V_6 \\ u_2 &= V_2 + x_1\theta_3 = V_2 + x_1V_6 \\ u_3 &= V_3 + x_2\theta_1 - x_1\theta_2 = V_3 + x_2V_4 - x_1V_5 \end{aligned} \tag{5.3.1}$$

The stresses in the loaded region are

$$\begin{aligned} t_1 &= \text{unknown} \\ t_2 &= \text{unknown} \\ t_3 &= \text{unknown} \end{aligned} \tag{5.3.2}$$

u_k and t_k are taken positive in the positive directions of the coordinate axes

The following stress integrals are defined

$$Q_1 = \int_{S_1} t_1 ds$$

$$Q_2 = \int_{S_1} t_2 \, ds$$

$$Q_3 = \int_{S_1} t_3 \, ds$$

$$Q_4 = \int_{S_1} \frac{x_2}{b} t_3 \, ds$$

$$Q_5 = \int_{S_1} \frac{x_1}{b} t_3 \, ds$$

$$Q_6 = \int_{S_1} \left(\frac{x_1}{b} t_2 - \frac{x_2}{b} t_1\right) \, ds$$

The harmonic time factor $e^{i\omega t}$ is being omitted. The stress integrals Q_4, Q_5, and Q_6 are couples opposing the rotation of the body about the x_1, x_2, and x_3 axes respectively.

Let F be some reference unit of force and m the mass, $\bar{J}_1$, $\bar{J}_2$, and $\bar{J}_3$ the moments of inertia about x_1, x_2, and x_3 axes respectively. We use the symbols $m_{jj} = m$, $j=1,2,3$

$$m_{44} = \bar{J}_1/b^2, \quad m_{55} = \bar{J}_2/b^2, \quad m_{66} = \bar{J}_3/b^2$$

The following dimensionless quantities are introduced

$$\bar{m}_{jj} = \frac{m_{jj}}{\rho b^3} , \quad j = 1,2,\ldots,6$$

$$\bar{u}_k = \frac{\mu b u_k}{F}$$

$$\bar{t}_k = \frac{b^2 t_k}{F}$$

$$\bar{V}_k = \frac{\mu b V_k}{F} \qquad (5.3.3)$$

$$\bar{Q}_k = \frac{Q_k}{F}$$

$$\bar{x}_k = \frac{x_k}{b}$$

$$\bar{s} = \frac{s}{b^2}$$

$$\eta_2 = \frac{b\omega}{c_2}$$

$$\eta_1 = \frac{b\omega}{c_1}$$

$$\bar{W}_k = \frac{\mu b W_k}{F}$$

The stress integrals become

$$\bar{Q}_1 = \int_{\bar{S}_1} \bar{t}_1 d\bar{s}$$

$$\bar{Q}_2 = \int_{\bar{S}_1} \bar{t}_2 \, d\bar{s}$$

$$\bar{Q}_3 = \int_{\bar{S}_1} \bar{t}_3 \, d\bar{s}$$

$$\bar{Q}_4 = \int_{\bar{S}_1} \bar{x}_2 \bar{t}_3 \, d\bar{s}$$

$$\bar{Q}_5 = \int_{\bar{S}_1} \bar{x}_1 \bar{t}_3 \, d\bar{s}$$

$$\bar{Q}_6 = \int_{\bar{S}_1} (\bar{x}_1 \bar{t}_2 - \bar{x}_2 \bar{t}_1) \, d\bar{s}$$

The equivalent dynamic stiffness (direct and coupled) is defined by

$$K_{jk} = \frac{Q_j}{\mu b V_k} = \frac{\bar{Q}_j}{\bar{V}_k} \tag{5.3.5a}$$

resulting in the following force-displacement relation

$$\begin{bmatrix} K_{11} & K_{12} & K_{13} & K_{14} & K_{15} & K_{16} \\ K_{21} & K_{22} & K_{23} & K_{24} & K_{25} & K_{26} \\ K_{31} & K_{32} & K_{33} & K_{34} & K_{35} & K_{36} \\ K_{41} & K_{42} & K_{43} & K_{44} & K_{45} & K_{46} \\ K_{51} & K_{52} & K_{53} & K_{54} & K_{55} & K_{56} \\ K_{61} & K_{62} & K_{63} & K_{64} & K_{65} & K_{66} \end{bmatrix} \begin{Bmatrix} \bar{V}_1 \\ \bar{V}_2 \\ \bar{V}_3 \\ \bar{V}_4 \\ \bar{V}_5 \\ \bar{V}_6 \end{Bmatrix} = \begin{Bmatrix} \bar{Q}_1 \\ \bar{Q}_2 \\ \bar{Q}_3 \\ \bar{Q}_4 \\ \bar{Q}_5 \\ \bar{Q}_6 \end{Bmatrix} \tag{5.3.5b}$$

Applying the same reasoning as for the two-dimensional problem in the previous chapter, the stiffnesses K_{jk} are computed by using six sets of values for the motions V_n of the body, namely $V_n^{(m)}$, $n,m = 1,2,\ldots,6$, and obtaining the stiffnesses from the following set of equations similar to the set (4.3.7)

$$V_k^{(m)} K_{jk} = Q_j^{(m)} \tag{5.3.6}$$
$$m,j,k = 1,2,\ldots,6$$

Summation over k is implied on the left hand side of (5.3.6)

The motions $\bar{W}_k$, k=1,2,...,6 of a given body with inertia properties $\bar{m}_{jk}$ are given by, refer to eq.(4.3.9)

$$(-\eta_2\bar{m}_{jk} + K_{jk})\bar{W}_k = f_j \tag{5.3.7}$$

(ii) Uncoupled Vertical Vibration

$\bar{V}_3$ is the only motion of the body considered in this case and the contact conditions are

Relaxed Contact Conditions:-

$$\begin{aligned} \bar{u}_1 &= \text{unknown} \\ \bar{u}_2 &= \text{unknown} \\ \bar{u}_3 &= \bar{V}_3 \\ \bar{t}_1 &= 0 \\ \bar{t}_2 &= 0 \\ \bar{t}_3 &= \text{unknown} \end{aligned} \tag{5.3.8}$$

Welded Contact Conditions:-

$$\begin{aligned} \bar{u}_1 &= 0 \\ \bar{u}_2 &= 0 \\ \bar{u}_3 &= \bar{V}_3 \\ \bar{t} &= \text{unknown} \\ \bar{t}_2 &= \text{unknown} \\ \bar{t}_3 &= \text{unknown} \end{aligned} \tag{5.3.9}$$

$\bar{V}_3 = 1$ is used and the dynamic stiffness is $K_{33} = \bar{Q}_3$. The

response $\bar{W}_3$ of a foundation with mass ratio $\bar{m}_{33}$ is obtained from

$$(-\eta_2\bar{m}_{33} + K_{33})\bar{W}_3 = f_3 \tag{5.3.9}$$

for excitation f_3.

(iii) Uncoupled Horizontal Vibration in x_2-direction

Only motion $\bar{V}_2$ is considered. The contact conditions are

Relaxed Contact Conditions:-

$$\begin{aligned} \bar{u}_1 &= \text{unknown} \\ \bar{u}_2 &= \bar{V}_2 \\ \bar{u}_3 &= \text{unknown} \\ \bar{t}_1 &= 0 \\ \bar{t}_2 &= \text{unknown} \\ \bar{t}_3 &= 0 \end{aligned} \tag{5.3.10}$$

$\bar{V}_2 = 1$ is prescribed. The dynamic stiffness is $K_{22} = \bar{Q}_2$ and the response $\bar{W}_2$ of a body of mass ratio $\bar{m}_{22}$ to excitation f_2 is

$$(-\eta_2\bar{m}_{22} + K_{22})\bar{W}_2 = f_2 \tag{5.3.12}$$

(iv) Uncoupled Rocking about x_1-axis

Motion $\bar{V}_4$ is considered. The contact conditions are

Relaxed Contact Conditions:-

$$\begin{aligned} \bar{u}_1 &= \text{unknown} \\ \bar{u}_2 &= \text{unknown} \\ \bar{u}_3 &= \bar{x}_2\bar{V}_4 \\ \bar{t}_1 &= 0 \end{aligned} \tag{5.3.13}$$

$$\bar{t}_2 = 0$$

$$\bar{t}_3 = \text{unknown}$$

Using $\bar{V}_4 = 1$ the dynamic stiffness is $K_{44} = \bar{Q}_4$, and the response of a body with inertia ratio $\bar{m}_{44}$ is $\bar{W}_4$ given by

$$(-\eta_2\bar{m}_{44} + K_{44})\bar{W} = f_4 \tag{5.3.15}$$

(v) Uncoupled Torsional Vibration

The motion of the body is $\bar{V}_6$, and we have the contact conditions

Relaxed Contact Conditions:-

$$\begin{aligned} \bar{u}_1 &= -\bar{x}_2\bar{V}_6 \\ \bar{u}_2 &= \bar{x}_1\bar{V}_6 \\ \bar{u}_3 &= \text{unknown} \\ \bar{t}_1 &= \text{unknown} \\ \bar{t}_2 &= \text{unknown} \\ \bar{t}_3 &= 0 \end{aligned} \tag{5.3.16}$$

Using $\bar{V}_6 = 1$ the dynamic stiffness is $K_{66} = \bar{Q}_6$, and the response $\bar{W}_6$ of a body with inertia ratio $\bar{m}_{66}$ is given by

$$(-\eta_2\bar{m}_{66} + K_{66})\bar{W}_6 = f_6 \tag{5.3.18}$$

The boundary conditions on the unloaded portion of the surface are, unmistakably,

$$\bar{u}_j = \text{unknown}, \quad \bar{t}_j = 0, \quad j=1,2,3 \tag{5.3.19}$$

5.4 APPLYING THE BOUNDARY INTEGRAL EQUATION

We recall the boundary integral equation (2.5.13) and put it in the dimensionless form

$$c_{jk}\bar{u}_k(P) + \int_{\bar{S}} \bar{T}_{jk}(P,Q)\bar{u}_k(Q)\ d\bar{s}(Q)$$

$$= \int_{\bar{S}} \bar{U}_{jk}(P,Q)\bar{t}_k(Q)\ d\bar{s}(Q) \qquad (5.4.1)$$

where $\bar{T}_{jk} = b^2 T_{jk}$ $\qquad$ $\bar{U}_{jk} = \mu b U_{jk}$

U_{jk} and T_{jk} are given by eqs.(2.4.7) and (2.4.6)

Expressions for $\bar{U}_{jk}$ and $\bar{T}_{jk}$ on the Half Space Boundary

The unit normal $\hat{n}$ to the half space boundary, has components

$$n_1 = 0 = n_2, \quad n_3 = -1$$

see fig.(5.1) for choice of coordinates. The distance between $P(\underline{y})$ and $Q(\underline{x})$ is given by

$$\bar{R}(P,Q) = \left\{(\bar{x}_1 - \bar{y}_1)^2 + (\bar{x}_2 - \bar{y}_2)^2\right\}^{\frac{1}{2}}$$

Note that

$$\frac{\partial \bar{R}}{\partial \bar{x}_j} = \frac{\bar{R}_j}{\bar{R}} = \frac{\bar{x}_j - \bar{y}_j}{\bar{R}}\ ; \qquad \frac{\partial \bar{R}}{\partial \bar{x}_3} = 0 = \frac{\partial \bar{R}}{\partial n}$$

$\bar{R}_j$ is the j-component of the position vector from P to Q.

Substituting these results into eqs.(2.4.6) and (2.4.7) we find

$$\bar{U}_{jk} = \begin{bmatrix} \bar{U}_{11} & \bar{U}_{12} & 0 \\ \bar{U}_{21} & \bar{U}_{22} & 0 \\ 0 & 0 & \bar{U}_{33} \end{bmatrix}$$

$$\bar{T}_{jk} = \begin{bmatrix} 0 & 0 & \bar{T}_{13} \\ 0 & 0 & \bar{T}_{23} \\ \bar{T}_{31} & \bar{T}_{32} & \bar{T}_{33} \end{bmatrix} \qquad (5.4.2)$$

where

$$\bar{U}_{11} = \tfrac{1}{4}\pi \frac{1}{\bar{R}} \left\{ \Psi + (3\Phi + \chi) \frac{\bar{R}_1 \bar{R}_1}{\bar{R}^2} \right\}$$

$$\bar{U}_{12} = \tfrac{1}{4}\pi \frac{1}{\bar{R}} \left\{ (3\Phi + \chi) \frac{\bar{R}_1 \bar{R}_2}{\bar{R}^2} \right\}$$

$$\bar{U}_{21} = \bar{U}_{12}$$

$$\bar{U}_{22} = \tfrac{1}{4}\pi \frac{1}{\bar{R}} \left\{ \Psi + (3\Phi + \chi) \frac{\bar{R}_2 \bar{R}_2}{\bar{R}^2} \right\}$$

$$\bar{U}_{33} = \tfrac{1}{4}\pi \frac{1}{\bar{R}} \Psi$$

$$\bar{T}_{13} = -\tfrac{1}{4}\pi \frac{\bar{A}_4}{\bar{R}^2}\frac{\bar{R}_1}{\bar{R}}$$

$$\bar{T}_{23} = -\tfrac{1}{4}\pi \frac{\bar{A}_4}{\bar{R}^2}\frac{\bar{R}_2}{\bar{R}}$$

$$\bar{T}_{31} = -\tfrac{1}{4}\pi \frac{\bar{A}_3}{\bar{R}^2}\frac{\bar{R}_2}{\bar{R}}$$

$$\bar{T}_{32} = -\tfrac{1}{4}\pi \frac{\bar{A}_3}{\bar{R}^2}\frac{\bar{R}_2}{\bar{R}}$$

$$\Psi = \gamma^2 \exp(i\eta_1\bar{R}) - \exp(i\eta_2\bar{R})$$

$$\Phi = \frac{1}{\eta_2^2\bar{R}^2}\left\{\exp(i\eta_2\bar{R})-\exp(i\eta_1\bar{R})\right\} + \frac{i}{\eta_2\bar{R}}\left\{\exp(i\eta_2\bar{R})-\gamma\exp(i\eta_1\bar{R})\right\}$$

$$\chi = \exp(i\eta_2\bar{R}) - \Phi$$

$$\bar{A}_3 = (i\eta_2\bar{R} - 1)\exp(i\eta_2\bar{R}) + 6\Phi + 2\chi$$

$$\bar{A}_4 = (1 - 2\gamma^2)(i\eta_1\bar{R} - 1)\exp(i\eta_1\bar{R}) + 6\Phi + 2\chi$$

The Boundary Elements.

The boundary is represented by eight-node quadrilateral elements as described in chapter 3, see fig.3.2. The arrangement of the elements on the boundary will be dictated mostly by the shape of the contact area. Figs.5.2., 5.3, and 5.4 show possible mesh arrangements for arbitrarily shaped

contact area, circular area and square area respectively. The mesh for a rectangular area is obtained by simply multiplying, say, the x_2-coordinates of the mesh points by the desired aspect ratio. It is observed that contact areas bounded by curved lines (e.g., circular or arbitrary shape) as well as straight lines (e.g., rectangular) are adequately represented.

In this problem where the nodal points are considerably more than those used in the two-dimensional case of previous chapter, we would like to take advantage of symmetry immediately where possible in order to reduce the computer storage requirements sufficiently to allow in-core matrix operations on the algebraic equations rather than employ disc-based methods. However, disc-based methods are unavoidable for the non-symmetric shapes as well as the coupled modes of vibration where the whole mesh has to be represented. Fig.5.5 shows the square mesh arrangement used for the results presented in this chapter. Any required ractangular shape may be obtained by multiplying, say, the x_2-coordinats by given width/length ratio. This leaves the half-length (x_1-dimension) of the rectangle fixed at unity while the width varies. Taking account of symmetry, only the variables at the first-quadrant nodes are computed although integration still had to be carried out on every individual element. The shaded area is the area of contact with the rigid foundation. The dimension of the outermost rectangle is indicated by R_o,

and is the area to which the BIE integrals are truncated as suggested in section 3.2. A rectangle is use here, instead of a circle as suggested in section 3.2, to indicate region R_o only for convenience. A circle would do equally well. The discretised boundary integral equation (3.3.10) is written

$$\tfrac{1}{2}\bar{u}_j(P^a) + \sum_{\ell=1}^{L}\sum_{c=1}^{8}\bar{u}_k\Big(d(\ell,c)\Big)\int_{\bar{S}_\ell}\bar{T}_{jk}\Big(P^a,Q(\underline{\xi})\Big)M_c(\underline{\xi})J(\underline{\xi})\ d\xi_1 d\xi_2$$

$$\sum_{\ell=1}^{L}\sum_{c=1}^{8}\bar{t}_k\Big(d(\ell,c)\Big)\int_{\bar{S}_\ell}\bar{U}_{jk}\Big(P^a,Q(\underline{\xi})\Big)M_c(\underline{\xi})J(\underline{\xi})\ d\xi_1 d\xi_2 \qquad (5.4.3)$$

The Jacobian of transformation $J(\underline{\xi})$ has been defined in section 3.3. The system of algebraic equations is formed by writing above equation for every nodal position of P ranging over only the first quadrant nodes if symmetry is employed. Fig.(5.5b) shows the mesh used for the circular foundation. One may choose to analyse the foundation by treating the base just like any arbitrary shape with the mesh arrangement indicated, and then proceed to solve for the variables at every node. But at this stage we shall simplify matter by introducing circular symmetry which applies to the vertical motions that we shall analyse. Circular cylindrical coordinates (r,θ,z) are introduced such that

$$x_1 = r.\cos\theta$$

$$x_2 = r.\sin\theta$$

$$x_3 = z$$

The implementation is to set up the algebraic equation (5.4.3) for a given position of point P by integrating over all elements. The variables in the equation which are with respect to rectangular coordinates x_1, x_2, x_3 are converted to variables in cylindrical coordinates using the relations

$$u_1 = u_r\cos\theta - ru_\theta\sin\theta$$

$$u_2 = u_r\sin\theta + ru_\theta\cos\theta$$

$$u_3 = u_z$$

and similarly for t_k.

Then we note that for the vertical and torsional vibrations corresponding variables at all nodes arranged on a given circle in the mesh are equal.

The following notation shall be used for the vector components in the cylindrical coordinate system.

t_r is shear stress component in radial direction,

t_θ, tensor component of shear stress in θ -direction,

$\tau \equiv rt_\theta$, physical component of shear stress in θ-direction,

$t_z \equiv t_3$, normal stress in z-direction,

Θ_3, angular motion of massive foundation about x_3-axis,

Υ_3, couple appied to the massive foundation about x_3-axis.

The next section gives details of the integration scheme over each element.

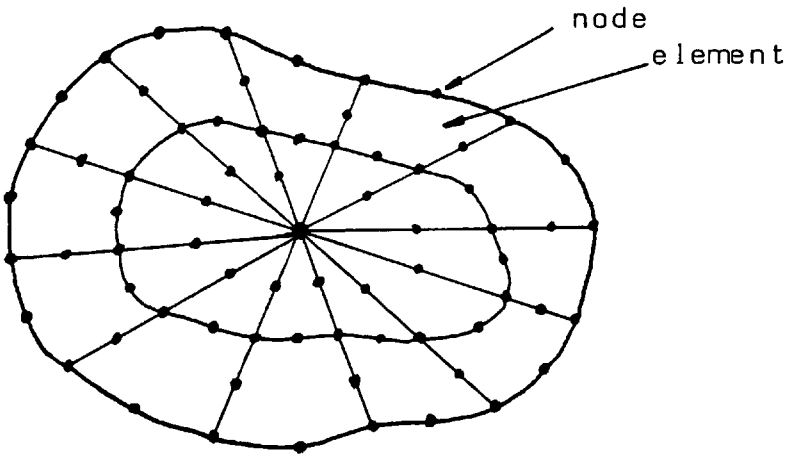

Fig 5.2 Arbitrary Shape

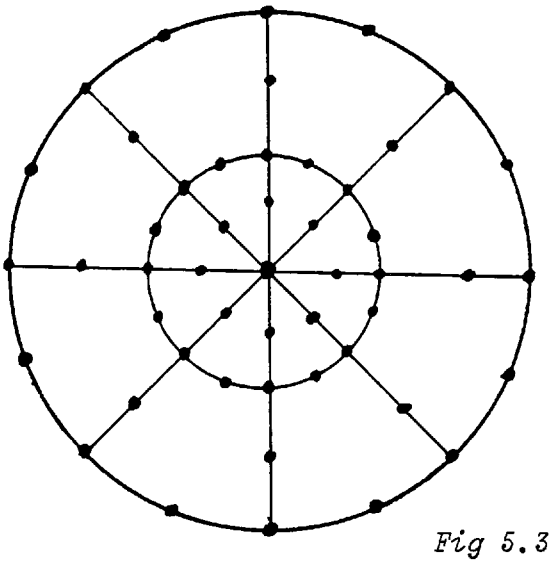

Fig 5.3 Circular Shape

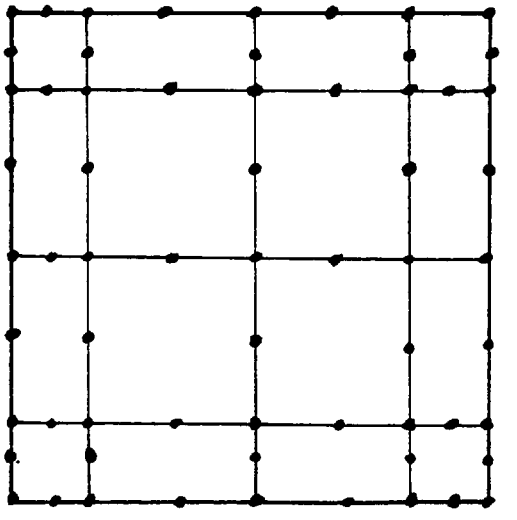

Fig 5.4 Square Shape

Example Mesh Node Arrangements on Various Shapes of Contact Surface

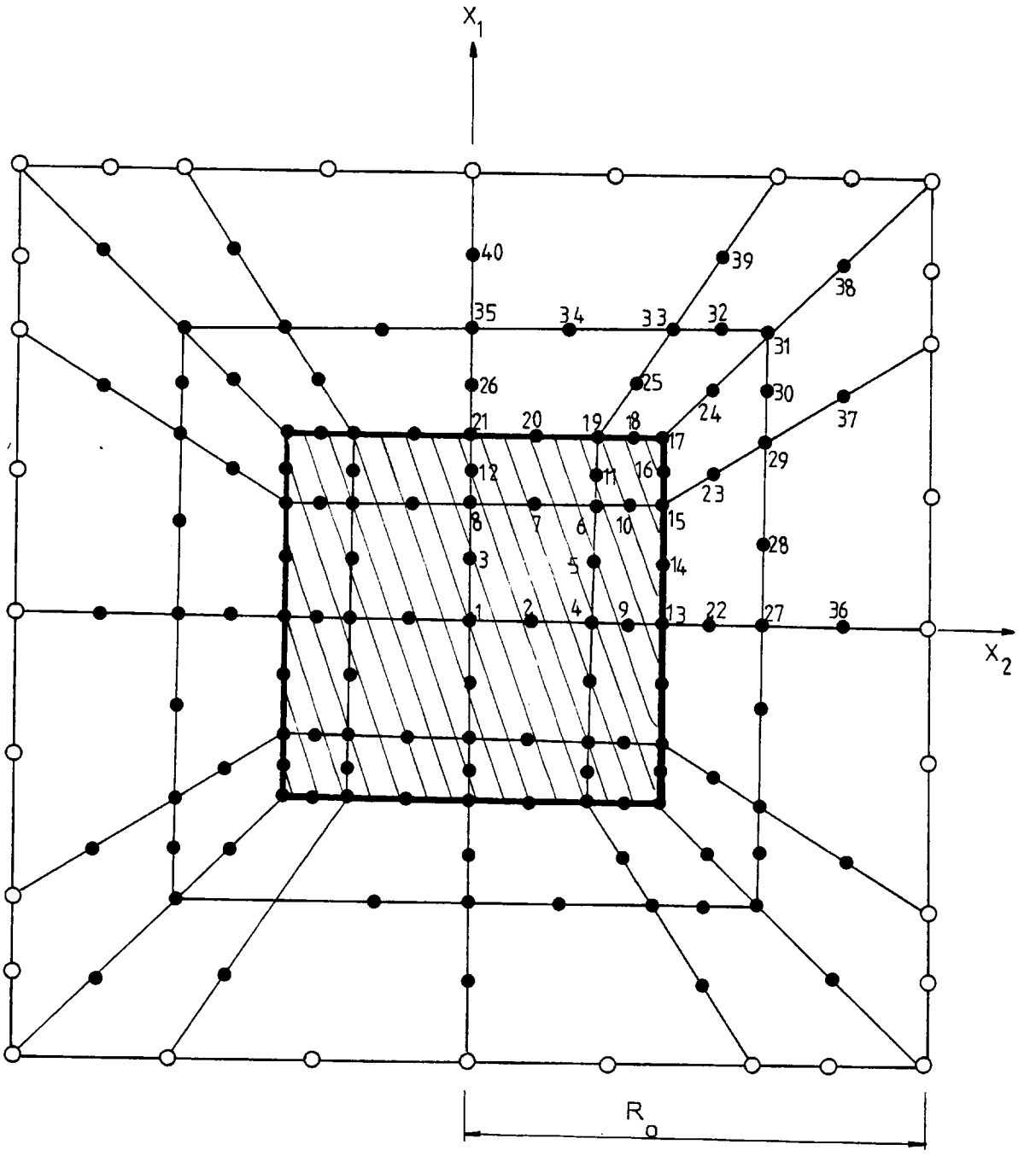

● nodes contributing to the BIE integrals

○ these and farther nodes do not contribute

Fig 5.5a Mesh Node Arrangement for Square Foundation (not to scale)

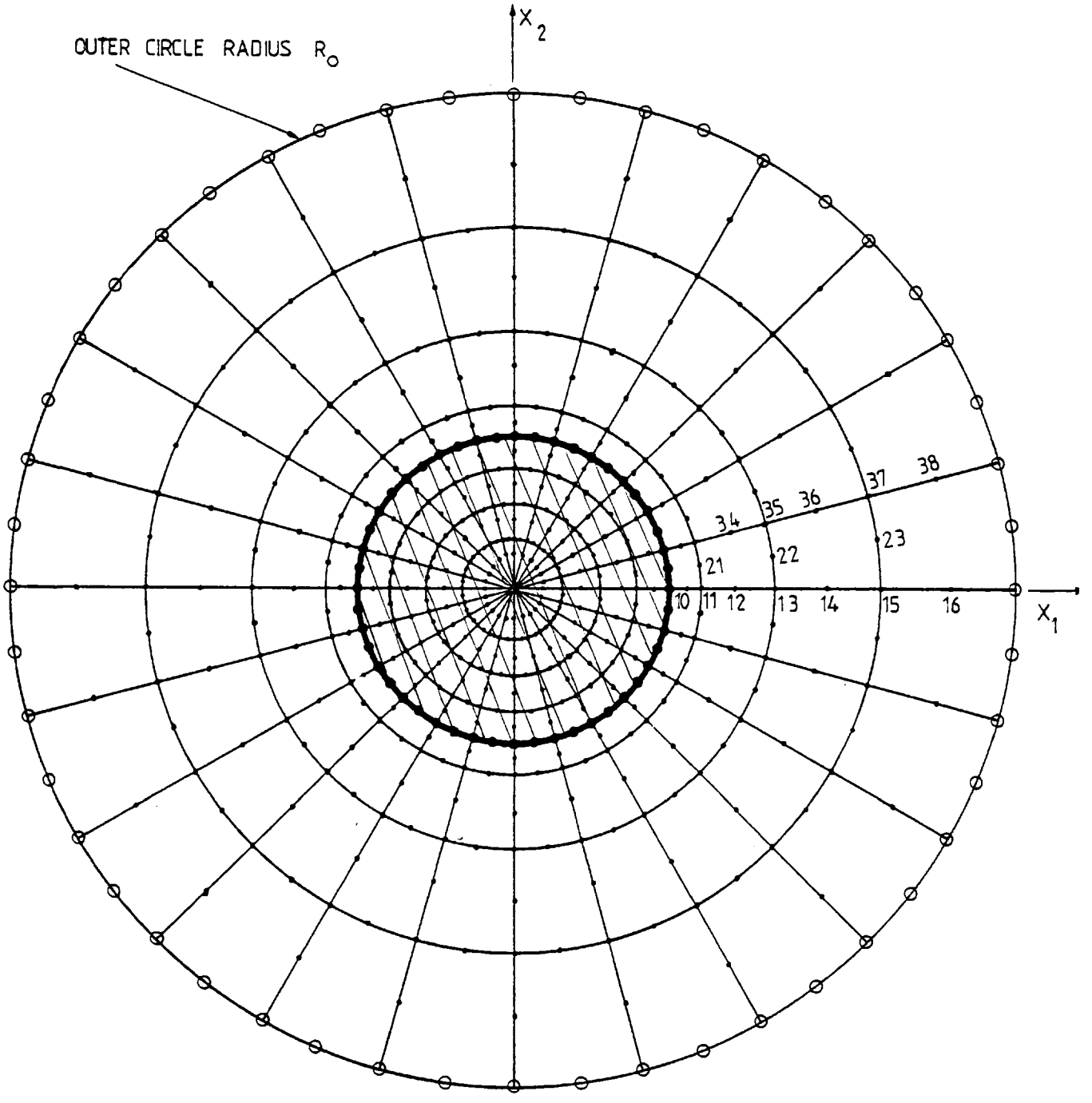

● nodes contributing to the BIE integrals

○ these and farther nodes do not contribute

Fig 5.5b Mesh Node Arrangement for Circular Foundation (not to scale)

5.5 NUMERICAL INTEGRATION SCHEME

The two-dimensional form of the Gauss-Legendre n-point quadrature scheme is employed. The integration of a function $f(\xi_1, \xi_2)$ is approximated by

$$\int_{-1}^{+1}\int_{-1}^{+1} f(\xi_1, \xi_2)d\xi_1 d\xi_2 \simeq \sum_{j=1}^{n_1}\sum_{k=1}^{n_2} f(\xi_{1j}, \xi_{2k})w_{1j}w_{2k} \qquad (5.5.1)$$

where w_{1j} and w_{2k} are the weights corresponding to abscissae ξ_{1j}, ξ_{2k}.

Cases to consider during the integrations are:

(i) Point P not a Member of Element:-

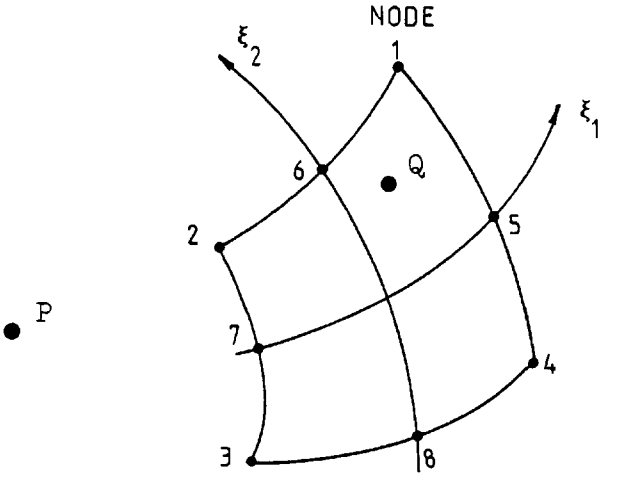

Fig 5.6 Point P Outside Integration Element

The Gauss-Legendre scheme (5.5.1) above is used directly over the element as no singularity of the integrands in (5.4.3) occurs. At a given point Q selected by values of ξ_1 and ξ_2, the coordinates are determined by interpolation over the nodal coordinates as described in section 3.3, see eq.(3.3.7)

$$\bar{x}_{jQ} = \sum_{c=1}^{8} M_c(\xi_1, \xi_2)(\bar{x}_j)_c$$

(ii) Point P a Member of the Element:-

The singularities of $\bar{U}_{jk}$ and $\bar{T}_{jk}$ at P now occur within the integration element. The procedure to deal with this is exactly as described by Lachat and Watson (1975) for elastostatics problems. The element is subdivided into two or three triangular subelements according as P is a corner or mid-point node, fig.5.7, each triangle having a vertex at P. A local system of coordinates ζ_j, j=1,2 is defined for each triangle, fig.5.8, such that the element coordinates ξ_j at a point Q in a triangle are interpolated linearly from the values at the corners of the triangle as

$$\xi_j = \xi_j(\underline{\zeta}) = \sum_{m=1}^{4} L_m(\underline{\zeta})\, \xi_{jm} \qquad (5.5.2)$$

ξ_{jm}, m=1,2,3,4, are the values of ξ_j at the four nodes of the triangular subelement.

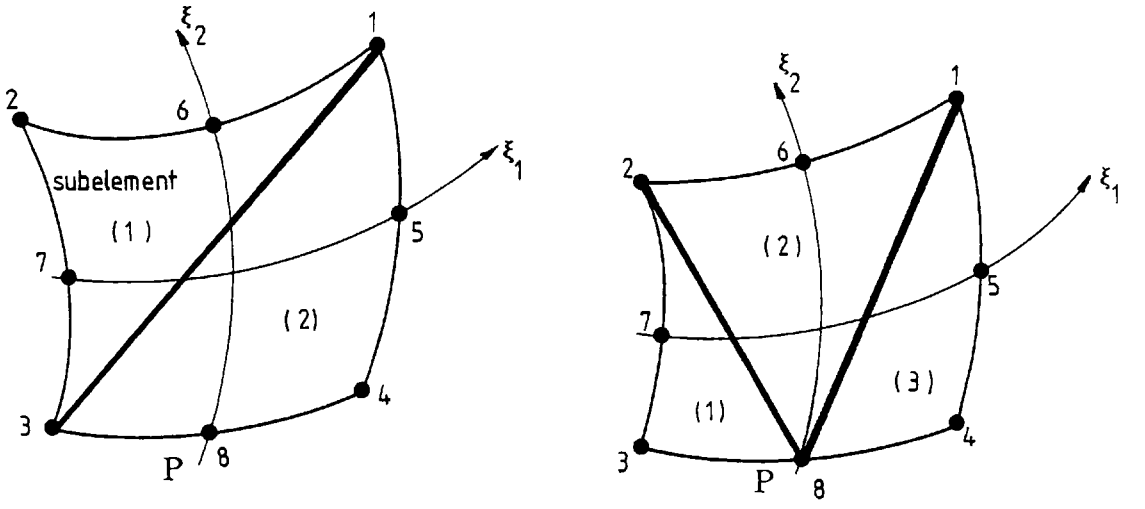

Fig 5.7 Element Subdivision

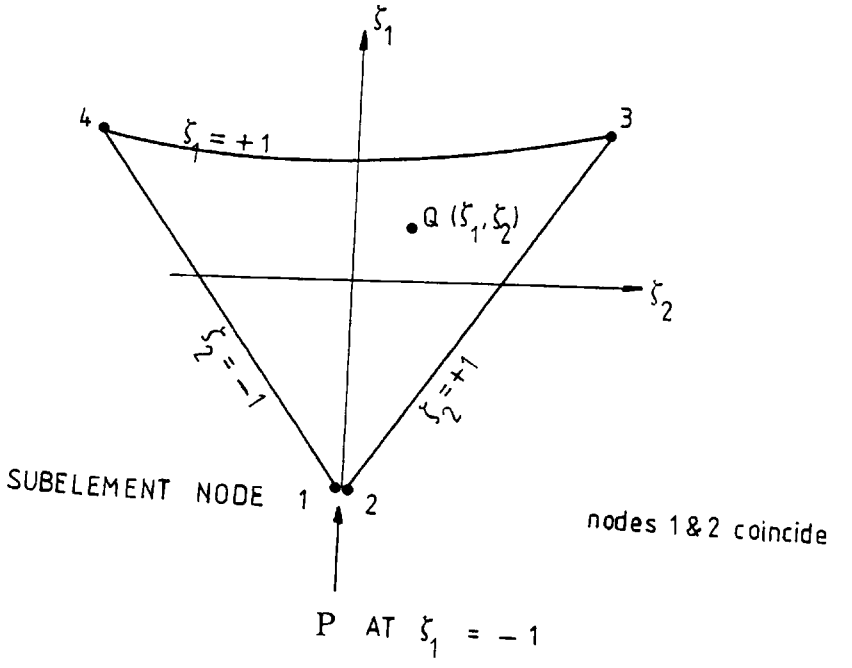

Fig 5.8 Subelement Coordinates ζ_j

$L_m(\underline{\zeta})$ are the linear interpolating functions defined by

$$\begin{aligned} L_1(\underline{\zeta}) &= \tfrac{1}{4}(1-\zeta_1)(1-\zeta_2) \\ L_2(\underline{\zeta}) &= \tfrac{1}{4}(1-\zeta_1)(1+\zeta_2) \\ L_3(\underline{\zeta}) &= \tfrac{1}{4}(1+\zeta_1)(1+\zeta_2) \\ L_4(\underline{\zeta}) &= \tfrac{1}{4}(1+\zeta_1)(1-\zeta_2) \end{aligned} \qquad (5.5.3)$$

The Jacobian of transformation from ξ_j to ζ_j is

$$H(\underline{\zeta}) = \begin{bmatrix} \dfrac{\partial \xi_1}{\partial \zeta_1} & \dfrac{\partial \xi_1}{\partial \zeta_2} \\ \dfrac{\partial \xi_2}{\partial \zeta_1} & \dfrac{\partial \xi_2}{\partial \zeta_2} \end{bmatrix} \qquad (5.5.4)$$

in which $\partial \xi_j / \partial \zeta_k$ is evaluated from representation (5.5.2). Thus the transformation from ζ_j to the global coordinates x_j is via the Jacobian $J(\underline{\xi})H(\underline{\zeta})$. A typical integral from eq.(5.4.3) takes the form

$$\int_{-1}^{+1}\int_{-1}^{+1} \bar{T}_{jk}\left(P^a, Q\left(\underline{\xi}(\underline{\zeta})\right)\right) M_c\left(\underline{\xi}(\underline{\zeta})\right) J\left(\underline{\xi}(\underline{\zeta})\right) H(\underline{\zeta})\, d\zeta_1 d\zeta_2 \qquad (5.5.5)$$

over a triangular subelement.

It is observed that at P the singularities of $\bar{T}_{jk}$ and $\bar{U}_{jk}$ are of order $O(1/\bar{R}^2)$ and $O(1/\bar{R})$ respectively, section 2.5. It may be seen that since lines $\zeta_2 = +1$ and $\zeta_2 = -1$ converge to a point at P, fig.5.8, the Jacobian $H(\underline{\zeta})$ is $O(\bar{R})$. Also the shape function $M_c(\underline{\xi})$ for all nodes other than that at P is also $O(\bar{R})$. Thus the integrand in (5.5.5) tends to a finite limit at P and the Gauss-Legendre scheme (5.5.1) can be used safely. Now the shape function $M_P(\underline{\xi})$ at node P tends to unity at P. The integrands containing $\bar{U}_{jk}$ still tends to a finite limit at P since $\bar{U}_{jk}$ is only $O(1/\bar{R})$ and the Jacobian $H(\underline{\zeta})$ of $O(\bar{R})$ is still available. So scheme (5.5.1) is still good for such integrals. The integral containing $\bar{T}_{jk}$ for node P, however, does not exist over element ℓ alone, but its principal value over all surrounding elements exists. Just as in the two-dimensional problem of previous chapter, ignoring this principal value does not introduce much error into our results. For the Gauss-Legendre quadrature scheme (5.5.1) the order (n_1, n_2) used was (4,4) for the small elements in the loaded region and (8,4) and (10,4) for the outer elements.

5.6 APPLYING THE BOUNDARY CONDITIONS TO THE ALGEBRAIC EQUATIONS

After the integration described in the previous section we end up with the system of equations

$$[B_1]\{u\} = [B_2]\{t\} \tag{5.6.1}$$

similar to system (4.6.1) in chapter 4. In expanded form

$$\begin{bmatrix} \begin{bmatrix} b_{11}^{(1)} \end{bmatrix} & \begin{bmatrix} b_{12}^{(1)} \end{bmatrix} & \begin{bmatrix} b_{13}^{(1)} \end{bmatrix} & \cdots & \begin{bmatrix} b_{1N}^{(1)} \end{bmatrix} \\ \cdots & \cdots & \cdots & \cdots & \cdots \\ \cdots & \cdots & \begin{bmatrix} b_{mn}^{(1)} \end{bmatrix} & \cdots & \cdots \\ \cdots & \cdots & \cdots & \cdots & \cdots \\ \begin{bmatrix} b_{N1}^{(1)} \end{bmatrix} & \begin{bmatrix} b_{N2}^{(1)} \end{bmatrix} & \begin{bmatrix} b_{N3}^{(1)} \end{bmatrix} & \cdots & \begin{bmatrix} b_{NN}^{(1)} \end{bmatrix} \end{bmatrix} \begin{Bmatrix} \begin{bmatrix} \bar{u}_1 \\ \bar{u}_2 \\ \bar{u}_3 \end{bmatrix}_1 \\ \cdots \\ \begin{bmatrix} \bar{u}_1 \\ \bar{u}_2 \\ \bar{u}_3 \end{bmatrix}_m \\ \cdots \\ \begin{bmatrix} \bar{u}_1 \\ \bar{u}_2 \\ \bar{u}_3 \end{bmatrix}_N \end{Bmatrix}$$

$$= \begin{bmatrix} \begin{bmatrix} b_{11}^{(2)} \end{bmatrix} & \begin{bmatrix} b_{12}^{(2)} \end{bmatrix} & \begin{bmatrix} b_{13}^{(2)} \end{bmatrix} & \cdots & \begin{bmatrix} b_{1N}^{(2)} \end{bmatrix} \\ \cdots & \cdots & \cdots & \cdots & \cdots \\ \cdots & \cdots & \begin{bmatrix} b_{mn}^{(2)} \end{bmatrix} & \cdots & \cdots \\ \cdots & \cdots & \cdots & \cdots & \cdots \\ \begin{bmatrix} b_{N1}^{(2)} \end{bmatrix} & \begin{bmatrix} b_{N2}^{(2)} \end{bmatrix} & \begin{bmatrix} b_{N3}^{(2)} \end{bmatrix} & \cdots & \begin{bmatrix} b_{NN}^{(2)} \end{bmatrix} \end{bmatrix} \begin{Bmatrix} \begin{bmatrix} \bar{t}_1 \\ \bar{t}_2 \\ \bar{t}_3 \end{bmatrix}_1 \\ \cdots \\ \begin{bmatrix} \bar{t}_1 \\ \bar{t}_2 \\ \bar{t}_3 \end{bmatrix}_m \\ \cdots \\ \begin{bmatrix} \bar{t}_1 \\ \bar{t}_2 \\ \bar{t}_3 \end{bmatrix}_N \end{Bmatrix} \tag{5.6.2}$$

$b^{(1)}_{mn}$ are 3x3 submatrices obtained from integrations of kernel tensor $\bar{T}_{jk}$, and $b^{(2)}_{mn}$ 3x3 submatrices obtained from $\bar{U}_{jk}$. As in the two-dimensional case we are now in a position to apply any boundary conditions we care to prescribe. The desired final system of equations is of the form

$$[A]\{z\} = \{B\} \tag{5.6.3}$$

in which $\{z\}$ is the vector of the unknowns and $\{B\}$ is formed from the prescribed boundary data.

The system (5.6.2) is partitioned to distinguish between variables in the loaded region S_1 and those in the stress-free surface S_o

$$\left[\begin{array}{c:c} S_1 & S_o \end{array}\right] \left\{\begin{array}{c} \bar{u}_{S_1} \\ \hdashline \bar{u}_{So} \end{array}\right\} = \left[\begin{array}{c:c} S_1 & S_o \end{array}\right] \left\{\begin{array}{c} \bar{t}_{S_1} \\ \hdashline \bar{t}_{So} \end{array}\right\} \tag{5.6.4}$$

The procedure for applying the boundary conditions described in section 5.3 is straightforward and exactly the same as described in chapter 4. The shuffling of the elements of matrices B_1 and B_2 applies only to the S_1-columns. We describe here the procedure only for the general six degrees-of-freedom motion, the others being even more straightforward.

The Six Degree-of-freedom Vibration

As in chapter 4 a suitable choice of the array $\bar{V}_n^{(m)}$ is selected to ensure that system (5.3.6) is not singular. To effect eqs.(5.3.1), multiply the u_1-columns of matrix B_1 by $\bar{V}_1^{(m)} - \bar{x}_2\bar{V}_6^{(m)}$, the u_2-columns by $\bar{V}_2^{(m)} + \bar{V}_6^{(m)}$ and the u_3-columns by $\bar{V}_3^{(m)} + \bar{x}_2\bar{V}_4^{(m)} - \bar{x}_1\bar{V}_5^{(m)}$, sum up the results and transfer the sum to the mth column of array B, which should have up to six columns available.

To effect eqs.(5.3.2), all the S_1-columns of matrix B_2 are transferred to replace those of B_1 as the coefficients of the unknown stresses. Again the procedure can very neatly be coded in a computer subprogram.

After sorting the final system the stress integrals $\bar{Q}_n^{(m)}$ are computed and the stiffnesses obtained as described in section 5.3, eq.(5.3.6)

Some Programming Hints

As in the problem of chapter 4 computer space does not have to be allocated for the entire size of array B_2. In this case only three rows of the S_1-columns are required at any one time because for a given position of point P, integration of eq.(5.4.3) yields three rows of equations simultaneously corresponding to j=1,2,3. The boundary conditions are applied immediately after the rows are computed and the space allocated to B_2 is released for the next round of integrations.

To solve the general six degrees-of-freedom motion as described above requires storage allocation for all the nodal variables in the entire mesh of figs.5.2, 5.3, 5.4 because no symmetry is expected. Disc-based method of solution would be required. The results presented in this chapter for vertical mode do admit symmetry, and requires only computer in-core handling of the matrices.

5.7 RESULTS AND DISCUSSIONS

(a)i Circular Foundation

The circular foundation is a good test case to check the accuracy of the BIE formulation because solutions of many aspects of the vibration are well known. In particular we shall use the vertical and torsional modes. The vertical mode has been well analysed by Awojobi and Grootenhuis (1965). Closed-form analytical solution for the torsional mode has been given by Reissner and Sagoci (1944), the graphical reproductions of which may be obtained from Eringen and Suhubi (1975) or Arnold, Bycroft and Warburton (1955). The latter reference also provides experimental results for the two modes of vibration.

(a)ii Circular Foundation, Vertical Vibration

It was found that the compliance curves converged to a definite limit for integration over regions indicated by radius R_o, fig.5.5b, greater than or equal to 5. This value is therefore used for all computations for the circular foundation.

Fig.5.10 shows the compliance for vertical vibration under relaxed conditions. In the figure the approximate analysis of Arnold, Bycroft and Warburton (1955) compares fairly well with the present results. The response of the foundation is calculated for three mass ratios and compared with the

analytical solutions of Awojobi and Grootenhuis (1965) in fig.5.11 where remarkable agreement is observed. The experimental results of Arnold et al are also included in the figure.

(a)iii Circular Foundation, Torsional Vibration

The shear stress under the rigid body is computed as the non-dimensional quantity $\bar{\tau} = \pi\tau/4\mu\Theta_3$ using the notation introduced in section 5.4 for the cylindrical coordinate system. The components of the stress in phase with and in quadrature with displacement are plotted in figs.5.12 and 5.13 respectively. The in-phase component decreases with increasing frequency factor η_2 while the quadrature component increases. The results are independent of Poisson ration.

The torsional stiffness is plotted in fig.5.14. The compliance, inverse of stiffness, is plotted in fig.5.15. The compliance, a non-dimensional ratio of angle of rotation V_6 and the resultant moment Q_6 of surface shear stress, is compared in fig.5.15 with the exact results by Reissner and Sagoci (1944). Remarkable agreement is achieved.

In fig.5.16 the non-dimensional torsional response amplitude $\bar{W}_6 = \mu b W_6/F = \mu b^3\Theta_3/T_3$ is computed for inertia ratios $m_{66} = \bar{J}_3/\rho b^5 = 5.34,\ 3.49$. Discrepancies exist between these results and those of Awojobi and Grootenhuis (1965), but good agreement is achieved with the experimental results of Arnold,

Bycroft and Warburton (1955) at frequencies below resonance.

(b)i Rectangular Foundation, Vertical Vibration

The effect of truncation of the BIE integrals on the results was examined with square foundation in vertical vibration. The compliance is plotted in fig.5.17 for various values of R_o. Convergence is rapidly achieved, and in fact the only results that are out of place are those corresponding to excluding the whole free surface from the integration (R_o=1). The results for R_o=5 and R_o=10 coincide, and indicate that no further increase in R_o will give any difference in the results. The value R_o=5 is used in subsequent results.

In fig.5.18a and 5.18b the real and imaginary parts of vertical compliance are compared respectively with similar results from Wong and Luco (1976) for Poisson ratio 1/3. Discrepancies are observed. It may also be noted that Wong and Luco obtained their results from numerical integration of complicated infinite integrals involving oscillatory functions whose accuracy is always difficult to guarantee. Results from Hamidzadeh (1978) are also included. The present results lie midway between the two previous works.

The dynamic stiffnesses for various width/length ratio a_r of the rectangular foundation are also computed and presented in figs.5.19. In figs.5.20a,b,c the vertical response is presented for aspect ratios a_r=1,8,16 respectively for various mass ratios $\bar{m}_{33}$.

The in-phase and quadrature components of the normal stress distribution are plotted in figs.5.21a and 5.21b respectively for a square foundation. The values plotted are those taken along one-half of the center line of the square, and are for Poisson ratio 1/4 of the supporting medium. The two-dimensional stress distribution is symmetric along the vertical x_3-axis. It is observed that the in-phase component of stress decreases with increasing frequency factor, fig.5.21a, while the quadrature component increases, fig.5.21b. The results clearly indicate the characteristic edge singularities of the stress distribution, and demonstrate that this significant feature is not lost in the BIE formulation, unlike other numerical methods such as that of Wong and Luco (1976).

A fuller picture of the stress distribution is presented in the three-dimensional computer graphical outputs of figs.5.22a,b for frequency factor 0.05, and figs.5.23a,b for frequency factor 0.8. The graphs show the stresses plotted as ordinates on one quadrant of the square base (the negative of the quadrature components are plotted). The edge singularities may be clearly observed, the peaks being sharper at the corners. Imagining the picture for the whole square base taken together presents a rather interesting image of a sporting arena surrounded by stepped seats with floodlight posts at the four corners.

(b)iii Rectangular Foundation, Horizontal Vibration

The horizontal vibration is considered for a square foundation and Poisson ration of the supporting medium of 1/3. The real and imaginary parts of the shear stress $\bar{t}_2$ are plotted in figs.5.24 and 5.25 respectively. The stresses plotted are those values selected along one half of the center line of the square in x_1-axis. The general picture for the entire square would be similar to the three-dimensional plots of figs.5.22a,b and 5.23a,b. As in the circular case, the stress component in phase with displacement decreases with increasing frequency factor while the quadrature component increases.

The horizontal stiffness is shown in fig.5.26. The compliance is plotted in fig.5.27 and compared with the results of Wong and Luco (1976). Large differences are noticed. It is interesting to note that Wong and Luco found that in their numerical integration scheme, the finer they made their mesh grid, see fig.1.1 in chapter 1, the lower their compliance curve. A still finer mesh may be required for their results to converge to the results of this study in fig.5.27.

The horizontal response of the foundation is plotted in fig.5.28 for mass ratios $\bar{m}_{22}$ = 150, 40, 10.

Next we present some interesting results.

(c) On the Idealisation of a "Long" Rectangular Foundation as Infinite Strip

It is informative to ivestigate the question of approximating a long rectangular foundation by an infinite strip. The accuracy of such approximation obviously depends on the length of the rectangle compared to its width. In this section the minimum length/width ratio required for a given approximation is examined.

We consider a rectangular foundation with a base of width/length ratio a_r=b/a, fig.5.9, excited in vertical direction (only vertical vibration is examined).

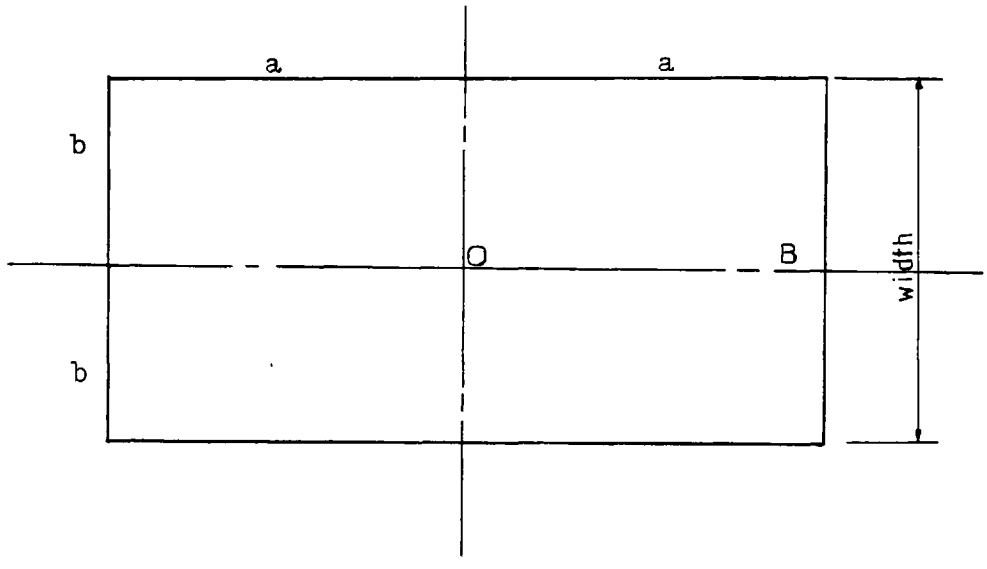

Fig 5.9 Rectangular Base

The mass per unit length is m'. First the analysis of chapter 4 is used to compute the resonance frequency, considering the foundation as an infinite strip of width 2b. Then the analysis of this chapter is used to compute the same quantity taking the foundation base as a finite rectangle that it is. The two results are then compared for various values of the ratio a_r. To be sure that the same quantities are compared in the two cases the frequency factor is taken as $\eta_0 = b\omega/c_2$ and a new mass ratio is defined by $m_o = m'/\rho b^2$. These quantities preserve the definitions used in chapter 4 for frequency factor η_2 and mass ratio $\bar{m}_{22}$ respectively since the half-width was identified with the characteristic length "b". In the three-dimensional analysis of this chapter the characteristic length "b" of the body has been taken as the half-length of the rectangle. Thus the mass ratio "$\bar{m}_{33}$" and frequency factor "η_2" relate to m_o and η_0 respectively by $\bar{m}_{33} = 2a_r^2 m_o$, $\eta_2 = \eta_0/a_r$.

In Table 5.1 the resonance frequency factor η_0 computed by the two methods are compared for various mass ratios m_o=40, 70, 100, 150. Some of the resonance curves for the three-dimensional analysis are shown in figs.5.20a,b,c. The difference between the two results is expressed as a percentage error based on the three-dimensional results. In fig.5.29 this error is plotted against $1/a_r$ for the various mass ratios considered. Thus suppose we have a rectangular foundation of width/length ratio a_r. If we proceed to

simplify matter by assuming an infinitely long ractangle so that the analysis of chapter 4 holds, the error involved in the predicted resonance frequency for a given mass ratio is indicated in fig.5.29 as a percentage of the true result, the true result meaning that obtainable by employing the proper three-dimensional analysis. The smaller the mass ratio the smaller the error. For mass ratio of 40 or less the length of the rectangular base must be at least six times greater than the width to achieve an error of less than 10%. The two-dimensional approximation under-estimates the resonance.

The fact that the error increases with increasing mass ratio may be understood in terms of the role that the mass of the supporting half space plays in the dynamics of foundations. At high mass ratio the rigid foundation provides the greater portion of the effective vibrating mass in the system, while the supporting medium serves mainly to provide the stiffness element. Analogous to an idealised mass-spring system, therefore, the response of the foundation becomes sensitive to the way in which the array of springs is assembled under it, so that it becomes less appropriate to equate the geometry a finite rectangular base imposes on the supporting medium to that imposed by an infinite strip. On the other hand at low mass ratio most ot the effective vibrating mass comes from the distributed mass in the half space, whicn now provides the mass as well as the stiffness elements. The distribution of the stiffness elements becomes

less important because it is followed by similar distribution of the mass elements.

We note interestingly that for a given mass ratio the error of infinite strip idealisation reduces with increasing length/width ratio ($1/a_r$) of the rectangular base. The longer the rectangle the less significant the edge singularity of the stress distribution at the ends (as far as contribution to the integrals of the stress is concerned), as may be observed from fig.5.30. In this figure the in-phase and quadrature components of the normal stresses are plotted along one half of the length-wise center line of the rectangle, i.e., line OB in fig.5.9. The distance along the line, divided by the semi-width "b", is the abscissa of fig.5.30. The stresses are plotted for rectangles of width/length ratio a_r=1,1/4,1/16 and frequency factor 0.6, the aim being to show the effect of the edge singularity on the integrals of the stress which form the dynamic stiffness. It may be observed that the larger the value of $1/a_r$, i.e., the longer the rectangle, the smaller the proportion of the stress integral contained in the region of the singularity. This is in agreement with what is expected from physical reasoning. Consequently the infinite strip analysis which ignores this end singularity becomes less inaccurate.

(d) Concluding Remarks.

The BIE method is as effective for the three-dimensional problem of foundation dynamics as it is for the two-dimensional problem. Again we observe that the same one equation is applicable to any shape of foundation or contact conditions. Many known results have been reproduced easily and cheaply. The agreement of the results for the circular foundation with experimental and exact results is remarkable, figs.5.11 and 5.16. The main computer program consists of setting up the system of equations (5.6.2). With circular symmetry introduced for the circular foundation we ended up only 32 algebraic equations. The calculation of dynamic stiffness for one particular frequency factor took 25 seconds on the average on the CDC Cyber 174 computer at Imperial College. For the rectangular foundation in which such simplification did not exist, 120 algebraic equations had to be solved, and the computation for one frequency factor took 40 seconds on the average.

The flexibility of the BIE method has allowed us to investigate quantitatively the question of how long a rectangular foundation should be compared to its width before it can be safely approximated as an infinitely long rectangular strip. It is hoped that the method will prove to be the easiest way of investigating more of those aspects of foundation dynamics that have so far appeared formidable to

analyse. In the next chapter an indication is given on how the BIE method may be used to investigate the interaction of many foundations on the earth surface and the analysis of flexible foundations.

TABLE 5.1 RESONANCE FREQUENCIES BY TWO TYPES OF ANALYSIS

$1/a_r$	RESONANCE FREQUENCY η_o		%
	INFINITE STRIP ANALYSIS (2)	FINITE RECTANGULAR ANALYSIS (3)	DIFFERENCE ((3) - (2))/(3)
	m_o = 40		
1	.165	.275	40
4	.66	.8	17.5
8	1.32	1.38	4.3
10			
16			
	m_o = 70		
1	.12	.21	42.8
4	.48	.63	23.8
8	.96	1.1	12.7
10	1.2	1.35	11.1
16	1.92	1.95	1.5
	m_o = 100		
1	.1	.175	42.8
4	.4	.54	26
8	.8	.95	15.8
10	1.0	1.17	14.5
16	1.6	1.70	5.9
	m_o = 150		
1	.085	.15	43.0
4	.34	.45	24.4
8	.68	.82	17.1
10	.85	.97	12.4
16	1.36	1.46	6.8

FIG.5.10 VERTICAL COMPLIANCE FOR CIRCULAR FOUNDATION.
POISSON RATIO = 0.

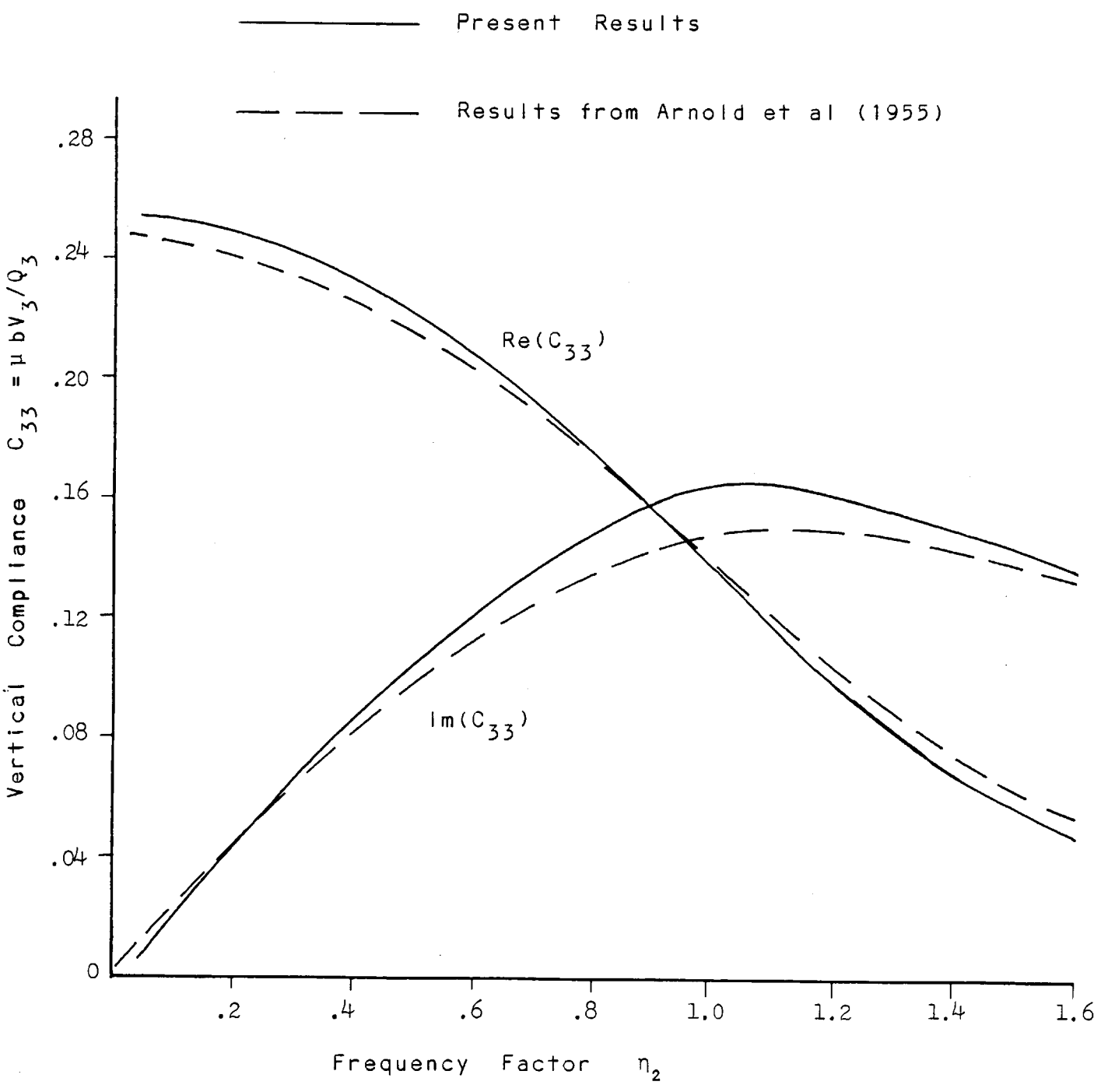

FIG.5.11 NON-DIMENSIONAL VERTICAL AMPLITUDE OF CIRCULAR FOUNDATION.

POISSON RATIO = 0.

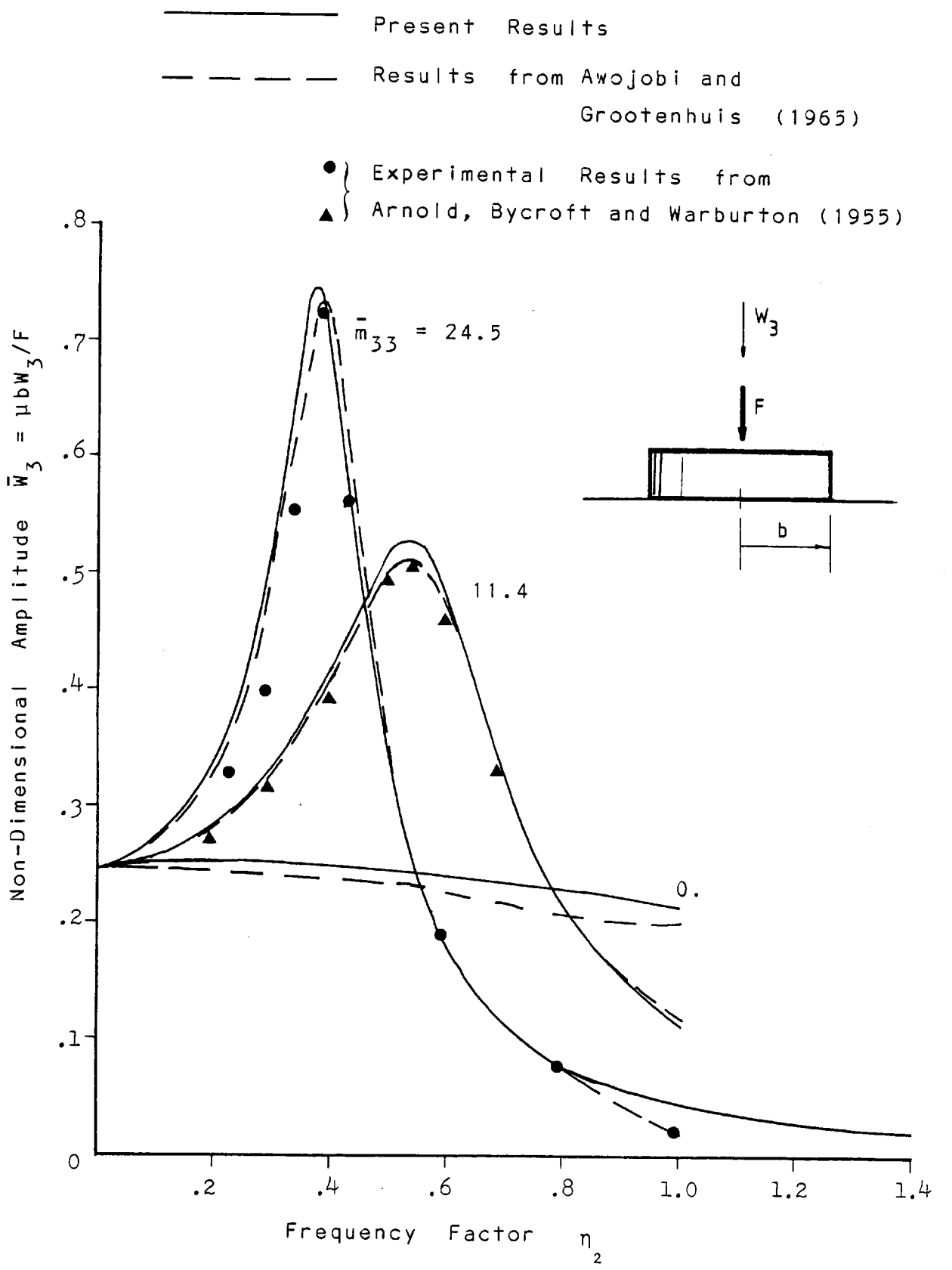

FIG 5.12 SHEAR STRESS DISTRIBUTION UNDER A RIGID CIRCULAR FOUNDATION IN TORSION.

(stress component in phase with displacement)

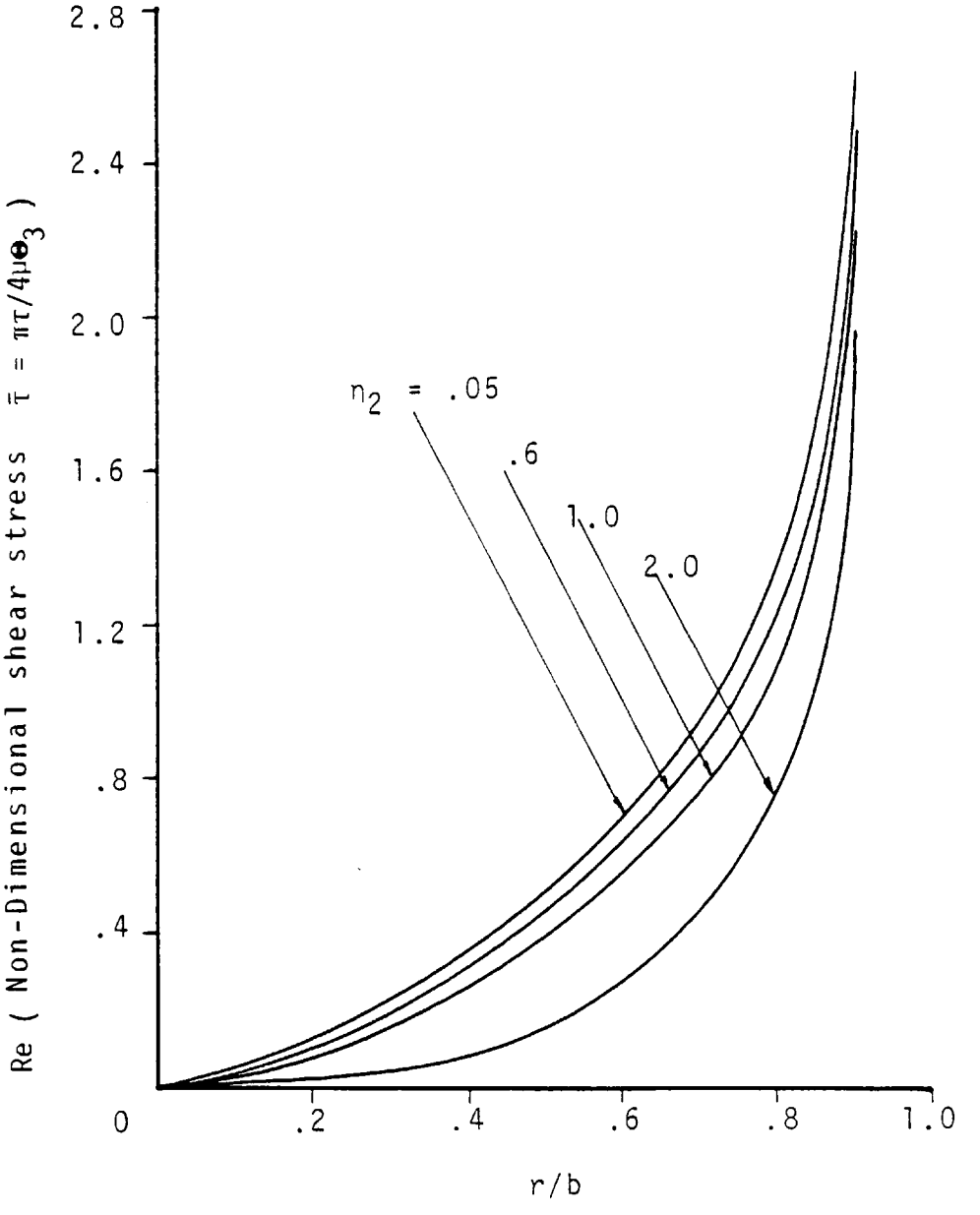

FIG 5.13 SHEAR STRESS DISTRIBUTION UNDER A RIGID CIRCULAR FOUNDATION IN TORSION.

(stress component in quadrature with displacement)

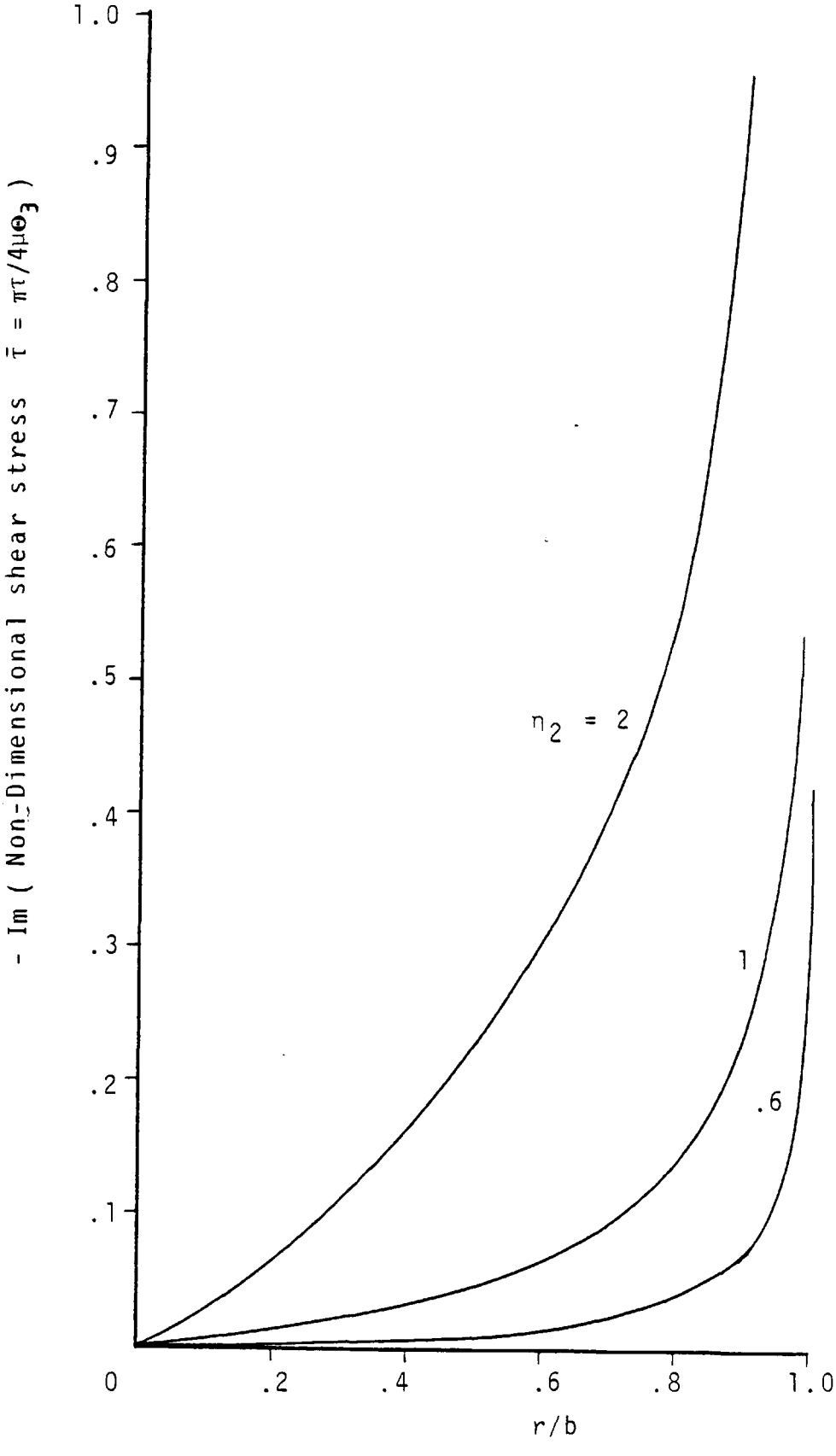

FIG 5.14 TORSIONAL STIFFNESS FOR CIRCULAR FOUNDATION.

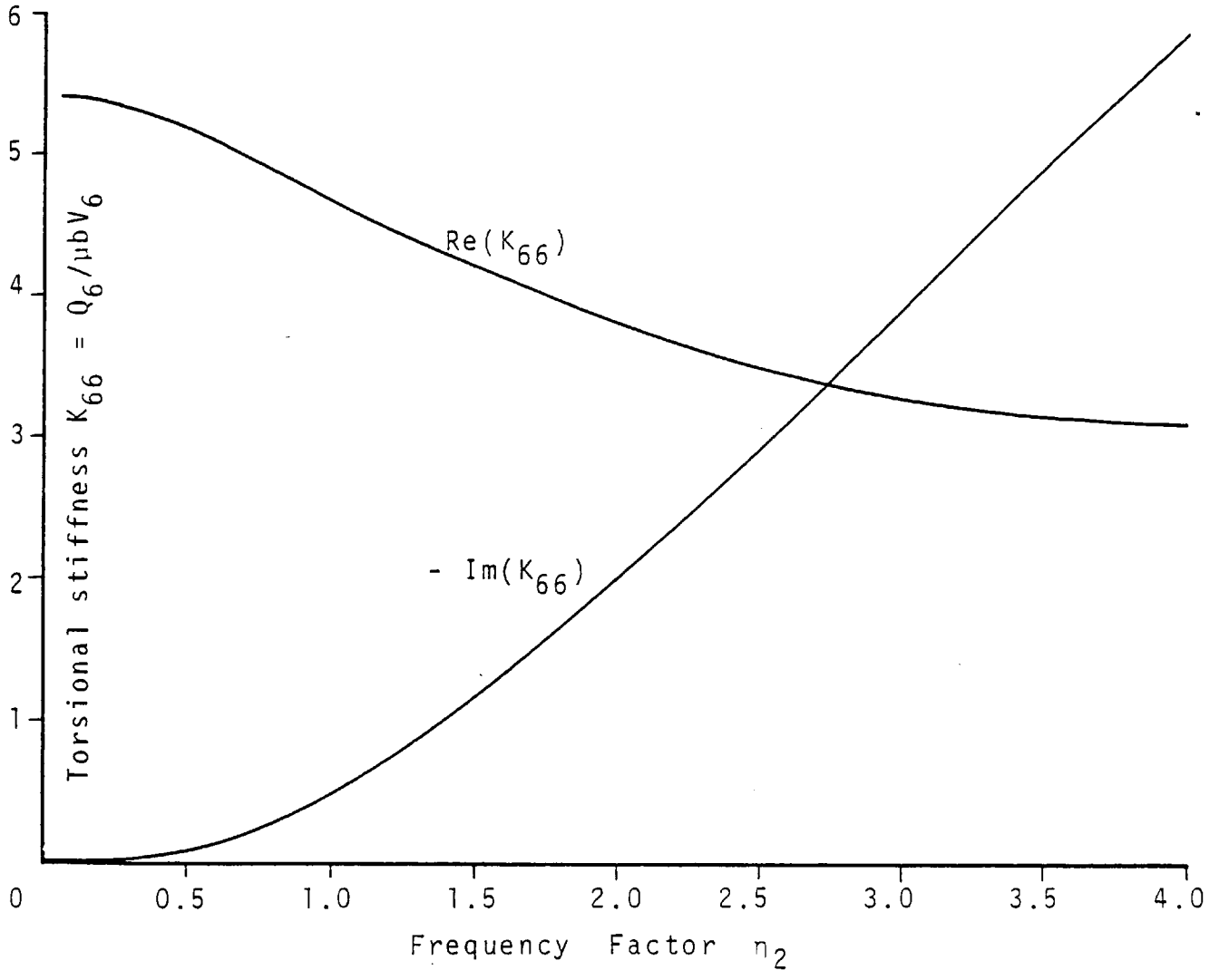

FIG 5.15 TORSIONAL COMPLIANCE FOR CIRCULAR FOUNDATION.

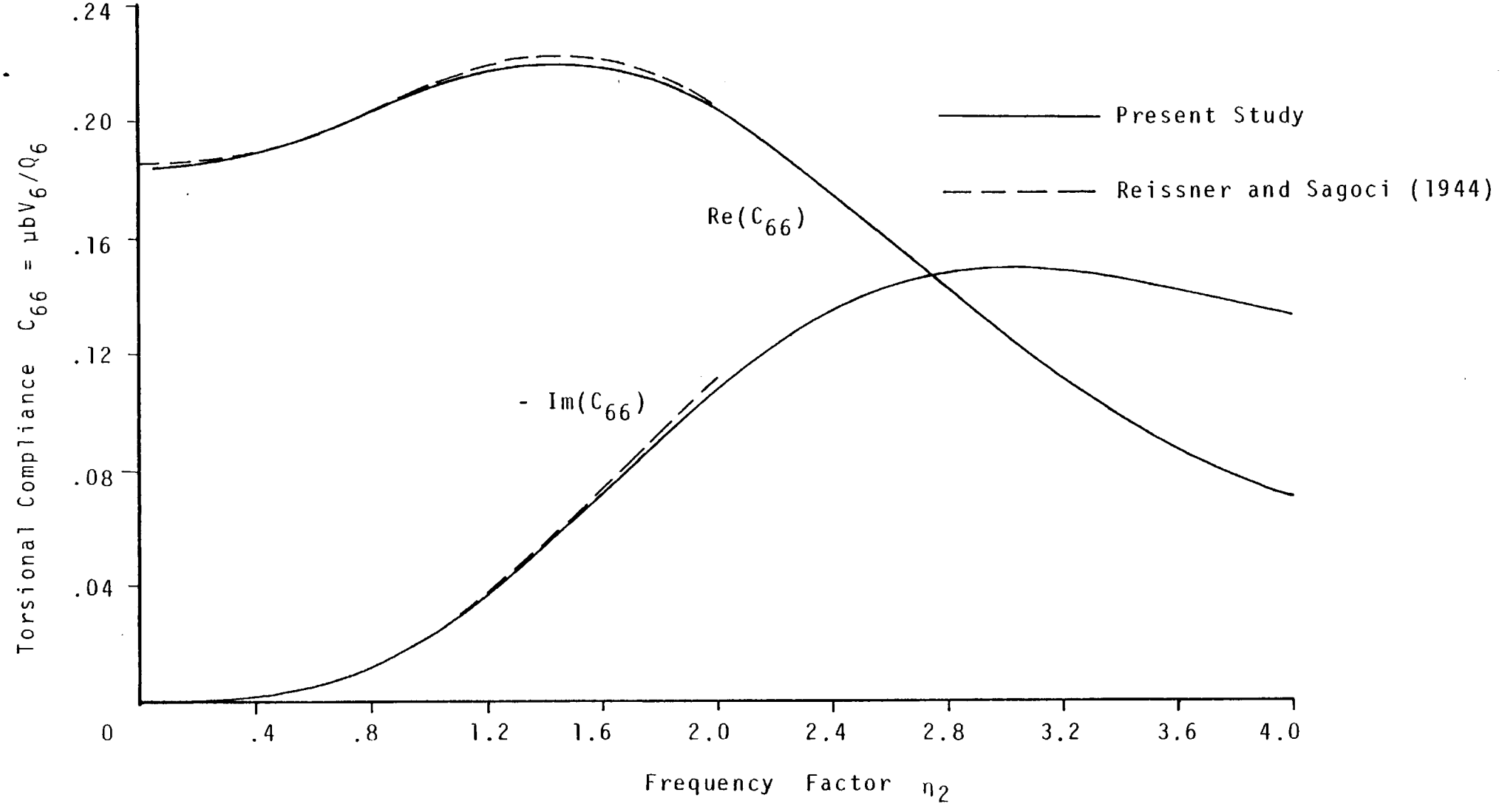

FIG 5.16 NON-DIMENSIONAL TORSIONAL RESPONSE AMPLITUDE OF CIRCULAR FOUNDATION.

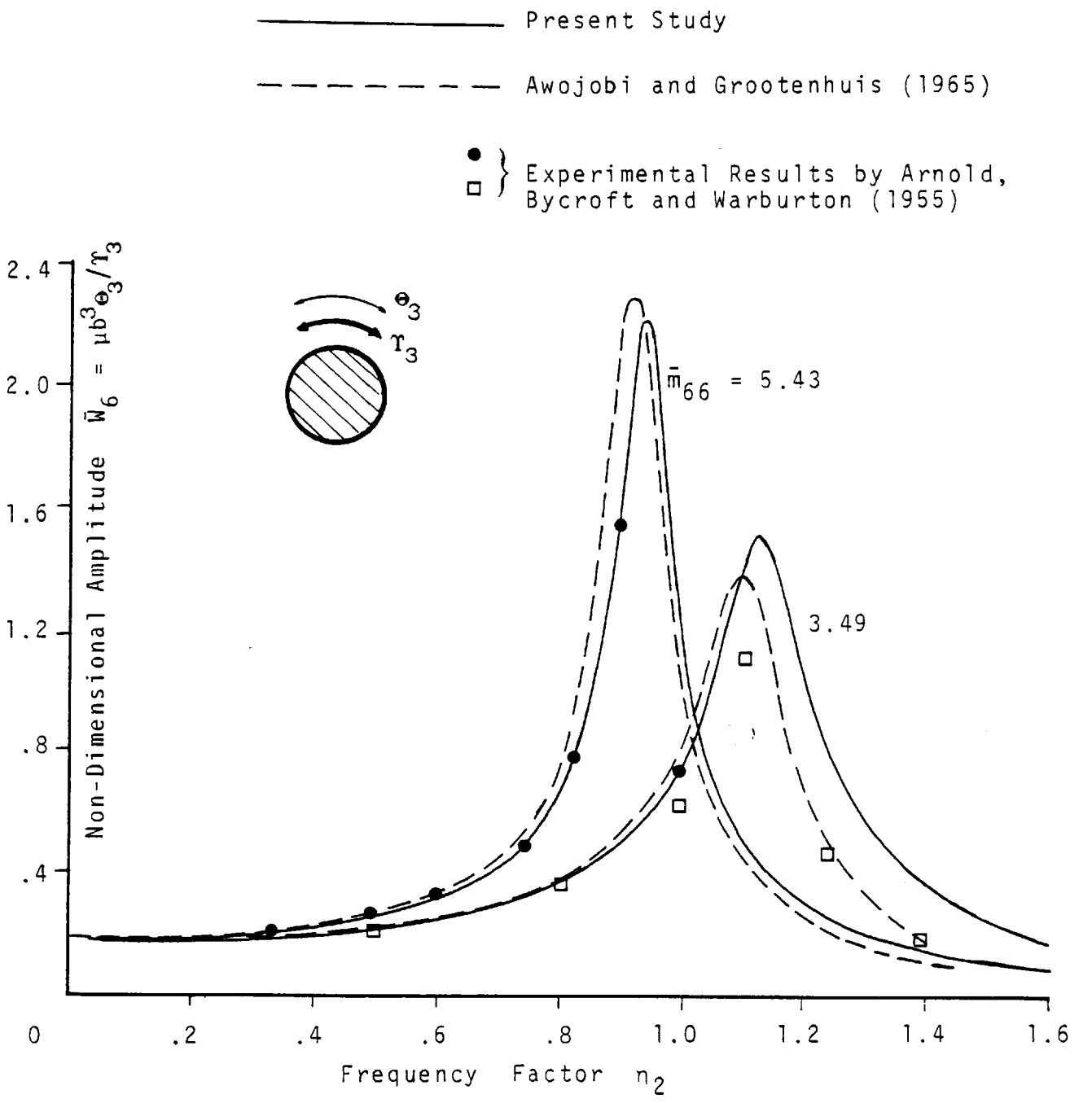

FIG.5.17 EFFECT OF R_o ON THE VERTICAL COMPLIANCE OF SQUARE FOUNDATION.

POISSON RATIO 1/3

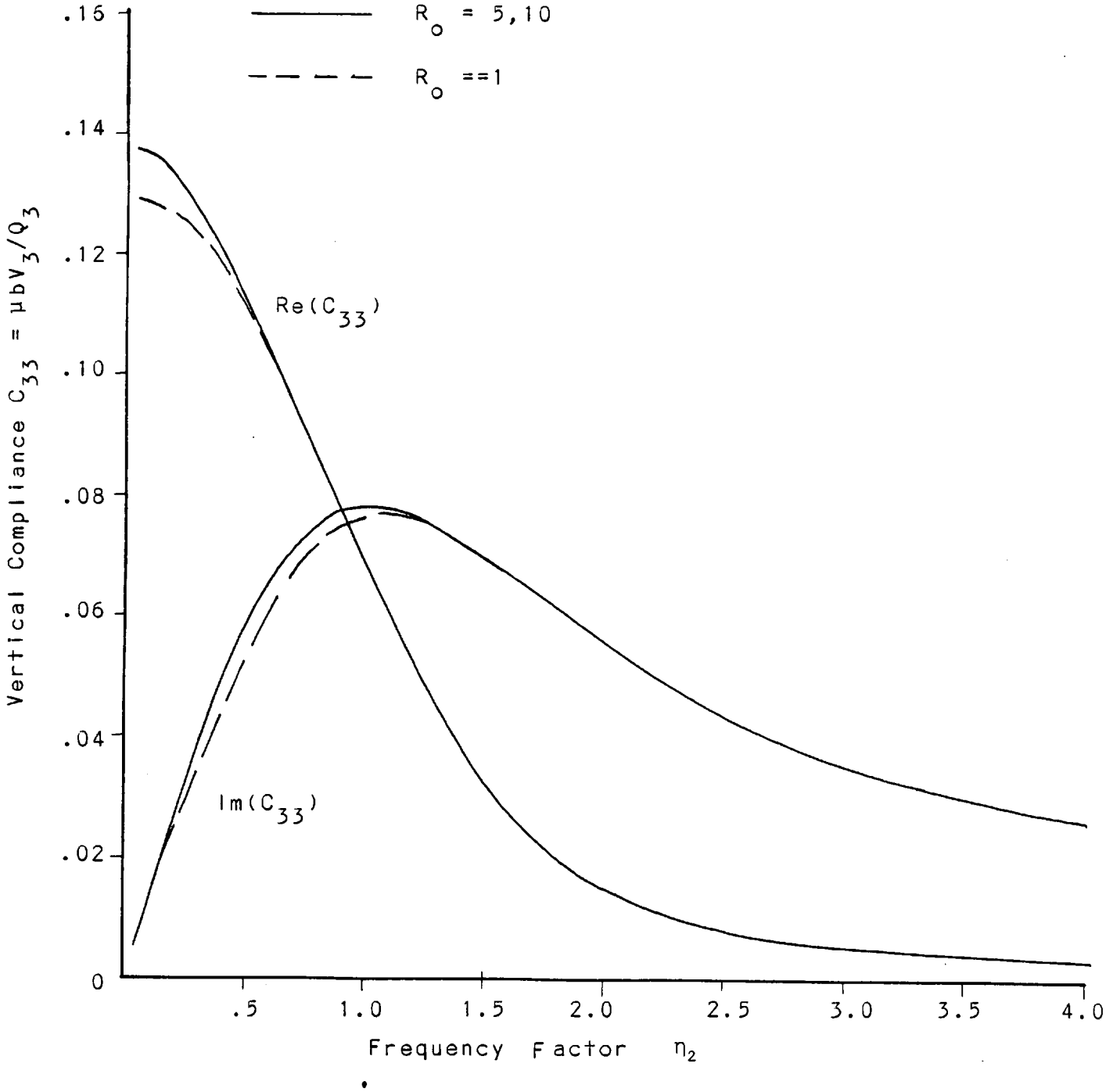

FIG.5.18a VERTICAL COMPLIANCE (REAL PART OF) FOR RIGID SQUARE FOUNDATION. POISSON RATIO = 1/3

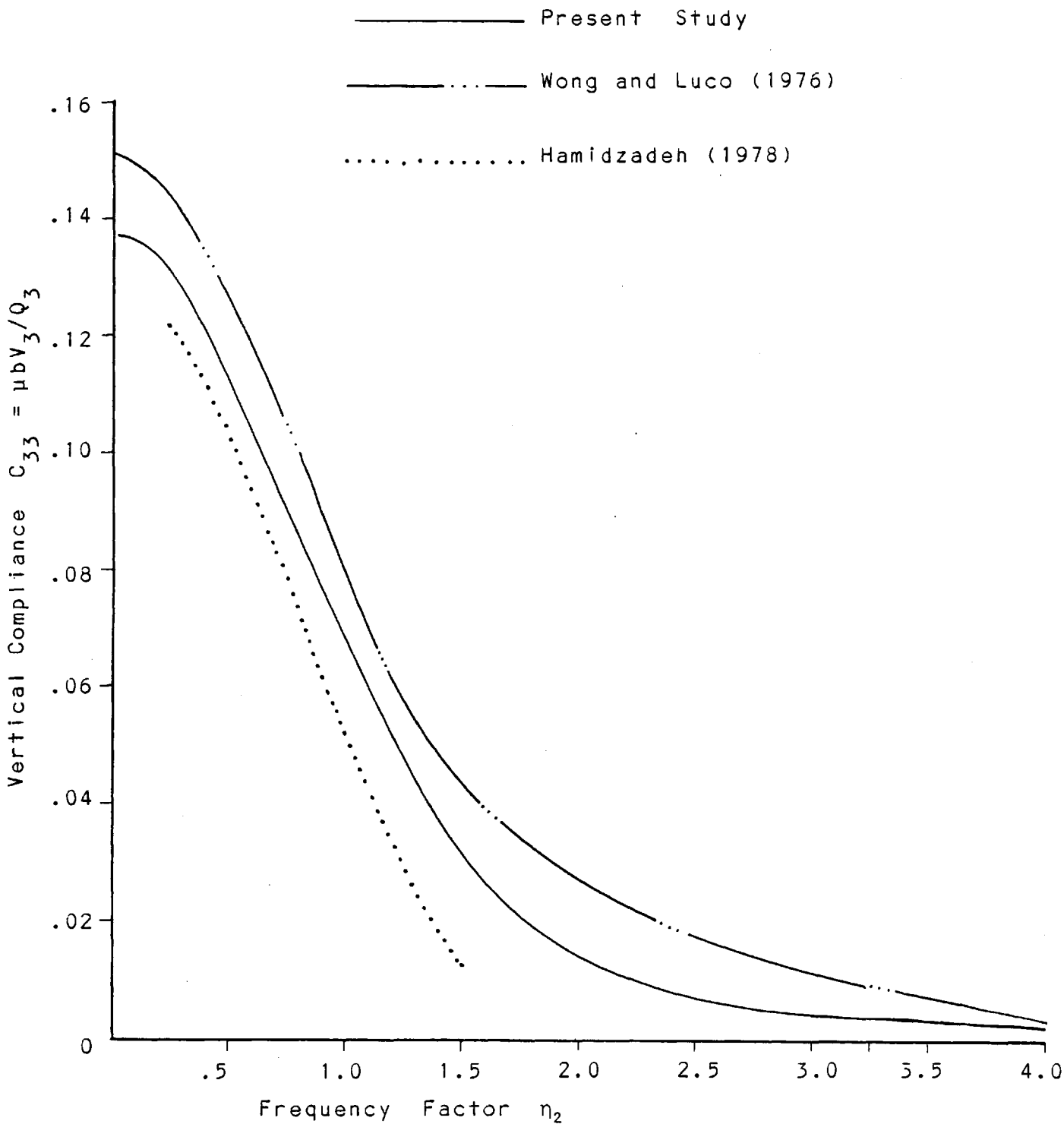

FIG.5.18b VERTICAL COMPLIANCE (IMAGINARY PART OF) FOR RIGID SQUARE FOUNDATION. POISSON RATIO = 1/3

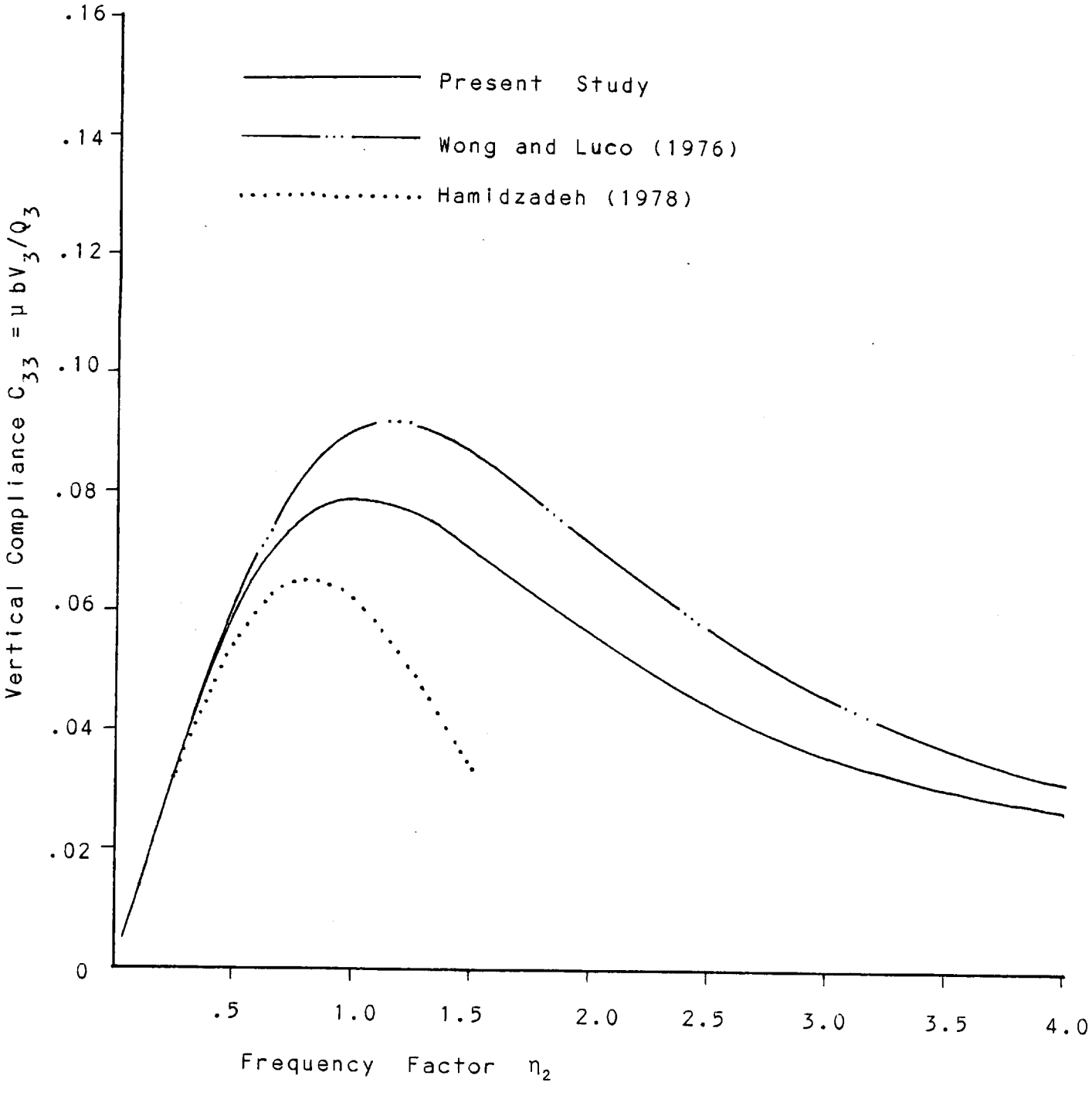

FIG.5.19 VERTICAL STIFFNESS FOR RECTANGULAR FOUNDATIONS OF VARIOUS WIDTH/LENGTH RATIOS a_r. POISSON RATIO 1/3

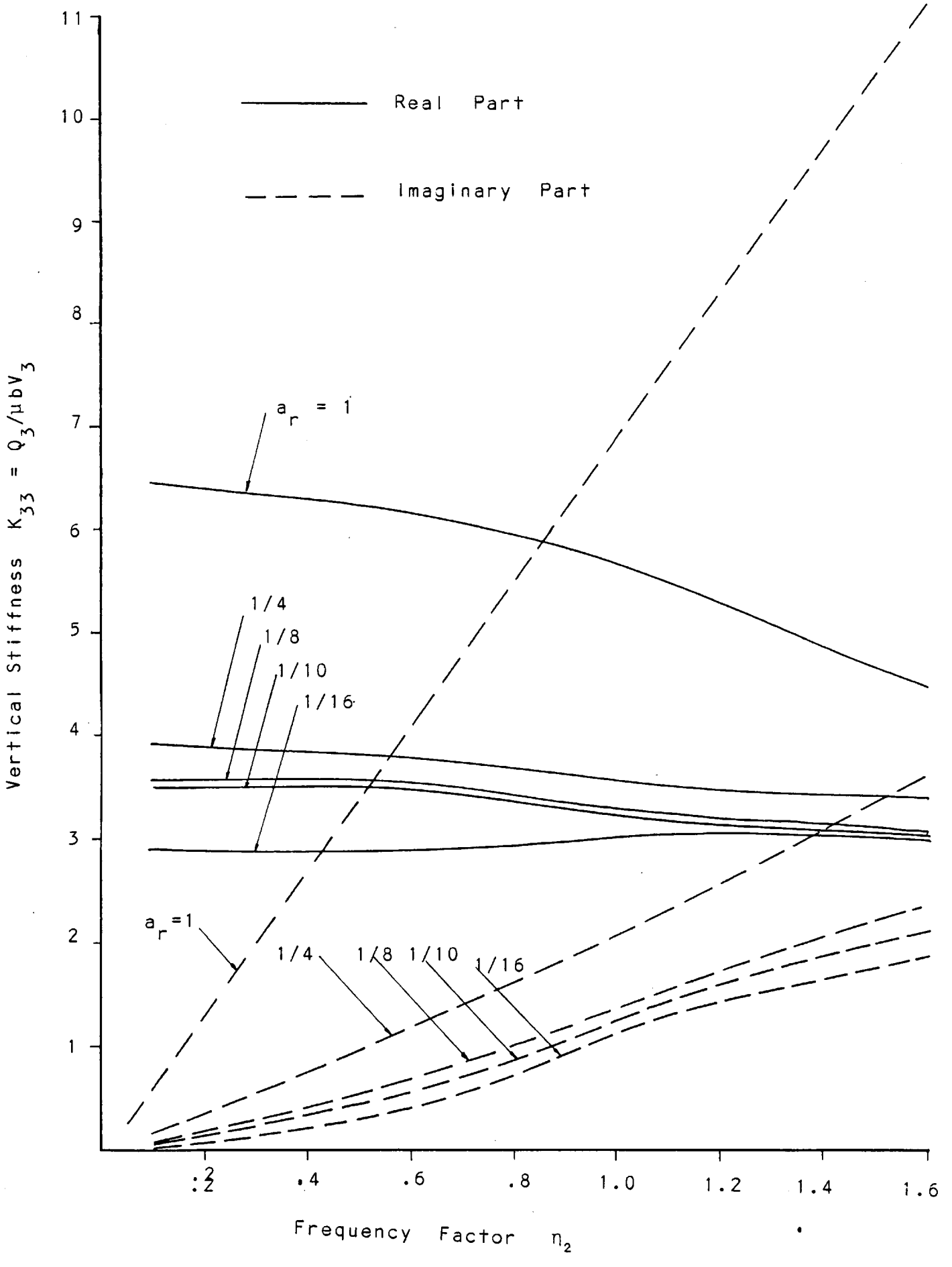

FIG.5.20a VERTICAL RESPONSE FOR RIGID SQUARE OUNDATION. POISSON RATIO = 1/4

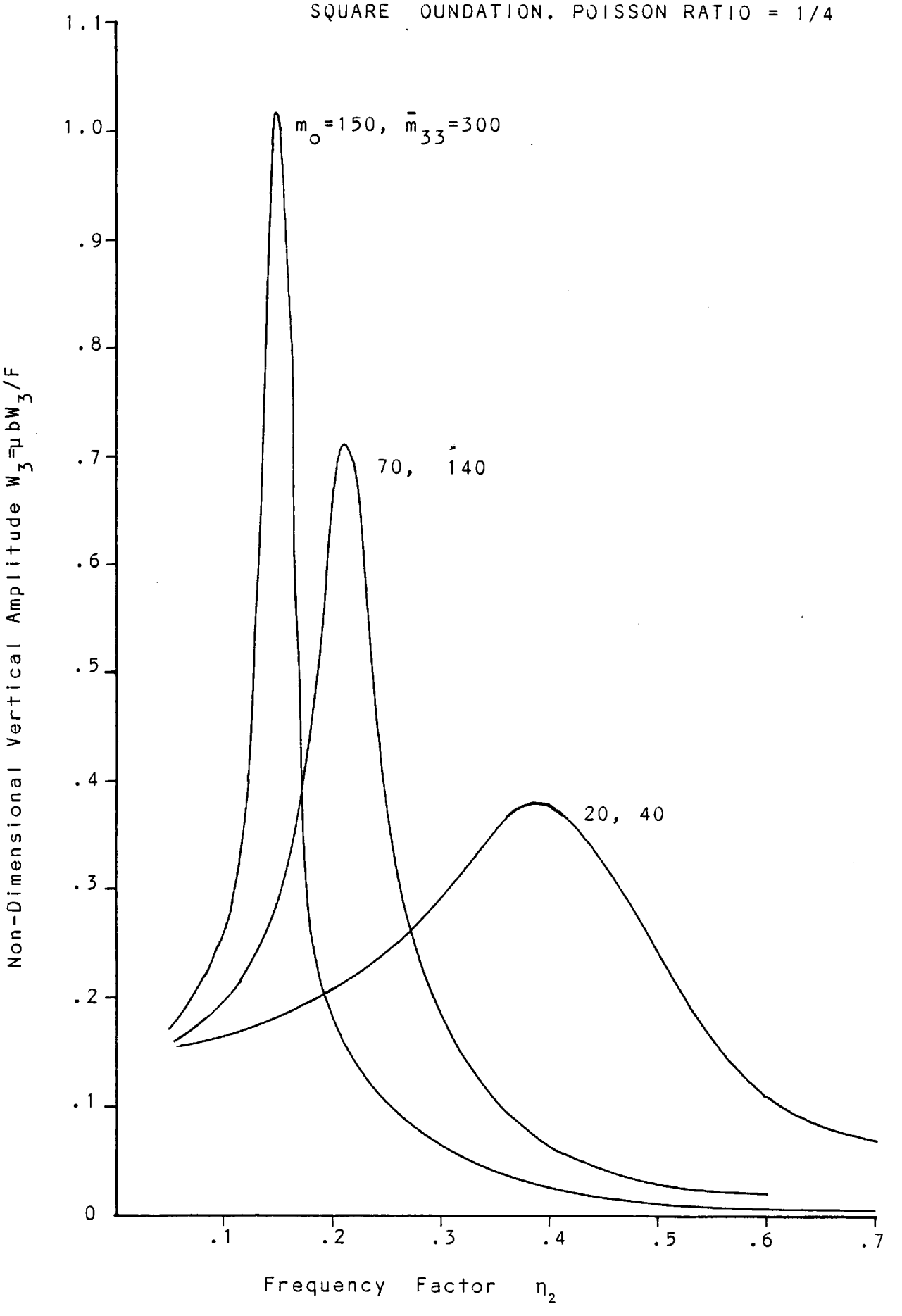

FIG. 5. 20b VERTICAL RESPONSE FOR RIGID RECTANGULAR FOUNDATION, WIDTH/LENGTH RATIO 1/8 POISSON RATIO 1/4

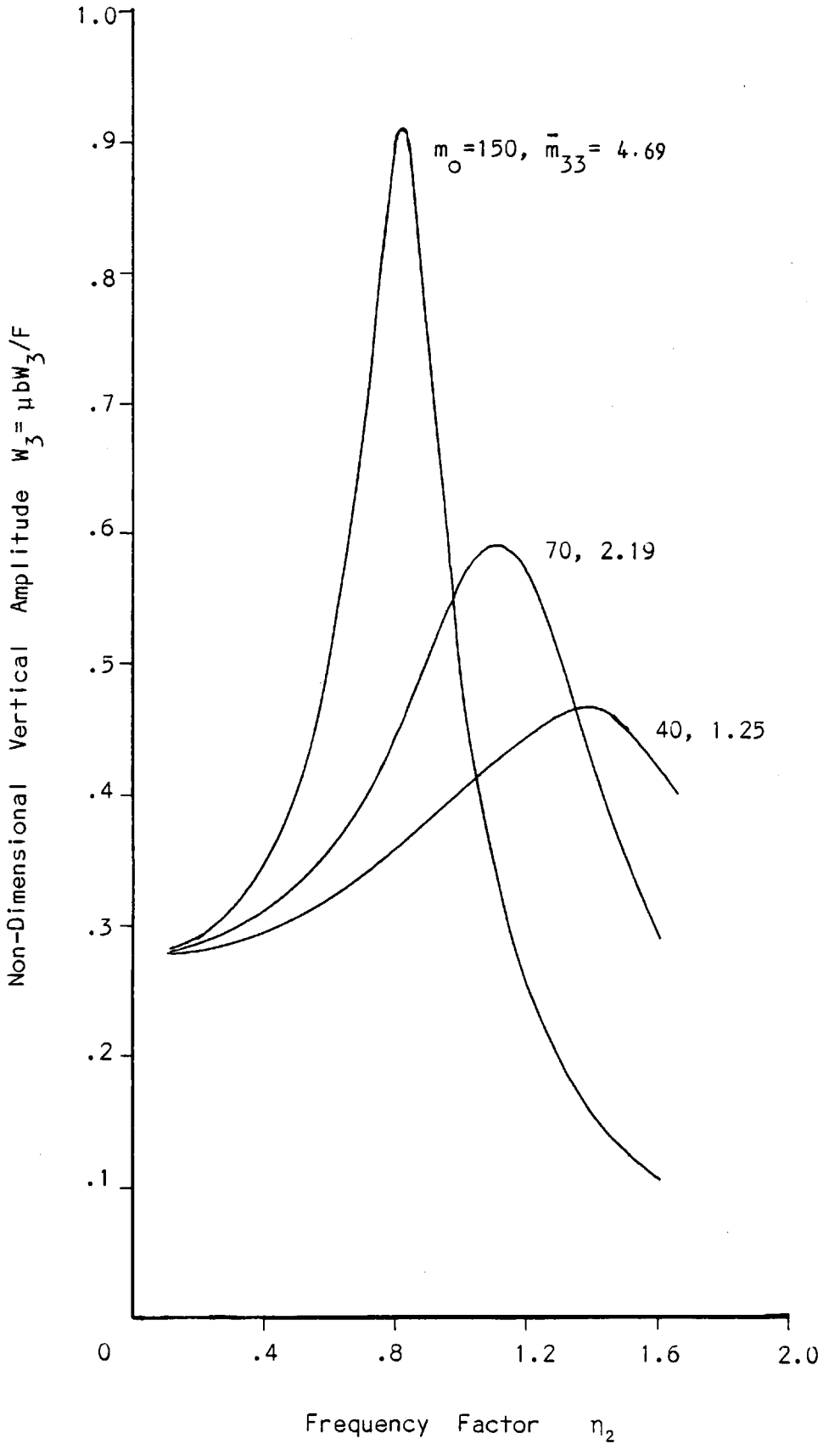

FIG.5.20c VERTICAL RESPONSE OF RIGID RECTANGULAR FOUNDATION, WIDTH/LENGTH RATIO 1/16. POISSON RATIO 1/4

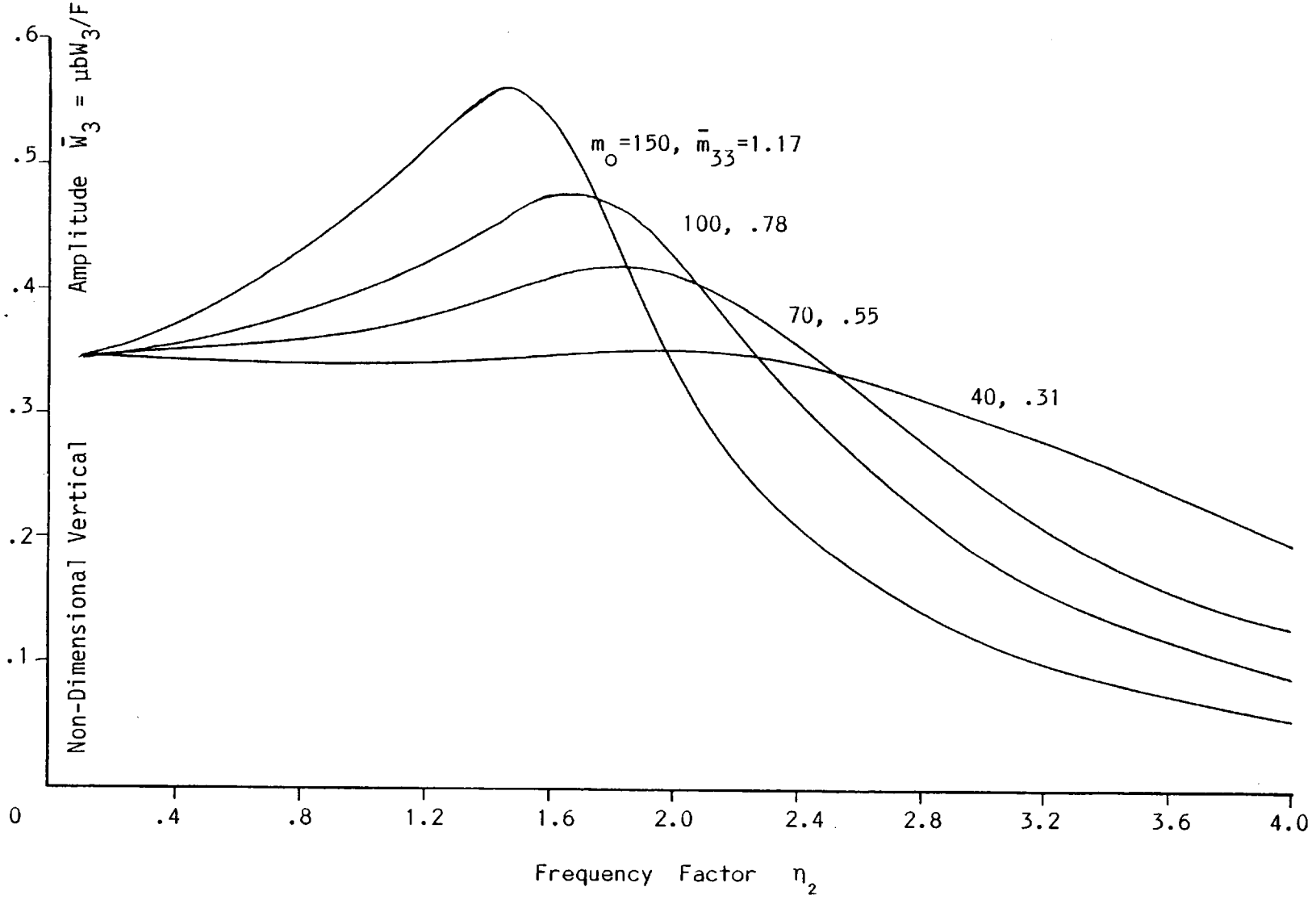

FIG. 5.21a NORMAL STRESS DISTRIBUTION ALONG CENTER LINE OF SQUARE FOUNDATION IN VERTICAL VIBRATION.
POISSON RATIO = 1/4
(Stress Component in Phase with Displacement)

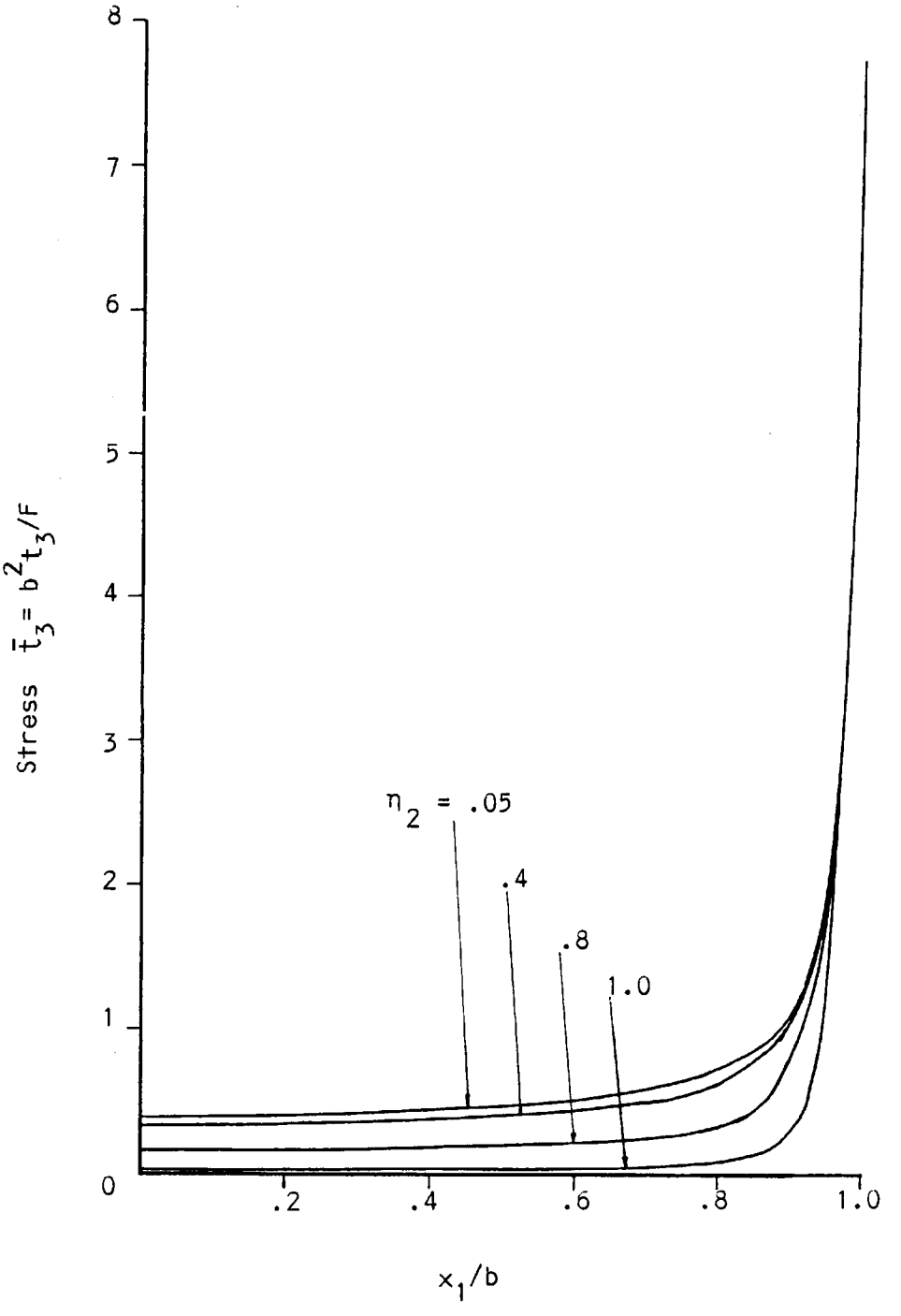

FIG.5.21b NORMAL STRESS DISTRIBUTION ALONG CENTER LINE OF SQUARE FOUNDATION IN VERTICAL VIBRATION.
POISSON RATIO = 1/4
(Stress Component in Quadrature with Displacement)

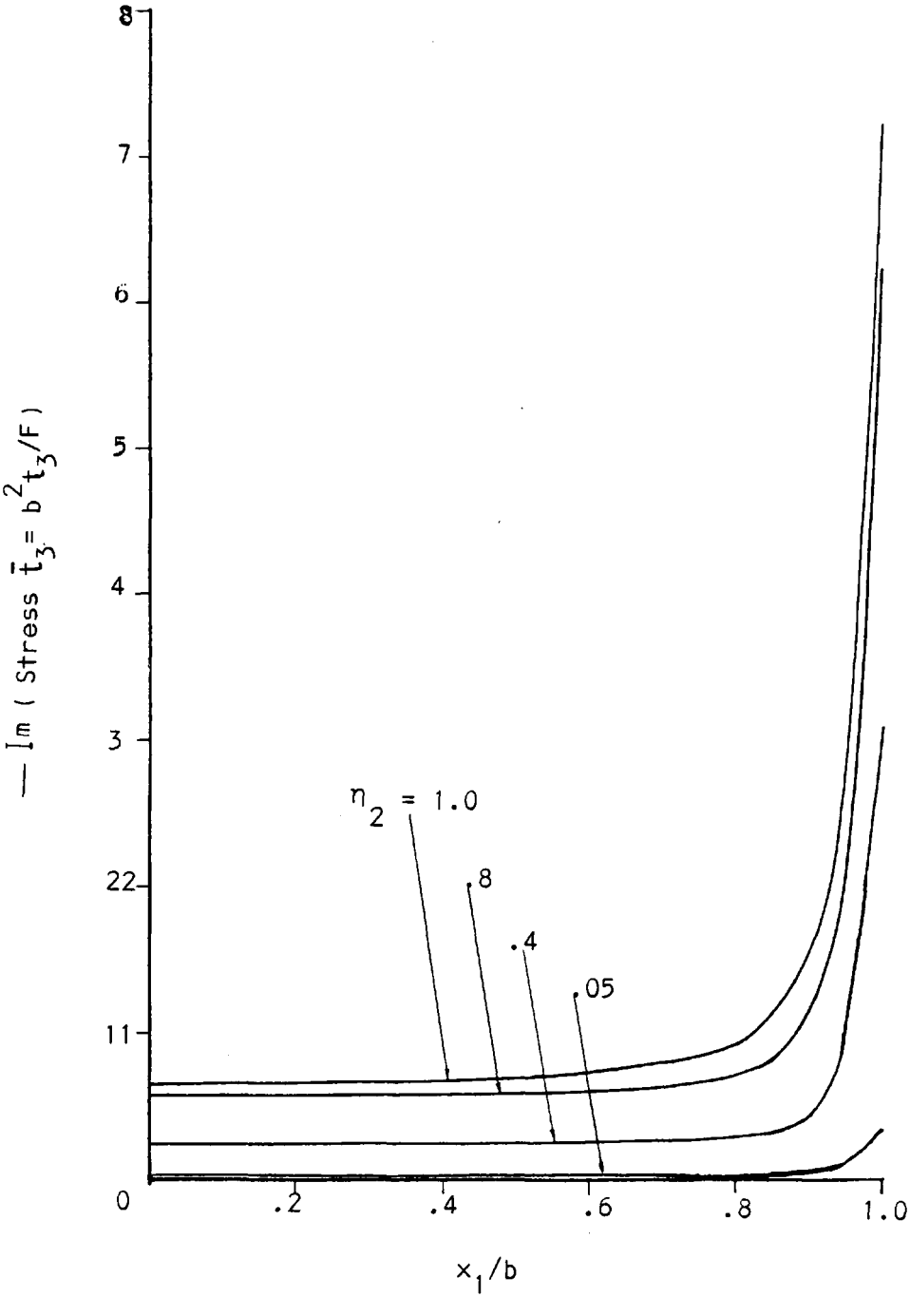

FIG 5.22a NORMAL STRESS DISTRIBUTION UNDER RIGID SQUARE FOUNDATION IN VERTICAL VIBRATION.
POISSON RATIO 1/4. FREQUENCY FACTOR 0.05.
(stress component in phase with displacement)

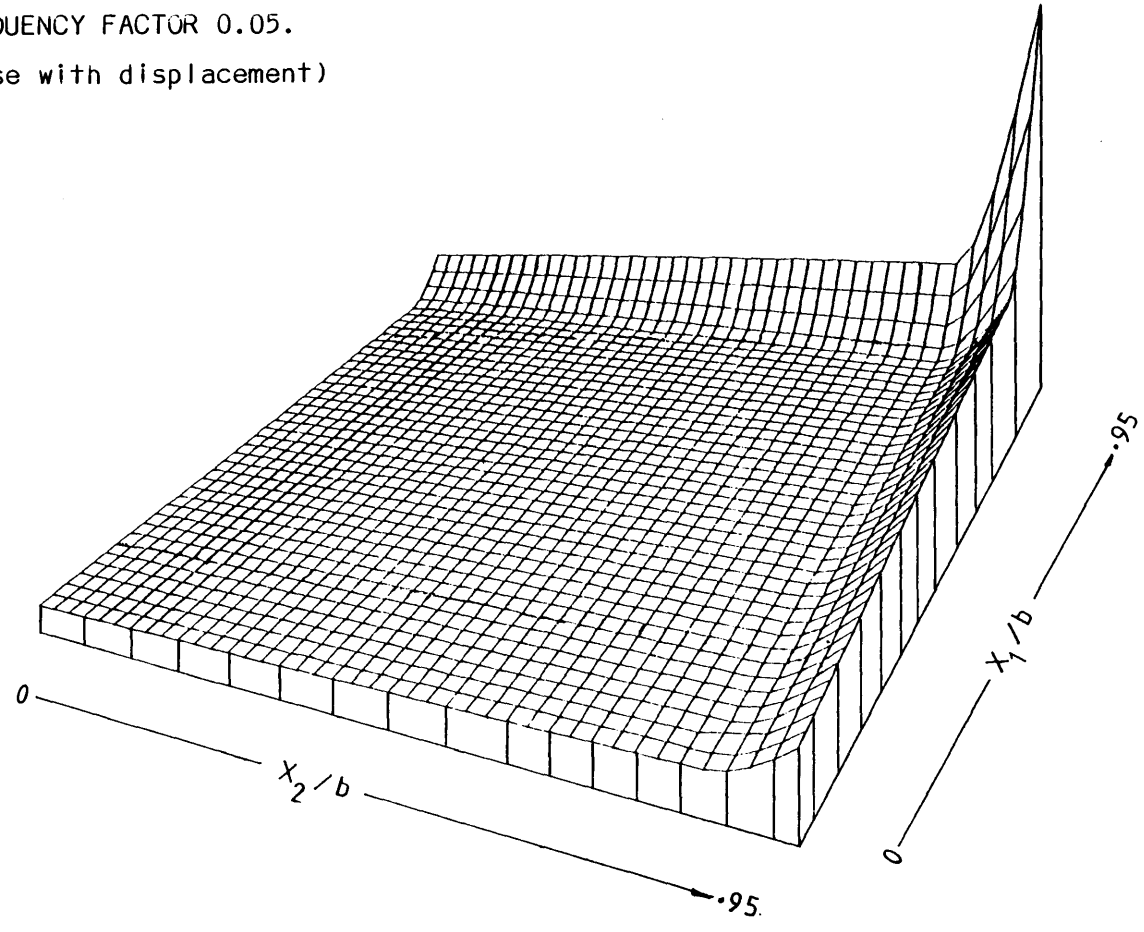

FIG 5.22b NORMAL STRESS DISTRIBUTION UNDER RIGID SQUARE FOUNDATION IN VERTICAL VIBRATION
POISSON RATIO 1/4. FREQUENCY FACTOR 0.05

— (stress component in quadrature with displacement)

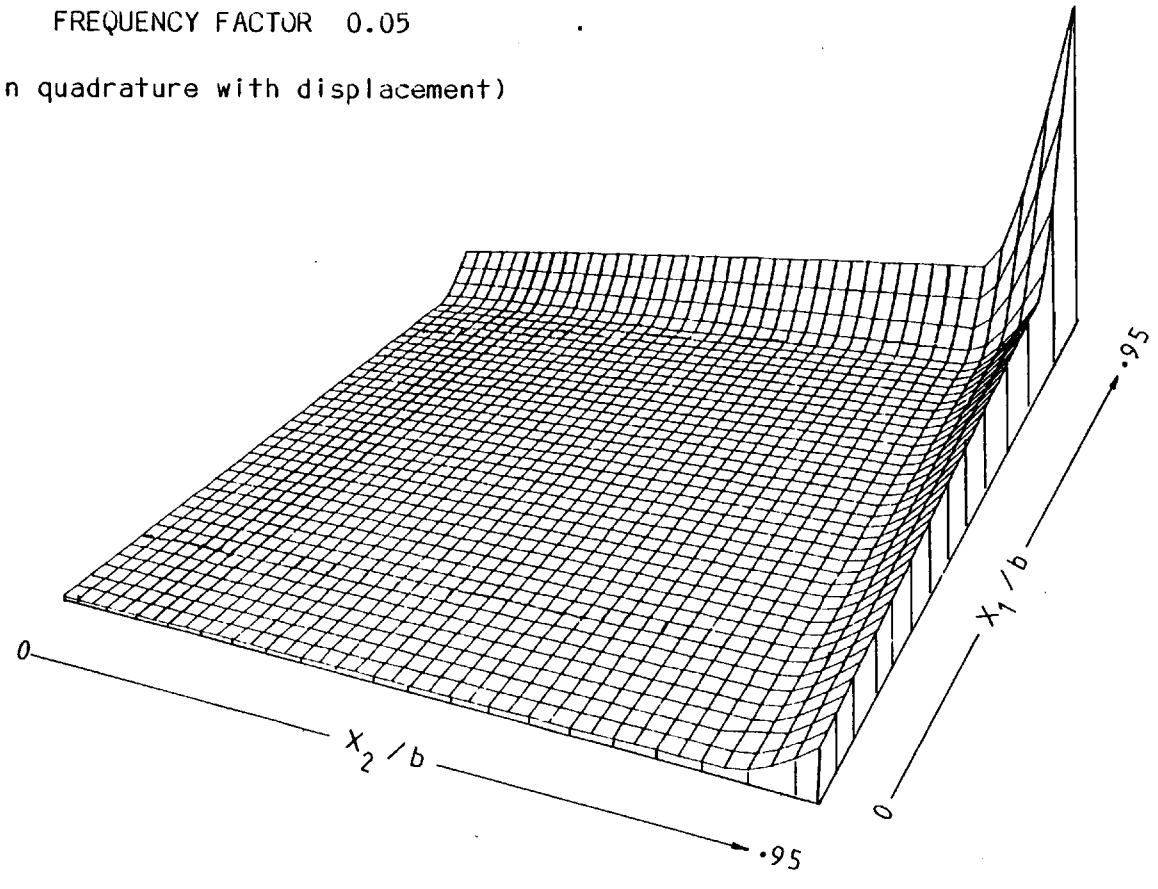

FIG 5.23a NORMAL STRESS DISTRIBUTION UNDER RIGID SQUARE FOUNDATION IN VERTICAL VIBRATION.
poisson ratio 1/4. frequency factor 0.8
(stress component in phase with displacement)

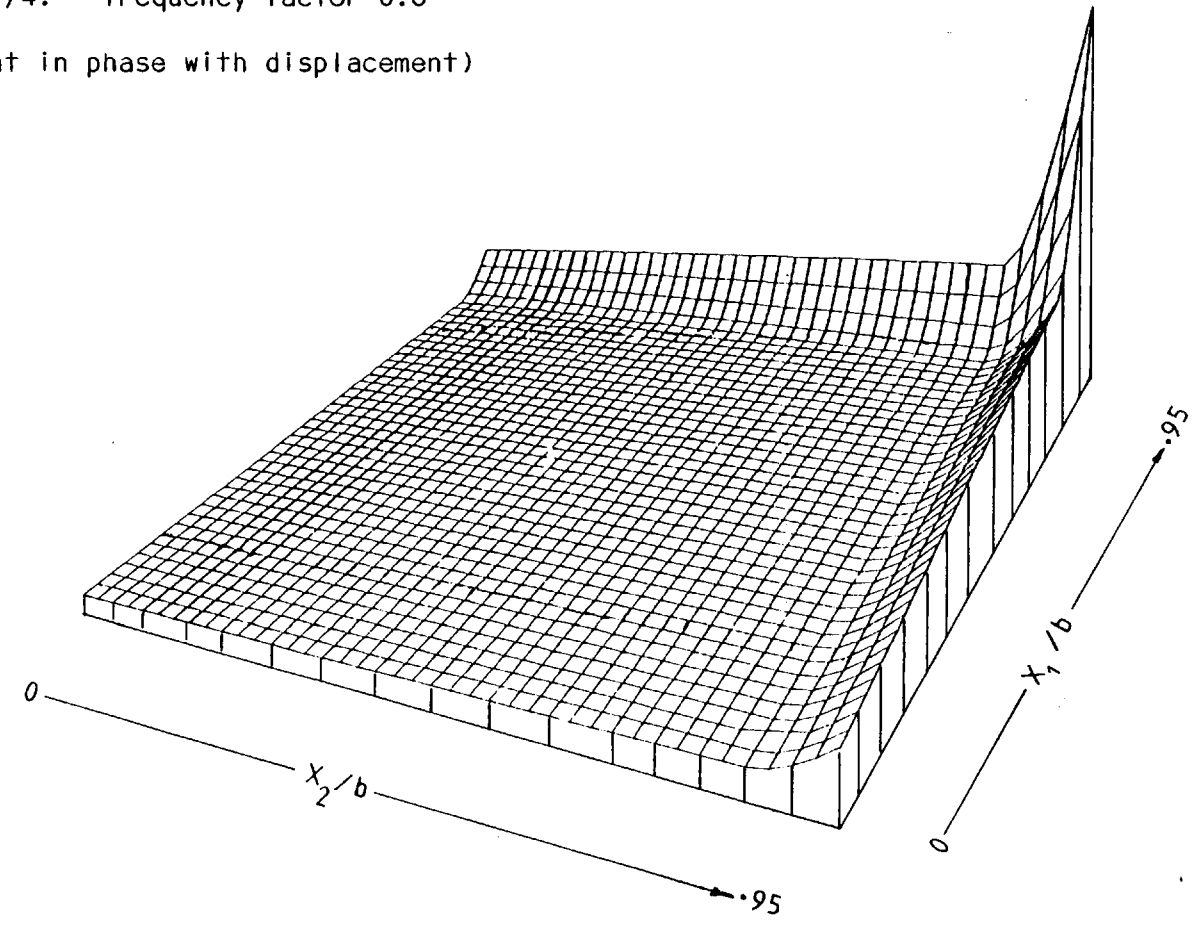

FIG 5. 23b NORMAL STRESS DISTRIBUTION UNDER RIGID SQUARE FOUNDATION IN VERTICAL VIBRATION.
POISSON RATIO 1/4. FREQUENCY FACTOR 0.8

— (stress component in quadrature with displacement)

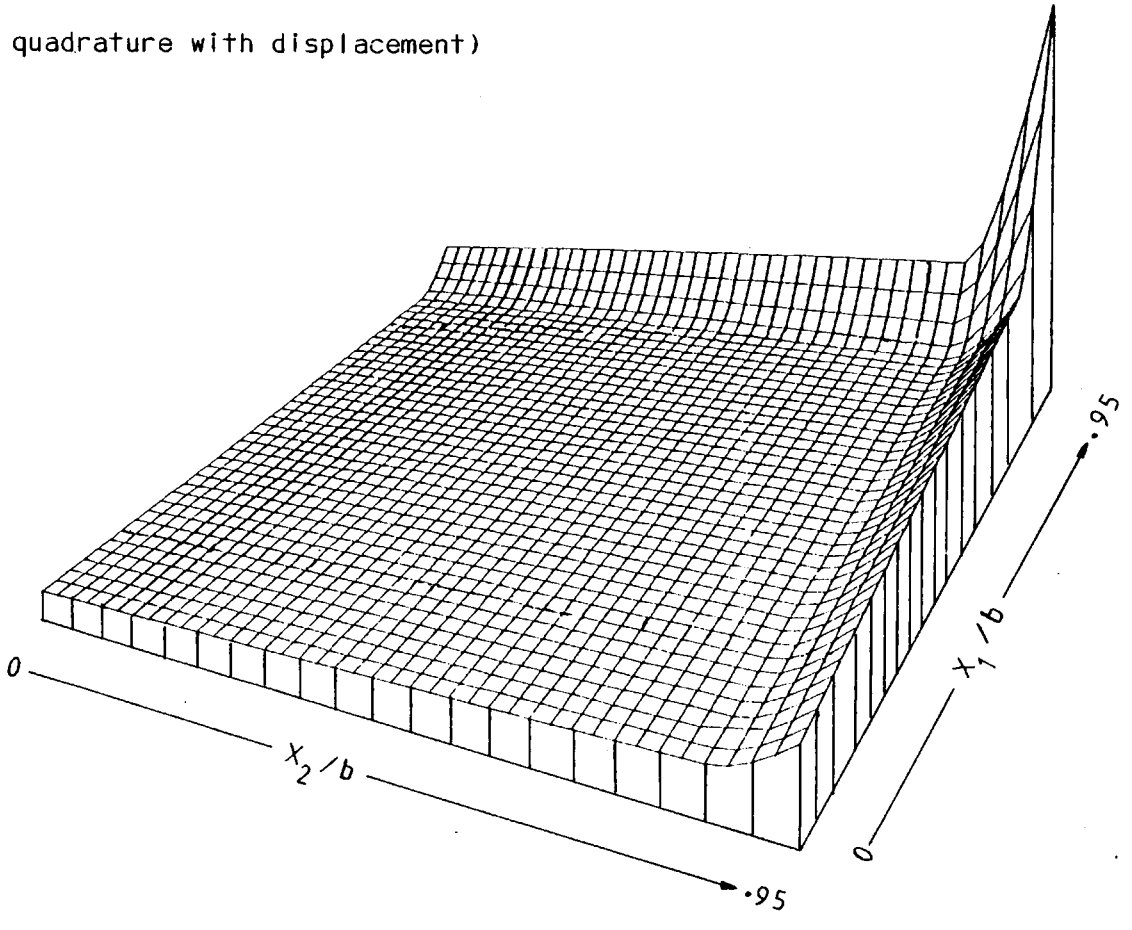

FIG.5.24 SHEAR STRESS DISTRIBUTION ALONG CENTER LINE OF RIGID SQUARE FOUNDATION IN HORIZONTAL VIBRATION. POISSON RATIO 1/3

(stress component in phase with displacement)

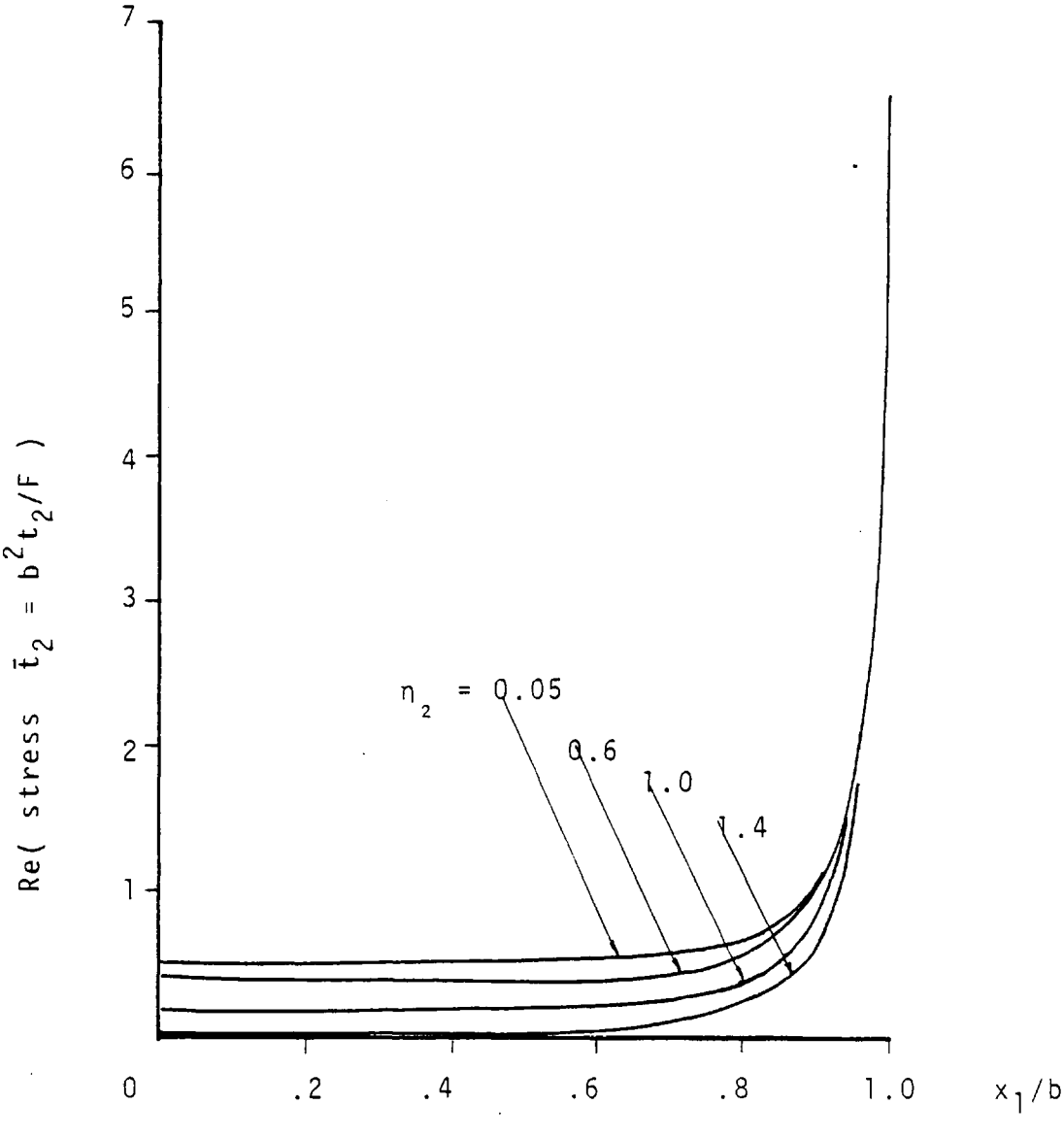

FIG 5.25 SHEAR STRESS DISTRIBUTION ALONG CENTER LINE OF RIGID SQUARE FOUNDATION IN HORIZONTAL VIBRATION. POISSON RATIO 1/3

(stress component in quadrature with displacement)

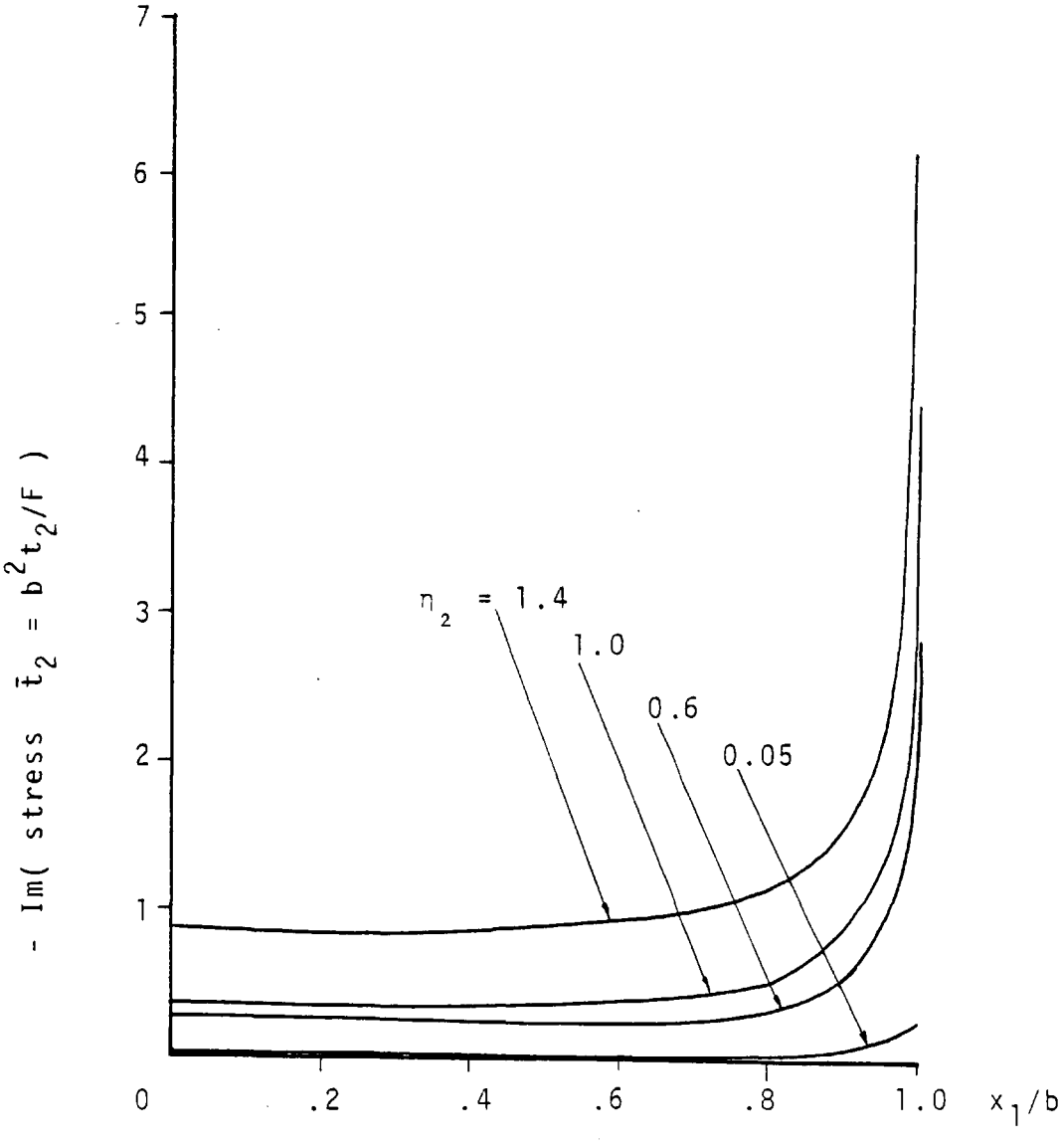

FIG.5. 26 HORIZONTAL STIFFNESS FOR SQUARE FOUNDATION POISSON RATIO 1/3.

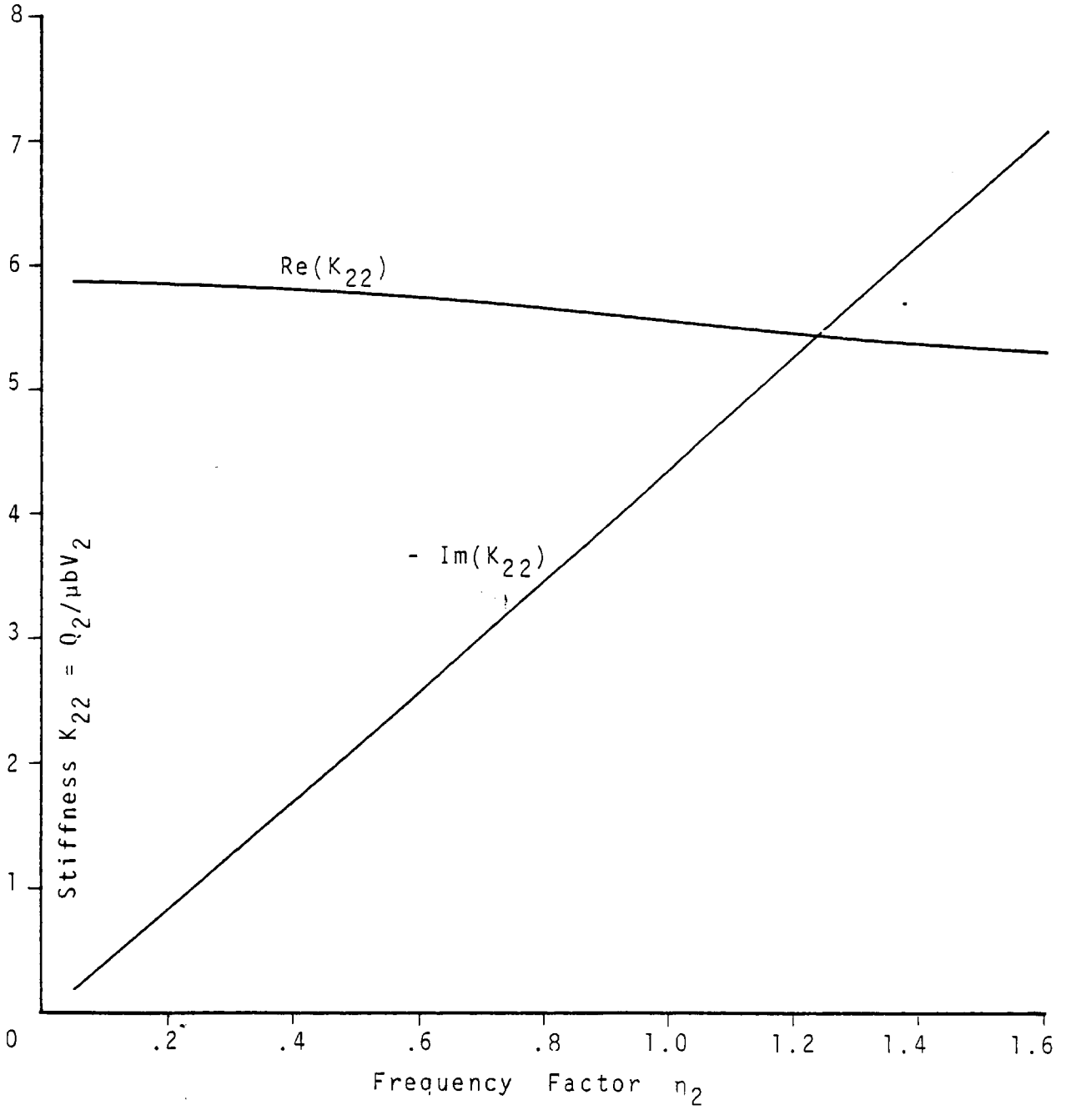

FIG 5.27 HORIZONTAL COMPLIANCE FOR RIGID SQUARE FOUNDATION. POISSON RATIO 1/3.

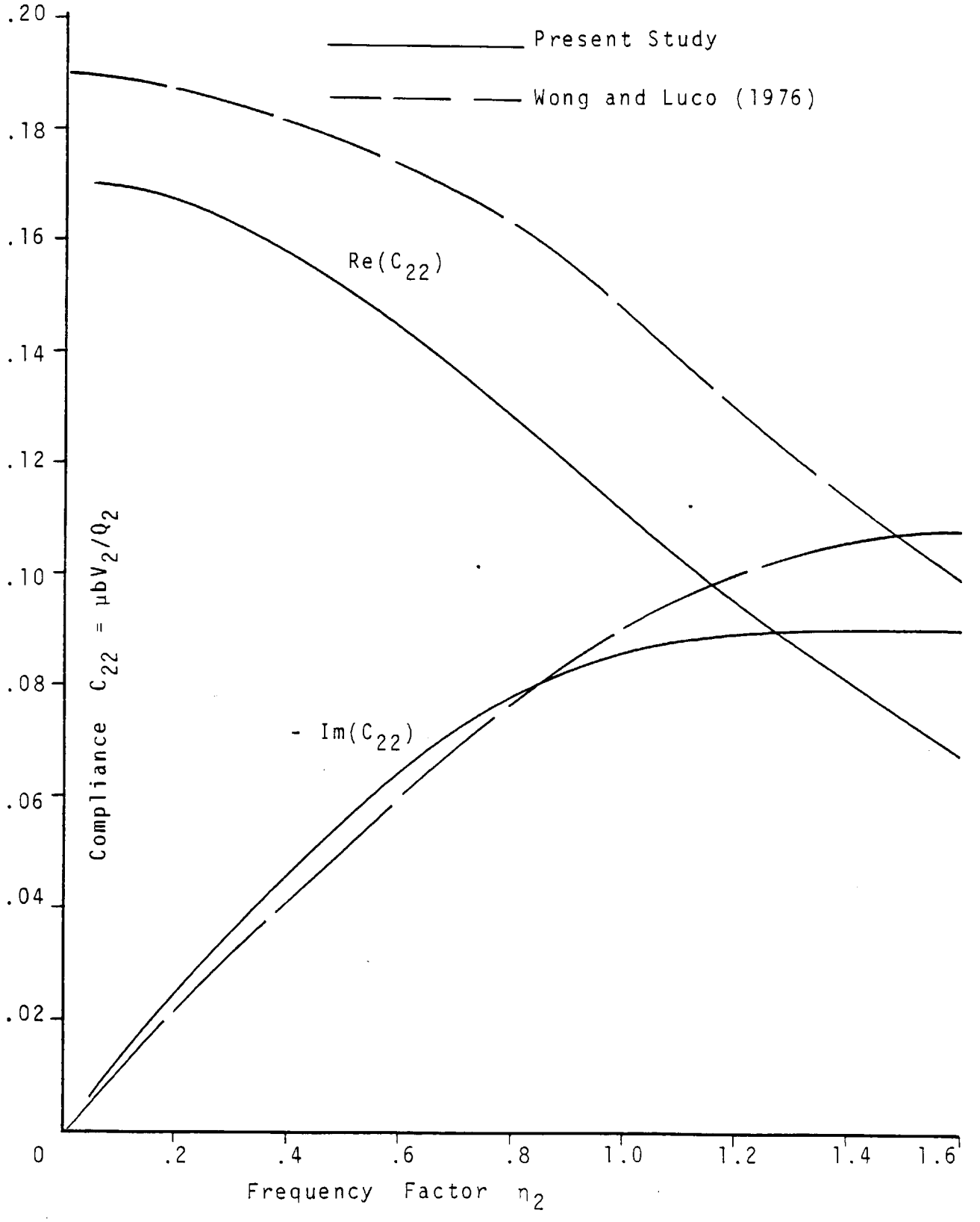

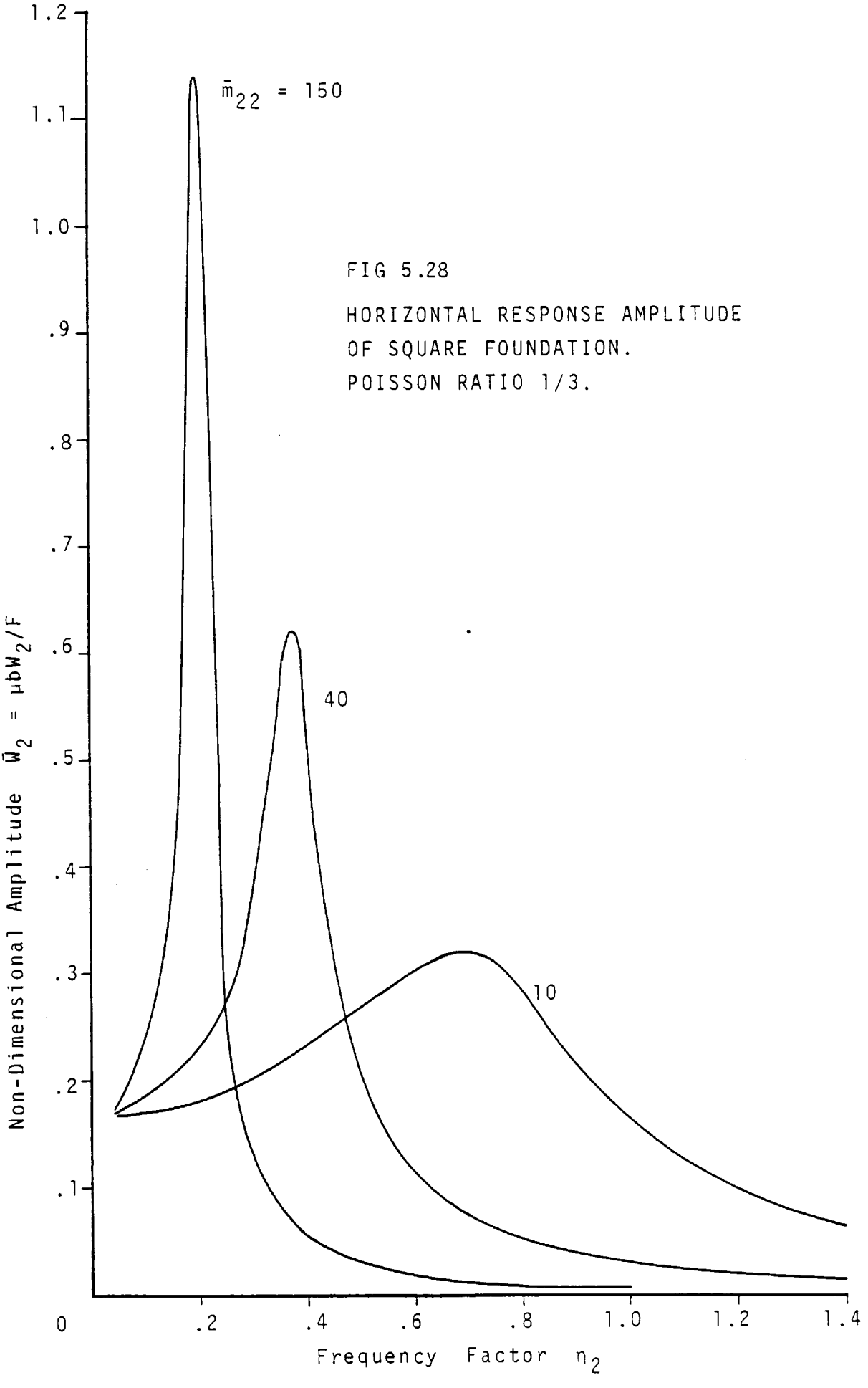

FIG 5.28

HORIZONTAL RESPONSE AMPLITUDE OF SQUARE FOUNDATION. POISSON RATIO 1/3.

FIG.5.29 % ERROR IN RESONANCE FREQUENCY PREDICTION BY THE INFINITE STRIP ANALYSIS. POISSON RATIO 1/4

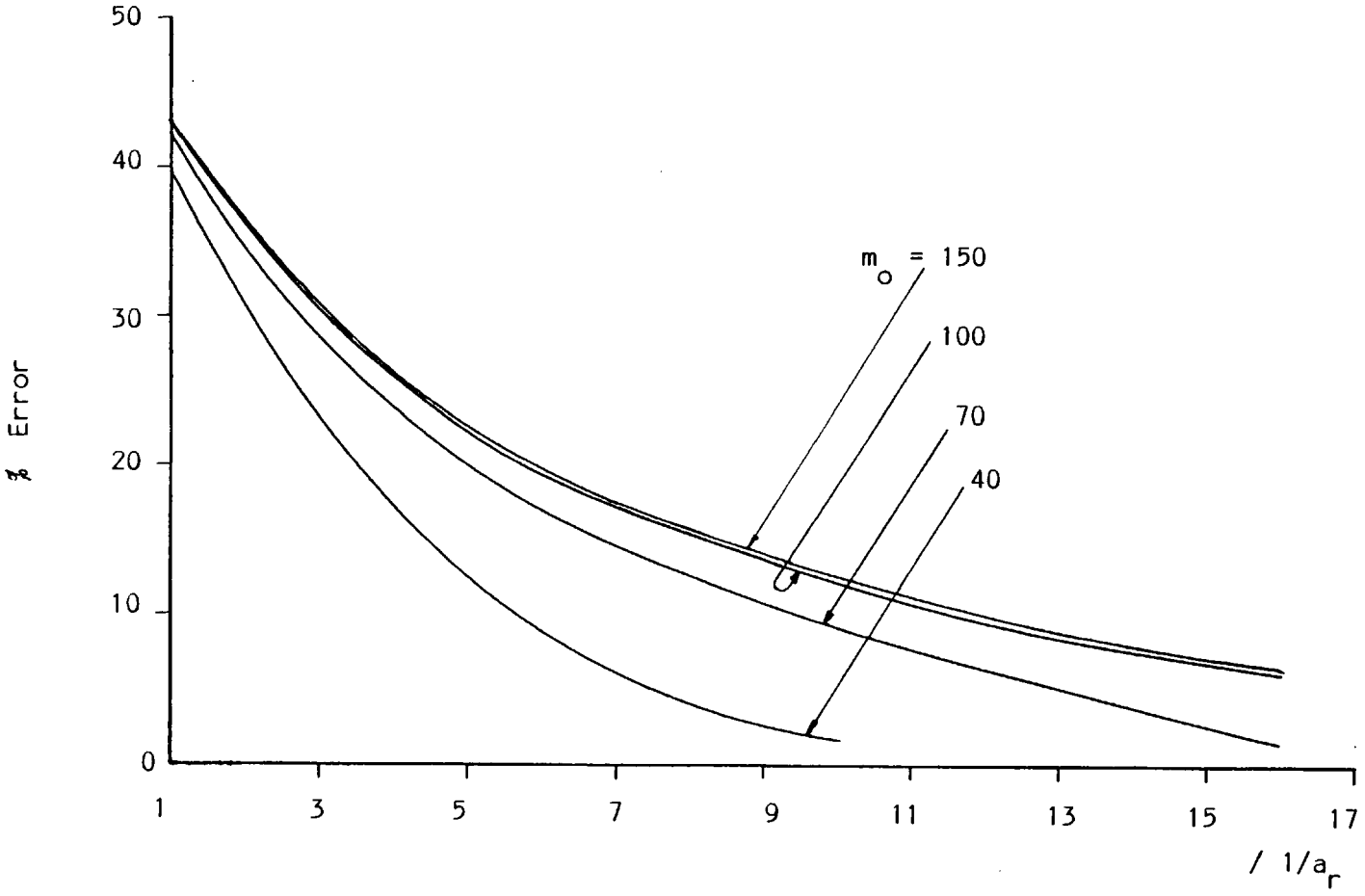

FIG. 5.30 NORMAL STRESS DISTRIBUTION ALONG LENGTH-WISE CENTER LINE OF RECTANGULAR FOUNDATION IN VERTICAL VIBRATION. POISSON RATIO = 1/4, FREQUENCY FACTOR 0.6

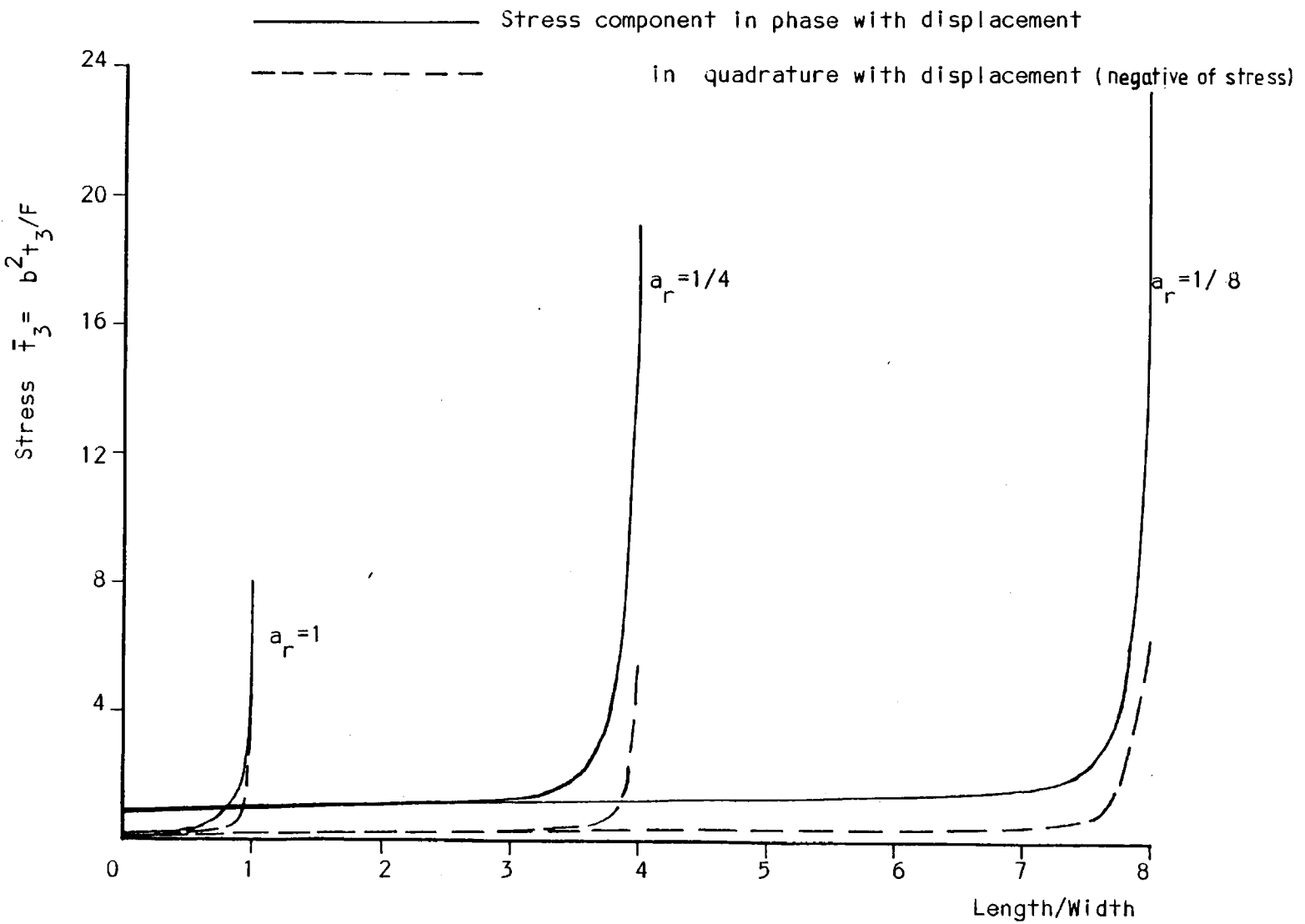

chapter 6

THE B.I.E. AND FUTURE DEVELOPMENTS IN FOUNDATION DYNAMICS

6.1 INTRODUCTION

This chapter examines the BIE method as a means of solving the general elastodynamic problem and, consequently, some of the more practical aspects of foundation dynamics such as vibration of flexible foundations. This particular aspect has been difficult to analyse, and the previous methods of analysis of vibration of foundation mentioned in chapter 1 are not easy to apply to such problems especially when arbitrary foundation shapes are involved. This problem is difficult because predicting the dynamic response of finite-size elastic solids and structures subjected to time-dependent loads and/or boundary conditions is a very formidable problem from the point of view of closed-form analytical solutions. In elastodynamics this is the problem of elastic wave propagation through solids. The Navier's wave equations (2.2.1) do admit to a simple solution in terms of trigonometric and/or Bessel functions. But it then becomes impossible in most cases to manipulate these functions to satisfy boundary conditions. It will be interesting to examine how the analytical difficulty mounts as we move from bodies of simpler geometry to those of more complicated geometry.

Analytical solutions have been obtained by Chree (1889) to the problem of longitudinal wave propagation through a cylinder of circular cross-section and infinite length. It

was possible to satisfy the boundary conditions of zero stresses all over the surface. The surface consists of the circular lateral face which is a single coordinate surface in cylindrical coordinate system. The end faces of the cylinder do not matter because they are far away at infinity. If we imagine an elastic plate of finite thickness in the z-direction and infinite extent in the x- and y-directions, fig.6.1, we also have a body whose boundary is describable with one coordinate surface (in x-y-z system), the other part of the boundary being at infinity. The problem of propagation of elastic wave through such a plate has been solved in close-form by Lamb (1917), and it appears only such simplified geometries can be analysed. A further example is the free vibrations of an elastic sphere, Lamb (1882).

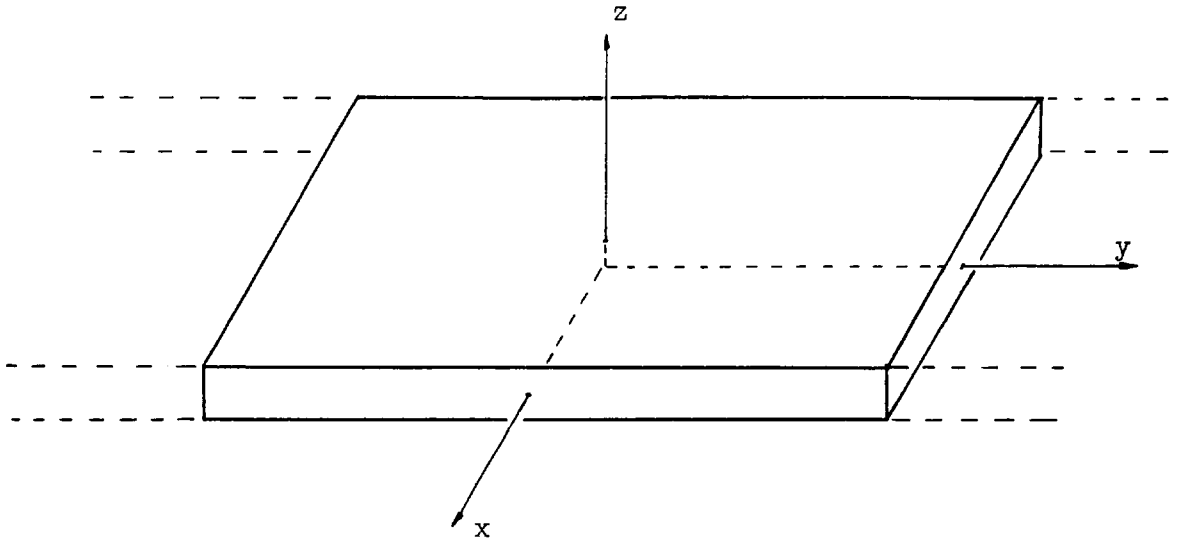

Fig 6.1 Elastic Plate

In fig.6.1 if we make, say, the x-dimension of the plate finite, the problem of wave propagation becomes unsolvable in closed-form, as observed by Morse (1950). The zero-stress conditions can be satisfied on either the x-faces or the z-faces. If the plate is sufficiently wide, the approximation usually made is to satisfy the boundary conditions on the wider z-faces while those on the narrow x-faces are ignored. If both x- and z-dimensions are of comparable sizes we have a bar of rectangular cross-section whose solution is not known. One could go further and make the y-dimension of the plate finite and comparable to other dimensions, so that we have a rectangular parallelopiped. This brings in one more dimension of intractability.

This analytical difficulty is responsible for the dearth of information on some practically useful aspects of foundation dynamics. For example the flexibility of the foundation is ignored because the elastic analysis of the half space is difficult enough let alone introducing that of the foundation.

The usual numerical methods employed in the elastic analysis of a finite body are the finite difference and the finite element methods. In elastostatics researchers have found that the Boundary Integral Equation (BIE) method has many more superior qualities. One therefore wonders if

these qualities cannot be similarly exploited in elastodynamics.

In this chapter the application of the BIE method to analysis of flexible foundations, as well as interaction of foundations, is examined qualitatively, beginning with analysis of a finite elastic body. Numerical results are not presented.

6.2 VIBRATIONS OF ELASTIC SOLIDS

Consider a block of elastic material of arbitrary shape. A rectangular block is shown in fig.6.2 for ease of drawing on the paper.

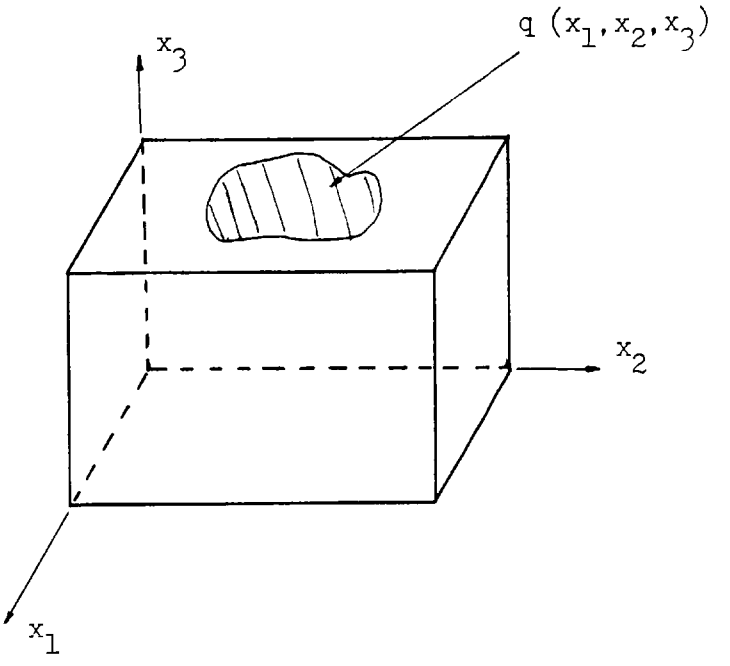

Fig 6.2 A Block of Elastic Material

It is subjected to a stress distribution $q(x_1,x_2,x_3)$ on a portion of the surface shown shaded. For the sake of argument we assume the block rests on a rigid x_1-x_2 surface. The stress q varies harmonically with time.

The boundary conditions are such that on the stress-free surfaces of the block, $t_k = 0$, u_k = unknown, $k = 1,2,3$. On the surface in contact with the rigid base, t_k = unknown, $u_k = 0$, and on the loaded area, t_k = known, u_k = unknown. These boundary data all related by the boundary integral equation, as before,

$$c_{jk}u_k(P) + \int_S T_{jk}(P,Q)u_k(Q)\ ds(Q)$$

$$= \int_S U_{jk}(P,Q)t_k(Q)\ ds(Q) \qquad (6.2.1)$$

From this one can determine the displacement u at some point of interest on the body and thus map out the mode shape at a given frequency, or one can determine the stress distribution at the contact with the rigid base.

Upon dicretising the boundary data we end up with the following system of algebraic equations

$$\left[A_1\right]\{u\} = \left[A_2\right]\{t\} \qquad (6.2.2)$$

the integration scheme being exactly as described for the foundation problem in chapter 5.

The free vibrations of the block may be similarly examined. In this case the whole surface is stress-free, the integral on the right hand side of eq.(6.2.1) is zero and the equation reduces to the form

$$c_{jk}u_k(P) + \int_S T_{jk}(P,Q)u_k(Q)\, ds(Q) = 0 \qquad (6.2.3)$$

Although this equation has an appearance similar to Fredholm's second integral equation, see Mikhlin (1957), it is essentially not the same because of the second-order singularity $O(1/R^2)$ of the kernel T_{jk}. But as shown by Kupradze (1963), Fredholm's second theorem can be proved for this singular integral equation. The equation has a discrete spectrum of proper frequencies (eigenvalues) ω^2 at which non-trivial solutions exists for u_k. Since the right hand side of (6.2.3) is zero, the discretised form is the same as eq.(6.2.2) with the right hand side zero. Also since T_{jk} is a non-linear function of ω^2, the problem is

a non-algebraic eigen-value problem in which the eigen-solution of matrix A in eq.(6.2.2) is to be obtained by root-searching method. The free vibration of an elastic sphere, Lamb (1882), would be a very good test case for this method. It is observed that since only the boundary data are discretised the problem size is considerably reduced compared with the finite difference and the finite element methods in which the data in the entire domain occupied by the block are discretised.

Next we shall be able to exploit this saving in problem size to introduce the elastic analysis of the half space and thus obtain an analysis of flexible foundations on the elastic half space.

6.3 VIBRATION OF AN ELASTIC FOUNDATION ON AN ELASTIC HALF SPACE

If the x_1-x_2 plane in fig.6.2 is taken as the surface of the elastic half space, the formulation described above applies to the block as the elastic foundation. The system of equations (6.2.2) applies except that both the stresses t_k and displacements u_k are unknown on the interface. The system of equations (5.6.1) in chapter 5 for the half space applies

$$\left[B_1\right]\left\{u\right\} = \left[B_2\right]\left\{t\right\} \tag{6.3.1}$$

except also that both the contact stresses and displacements with the foundation are unknown. At the interface the displacement compatibility conditions and stress equilibrium conditions are employed

$$\begin{aligned} u_k^{(f)} &= u_k^{(h)} \\ t_k^{(f)} &= -t_k^{(h)} \end{aligned} \tag{6.3.2}$$

where superscripts (f) and (h) refer to foundation and the half space respectively. Eqs.(6.2.2), (6.3.1) and (6.3.2) form a linear system which can be solved for the unknown interfacial functions.

The work of Krent and Schmidt (1979) on the vibration of elastic circular plate on an elastic half space is interesting, particularly the semi-numerical approach employed. Just as in the initial studies on rigid foundations, such approaches start with simpler geometries like the circular shape and get stuck on more complicated shapes. The method of Krent and Schmidt depends on the availability of a closed-form expression relating the deformation of the elastic plate to the applied stresses. They used the approximate plate equations of Mindlin

(1951). Since such expressions are not forthcoming for bodies of arbitrary shapes the only choice at present is an efficient numerical method. The method described here applies to elastic bodies of arbitrary shape.

6.4 INTERACTION OF RIGID FOUNDATIONS ON AN ELASTIC HALF SPACE

In a survey of soil dynamics, Whitman (1969) stated that among important unresolved problems is the study of the interaction of nearby masses on the ground. This is another aspect of foundation dynamics in which the BIE appears very effective. The application of the method dwells on the fact that all motions of a given foundation are determined by the three components of stress t_k, $k = 1,2,3$ at the interface. The implementation is feasible due to the fact that the algebraic system of equations (5.6.1) can be set up for a stress distribution over an area of arbitrary shape on the half space as indicated by the shaded area in fig.5.2. Then the area is partitioned into a number of zones e, f, g in fig.6.3 below. Region h separates the zones. The outer curve C is that within which the BIE integrals have been truncated. The inner curve E is the boundary of the area on which we have some stress distribution. If after setting up the algebraic equations we prescribe zero stresses and unknown

displacements for all nodes within region h, we shall have the zones e, f, g representing the contact areas of three foundations separated by region h.

In this case the characteristic dimension "b" of the region E used for the dimensionless quantities in eqs.(5.3.3) and (5.3.4) must be chosen so that the entire region E falls within a circle of some convenient radius, say, unity. This is to ensure that for foundations positioned any reasonable distance apart the region E can still permit numerical integration over an area that is not too wide.

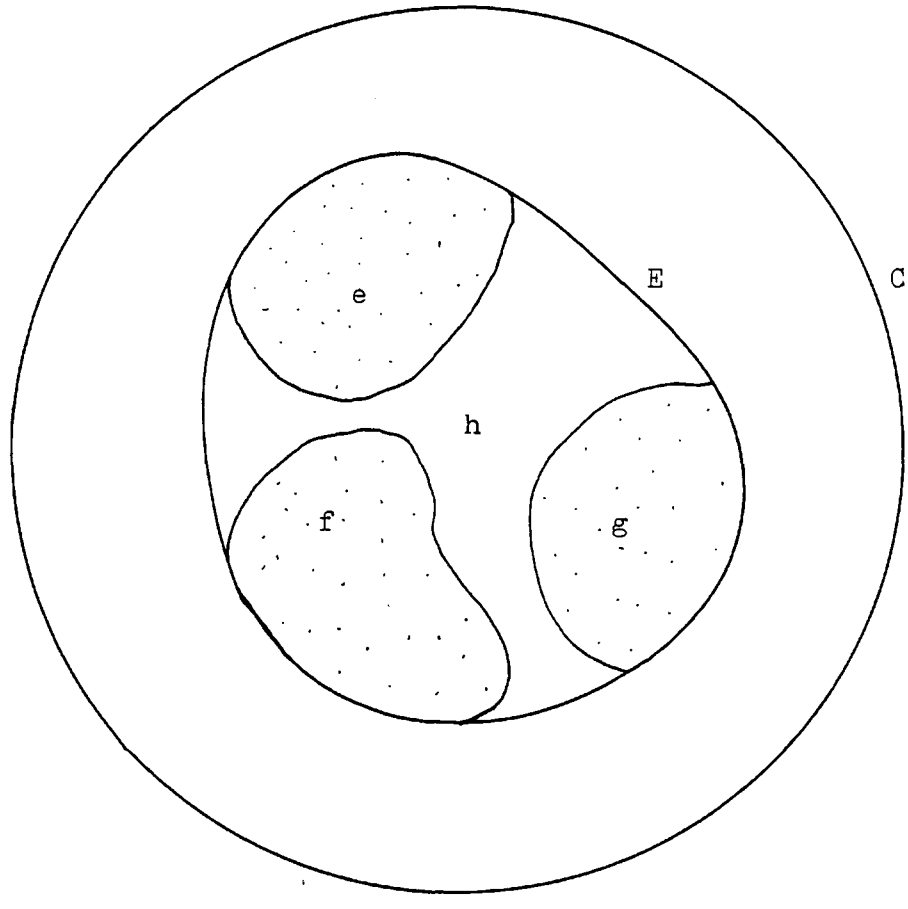

Fig 6.3 The Contact Areas of Three Foundations

The formulation of the problem is very similar to that in section 5.3, chapter 5, for the general six degrees-of-freedom single foundation system - and it must be remembered that each foundation in the present multi-foundation system is exposed to the full six degrees-of-freedom excitation. Unlike section 5.3, however, it will be more convenient to formulate the problem directly in terms of response of a given system of massess, excitation forces/couples, etc, instead of first solving for stiffness which may not be easy to define unambiguously in the present case. We shall assume, as before and without loss of generality, that the centers of mass of the foundations are very close to the centroids of the bases. m^r, r=e,f,g, is the mass of foundation r where superscript r is used to refer to the foundation e, f, or g in fig.6.3. $\bar{J}_{jk}$, j,k=1,2,3, are the mass moments of inertia. In order to employ a homogeneous set of notation we may use m^r_{jk} to indicate the inertia properties of the foundations in the six possible directions of motion, such that

$$m^r_{jk} = m^r, \quad j = k, \quad j,k = 1,2,3$$

$$m^r_{jk} = \bar{J}_{jk}/b^2, \quad j,k = 4,5,6$$

b is a characteristic length of the system of foundations. We put the motions of the foundations as

w_1^r, translation in x_1-direction,

w_2^r, translation in x_2-direction,

w_3^r, translation in x_3-direction,

Θ_1^r, rotation about x_1-axis,

Θ_2^r, rotation about x_2-axis,

Θ_3^r, rotation about x_3-axis,

and define

w_4^r as $b\Theta_1^r$,

w_5^r $b\Theta_2^r$,

w_6^r $b\Theta_3^r$,

so that the complete motion of a foundation is described by w_k^r, $k = 1,2,3,\ldots,6$.

The reactions of the supporting medium to a given foundation are indicated by the stress integrals Q_k^r, $k = 1,2,3,\ldots,6$, where Q_k are given are given by the stress integrals defined below eq.(5.3.2) with the understanding that integration pertaining to a given foundation is restricted to the contact area between that foundation and the soil.

The excitation forces applied to a foundation are

F_1^r, force applied in x_1-direction,

F_2^r, force applied in x_2-direction,

F_3^r, force applied in x_3-direction,

Υ_1^r, couple applied about x_1-axis,

Υ_2^r, couple applied about x_2-axis,

Υ_3^r, couple applied about x_3-axis.

Define

F_4^r as Υ_1^r/b,

F_5^r, Υ_2^r/b,

F_6^r, Υ_3^r/b,

so that the forces and couples are described by F_j^r, $j = 1,2,3,\ldots,6$.

The six equations of harmonic motion of a foundation are

$$- \omega^2 m_{jk}^r W_k^r + Q_j^r = F_j^r \qquad (6.4.1)$$

$$j,k = 1,2,\ldots,6$$

$$r = e,f,g$$

If we had taken account of the coordinate distances of

the centers of mass of the foundations from their respective centroids of base, we would only need to redefine the motions W_k^r and forces Q_j^r and F_j^r in terms of components through the centers of mass. This omission does not impair the generality of the formulation of the elasticity problem.

The components of displacement and stress on the surface of the half space are indicated by u_k and t_k as before. Under each foundation these components are u_k^r and t_k^r respectively. t_k^r appear under the integrals involved in the quantities Q_j^r in eq.(6.4.1) above. u_k^r are related to W_k^r through the requirements that each foundation remains rigid during motion,i.e.,

$$u_1^r = W_1^r - x_2\Theta_3^r = W_1^r - x_2 W_6^r/b$$

$$u_2^r = W_2^r + x_1\Theta_3^r = W_2^r + x_1 W_6^r/b$$

$$u_3^r = W_3^r + x_2\Theta_1^r - x_1\Theta_2^r = W_3^r + (x_2 W_4^r - x_1 W_5^r)/b \qquad (6.4.2)$$

as in eqs.(5.3.1). So u_k^r are known in terms of W_k^r under the foundations, while t_k remain unknown. But u_k remain unknown elsewhere while $t_k = 0$.

All the displacements and stresses are related by the boundary integral equation, as before,

$$c_{jk}u_k(P) + \int_S T_{jk}(P,Q)u_k(Q)\ ds(Q)$$

$$= \int_S U_{jk}(P,Q)t_k(Q)\ ds(Q) \qquad (6.4.3)$$

The aim is to extract the stress integrals Q_j in terms of W_k from above equation using eq.(6.4.2) and then substitute them into the equations of motion (6.4.1). The implementation is to discretise the equations over a suitable mesh of nodes superposed over fig.6.3 and solve the resulting set of algebraic equations simultaneously.

The numerical integration scheme for the boundary integral equation is exactly as described in chapter 5, with the mesh elements covering up to the circle C in fig.6.3. Some of the elements are arranged to have part of their boundaries coincide with the appropriate bondary lines in fig.6.3, just like the single foundation problem. It is noted that the quadratic variation of variables employed over an element is adequate for modelling curved boundary lines, e.g., the circular foundation problem of previous chapter. After the integration we arrive at the algebraic

system of equations

$$[B_1]\{u\} = [B_2]\{t\} \tag{6.4.4}$$

which may be set up immediately without regard yet to any particular mode of vibration, contact conditions, or any special aspect of the system we wish to investigate. Equation (6.4.4) above is simply a numerical version of the boundary integral equation. {u} is the vector of nodal displacements and {t} that of the nodal stresses. The coefficient matrices B_1 and B_2 may be partitioned to indicate which terms pertain to nodes in which region in fig.6.3.

$$\left[\begin{array}{c|c|c|c|c} e & f & g & h & S_o \end{array}\right] \left\{\begin{array}{c} u^e \\ \hline u^f \\ \hline u^g \\ \hline u^h \\ \hline u^{So} \end{array}\right\} = \left[\begin{array}{c|c|c|c|c} e & f & g & h & S_o \end{array}\right] \left\{\begin{array}{c} t^e \\ \hline t^f \\ \hline t^g \\ \hline t^h \\ \hline t^{So} \end{array}\right\}$$

S_o indicates the stress-free region between curves E and C. It is observed again, as in chapters 4 and 5, tnat it is not necessary to compute the terms of matrix B_2 belonging to S_o and h because zero stresses shall be

prescribed there. In this system of equations we wish to shuffle between the knowns and unknowns and regroup the unknowns to the left and the knowns to the right.

The vectors $\{u^{So}\}$ and $\{u^{h}\}$ are unknown. The vectors $\{u^{e}\}$, $\{u^{f}\}$ and $\{u^{g}\}$ are regrouped in terms of the new variables $\{w^{e}\}$, $\{w^{f}\}$ and $\{w^{g}\}$ using the discretised forms of the rigidity equations (6.4.2) to form $6x3=18$ additional columns to the left hand side matrix. The positions vacated by the coefficients of $\{u^{e}\}$, $\{u^{f}\}$ and $\{u^{g}\}$ are then taken up by tne coefficients of the unknown $\{t^{e}\}$, $\{t^{f}\}$ and $\{t^{g}\}$ respectively transferred from the right hand side, which now becomes zero. The new system of equations has a rectangular coefficient matrix on the left hand side and zero on the right, there being 18 less equations than unknowns.

$$\left[\begin{array}{c|c|c|c|c} e & f & g & h & S_o \end{array}\right] \left\{\begin{array}{c} t^{e} \\ \hline t^{f} \\ \hline t^{g} \\ \hline u^{h} \\ \hline u^{So} \\ \hline w^{e} \\ w^{f} \\ w^{g} \end{array}\right\} = 0 \qquad (6.4.6)$$

The system is completed by bringing in the discretised forms of the 18 equations of motion (6.4.1) of the rigid foundations, i.e.,

$$\left[\begin{array}{c|c|c|c|c|c} e & f & g & (\text{zero}) & (\text{zero}) & \end{array}\right] \left\{\begin{array}{c} t^e \\ \hline t^f \\ \hline t^g \\ \hline u^h \\ \hline u^{So} \\ \hline w^e \\ w^f \\ w^g \end{array}\right\} = \left\{\begin{array}{c} F^e \\ F^f \\ F^g \end{array}\right\} \tag{6.4.7}$$

Eqs.(6.4.6) and (6.4.7) form a complete set of equations that may be solved simultaneously for the response $\{W^r\}$ of the foundations together with the nodal stress distributions $\{t^r\}$ under each foundation. Any aspect of the system may be investigated from this set of equations. For example, if only one foundation is excited in one particular manner, the appropriate force components F_j^r are made zero in eq.(6.4.7). The displacement transmission ratio can be found by computing the ratio of the appropriate values of W_k^r, or the force transmission ratio may be found by computing the ratio of the appropriate excitation force and

stress integrals.

It may be observed that above is the complete formulation of the problem. It takes care of the simultaneous presence of all the foundations and the inter-dependence of the stress distribution under them. The foundations may be of any shape. The only approximation is the discretisation of the equations. The analysis of multi-foundation systems is very rare in the literature. It is worthwhile to compare now the users of the previous methods of analysis of foundation vibrations approached (or might have approached) the problem of interaction of foundations.

6.5 COMPARISON WITH PREVIOUS METHODS OF ANALYSIS.

The grouping of previous methods of analysis is that used in section 1.2 of chapter 1.

(a) Finite Model of the Semi-Infinite Half Space.

As far as the author is aware no work has appeared in the literature employing this method to multi-foundation problems. The method would be difficult to implement because, as observed in chapter 1, the finite model would probably have to be very large before satisfactory accuracy can be achieved. The discretisation over the volume of a

domain is very expensive and less accurate than the BIE method which approximates only over the boundary. After their attempt on the two-foundation problem, discussed below, Warburton, Richardson and Webster (1971) suggested that such problems would more likely be better investigated using three-dimensional finite elements. Truly a numerical approach is best for this type of problem, and the BIE seems to be more attractive.

(b) Analytical Method of Dual Integral Equations.

This method can only be used for simple shapes as circles that can be described by a simple closed-form algebraic expression, and even then only for single-foundation systems. When there are more than one foundation, the shapes of the contact areas (even if individually circular) taken together cannot be so described and the method becomes cumbersome when it comes to applying the boundary conditions of non-zero surface stresses on patches of the surface.

This is probably why researchers have been forced to first analyse a single foundation before imposing the presence of the second one by some approximations. Richardson, Webster and Warburton (1971) computed displacements on the surface of the half space near to a single harmonically excited circular foundation. Then Warburton, Richardson and Webster (1971) employed an averaging technique over these

displacements on a selected region to determine the response of a second foundation that would occupy that region. The drawback in this approach is the implied assumption that the presence of the second foundation would not nave affected those displacements that were computed in its absence. As the authors rightly observed, the presence of the second foundation can be appreciable, and no estimate of the amplitude of its response can be made solely by considering the surface displacements which would exist without it being present. This simplified approach has been employed by a number of researchers. Lee and Wesley (1973) determined the dynamic response to seismic loading of a group of flexible structrures which are bonded in close proximity to an elastic half space. They represented discrete values of free-surface displacements computed by Richardson et al (1971) for the single-foundation system by a set of continuous functions and integrated them over regions designated for other foundations. MacCalden and Mathieson (1973) gave experimental and theoretical results for the transmission of harmonic vibrations from an excited rigid circular foundation to a nearby unexcited one. For their theory they used the single-foundation solution of Bycroft (1956). Clement (1974) used the technique with his single-foundation theory which included hysteretic damping.

(c) Green Function Approach.

The approach of Hamidzadeh (1978) on a system of two square foundations is the same averaging technique over displacements computed in the absence of one of the foundations. Probably because of some untidiness inherent in his single-foundation analysis, he could only allow for certain modes of vibration by each of the foundations instead of letting them execute their coupled motions.

The Green function approach by Wong and Luco (1976) is worth mentioning here even though there has been no application of that method to the multi-foundation problem. By now it is clear that the integral representation of the single-foundation problem by Wong and Luco, see eq.(1.2.2) in chapter 1, is rather similar to the BIE formulation in that the stress is multiplied by a kernel function and integrated over the soil-foundation interface. So a formulation for the multi-foundation problem similar to the BIE formulation above can be made using the Wong-Luco equation. But the problem with that equation is in the kernel function which itself contains finite and infinite double integrals of oscillatory functions as discussed in section 1.2, whereas the kernels U_{jk} and T_{jk} in the BIE formulation are simple closed-form expressions.

(d) Conformal Mapping of the Half Space.

It is possible to think of applying this technique to the

multi-foundation problem by transforming the entire half space volume to a rectangular parallelopiped and then apply finite difference discretisation. As observed in chapter 1, the resulting large set of equations to solve would be too cumbersome to handle. Moreover, an observation similar to that in paragraph (a) above may be made about this approach, namely, the efforts spent computing quantities at points within the half space are wasted and irrelevant to the foundation problem, and the discretisation of equations throughout the domain leads to less accuracy.

chapter 7

CONCLUSION

7.1 ACHIEVEMENTS OF THE PRESENT WORK

The contribution of the present study to the knowledge of the dynamics of foundations on the elastic half space may be summarised as follows.

A new mathematical tool, the Boundary Integral Equation method, has been developed for analysing the dynamics of foundations on the elastic half space. Addressing directly the physics of the problem, the BIE method is able to seize on the physical requirements in the form of the radiation conditions of elastodynamics to make itself particularly suited to the problems of foundation dynamics. This quality of the method is further enhanced as it deals directly with boundary data, the only data that is most relevant to the foundation problem, and consequently achieves tremendous reduction in problem size. The integrands involved in the method are only simple closed-form expressions, and so numerical implementation is cheap. The BIE is a one equation that provides solutions to all modes of vibration, pure or coupled, as well as various types of contact conditions. As such it sort of presents itself as a universal statement of the dynamics of foundations in so far as it has been tested in this study.

All possible motions of the rigid infinite rectangular

strip foundation have been analysed, including the general three degrees-of-freedom. The pure modes have been compared with existing results. The results for pure vertical mode shows very good agreement with analytical results by Karasudhi, Keer and Lee (1968) and Luco and Westmann (1972). The conditions of frictionless contact and those of fully bonded contact have been investigated. Just as Luco et al observed, fig.4.15 shows little difference between the two types of contact conditions for Poisson ratio of 1/4 (and higher). The compliance for the pure horizontal mode as computed by the BIE method shows equally good agreement with results by Luco et al. But for the pure rocking mode, the compliance by Luco et al shows slight over-estimation compared with that by this study, fig.4.19. The approximations made by Luco et al in evaluating their integrals were probably biginning to show. The compliances, direct and coupling, for the coupled horizontal-rocking modes also show very good agreement between this study and that by Luco et al, except again for the direct rocking compliance and the coupling compliances. The three degrees-of-freedom motion is mentioned later.

To leave the accuracy of the BIE method in no doubt the well known problem of vibration of foundation with circular base has been analysed. The vertical response amplitude shows remarkable agreement with the well known

results of Awojobi and Grootenhuis (1965) and the experimental results of Arnold, Bycroft and Warburton (1955), fig.5.11. As for the torsional mode, a closed-form analytical solution is available from Reissner and Sagoci (1944) and Sagoci (1944). The agreement between these and the BIE results is remarkable, fig.5.15. We observe equally close agreement with the experimental results of Arnold, Bycroft and Warburton (1955) for the torsional response amplitude.

The rectangular foundation is also analysed. The pure vertical compliance by the BIE method for a square foundation shows the results of Hamidzadeh (1978) to be underestimations and those of Wong and Luco (1976) to be overestimations, figs.5.18a,b. The same observation can be made about pure horizontal vibration in fig.5.27, which probably points to the effect of the difficulties that Wong et al might have had in evaluating the infinite integrals of oscillatory functions involved in their kernel function G_{jk}, see eq.(1.2.2) in chapter 1 of this thesis and the subsequent discussions. The vertical vibration has been analysed for rectangular foundations of length/width ratio 1, 4, 8, 10, 16.

The stress distribution under the rigid foundation have also been plotted in some of the cases mentioned above - normal stress under infinite rectangular foundation in

vertical vibration, the shear stress under circular foundation in torsion, the shear stress under square foundation in horizontal translation, the normal stress under rectangular foundation of various length/width ratios in vertical vibration. In all of the cases the characteristic edge singularity in the stress distribution is clearly shown even though the value of infinity at the edge of the loaded region was, of course, not obtained in the numerical implementation. The three-dimensional stress plots of figs.5.22a,b and 5.23a,b for the square foundation in vertical vibration are very informative. It is interesting to note that this important feature of foundation dynamics is not lost in the BIE formulation and implementation unlike some numerical methods such as that by Wong and Luco (1976) which only hoped that even though the stress singularity was not adequately represented, the stress integral would be accurate enough for engineering purposes. Knowledge of the stress distribution is important because in addition to consideration of resonance, a foundation designer would like to know the magnitudes and distribution of the stresses he is designing to withstand.

The benefit of the advent of the modern digital computer is felt in most fields of research, and it is desirable that the field of foundation dynamics is not left out. The convenience of investigating most aspects of foundation

dynamics from the same BIE equation allows the problem solution to be presented in a cheap and versatile computer program, see concluding paragraphs of chapters 4 and 5. For example all the results for the infinite rectangular strip foundation in chapter 4 are produced from one program, from which various aspects were investigated by changing a word of input data to read, for example, ROCKING instead of VERTICA mode of vibration, or RELAXED instead of WELDEDD contact conditions. The program requires only 21,000 words of computer memory for in-core handling of all the codes and equations, and takes typically 8 seconds to compute the dynamic stiffness and stress distribution at a particular frequency (by a CDC Cyber 174 batch processor). The results in chapter 5 for foundation of finite size are similarly coded into another program requiring 51,000 memory words and typically 40 seconds to execute at one value of frequency factor. Wong and Luco (1976) reported that at one particular frequency, the evaluation of their influence function G_{jk}, see eq.(1.2.2), took 2 minutes (on an IBM 370/158 batch processor), presumably before proceeding to solve the vibration problem for the square foundation.

It has been intended to present the BIE not only as a more convenient way of analysing foundation dynamics, but also as a means of going beyond where other methods have usually stopped, and looking ahead to future developments

in this field and in the field of elastodynamics in general. The three degrees-of-freedom vibration of the infinite rectangular strip foundation has been investigated, and the usually implied assumption has been verified that there is no coupling between the vertical and other modes. The vertical vibration has been analysed for rectangular foundations of length/width ratio of up to 16. It is common to approximate such "long" foundations as infinite strips in order to simplify analysis, without examining the errors involved in such approximations. The errors involved have been investigated quantitatively as far as predicting vertical resonance frequencies is concerned. The approximation usually results in underestimation of resonance frequency. For a mass ratio of 40 or less the length of the rectangular base must be at least six times greater than the width to achieve an error of less than 10%, see fig.5.29. As expected the longer the rectangle the smaller the error. But for a given rectangle, the error increases with increasing mass ratio. It is expected that the same trend will hold for other modes.

The BIE is not restricted to the field of foundation dynamics. It is, presumably, a statement of the general elastodynamic problem. An indication has been given of how it may be applied as such to the analysis of dynamic response of elastic solids subjected to harmonic loads.

This subject has been the obstacle to the study of some of the more practical aspects of foundation dynamics. The way the BIE can cope with such aspects as the combined problem of vibration of elastic foundation on the elastic half space has been outlined. Also details have been given of a complete formulation with the BIE of the problem of interaction of rigid foundations on the elastic half space.

The formulation presented in this thesis is valid for foundations of arbitrary shape including discontinuities. The formulation of the necessary equations leading to the BIE method has been presented. The use of the method to meet the requirements of foundation dynamics, the necessary numerical manipulation of the method, and solution capabilities to new aspects of foundation problems have been demonstrated. It is felt that the way is now open to the investigation of much more sophisticated problems, with the formulation in this thesis an invaluable tool.

7.2 SUGGESTIONS FOR FUTURE RESEARCH

It was mentioned in section 2.1, chapter 2, that the Boundary Integral Equation method has not been as developed in the field of elastodynamics as it is in elastostatics. In the latter field the method appears to represent a universal statement of elastostatics in that the same equation solves virtually all types of problems ranging from elastic fracture mechanics and rock mechanics to elastoplastic and thermo-elasticity analysis. It is desirable to carry over the benefits of this new-found tool to elastodynamics, so that hopefully the BIE method could also be regarded as embodying solutions to almost all types of elastodynamic problems. Simple problems to start with include elastic wave diffraction through circular cylinders of infinite or semi-infinite length whose solutions are known, as well as through cylinders of rectangular cross-section whose solutions are difficult to obtain in closed-form. Then bodies of finite shapes can be studied, such as the free vibration of an elastic sphere whose solution is known, and then the rectangular parallelopiped whose solution is not known. Once the elastodynamic deformation of finite bodies can be successfully analysed, the way is paved for introducing flexibility into foundations of arbitrary shape, and then for such studies as the effect of topology on surface waves.

The interaction of foundations on the elastic half space may now be fully studied. But this requires first a fuller investigation of the unconstrained (six degrees-of-freedom) vibration of foundation of arbitrary shape.

It must be stated that there is plenty of scope for improvement on the implementation of this BIE scheme. This thesis is simply to draw the attention of researchers to this convenient method of analysis. As new and improved methods of numerical implementation of the scheme continue to evolve in elastostatics it is desirable that elastodynamics does not fall behind.

appendix A

THE CONCEPT OF "ELASTODYNAMIC STATE"

A.1 DEFINITIONS

Following Eringen and Suhubi (1975), we may use the notation $C^{m,n}(D,\mathbf{r})$ where m and n are integers, to define the class of all functions that exist and are continuous with their spatial derivatives of order up to and including m and time derivatives of order up to and including n, on $D\times\mathbf{r}$. The latter notation $D\times\mathbf{r}$ denotes a spatial region D and a time interval $\mathbf{r}$. $\Phi \in C^{m,n}(D\times\mathbf{r})$ implies that the function Φ belongs to class $C^{m,n}$. $\mathbf{r}^-$ is used to denote the state of the past, and $\mathbf{r}^+$, that of the present and henceforth.

This latter classification of $\mathbf{r}$ is needed only for transient problems. In our present case of steady state elastodynamics, harmonic time variation is assumed. It is therefor sufficient to write the class $C^m(D)$ and bear in mind that a function $\Phi \in C^m(D)$ is a function of frequency.

A.2 THE ELASTODYNAMIC STATE

This is a convenient reference to all the parameters and field variables existing in an elastic domain during a given (steady state) event. Let D be a spatial domain

with boundary S. If $\underline{u}$ and $\underline{\sigma}$ are, respectively, a vector-valued and a symmetric second-order tensor-valued function defined on D, we call the ordered pairs $\mathscr{A}=[\underline{u},\underline{\sigma}]$ an elastodynamic state on D with the displacement field $\underline{u}$ and the stress field $\underline{\sigma}$, corresponding to a body force density $\underline{f}$, mass density ρ, irrotational wave speed c_1, and equivoluminal wave speed c_2. The following provisions are assumed to hold.

(a) $\underline{u} \in C^2(D)$, $\underline{u} \in C^1(D)$, $\underline{\sigma} \in C^0(D)$, $\underline{f} \in C^0(D)$.

The stress and body force functions are allowed to be discontinuous. The constants ρ, c_1, and c_2 are subject to

$$\rho > 0, \quad c_1 > 2/\sqrt{3}c_2 > 0$$

(b) $\underline{u}$, $\underline{f}$, c_1 and c_2 satisfy the Navier's elastodynamic equation of motion (2.2.2) with body force included, namely,

$$(c_1^2 - c_2^2)\,\nabla\nabla\cdot\underline{u} + c_2^2\,\nabla^2\underline{u} + \omega^2\underline{u} + \underline{f} = 0$$

With this definition the notion of elastodynamic states (1), $\mathscr{A}_1[\underline{u},\underline{\sigma}_1]$, and (2), $\mathscr{A}_2[\underline{u}_2,\underline{\sigma}_2]$ become clear as belonging to two different events. For example in the formulation of the boundary integral equation in section

2.5, chapter 2, one of the two distinct elastodynamic states involved in the Betti-Rayleigh equation (2.3.4) of section 2.3, namely $\mathscr{A}_1$, is taken to correspond to the Stoke's problem of a concentrated time-harmonic body force acting in a given direction in an infinite domain. The other state $\mathscr{A}_2$ is the problem we wish to solve.

appendix B

SOME ALGEBRAIC DETAILS

B.1 EXPANSION OF U_{jk} FOR TWO-DIMENSIONAL PROBLEMS

The expression for U_{jk} is given by eq.(2.4.3)

$$U_{jk}(P,Q) = \frac{i}{4\rho}\left\{ \frac{1}{c_2^2} H_o^{(1)}\{k_2 R\}\delta_{jk} + \frac{1}{\omega^2}\frac{\partial^2}{\partial x_j \partial x_k}\left(H_o^{(1)}\{k_2 R\} - H_o^{(1)}\{k_1 R\}\right)\right\}$$

$$j,k = 1,2 \qquad \text{(B.1.1)}$$

in which

$$R = \left((x_1 - y_1)^2 + (x_2 - y_2)^2\right)^{1/2}$$

It will be convenient to employ the following short form notations.

$$\left\{ \bullet \right\}_{,j} \equiv \frac{\partial}{\partial x_j}\left\{ \bullet \right\}$$

where the dot within the brackets indicate any given expression.

Also

$$\beta_{mn} \equiv R_{,m} R_{,n}$$

$$\delta_{mn} \equiv \text{the Kroenecker delta}$$

$\frac{\partial}{\partial n}$ ≡ directional derivative along unit normal n.

summation is implied on repeated subscripts.

The following identities will be useful and may be verified

$$\left\{H_o(k_jR)\right\}_{,m} = - k_j H_1(k_jR) R_{,m}$$

Therefore it is easy to show that

$$\left\{H_o(k_jR)\right\}_{,m,n} = k_j^2 H_2(k_jR) \delta_{mn} + \frac{k_j}{R} H_1(k_jR) \beta_{mn}$$

The second term in eq.(B.1.1) above may then be evaluated and the results substituted back into the expression. After grouping terms, the functions Ψ and χ are then introduced as defined for eqs.(2.4.4) and (2.4.5) in chapter 2. The final result is obtained as in eq.(2.4.4).

$$U_{mn} = \frac{i}{4\mu} (\Psi\delta_{mn} + \chi\beta_{mn}) \qquad (B.1.2)$$

Let's put $\alpha_1 = i/4\mu$ to save some writing.

B.2 DIFFERENTIATIONS OF U_{jk} TO OBTAIN T_{jk}, TWO-DIMENSIONAL PROBLEM.

Recall eq.(2.4.2)

$$T_{jm} = \lambda U_{jr,r} n_m + \mu(U_{jm,s} + U_{js,m}) n_s \qquad (B.2.1)$$

By careful manipulations, the following expressions may be simplified.

$$U_{jr,r} = \alpha_1 (\Psi\delta_{jr} + \chi\beta_{jr})_{,r}$$

$$= \alpha_1 (\Psi_{,r}\, \delta_{jr} + \chi_{,r}\, \beta_{jr} + \chi\beta_{jr,r})$$

$$U_{jm,s} = \alpha_1 \left\{ (\Psi\delta_{jm})_{,s} + (\chi\beta_{jm})_{,s} \right\}$$

$$= \alpha_1 \left\{ \Psi_{,s}\, \delta_{jm} + \chi_{,s}\, \beta_{jm} + \chi\beta_{jm,s} \right\}$$

and similarly for $U_{js,m}$

$$U_{js,m} = \alpha_1 \left\{ (\Psi\delta_{js})_{,m} + (\chi\beta_{js})_{,m} \right\}$$

$$= \alpha_1 \left\{ \Psi_{,m}\, \delta_{js} + \chi_{,m}\, \beta_{js} + \chi\beta_{js,m} \right\}$$

Collecting results into expression (B.2.1),

$$T_{jm} = \alpha_1 \Big\{ (\Psi_{,r}\,\delta_{jr} + \chi_{,r}\,\beta_{jr} + \chi\beta_{jr,r}) + \mu n_s(\Psi_{,s\ jm} + \chi_{,s}\,\beta_{jm} + \chi\beta_{jm,s}) + \mu n_s(\Psi_{,m}\,\delta_{js} + \chi_{,m}\,\beta_{js} + \chi\beta_{js,m}) \Big\}$$

After a considerable amount of indicial manipulation we find

$$T_{jk}(P,Q) = \frac{i}{4}\left(A_1 \frac{\partial R}{\partial n}\,\delta_{jk} + A_2 \frac{\partial R}{\partial n}\,R_{,j}R_{,k} + A_3\,R_{,k}n_j + A_4\,R_{,j}n_k \right)$$

which corresponds to eq.(2.4.5) for which the functions A_1, A_2, A_3, and A_4 have been defined in chapter 2.

B.3 EXPANSION OF U_{jk} FOR THREE-DIMENSIONAL PROBLEMS

The expression for U_{jk} is given by eq.(2.4.1)

$$U_{jm} = \frac{1}{4\pi\rho}\left\{ \frac{1}{c_2^2 R} \exp(\imath k_2 R)\, \delta_{jk} + \frac{\partial^2}{R\,\omega^2\, \partial x_j \partial x_m} \left(\exp(\imath k_1 R) - \exp(\imath k_2 R) \right) \right\}$$

$$j,m = 1,2,3$$

in which

$$R = \left((x_1 - y_1)^2 + (x_2 - y_2)^2 + (x_3 - y_3)^2 \right)^{1/2}$$

The short form notation introduced in section B.1 above holds except that the indices range over 1,2,3 instead of just 1,2

If R_j is the compnent of the vector of position from $P(\underline{y})$ to $Q(\underline{x})$, we find, after carrying out the differentiations indicated in expression (B.3.1) above,

$$U_{jm} = \frac{1}{4\pi\rho}\left\{ \left(\frac{3R_jR_m}{R^3} - \frac{\delta_{jm}}{R}\right)\left[(\exp(ik_2R) - \exp(ik_1R))/\omega^2R^2 \right.\right.$$

$$\left. + \left(\frac{1}{c_2}\exp(ik_2R) - \frac{1}{c_1}\exp(ik_1R) \right)\right]$$

$$+ \frac{R_jR_m}{R^2}\left(\frac{1}{c_1^2}\exp(ik_1R) - \frac{1}{c_2^2}\exp(ik_1R) \right.$$

$$\left.\left. + \frac{\delta_{jk}}{Rc_2}\exp(ik_2R) \right\}\right.$$

After simplification involving long manipulation, and regrouping terms,

$$U_{jm} = \frac{1}{4\pi\rho}\frac{1}{R}\left(\Psi\delta_{jk} + (3\Phi + \chi)R_{,j}R_{,m}\right)$$

where the functions Ψ, Φ and χ have been defined for eqs.(2.4.6) and (2.4.7) in chapter 2. The symbols Φ and χ are used just for convenience and should not be confused with those used in section B.1

B.4 DIFFERENTIATION OF U_{jk} TO OBTAIN T_{jk} FOR THREE-DIMENSIONAL PROBLEMS

Recall again eq.(2.4.2)

$$T_{jm} = \lambda U_{jr,r} n_m + \mu(U_{jm,s} + U_{js,m}) n_s$$

It is useful to observe that

$$U_{jr,r} = \text{Div.}\underline{U}$$

where $\underline{U}$ is the second order tensor-valued function U_{jm}
If the definition

$$U_{jp,q} = \frac{\partial}{\partial x_q}(U_{jp})$$

is recalled, the differentiations involved in eq.(B.4.1) above is a question of algebra.
The notations A_1, A_2, A_3, A_4 are e ployed again, but with definitions as given below eq.(2.4.6) and (2.4.7) in chapter 2. The expression for T_{jk} below m be conveniently grouped in terms of the notations to obtain a further simplification.

$$T_{jk}(P,Q) = \frac{1}{4\pi}\frac{1}{R^2}\left(A_1 \frac{\partial R}{\partial n}\delta_{jk} + A_2 \frac{\partial R}{\partial n} R_{,j}R_{,k} \right.$$

$$\left. + A_3 R_{,k}n_j + A_4 R_{,j}n_k \right)$$

corresponding to eq.(2.4.7)

references

1. ABRAMOWITZ M. and STEGUN I.A. eds. (1972)
Handbook of Mathematical Functions
Dover Publications, 10th Printing

2. AGABEIN M.E., PARMELEE R.A. and LEE S.L. (1968)
"A Model for the Study of Soil-Structure Interaction"
International Association for Bridge and Structural Engineering,
8th Congress. Theme VI, New York, p.1

3. ALABI B. (1979)
"A Conformal Mapping Solution To Elastodynamic Boundary Value Problems"
Ph.D Thesis, Imperial College, University of London

4. ANG A.H.S. and HARPER G.N. (1964)
"Analysis of Contained Plastic Flow in Plane Solids"
J. Eng. Mech. Div., ASCE Vol.90 p.397

5. ANG A.H.S. and NEWMARK N.M (1971)
"Development of a Transmitting Boundary for Numerical Wave Motion Calculation"
Report to the Defence Atomic Support Agency,
Washington D.C., April

6. ARNOLD R.N., BYCROFT G. N. and WARBURTON G.B. (1955)
"Forced Vibrations of a Body on an Infinite Elastic Solid"
J. Applied Mechanics, Vol.22 p.391

7. AWOJOBI A. O. (1966)
"Harmonic Rocking of a Rigid Rectangular Body on a Semi-Infinite Elastic Medium"
J. Applied Mechanics, Vol.88 p.547

8. AWOJOBI A. O. (1971)
"Approximate Solution of High-Frequency-Factor Vibrations of Rigid Bodies on Elastic Media"
J. Applied Mechanics, Vol.38 p.111

9. AWOJOBI A. O. and GROOTENHUIS P. (1965)
"Vibrations of Rigid Bodies on Semi-Infinite Elastic Media"
Proc. Royal Society of London, Vol.287A p.27

10. BAKER B. B. and COPSON E. T. (1950)
The Mathematical Theory of Huygen's Principle
Oxford (Clarendon), 1950, 2nd Ed.

11. BANAUGH R. P. (1963)
"Diffraction of Steady Acoustic Waves by Surface of Arbitrary Shape"
J. Acoustical Soc. of America, Vol.35 p.1590

12. BANAUGH R. P. (1964)
"Application of Integral Representations of Displacements Potentials in Elastodynamics"
Bulletin, Seismological soc. of America, Vol.54 p.1073

13. BANAUGH R. P. and GOLDSMITH W. (1963)
"Diffraction of Steady Waves by Surfaces of Arbitrary Shape"
J. Applied Mechanics, Vol.30 p.589

14. BERGER B. S. and ALABI B. (1978)
"Solution of Navier's Equation in Cylindrical Curvilinear Coordinates"
J. Applied Mechanics, Vol.45 p.812

15. BETTI E. (1872)
"Teoria dell' Elasticita"
II Nuovo Ciemento, 7-10, 5

16. BREBBIA C. A. (1978)
The Boundary Element Method For Engineers
Pentech Press, London, 1978

17. BYCROFT G.N. (1956)
"Forced Vibrations of Circular Plate on a Semi-Infinite Elastic Space and on an Elastic Stratum"
Phil. Trans. of the Royal Society, Vol.248A, p.327

18. CHERTOCK G. (1964)
"Sound Radiation from Vibrating Surfaces"
J. Acousical Soc. of America, Vol.36 p.1305

19. CHREE C. (1889)
"The Equations of an Isotropic Elastic Solid in Polar and Cylindrical Coordinates. Their Solution and Application"
Trans. Cambridge Philosophical Society, Vol.14 p.251

20. CLEMENT J.F. (1974)
"Dynamic Response of Structures on Elastic Media"
Ph.D Thesis, Nottingham University.

21. CRUSE T. A. (1967)
"The Transient Problem in Classical Elastodynamics

Solved by Integral Equations"
Ph.D Thesis, University of Washington, 1967

22. CRUSE T. A. (1969)
"Numerical Solutions in Three Dimensional Elastostatics"
International Journal of Solids and Structures Vol.5
p.1259

23. CRUSE T. A. (1972)
The Surface Crack: Physical Problems and Computational Solutions
Ed. J.L. Swedlow
New York: ASME p.153

24. CRUSE T. A. (1973)
"Application of the Boundary Integral Equation Method to Three Dimensional Stress Analysis"
Computers and Structures, Vol.3 p.509

25. CRUSE T. A. and RIZZO F. J. (1968)
"A Direct Formulation and Numerical Solution of the General Transient Elastodynamic Problem: I"
J. Math. Ananalysis and Applications, Vol.22 p.244

26. CRUSE T. A. and RIZZO F. J. (1968)
"A Direct Formulation and Numerical Solution of the General Transient Elastodynamic Problem: II"
J. Math. Ananalysis and Applications, Vol.22 p.341

27. CRUSE T. A. and RIZZO F. J. (eds.) (1975)
"Boundary Integral Equation Method: Computational Applications in Applied Mechanics"
ASME Proc. AMD, Vol.11 1975

28. DOYLE J. M. (1965)
"Radiation Conditions in Elasticity"
J. Applied Math. and Physics (ZAMP), Vol.16 p.527

29. DOYLE J. M. (1966)
"Integration of the Laplace Transformed Equations of Classical Elastokinetics"
J. Math. Analysis and Applications, Vol.13 p.118

30. ELORDUY J., NIETO J. A. and SZEKELY E. M. (1967)
"Dynamic Response of Bases of Arbitrary Shape Subjected to Periodic Vertical Loading"
Proc. Intern. Symp. on Wave Propagation and Dynamic Properties of Earth Materials
Albuquerque, University of New Mexico, p.105

31. ERINGEN A. C. and SUHUBI E. S. (1975)
Elastodynamics, Volume II
Academy Press, 1975

32. GUPTA D.C, PARMELEE R. A. and KRIZEK R. J. (1973)
"Coupled sliding and Rocking Vibrations of a Rigid Foundation on an Elastic Medium"
Symp. Earth and Earth Structures under Earthquakes and Dynamic Loads. Vol.1
The Technical Institute Northwestern University, Evanston III U.S.A

33. HAMIDZADEH ERAGHI H. R. (1978)
"Dynamics of Rigid Foundations on the Surface of an Elastic Half-Space"
Ph.D Thesis, Imperial College, University of London.

34. INTERNATIONAL COMMISSION ON LARGE DAM S (1979)
"Transaction of the 13th International Congress on Large Dams, New Delhi"
Int. Commission on Large Dams, Paris 1979)

35. JASWON M. A. and PONTER A. R. (1963)
"Integral Equation Methods in Potential Theory, I"
Proc. Royal Society of London, Series A, p.273

36. KARASUDHI P., KEER L. M. and LEE S. L (1968)
"Vibratory Motion of a Body on an Elastic Half Space"
Ph.D Thesis, Northwestern University, Evanston, Illonois, 1968

37. KARASUDHI P., KEER L. M. and LEE S. L. (1968)
"Vibratory Motion of a Body on an Elastic Half Plane"
J. Applied Mechanics, Vol.35 p.697

38. KELLOGG O. D. (1953)
Foundations of Potential Theory
Dover, 1953

39. KELVIN, LORD (Sir W. Thomson) (1848)
Cambridge and Dublin Mathematical Journal

40. KRENT S. and SCHMIDT H. (1979)
"Vibration of an Elastic Circular Plate on an Elastic Half Space. A Direct Approach"
The Danish Center for Applied Mathematics and Mechanics
Report No.169, Dec.1979

41. KUPRADZE V. D. (1963)
"Dynamical Problems in Elasticity"
in Progress in Solid Mechanics, Vol.3, 1963
Eds. I.N. Sneddon, R. Hill
Wiley and Sons

42. LACHAT J. C. and WATSON J. O. (1975)
"A Second Generation Boundary Integral Equation Program for Three Dimensional Elastic Analysis
found in reference number 27

43. LAMB H. (1882)
"On the Vibrations of an Elastic Sphere"
Proc. London Math. Soc, Vol.13 p.189

44. LAMB H. (1904)
"On the Propagation of Tremors Over the Surface of an Elastic Solid"
Philosophical Transactions, Royal Society of London
Vol.203A p.1

45. LAMB H. (1917)
"On Waves in an Elastic Plate"
Proc. Royal Society of London, Vol.93A p.114

46. LEE T.H. and WESLEY D.A. (1973)
"Soil-Structure Interaction of Nuclear Reactor Structure Considering Through-Soil Coupling Between Adjacent Structure"
Nuclear Engineering and Design, Vol.24

47. LOVE A.E. H. (1944)
A Treatise on the Mathematical Theory of Elasticity
Dover, 1944

48. LUCO J. E. and WESTMANN R. A. (1972)
"Dynamic Response of a Rigid Footing Bonded to an Elastic Half Space"
J. Applied Mechanics, Vol.39 p.527

49. LYSMER J. and KUHLEMEYER R. L. (1969)
"Model for Infinite Media"
Journal of Engineering Mechanics Division, ASCE, Vol.95 p.1381

50. LYSMER J. and WASS G. (1972)
"Shear Waves in Plane Infinite Structures"
J. Eng. Mech. Division, ASCE, Vol.98 p.85

51. MacCALDEN P.B. and MATTHIESON R.B. (1973)

"Coupled Response of Two Foundations"
5th World Conference on Earthquake Engineering, Rome, p.1913

52. MEYER W.L., BELL W.A., ZINN B. T. and STALLYBRASS M. P. (1978)
"Boundary Integral Solutions of Three Dimensional Acoustic Radiation Problem"
J. Sound and Vibrations, Vol.59 p.245

53. MIKHLIN S. G. (1957)
Integral Equations
Pergamon, 1957

54. MILLER G. F. and PURSEY H. (1954)
"The Field and Radiation Impedance of Mechanical Radiators on the Free Surface of Semi-Infinite Isotropic Solid"
Proc. Royal Society of London, Series A, p.521

55. MINDLIN R. D. (1951)
"Influence of Rotary Inertial and Shear on Flexural Motion of Isotropic Elastic Plates"
J. Applied Mechanics, Vol.18 p.31

56. MORSE R. W. (1950)

"The Velocity of Compressional Waves in Rods of Rectangular Cross Section"

The J. Acoustical Soc. of America, Vol.22 p.219

57. MORSE P. M. and FESHBACK H. (1953)

Methods of Theoretical Physics Part II

McGraw-Hill, New York, 1953

58. NOWACKI W. (1964)

"Mixed Boundary-Value Problems in Elastodynamics"

Proceedings of Vibration Problems, Warsaw Vol.3

59. PAPADOPOULIS M. (1963)

"The Use of Singular Integrals in Wave Propagation Problems With Application to the Point Source in a Semi-Infinite Medium"

Pro. Royal Society of London, Vol.276A P.1365

60. PEKERIS C. L. (1955)

"The Seismic Buried Pulse"

Proc. National Academy of Science, USA, Vol.41 P.629

61. QUINLAN P. M. (1953)

"The Elastic Theory of Soil Dynamics"

Special Technical Publication 156.
American Society for Testing and Materials, P.3

62. REISSNER E. (1936)
"Stationary, Axially Symmetric Oscillations on a Homogeneous Elastic Half Space Caused by a Vibration Body"
Ingenieur Archiv. Vol.7 p.381

63. REISSNER E. and SAGOCI H. F. (1944)
"Forced Torsional Oscillations of Elastic Half-Space I"
J. Applied Physics, Vol.15 p.652

64. RICHARDSON J.D., WEBSTER J. J. and WARBURTON G. B. (1971)
"The Response on the Surface of an Elastic Half Space Near to a Harmonically Excited Mass"
J. Sound and Vibrations, Vol.14

65. RIZZO F. J. (1967)
"An Integral Equation Approach to Boundary Value Problems of Classical Elastostatics"
Q. Applied Math, Vol.25 p.83

66. RIZZO F. J. and SHIPPY D. J. (1968)
"A Formulation and Solution Procedure for the General Non-homogeneous Elastic Inclusion Problem"

Int. J. Solids and Structures, Vol.4 p.1161

67. SAGOCI H. F. (1944)
"Forced Torsional Oscillations of an Elastic Half-Space II"
J. Applied Physics, Vol.15 p.655

68. SHARMA D. L. (1967)
"Scattering of Steady Elastic Waves by Surfaces of Arbitrary Shape"
Bull. Seismological Soc. of America, Vol.57 p.795

69. SHAW R. P. (1968)
"Scattering of Elastic Waves by Rigid Obstacles of Arbitrary Shape"
J. Acoustical Soc. of America, Vol.44 p.745

70. SEVERN R.T., JEARY A. P. and ELLIS B. R. (1980)
"Forced Vibration Tests and Theoretical Studies on Dams"
Proc. Inst. Civil Engineers, Part 2, Vol.69 p.605

71. SOKOLNIKOFF I. S. and REDHEFFER R. M. (1958)
Mathematics of Physics and Modern Engineering
McGraw-Hill, 2nd edition, 1958

72. STERNBERG E. and EUBANKS R. A. (1957)
"On Stress Functions for Elastokinetics and the Integration of the Repeated Wave Equation"
Q. Applied Math., Vol.15 p.149

73. STOKE G. G. (1849)
"On the Dynamical Theory of Diffraction"
Trans. Cambridge Philosophical Soc., Vol.9 p.1

74. SYMM G. T. (1963)
"Integral Equation Methods in Potential Theory"
Proc. Royal Society of London, Series A, p.275

75. TAN C. L. and FENNER R. T. (1978)
"Three-Dimensional Stress Analysis by the Boundary Integral Equation Method"
J. Strain Analysis, Vol.13 p.213

76. TAN C. L. and FENNER R. T. (1979)
"Elastic Fracture Mechanics Analysis by the Boundary Integral Equation Method"
Proc. Royal Society of London, Vol.369A p.243

77. THOMAS D. P. (1968)
"Torsional Oscillations of an Elastic Half Space"
Quarterly J. Mech. and Applied Math., Vol.21 p.51

78. THOMSON W. T. and KOBORI T. (1963)
"Dynamical Compliance of Rectangular Foundations on an Elastic Half Space"
J. Applied Mechanics, Vol.30 p.579

79. WARBURTON G.B., RICHARDSON J. D. and WEBSTER J. J. (1971)
"Forced Vibrations of Two Masses on an Elastic Half Space"
J. Applied Mechanics, Vol.38 p.148

80. WARBURTON G.B., RICHARDSON J.D. and WEBSTER J.J. (1972)
"Harmonic Response of Masses on an Elastic Half Space."
Jnl. Engineering for Industry, ASME, Vol.94, p.193

81. WHITMAN R.V. (1969)
"The Current Status of Soil Dynamics"
Applied Mechanics Reviews, Vol.22, p.1

82. WONG H. L. and LUCO J. E. (1976)
"Dynamical Response of Rigid Foundations of Arbitrary Shape"
Earthquake Eng. and Structural Dynamics,
Vol.4 p.579

83. ZIENKIEWICZ O. C. and CHEUNG Y. K. (1967)

The Finite Element Method in Structural and Continuum Mechanics

McGraw-Hill, London, 1967